

**POTENTIAL ASSESSMENT OF NONPOINT SOURCE
POLLUTION ON SURFACE WATER QUALITY IN
UPPER LAM PHRA PHLOENG WATERSHED USING
GEOSPATIAL MODELS**

Tharapong Phetprayoon

A Thesis Submitted in Partial Fulfillment of the Requirements for the

Degree of Doctor of Philosophy in Geoinformatics

Suranaree University of Technology

Academic Year 2010

การประเมินศักยภาพของมดพิษประเภทไม่ทราบแหล่งกำเนิดแน่นอน
ต่อคุณภาพน้ำผิวดิน ในลุ่มน้ำลำพระเพลิงตอนบน โดยใช้แบบจำลองเชิงพื้นที่

นายธราพงษ์ เพ็ชรประยูร

วิทยานิพนธ์นี้เป็นส่วนหนึ่งของการศึกษาตามหลักสูตรปริญญาวิทยาศาสตรดุษฎีบัณฑิต

สาขาวิชาภูมิสารสนเทศ

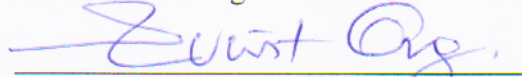
มหาวิทยาลัยเทคโนโลยีสุรนารี

ปีการศึกษา 2553

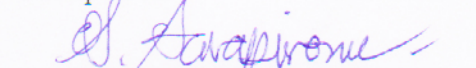
**POTENTIAL ASSESSMENT OF NONPOINT SOURCE
POLLUTION ON SURFACE WATER QUALITY IN UPPER LAM
PHRA PHLOENG WATERSHED USING GEOSPATIAL MODELS**

Suranaree University of Technology has approved this thesis submitted in partial fulfillment of the requirements for the Degree of Doctor of Philosophy.

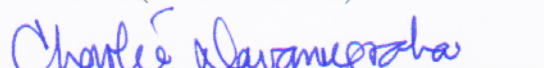
Thesis Examining Committee


(Asst. Prof. Dr. Suwit Ongsomwang)

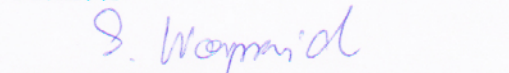
Chairperson


(Asst. Prof. Dr. Sunya Sarapirome)

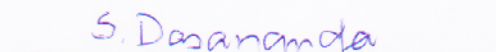
Member (Thesis Advisor)


(Assoc. Prof. Dr. Charlie Navanugraha)

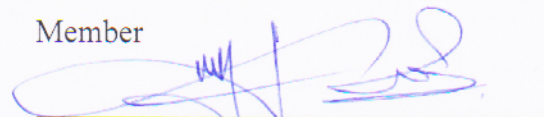
Member


(Asst. Prof. Dr. Sodchol Wonprasaid)

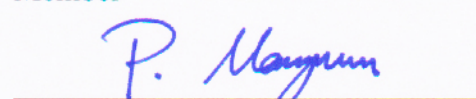
Member


(Asst. Prof. Dr. Songkot Dasananda)

Member


(Dr. Dusdi Chanlikit)

Member


(Assoc. Prof. Dr. Prapun Manyum)


(Dr. Wut Dankittikul)

Acting Vice Rector for Academic Affairs

Dean of Institute of Science

ธราพงษ์ เพ็ชรประยูร : การประเมินศักยภาพของมลพิษประเภทไม่ทราบแหล่งกำเนิด
แน่อนต่อคุณภาพน้ำผิวดิน ในลุ่มน้ำลำพระเพลิงตอนบน โดยใช้แบบจำลองเชิงพื้นที่
(POTENTIAL ASSESSMENT OF NONPOINT SOURCE POLLUTION ON SURFACE
WATER QUALITY IN UPPER LAM PHRA PHLOENG WATERSHED USING
GEOSPATIAL MODELS) อาจารย์ที่ปรึกษา : ผู้ช่วยศาสตราจารย์ ดร.สัญญา สราภิรมย์,
226 หน้า.

การวิจัยครั้งนี้มุ่งพัฒนาแบบจำลองเชิงพื้นที่สำหรับจำลองปริมาณน้ำท่า ตะกอน และ
สารอาหาร ซึ่งใช้เป็นดัชนีบ่งชี้ภาวะผลกระทบเชิงพื้นที่ในพื้นที่ศึกษา และจัดทำดัชนีบ่งชี้ศักยภาพ
การปนเปื้อนจากมลพิษประเภทไม่ทราบแหล่งกำเนิดแน่อนเพื่อใช้กำหนดลำดับความต้องการ
การจัดการของพื้นที่

แบบจำลองเชิงพื้นที่ที่รวมกับวิธีการหมายเลขโค้งน้ำท่า (Runoff Curve Number
Method) ได้รับการพัฒนาขึ้นเพื่อใช้ประเมินปริมาณน้ำท่าโดยมีการคำนวณในรูปแบบกริด และทำ
การเปรียบเทียบค่าและตรวจสอบความถูกต้องของแบบจำลอง โดยนำผลที่ได้จากแบบจำลอง
เปรียบเทียบกับผลการตรวจวัด ณ สถานี M.171 และ M.145 แบบรายเหตุการณ์ ในช่วงฤดูฝน พ.ศ.
2551 พบว่า แบบจำลองมีค่าสัมประสิทธิ์ประสิทธิภาพ (E) เท่ากับ 0.87 และ 0.68 และค่า
สัมประสิทธิ์การตัดสินใจ (R^2) เท่ากับ 0.89 และ 0.75 ของสถานี M.171 และ M.145 ตามลำดับ
ชี้ให้เห็นว่าแบบจำลองที่พัฒนาขึ้นมีความถูกต้องอยู่ในเกณฑ์ที่ยอมรับได้

การประเมินปริมาณตะกอนโดยใช้แบบจำลองเชิงพื้นที่ที่รวมกับสมการสูญเสียดินสากล
(MUSLE) และแบบจำลองสัดส่วนการพัดพาตะกอน (SEDD) โดยการคำนวณในรูปแบบกริด ผล
การศึกษาพบว่า แบบจำลองมีค่า E เท่ากับ 0.79 และ R^2 เท่ากับ 0.92 ชี้ให้เห็นว่าแบบจำลองที่
พัฒนาขึ้นมีความถูกต้องอยู่ในเกณฑ์ที่ยอมรับได้

การประเมินมลสารที่ละลายมากับน้ำท่าและที่ติดมากับตะกอนโดยใช้แบบจำลองเชิงพื้นที่
ที่รวมกับสมการการสูญเสียธาตุอาหารในแบบจำลอง AGNPS โดยการคำนวณในรูปแบบกริด ผล
การศึกษาพบว่า ผลของแบบจำลองในการประเมินไนโตรเจนทั้งที่ละลายมากับน้ำท่าและที่ติดมา
กับตะกอน และฟอสฟอรัสที่ละลายมากับน้ำท่า มีค่า E อยู่ในช่วง 0.52 ถึง 0.70 และ R^2 เท่ากับ 0.78
ถึง 0.93 ส่วนผลของแบบจำลองในการประเมินฟอสฟอรัสที่ติดมากับตะกอน มีค่า E เท่ากับ 0.13
และ R^2 เท่ากับ 0.87 พบว่าในบางเหตุการณ์ผลจากแบบจำลองมีความผิดพลาดค่อนข้างสูงและเป็น
สาเหตุสำคัญที่ส่งผลให้ E มีค่าต่ำมาก อย่างไรก็ตาม หลายเหตุการณ์มีผลจากแบบจำลองที่ให้ความ
ถูกต้องพอสมควร เมื่อพิจารณาในภาพรวมแล้วพบว่าแบบจำลองทำงานร่วมกับ GIS ได้ดี อย่างไรก็ตาม

ตาม ความถูกต้องของแบบจำลองควรได้รับการปรับปรุงให้ดีขึ้นในโอกาสต่อไปด้วยการพิจารณาถึงพารามิเตอร์ทั้งหมดที่เกี่ยวข้องและความน่าเชื่อถือในการได้มา

ข้อมูลมลพิษประเภทไม่ทราบแหล่งกำเนิดแน่นอนที่ได้จาก 3 ส่วนแรกทีกล่าวมาแล้ว สามารถระบุถึงความรุนแรงเชิงพื้นที่ของผลกระทบจากมลพิษแต่ละประเภทได้ สำหรับการพิจารณาผลกระทบของมลพิษเชิงพื้นที่ทั้ง 3 ส่วนในภาพรวม ได้ทำการพัฒนาดัชนีโดยรวมที่บ่งชี้ศักยภาพของพื้นที่ต่อมลพิษประเภทไม่ทราบแหล่งกำเนิดแน่นอนโดยใช้เทคนิคการวิเคราะห์ตัดสินใจแบบหลากหลายเกณฑ์ ร่วมกับ GIS ดัชนีย่อยที่ใช้ในการวิเคราะห์ ได้แก่ ดัชนีศักยภาพน้ำท่า ดัชนีศักยภาพตะกอน ดัชนีศักยภาพมลสาร ค่าดัชนีรวมที่ได้จะบ่งบอกถึงศักยภาพในการเป็นแหล่งกำเนิดมลสารของพื้นที่ และสามารถนำไปใช้กำหนดลำดับก่อนหลังตามความจำเป็นเร่งด่วนสำหรับการวางแผนและจัดการมลพิษประเภทไม่ทราบแหล่งกำเนิดแน่นอนในพื้นที่ลุ่มน้ำต่อไป

สาขาวิชาการรับรู้จากระยะไกล
ปีการศึกษา 2553

ลายมือชื่อนักศึกษา อรุณพร
ลายมือชื่ออาจารย์ที่ปรึกษา Dr. Anuphono
ลายมือชื่ออาจารย์ที่ปรึกษาร่วม Charlie Navanvongsa
ลายมือชื่ออาจารย์ที่ปรึกษาร่วม S. Wannich

THARAPONG PHETPRAYOON : POTENTIAL ASSESSMENT OF
NONPOINT SOURCE POLLUTION ON SURFACE WATER QUALITY IN
UPPER LAM PHRA PHLOENG WATERSHED USING GEOSPATIAL
MODELS. THESIS ADVISOR : ASST. PROF. SUNYA SARAPIROME,
Ph.D. 226 PP.

NONPOINT SOURCE POLLUTION, GRID-BASED APPLICATION, RUNOFF,
SEDIMENT YIELD, NUTRIENT YIELD, INDEX OF ENVIRONMENTAL
IMPACT.

This research aims at developing geospatial models to simulate runoff, sediment, and nutrient yield which are indicators to determine impact conditions spatially within the study area and to set up Nonpoint Source Pollution Potential Index (NPSI) for prioritizing management requirement of areas.

Calibration and validation of the grid-based Curve Number method for the Upper Lam Phra Phloeng watershed was performed by comparing observed and simulated runoff at the M.171 and M.145 stations during rainy season in 2008. The results of the model validation show that coefficient of efficiency (E) is 0.87 and 0.68 and coefficient of determination (R^2) is 0.89 and 0.75 at the M.171 and M.145 stations, respectively. This indicates that the model working under the Geographic Information System (GIS) reasonably well with acceptable accuracy.

The grid-based approach has been applied with Modified Universal Soil Loss Equation (MUSLE) and Sediment Delivery Distributed (SEDD) models for the sediment yield simulation. Evaluation of sediment yield models was performed by

comparing the observed and simulated results. The results of model validation show that E is 0.79 and $R^2 = 0.92$. This indicates that the model working under the GIS reasonably well with acceptable accuracy.

The Agricultural Nonpoint Source Pollution Model (AGNPS) algorithm integrated with grid-based geospatial model was developed to simulate the nutrient processes in forms of dissolved and sediment-adsorbed loads. The overall results of the model validation show that E and R^2 values range from 0.52-0.70 and 0.78-0.93, respectively. However, phosphorus adsorbed by sediments shows exceptionally poor model performance with $E = 0.13$ and $R^2 = 0.87$. This is because in few events errors become abnormally high that can lead E to be low while some other events show much less errors. Overall consideration, the evaluation of the grid-based nutrient yield model demonstrated that this model working under the GIS reasonably well.

The NPS pollutants in three different forms mentioned above can indicate impact intensity of each type of pollutant spatially. For overall impact consideration, the NPSI was established using GIS and Multi-criteria Decision Analysis (MCDA) technique, particularly for identifying and prioritizing critical areas. The index was integrated from indices of surface runoff, sediment yield, and nutrient yield. The map of NPSI will be helpful for examining the pattern of diffuse pollution and could facilitate the decision on NPS pollution management at local level.

School of Remote Sensing

Academic Year 2010

Student's Signature Tharapong.

Advisor's Signature S. Sarapinome

Co-advisor's Signature Charlie Sawanyakul

Co-advisor's Signature S. Wanyard

ACKNOWLEDGEMENTS

It is my pleasure to express my gratitude to all people who have encouraged me to finish this work. For sure, the fulfillment of this research is due to the cooperation of many people. Therefore, I can only hope that I mention you all – and those who I forget at this moment, please forgive me and think that despite this lapse I really do appreciate you all.

First of all, I would like to express my sincere gratitude to my advisor, Asst. Prof. Dr. Sunya Sarapirome, whose encouragement, guidance and support from the initial to the final enabled me to develop an understanding of the subject.

I would like to appreciate the co-advisor, Assoc. Prof. Dr. Charlie Navanugraha and Asst. Prof. Dr. Sodchol Wonprasaid in help, guidance, discussion on many concerned problems.

I am also very grateful to the committee, Asst. Prof. Dr. Suwit Ongsomwang, Asst. Prof. Dr. Songkot Dasananda, and Dr. Dusdi Chanlikit, for always being interested in the progress of my work, and for all valuable suggestions and critical comment during seminars and progress meeting.

I would like to express my sincere gratitude to Asst. Prof. Dr. Pratueng Jintasakul and Assoc. Prof. Dr. Napat Noinumsai, for all valuable suggestions and moral support.

Thanks to all staffs of The Hydrology and Water Center Management for Lower Northeastern Region, who help fieldwork at M.145 and M.171 stations.

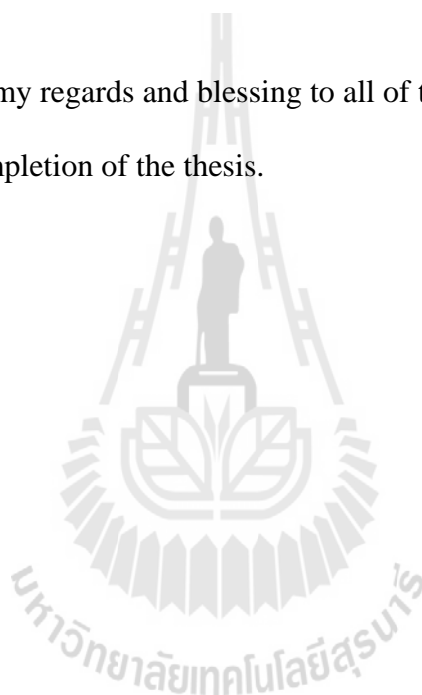
I would also like to express my sincere thanks to friends from the SUT School of Remote Sensing for all invaluable questions and suggestions during seminars and progress meeting, which really improved the thesis content.

I wish to acknowledge the Nakhon Ratchasima Rajabhat University for the financial support.

Special thanks go to my family for great love, care, and patience during my study.

Lastly, I offer my regards and blessing to all of those who supported me in any aspects during the completion of the thesis.

Tharapong Phetprayoon



CONTENTS

	Page
ABSTRACT IN THAI.....	I
ABSTRACT IN ENGLISH	III
ACKNOWLEDGEMENTS.....	V
CONTENTS.....	VII
LIST OF TABLES.....	XIII
LIST OF FIGURES	XVI
LIST OF ABBREVIATIONS.....	XX
CHAPTER	
I INTRODUCTION.....	1
1.1 Rational of the study	1
1.2 Problem in the study area.....	4
1.3 Research objectives.....	5
1.4 Scope and limitation of the study.....	6
1.4.1 Limitation of data	6
1.4.2 Scope of the model.....	9
1.5 Study area.....	10
1.5.1 Physical characteristics	10
1.5.2 Agricultural features.....	12
1.6 Benefits of the study	13

CONTENTS (Continued)

	Page
1.7 Structure of the thesis.....	13
1.8 References.....	16
II LITERATURE REVIEWS.....	20
2.1 Nonpoint source pollution characteristics.....	20
2.1.1 Runoff processes	21
2.1.2 Sedimentation processes	22
2.1.3 Nutrients processes.....	24
2.2 Modeling environment of NPS	25
2.2.1 Spatial context.....	26
2.2.2 Temporal context.....	27
2.2.3 Processes context.....	28
2.3 Tools for NPS pollution model	31
2.3.1 Existing NPS pollution model.....	31
2.3.2 Tool selected for the study	34
2.4 GIS technology and NPS model	35
2.5 Previous NPS studies	37
2.6 References.....	41
III SURFACE RUNOFF SIMULATION USING GRID-BASED	
CURVE NUMBER METHOD.....	48
3.1 Abstract	48

CONTENTS (Continued)

	Page
3.2 Introduction	49
3.3 Materials and methods	50
3.3.1 Curve number method	50
3.3.2 Data collection	54
3.3.3 Assignment of appropriate curve number values	59
3.3.4 Model development of grid-based approach	64
3.3.5 Model evaluation	65
3.4 Results and discussion	67
3.4.1 Model calibration	67
3.4.2 Model validation	71
3.5 Conclusion	75
3.6 References	76
 IV SEDIMENT YIELD ESTIMATION USING MODIFIED	
UNIVERSAL SOIL LOSS EQUATION AND SEDIMENT	
DELIVERY DISTRIBUTED MODEL	79
4.1 Abstract	79
4.2 Introduction	80
4.3 Materials and methods	81
4.3.1 Modified Universal Soil Loss Equation (MUSLE)	83
4.3.2 Data collection for MUSLE	84
4.3.3 Sediment delivery distributed model (SEDD)	98

CONTENTS (Continued)

	Page
4.3.4 Model development of grid-based approach	102
4.3.5 Event-based sediment yield measurement	103
4.4 Results and discussion	105
4.4.1 Model calibration	105
4.4.2 Model validation	106
4.5 Conclusions	111
4.6 References	111
V NUTRIENT YIELD ESTIMATION USING GRID-BASED	
AGNPS MODEL	116
5.1 Abstract	116
5.2 Introduction	118
5.3 Materials and methods	119
5.3.1 Nitrogen yield in runoff simulation model	120
5.3.2 Phosphorus yield in runoff simulation model	125
5.3.3 Nitrogen yield in sediment simulation model	128
5.3.4 Phosphorus yield in sediment simulation model	130
5.3.5 Nutrient observation and analysis	132
5.4 Results and discussion	135
5.4.1 Results of nitrogen yield in runoff	135
5.4.2 Results of phosphorus yield in runoff	139
5.4.3 Results of nitrogen yield in sediment	144

CONTENTS (Continued)

	Page
5.4.4 Results of phosphorus yield in sediment.....	149
5.5 Conclusion	155
5.6 References	155
VI DEVELOPMENT OF NONPOINT SOURCE POLLUTION	
POTENTIAL INDEX	157
6.1 Abstract	157
6.2 Introduction.....	158
6.3 Materials and methods	159
6.3.1 GIS and Multi-Criteria Decision Analysis (MCDA)	159
6.3.2 Runoff potential index.....	164
6.3.3 Sediment potential index.....	165
6.3.4 Nutrient potential index.....	167
6.4 Results and discussion	170
6.5 Conclusion	173
6.6 References.....	174
VII GENERAL CONCLUSION AND RECOMMENDATION.....	177
7.1 General conclusion.....	178
7.1.1 Surface runoff model development	178
7.1.2 Sediment yield model development	179
7.1.3 Nutrient yield model development.....	181
7.1.4 Nonpoint source pollution potential index (NPSI) development..	182

CONTENTS (Continued)

	Page
7.2 Recommendation for further research.....	183
APPENDICES	
APPENDIX A CRITERIA FOR HYDROLOGIC SOIL GROUP.....	186
APPENDIX B ANTECEDENT SOIL MOSITURE CONDITION (AMC)	188
APPENDIX C SOURCE CODE OF RUNOFF MODEL.....	189
APPENDIX D MANNING’S ROUGHNESS COEFFICIENTS FOR CERTAIN TYPES OF LAND USE FOR THIS STUDY ..	195
APPENDIX E 24-HOUR DURATION PRECIPITATION WITH A 2-YEAR RETURN PERIOD DATA.....	196
APPENDIX F K VALUES BASED ON GEOLOGICAL DATA	197
APPENDIX G C VALUES BASED ON LAND USE DATA.....	198
APPENDIX H COEFFICIENT RELATED TO LAND USE FOR SEDD MODEL.....	199
APPENDIX I SOURCE CODE OF SEDIMENT YIELD MODEL.....	200
APPENDIX J SOURCE CODE OF NUTRIENT YIELD MODEL.....	204
APPENDIX K SOME PICTURES OF AREA CHARACTERISTICS	218
APPENDIX L SOME PICTURES OF SAMPLING AND LABORATORY	221
CURRICULUM VITAE.....	226

LIST OF TABLES

Table	Page
2.1 Summary of the characteristics from some of the reviewed NPS models	31
3.1 Rainfall station (The rainfall station map is shown in Figure 1.1)	54
3.2 Soil series properties for hydrologic soil group determination.....	57
3.3 Modified curve number values of Upper Lam Phra Phloeng watershed	61
3.4 Data comparison of model simulations (Q_{sim}) and field observations (Q_{obs}) of ten events for model calibration	68
3.5 Data comparison of calibrated model simulations (Q_{sim}) and field observations (Q_{obs}) of eight events for model validation.....	72
4.1 Observed sediment yield data at M.171 and M.145 stations	104
4.2 Data comparison of sediment yield simulation (SY_{sim}) and observation (SY_{obs}) of eight events for sediment yield model calibration	105
4.3 Data comparison of calibrated-sediment yield simulation (SY_{sim}) and observation (SY_{obs}) of eight events for sediment yield model validation.....	107
5.1 Observed nutrient concentration in runoff at M.171 and M.145 stations	132
5.2 Observed nutrient attached in sediment at M.171 and M.145 stations	134
5.3 Data comparison of nitrogen yield in runoff simulation and observation of eight events for model calibration	136
5.4 Data comparison of nitrogen yield in runoff simulation and observation of eight events for model validation	137

LIST OF TABLES (Continued)

Table	Page
5.5 Data comparison of phosphorus yield in runoff simulation and observation of eight events for model calibration.....	140
5.6 Data comparison of phosphorus yield in runoff simulation and observation of eight events for model validation.....	142
5.7 Data comparison of nitrogen yield in sediment simulation and observation of eight events for model calibration.....	145
5.8 Data comparison of nitrogen yield in sediment simulation and observation of eight events for model validation.....	147
5.9 Data comparison of phosphorus yield in sediment simulation and observation of eight events for model calibration.....	150
5.10 Data comparison of phosphorus yield in sediment simulation and observation of eight events for model validation.....	152
6.1 Potential loading values of fertilizer for different main land uses in the Upper Lam Phra Phloeng watershed during year 2008	169
A-1 Criteria for hydrologic soil group determination	186
B-1 AMC for this study	188
B-2 Criteria for AMC classification	188
D-1 Manning's roughness coefficients for certain types of land use for this study	195
E-1 24-hour duration precipitation with a 2-year return period	196

LIST OF TABLES (Continued)

Table	Page
F-1 K values based on major rock types of each of the geological formations	197
G-1 C values based on land use data in the study area	198
H-1 Coeffieicnt (a_i) related to land use for SEDD model.....	199



LIST OF FIGURES

Figure	Page
1.1 Study area.....	11
1.2 Structure of the thesis.....	15
3.1 Flow diagrams of the grid-based curve number method	53
3.2 Rainfall data (mm) for calibration events	55
3.3 Rainfall data (mm) for validation events	56
3.4 Hydrologic soil group data.....	58
3.5 Land use data (Level 3 Classification)	69
3.6 Curve number values according to antecedent soil moisture condition	63
3.7 Simulated surface runoff from grid-based Curve Number method	64
3.8 Runoff depth (mm) for calibration events (M.171)	69
3.9 Runoff depth (mm) for calibration events (M.145)	70
3.10 Comparison of observed and simulated runoffs at M.171 and M.145 stations ...	71
3.11 Runoff depth (mm) for validation events (M.171)	73
3.12 Runoff depth (mm) for validation events (M.145)	74
3.13 Relationships of observed and calibrated-simulated runoffs for model validation at the M.171 and M.145 stations.....	75
4.1 Flow diagrams of the sediment yield estimation	82
4.2 Runoff factor	85
4.3 Spatial distribution of peak discharge ($\text{m}^3 \text{s}^{-1}$) of eight events.....	88

LIST OF FIGURES (Continued)

Figure	Page
4.4 Spatial distribution of K factor in the study area	90
4.5 Spatial distribution of L factor	93
4.6 Spatial distribution of S factor	94
4.7 Spatial distribution of C factor.....	95
4.8 Spatial distribution of P factor.....	97
4.9 Spatial variation of event-based MUSLE simulated.....	98
4.10 Spatial distribution of SDR.....	102
4.11 Flow diagrams of event-based sediment yield measurement	104
4.12 Scatter plot of results of observed and simulated sediment yield.....	106
4.13 Spatial variation of event-based simulated sediment yields	108
4.14 Relationships of observed and calibrated-simulated sediment yield for model validation.....	109
5.1 Flow diagrams of the nitrogen yield in runoff estimation	124
5.2 Flow diagrams of the phosphorus yield in runoff estimation	127
5.3 Flow diagrams of the nitrogen yield in sediment estimation.....	129
5.4 Flow diagrams of the phosphorus yield in sediment estimation.....	131
5.5 Observed nitrogen concentration in runoff at M.171 and M.145	133
5.6 Observed phosphorus concentration in runoff at M.171 and M.145	133
5.7 Observed nitrogen attached in sediment at M.171 and M.145	134
5.8 Observed phosphorus attached in sediment at M.171 and M.145	135
5.9 Calibration results of observed and simulated nitrogen yield in runoff.....	136

LIST OF FIGURES (Continued)

Figure	Page
5.10 Relationships of observed and calibrated-simulated nitrogen yield in runoff.....	138
5.11 Spatial variation of event-based simulated nitrogen yield in runoff.....	139
5.12 Calibration results of observed and simulated phosphorus yield in runoff ..	141
5.13 Relationships of observed and calibrated-simulated phosphorus yield in runoff.....	143
5.14 Spatial variation of event-based simulated phosphorus yield in runoff.....	144
5.15 Calibration results of observed and simulated nitrogen yield in sediment ...	146
5.16 Relationships of observed and calibrated-simulated nitrogen yield in sediment	148
5.17 Spatial variation of event-based simulated nitrogen yield in sediment	149
5.18 Calibration results of observed and simulated phosphorus yield in sediment	151
5.19 Relationships of observed and calibrated-simulated phosphorus yield in sediment	153
5.20 Spatial variation of event-based simulated phosphorus yield in sediment ...	154
6.1 Flow diagram of the NPSI development.....	163
6.2 Flow diagram of the runoff potential index development	164
6.3 Distribution of the runoff potential index	165
6.4 Flow diagram of the sediment potential index development	166
6.5 Distribution of the sediment potential index.....	167

LIST OF FIGURES (Continued)

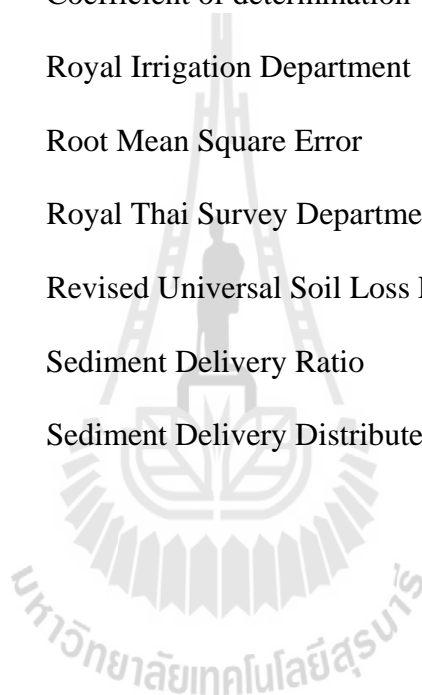
Figure	Page
6.6	Flow diagram of the nutrient potential index development..... 168
6.7	Distribution of the nutrient potential index..... 170
6.8	The NPSI distribution in the study area..... 172
6.9	Average NPSI in the village level..... 173
A-1	Direction of tillage for maize often across the contour..... 218
A-2	Maize cropping in undulating-rolling topography 218
A-3	Cassava cropping in undulating rolling topography 219
A-4	Mungbean cropping 219
A-5	Sugarcane cropping..... 220
A-6	Mango orchard 220
B-1	M.145 station (Cable way)..... 221
B-2	M.171 station (Bridge)..... 221
B-3	Sampling instrument 222
B-4	Stream flow velocity measurement, suspended sediment sampling, water quality sampling at M.145 223
B-5	Stream flow velocity measurement, suspended sediment sampling, water quality sampling at M.171 223
B-6	Sediment yield analysis laboratory 224
B-7	Sediment yield analysis by drying at 103°C method..... 224
B-8	Nutrient yield analysis instrument 225

LIST OF ABBREVIATIONS

AGNPS	=	Agricultural Nonpoint Source Pollution Model
AMC	=	Antecedence soil moisture condition
APPI	=	Agricultural pollution potential index
<i>CN</i>	=	Curve Number
CREAMS	=	Chemicals, Runoff and Erosion from Agricultural Management System
DEM	=	Digital Elevation Model
DEQP	=	Department of Environmental Quality Promotion
DMR	=	Department of Mineral Resources
<i>E</i>	=	Coefficient of efficiency
EPA	=	Environmental Protection Agency
<i>ER</i>	=	Enrichment Ratio
GIS	=	Geographic Information System
HSG	=	Hydrologic Soil Group
LDD	=	Land Development Department
MCDA	=	Multi-criteria Decision Analysis
MUSLE	=	Modified Universal Soil Loss Equation
N	=	Nitrogen
NPS	=	Nonpoint source
NPSI	=	Nonpoint source pollution potential index

LIST OF ABBREVIATIONS (Continued)

NRCS	=	Natural Resources Conservation Service
P	=	Phosphorus
PCD	=	Pollution Control Department
R^2	=	Coefficient of determination
RID	=	Royal Irrigation Department
<i>RMSE</i>	=	Root Mean Square Error
RTSD	=	Royal Thai Survey Department
RUSLE	=	Revised Universal Soil Loss Equation
SDR	=	Sediment Delivery Ratio
SEDD	=	Sediment Delivery Distributed Model



CHAPTER I

INTRODUCTION

1.1 Rational of the study

Maintaining or improving the quality of surface and groundwater is of primary concern for future sustainability. Water pollution come form two different sources- *point source* and *nonpoint source* (NPS). Point-source pollution can be controlled by discharge permits. Unlike point-source pollution, the NPS pollution depends on land-based activities and hydrologic phenomena. Little progress has been made in controlling NPS water pollution because of the difficulties of source identification and discharge control from so many diffused sources. Agricultural is now considered the most important NPS pollution loading into water bodies. Surface water and groundwater quality degradation due to agricultural practices and conversion of land to agriculture can be categorized as follows: a) degradation due to land use conversion from native lands to agriculture, b) increase of erosion and soil loss due to agricultural practices, c) chemical pollution by fertilizers and pesticides, and d) pollution from animal operations (Novotny, 1999). Abatement of agricultural NPS can be and must be conducted in the context of moving toward sustainable agriculture.

Prioritization or targeting of impaired water bodies and critical NPS areas in watershed is required for effective management (Caruso and Ward, 1998). With limited resources available, control and implementation programs focusing on critical NPS areas and adequate consideration of the impacts on alternative management, land

use, and conservation approaches are important (Srivastava et al., 2001). Water quality monitoring program plays an important role in water resource management, particularly for impaired water bodies where NPS are the overwhelming sources. This would require extensive monitoring activities. However, water quality monitoring programs can be extremely time consuming and costly. Along with laboratory and field studies, models can provide improved understanding leading to better management of environmental quality and sustainability (Ramaswami et al., 2005). The modeling alternative requires the description and understanding of several environmental phenomena with spatial and temporal variation (Luzio et al., 2004). Spatial modeling for surface water quality protection and improvement is therefore considered effective approach for environment management.

However, in Thailand the governing policies on watershed management in the past did not appreciate the importance of NPS pollution (Simachaya, 2003). Studies on the application modeling to explore the environmental problem arising from NPS pollution due to agricultural activities and to generate possible remedial measures and strategies to solve this problem are very few (กรมควบคุมมลพิษ, 2545; Babel et al., 2004). Although, the Tenth National Economic and Social Development Plan (2007-2011) emphasize on upgrade standards of environmental management in order to protect the resource base and maintain a sustainable balance in the natural environment and water quality as an important component. Moreover, The Policy and Prospective Plan for Enhancement and Conservation of National Environment Quality (1997-2016) recognized the role of local governments and civil society in improving and protecting water quality (Department of Environmental Quality Promotion [DEQP], 2005). None of the strategies mentioned above states directly about the

management of NPS pollution from agricultural. However, there are some words in the explanation of these strategies (i.e., sustainable balance, natural environment, water quality, local governments) which imply that NPS pollution is a part of these plans (Thapinta et al., 2009). They still lack of enough information and tools that could help in evaluating and managing a NPS pollution problem of surface water quality.

The problem associated with NPS pollution can be addressed with remote sensing and GIS technologies. The utility of the data and technologies are due to the size and distribution of the problem, the need for quantitative assessment to manage the pollution, and the widespread sources of the problem (Ward and Trimble, 2003). The advantages of linking the models with GIS are efficiently and consistently assigning parameter values to all parts of a study area, and to facilitate modeling with increased spatial resolution (Yagow, 1997). There are increasing efforts to develop and apply distributed parameters of models in a GIS environment for identifying and assessing critical NPS loading areas (Endreny and Wood, 1999; Chowdary et al., 2001; Leon et al., 2001; He, 2003; Babel et al., 2004).

The techniques for assessing surface water quality affected by NPS pollution are needed to establish. These techniques would help identify areas where NPS pollutions adversely impact on surface water. In this study, an effort will be made to develop geospatial models and methodologies for simulation and assessment of NPS pollution to support environmental management in the Upper Lam Phra Phloeng watershed.

1.2 Problem in the study area

In Thailand, water pollution from land-based activities is largely associated with urbanization, industrialization, and agricultural activities (Simachaya, 2002). The main pollutants from agricultural activities that cause problem to surface water quality problem are sediment, nutrient and other chemical substances. The Upper Lam Phra Phloeng watershed pollution is mostly associated with agricultural activities, especially when crop areas are increased from 44.97 to 65.49 percent during 1973-2000 (Charupatt, 2002). In the study area, fertilizer application has been increased rapidly over the past decade, especially for maize. The rate of application has doubled since fertilizer was first used, from around 210 kg ha^{-1} in 1998 or longer ago to about 470 kg ha^{-1} in 2003 (Cho and Zoebisch, 2003). Amount of fertilizer usage tends to be increased considerably. Although fertilizer usage can accelerate agricultural production, it is the source of surface water contamination. The more the fertilizers are used, the higher the potential of surface water contamination is (Chandler et al., 1998).

Regarding on agricultural land preparation, the farmers have changed from hand hoeing and animal powered tillage to tractor drawn land preparation. This leads to more intensive soil mixing and deeper tillage. Also, due to the nature and capacity of large machinery, the direction of tillage is often across the contour, thus encouraging soil erosion (Cho and Zoebisch, 2003). In the study area, maize is the dominant crop, as maize-maize (2 crops per year), maize-mungbean, and maize-fallow rotation (Cho et al., 2004). After the crop has been harvested the land is tilled and becomes sensitive to sheet erosion. Moreover, the forest land is being destroyed continuously which leads to increasing soil erosion. Lam Phra Phloeng reservoir is one of the targets most

serious affected by soil erosion related to sedimentation (Heijnis et al., 2003; Lorsirirat, 2007). Its storage capability was decreased from 150 million cubic meters to 108 million cubic meters during 1970-1991.

The problem of surface water quality deterioration in the Upper Lam Phra Phloeng watershed caused by agricultural NPS pollution is taken spatially into consideration in this study.

1.3 Research objectives

As increasing agricultural land and use of fertilizer in the Upper Lam Phra Phloeng watershed, the surface water protection becomes unavoidably needed. Monitoring on surface water quality is required in the first step. However, it is impractical to monitoring the whole areas by field investigation because of time and budget constraints. Therefore, techniques for assessing surface water quality affected by agricultural practices through spatial modeling are required to be established. These techniques would help identify areas where surface water is impacted by NPS pollution. Once the areas are identified, field surface water monitoring programs can be focused in such areas.

The purpose of this research is to develop tools and procedures to assess and identify areas in the Upper Lam Phra Phloeng watershed where surface water quality is affected by NPS pollution using GIS techniques. The specific objectives of this study are as follows:

1.3.1 To develop geospatial models to simulate runoff, sediment, and nutrient yields as indicators to determine impact conditions spatially within the study area.

1.3.2 To set up model results as index of pollution levels for further land management.

1.4 Scope and limitation of the study

This study deals with using geospatial modeling to potential assessment NPS pollution from agricultural activities which can impact on surface water quality of the study area and the downstream reservoir. The geospatial modeling is: 1) an attempt to simulate real world processes through the use of spatial input data describing physical characteristics of the system, 2) a set of algorithms to transform input data to output parameters of interest, and 3) simplifying assumptions to limit the scope of the model. The following aspects imposed limits and scope of the study.

1.4.1 Limitation of data

1.4.1.1 Resolution of spatial data

The data resolution can affect to simulation output of NPS pollution. In general increasing level of spatial resolution can increase the accuracy of the simulation. Values assigned to any grid cell represent an average value over the area of each cell. The greater the variability over the cell, the greater the error will be induced through the use of an average value. However, the cell size in this study will be based on the finest resolution of data set (30×30 meters) to reduce uncertainty caused by spatial averaging.

1.4.1.2 Rainfall data

Rainfall is driving force parameter of NPS pollution model. For improving accuracy, data obtained from stations must capture the variability of rainfall in the watershed. In this study, rainfall data were gathered from 11 manual

rain gauges located within and near the watershed. Considerable variation of rainfall existing among these stations, and rainfall distribution was not uniform over the watershed. The spatial rainfall variability within a watershed is presented. The Inverse Distance Weight (IDW) interpolation method was used to determine the spatial distribution of event based rainfall amount from a series of rain gauges.

1.4.1.3 Field observation data

Field observation data based on event consist of runoff, sediment yield, and nutrient yield. This used for calibration and validation the geospatial model. Especially, runoff data are very important to help quantify amount of pollutants transported by stream flow. The Upper Lam Phra Phloeng watershed has no historical observed data. So it is necessary to design and implement samplings for runoff, sediment, and nutrient along the main stream and also at the outlet of watershed. The measurement is confined to the stream flow measurement, sediment yield, and nutrient yield. Nutrient yield of nitrogen and phosphorus are in forms of both adsorbed in sediment and dissolved in runoff.

Observed data of the Royal Irrigation Department (RID), M.145 with 335 km² drainage area at the upstream outlet and M.171 with 556 km² drainage area at down stream outlet are used for model evaluation. Field observation data was conducted only in monsoon period between June – October 2008. The collection of sediment and nutrient samples coincides with the runoff peaks of the events, and also temporally over the rising and descending portion of the hydrograph curves. Prior to collecting a sample, measurement of the stream flow was conducted. The method of sampling and analysis was followed the standard method for the examination of water and wastewater (American Public Health Association, 1998).

Although an attempt was made to collect samples for every storm event, some storm events were not sampled due to unforeseen circumstances, such as equipment malfunctions. Therefore, comparison between data from model simulations and observed data were made only 18 events for runoff model, 16 events for sediment yield and nutrient yield models.

1.4.1.4 Land use data

All forms of land use can potentially affect the quality of storm water runoff from the land surface. Land use data are required for NPS pollution assessment because they donate the activities on land that generate the pollutants. The digital land use data at scale 1:25,000 were obtained from Land Development Department (LDD), which were updated to the year 2007. The model simulation conducted in the year 2008, this study assumed that there was a little change of land use of 2007 to 2008.

1.4.1.5 Digital Elevation Model (DEM)

The physical features of the topography substantially influence the magnitude and dynamics of surface runoff. Thus, they also influence NPS pollution. The Digital Elevation Model (DEM) contains spatially distributed elevation information to allow an automatic delineation of watershed. Topographic maps of the Royal Thai Survey Department (RTSD) at the scale 1:50,000 were used to generate DEM. The relevant parameters can be generated from DEM are slope, flow direction, flow length, and flow accumulation.

1.4.1.6 Soil data

The important properties of soil data including soil texture, permeability, structure, porosity, and the amount of existing nutrient are related to NPS pollution study. Soil data can be obtained at the scale of 1:25,000 from LDD and field survey.

However, this data set has no information in slope complex areas. Therefore, derived data of geological formations of the Department of Mineral Resources (DMR) were identified and used for complementing where soil data are absent.

1.4.1.7 Agricultural practice data

Information on agricultural practices was collected. Tillage types, the amount and types of fertilizer, application methods, and other practices can affect both the quantity and quality of surface runoff (Cooke et al., 2005) and substantially influence the magnitude and dynamic of NPS pollution. In this study, information regarding the agricultural practices can be obtained from 1) literature and fertilizer fact sheets and 2) field visits to some farms.

1.4.2 Scope of the model

Efficiency to develop a new model can be based on several facts such as research budget, study objectives and available time. It could take several years before it can be successfully applied to a specific situation. Therefore, this study decided to employ existing geospatial models to serve the objectives. The main criteria for choosing the models are: to be line with specific problem, data requirements, model accuracy, model capability, and ease of use. Previous model validation and study results observed should play a key role in determining which model to use. Base on extensive literature searches and consideration, Agricultural Nonpoint Source Pollution Model (AGNPS) was chosen for this study and was calibrated for more appropriate to the local.

The application scope of the AGNPS model includes:

- Event-based simulation
- Local cell-based operation.

- Surface runoff simulation
- Sediment yield simulation
- Nutrient yield simulation in forms of both adsorbed on sediment and dissolved in runoff.

Calibration technique for model results is required to minimize errors.

1.5 Study area

1.5.1 Physical characteristics

The 786.26 km² of Upper Lam Phra Phloeng watershed was selected for this study (Figure 1.1). The topography of the area is generally characterized by hilly-rolling terrain, with less undulating and flat areas. Elevation ranges from 260 m above mean sea level (msl.) in the northeastern parts to about 1,307 m above msl. in the southwestern parts of the watershed. This watershed is upstream area of the Lam Phra Phloeng reservoir. Therefore, any activities presence in the area can affect to the downstream reservoir. The climate is influenced by both the northeast and southwest monsoons, with an average annual rainfall of around 1,117 mm. The soils in the area vary to be 15 series with different soil textures as clay, clay loam, loam, loamy sand, sandy clay loam, sandy loam, and silty clay. The land use of the watershed consists of dense and disturbed evergreen forests, dense and disturbed deciduous forests, forest plantation, field crops, and orchards. In year 2007, more than 41.52% of the watershed is classified as field crop area. The dominant crops are maize, sugarcane, and cassava. Only 24.83% of the area is classified as forests.

In the lower reaches of the watershed, agriculture has been practiced for considerable a long time and the forests have completely disappeared. The upper

reaches of the watershed still have some forest cover, especially in the areas bordering the Khao Yai national park.

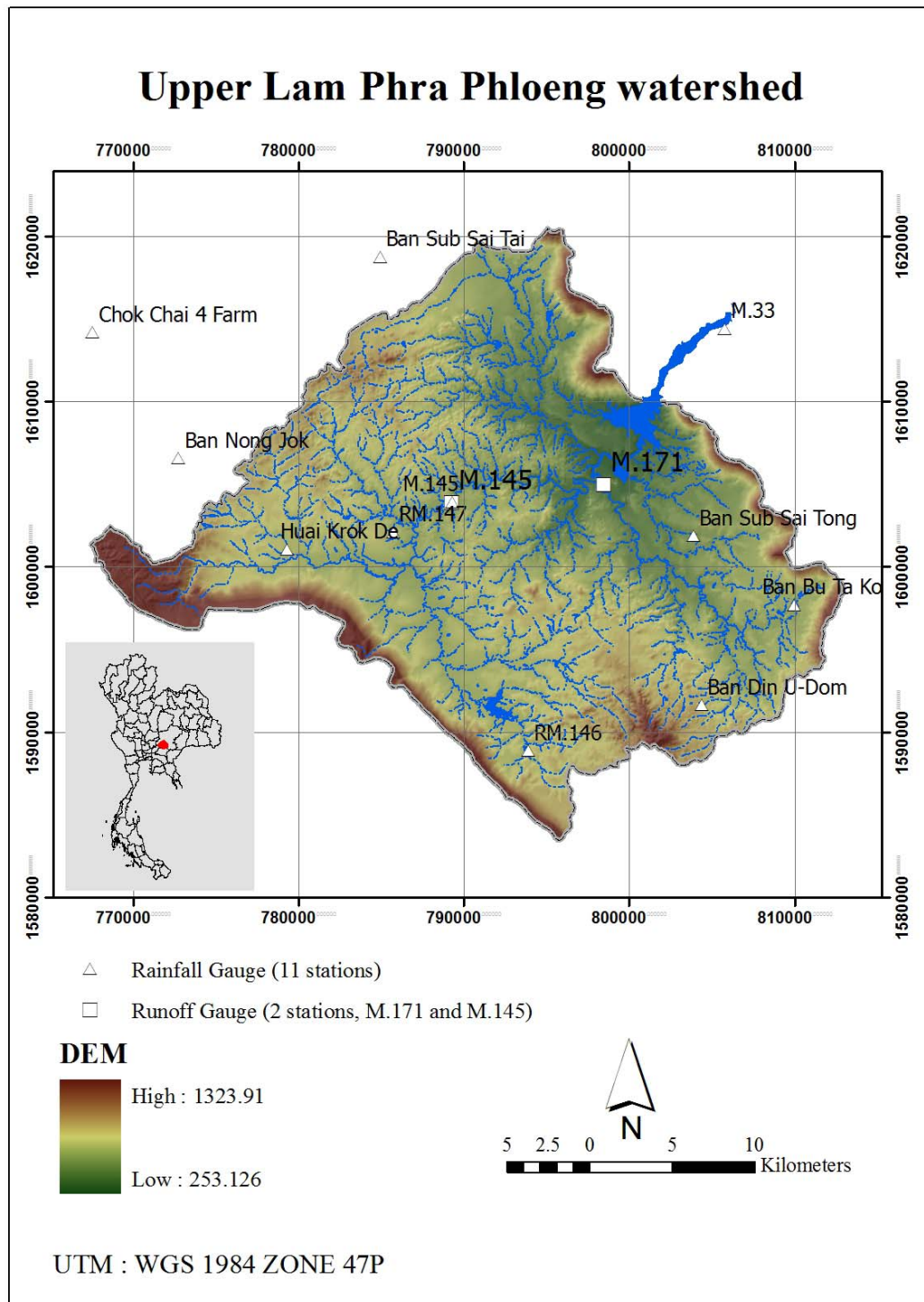


Figure 1.1 Study area.

1.5.2 Agricultural features

The area has a relatively short agricultural history. From the 1960 most of the land remains government property. People started to settle in the area and began to clear-cut the forest to grow subsistence crops, upland rice and castor beans. After a relatively short period of subsistence crops domination, the land use has been rapidly developed into maize-based cash-crop systems. Maize is still the main crop now. Due to the influx of more people, the agricultural land is expanded rapidly (Cho and Zoebisch, 2003).

Lately in 2003, limited land rights for the farmers are being issued. The land-use system of the area has been changed overtime from subsistence to more market-oriented farming. The application of inorganic fertilizers, herbicides, and pesticides became standard practice. The use of these inputs led to a significant increase in land productivity. However, most farmers do not have sufficient capital to purchase all required inputs for cultivation and they largely depend on private money lenders and middlemen for input supply at high interest rates (Cho and Zoebisch, 2004).

There is the general perception among farmers of a considerable soil-fertility decline. Therefore, more and more fertilizers are needed to be applied to maintain the current yield crop level. Usage of fertilizers has greatly increased agricultural production. However, there has also been an increase risk for surface water contamination.

1.6 Benefits of the study

Generally, the research provided useful means for examining and assessment the NPS pollution in watershed systems. The research outputs should be useful as basic information to support NPS pollution control and management. The benefits of research results are as follows:

1.6.1 Reliable geospatial model appropriate to simulation the runoff, sediment, and nutrient yields in the study area.

1.6.2 NPS index to prioritize areas in the study area for further land/water pollution reduction management at local level.

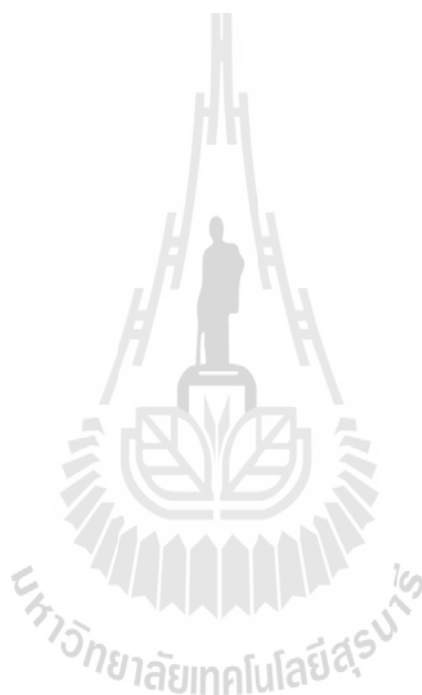
1.6.3 Well-organized geo-database of the area for future research and management.

1.6.4 Research methodology as a study prototype for other watersheds with the same geographic and practical conditions.

1.7 Structure of the thesis

The structure of this thesis is shown in Figure 1.2. The arrows indicate the relations among chapters. Chapter I introduces rational and background problem of the study, research objectives and its scope, limitations, and benefit, including characteristics of the study area. The remaining chapters of the thesis have the following structure. Chapter II provides a comprehensive literature review of the NPS characteristics, NPS model, and previous studies. The recent developed technologies in NPS modeling are discussion in this chapter. Chapter III emphasizes the development of grid-based curve number method for runoff simulation. Chapter IV explains the sediment yield simulation using modified universal soil loss equation and

sediment delivery distribute model. Chapter V deals with the nutrient yield simulation using grid-based AGNPS model. Chapter VI covers spatially NPS pollution indexing from the quantitative results of Chapter III, IV, and V using GIS multi-criteria decision analysis (MCDA). The NPS pollution index is proposed to prioritize parts of the study area for proper watershed management at local level. Finally, conclusion of this thesis and recommendation for future research are drawn towards the end in Chapter VII.



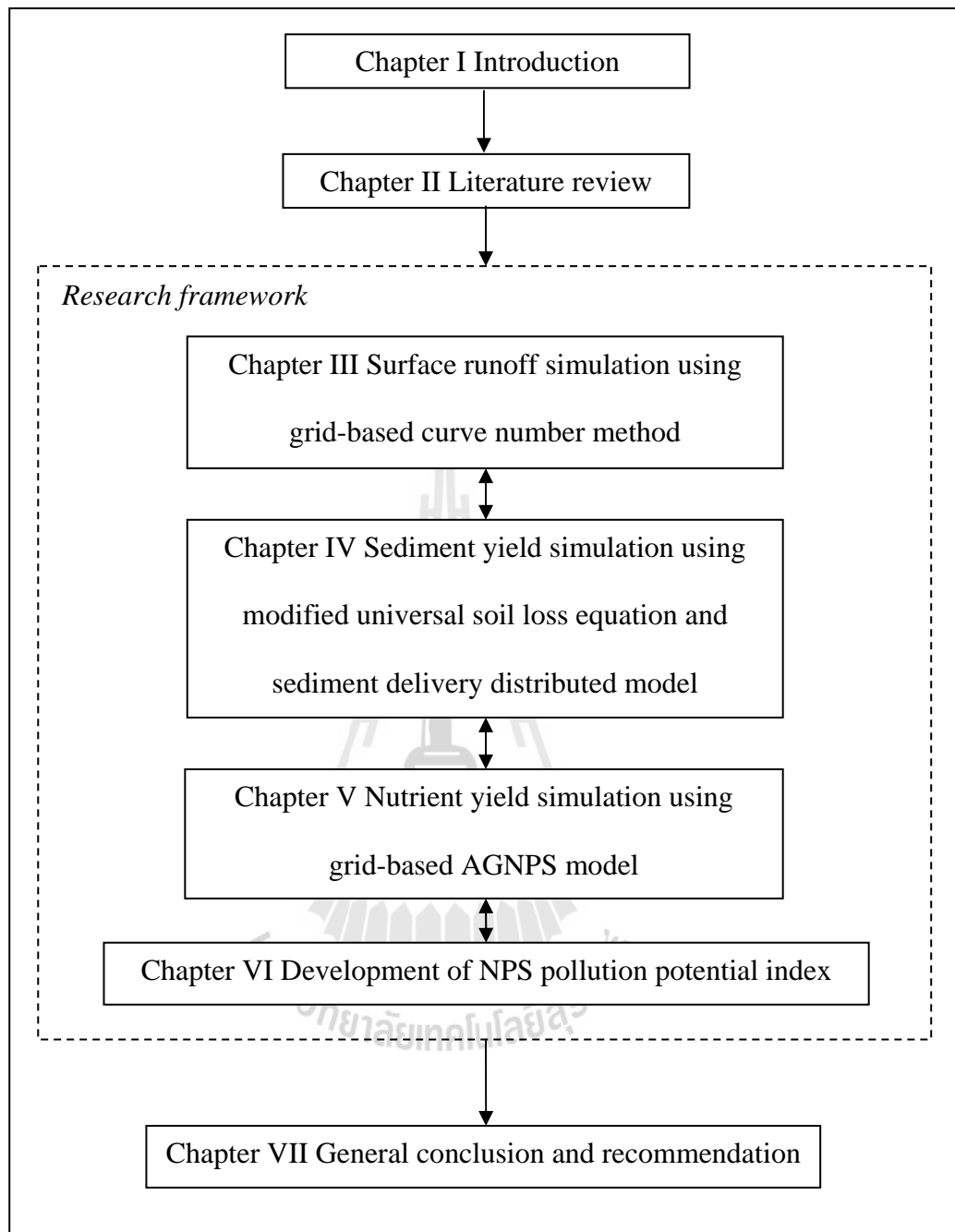


Figure 1.2 Structure of the thesis.

1.8 References

- กรมควบคุมมลพิษ. (2545). รายงานสถานการณ์และการจัดการปัญหามลพิษทางน้ำปี 2544-2545. กรุงเทพฯ: กรมควบคุมมลพิษ.
- American Public Health Association. (1998). **Standard Methods for the Examination of Water and Wastewater**. 18th American Public Health Association, Washington.
- Babel, M.S., Najim, M.M.M., and Loof, R. (2004). Assessment of agriculture nonpoint source model for a watershed in tropical environment. **Journal of Environmental Engineering**. 130(9): 1032-1041.
- Caruso, B.S., and Ward, R.C. (1998). Assessment of nonpoint source pollution from inactive mines using a watershed-based approach. **Environmental Management**. 22(2): 225-243.
- Chandler, J., Holland, M.M., Forster D.L., Southgate D.D., Thornton J.A., and Weinberg, A. (1998). Development and implementation of a nonpoint source pollution control programme. In Thornton, J.A., Rast W., Holland M.M., Jolankai G., and Ryding, S.O. (eds.). **Assessment and control of nonpoint source pollution of aquatic ecosystems a practical approach**. (pp 17-38). UK: The Parthenon publishing group.
- Charupatt, T. (2002). **Land use change detection, land evaluation and land use planning in Lam Phra Phloeng watershed**. Ph.D. Thesis, Khon Kaen University, Thailand.

- Cho, K.M., and Zebisch, M.A. (2003). Land-use change in the Upper Lam Phra Phloeng watershed, Northeastern Thailand characteristics and driving forces. **Journal of Agriculture and Rural Development in the Tropics and Subtropics**. 104 (1): 15-29.
- Cho, K.M., Zebisch, M.A., and Ranamukhaarachchi, S.L. (2004). Land-use dependent soil quality in the Lam Phra Phloeng watershed, Northeast Thailand. In **International Soil Conservation Organization Conference 2004**. (pp 1-6). Brisbane, Australia.
- Chowdary, V.M., Yatindranath, Kar, S., and Adiga, A. (2001). Assessment of non-point source pollution on watershed basis using remote sensing, GIS and AGNPS model. In **22th Asian Conference on Remote Sensing**. Singapore: National University of Singapore.
- Cooke, S.E., Ahmed, S.M., and MacAlpine, N.D. (2005). **Introduction guide to surface water quality monitoring in agricultural**. Conservation and Development Branch, Alberta Agricultural, Food and Rural Development. Edmonton, Alberta.
- Department of Environmental Quality Promotion [DEQP]. (2005). **Thailand environmental performance assessment** [On-line]. Available : <http://www.deqp.go.th/SepII/SepII.htm>.
- Endreny, T.A., and Wood, E.F. (1999). Distributed watershed modeling of design storm to identify nonpoint source loading areas. **Journal of Environmental Quality**. 28(2): 388-397.

- He, C. (2003). Integration of geographic information systems and simulation model for watershed management. **Environmental Modelling & Software**. 18(8-9): 809-813.
- Heijnis, H., Zawadzki, A., Srisukasawad, K., and Lorsirirat, K. (2003). Lam Phra Phloeng dam, Thailand - A high resolution record of human activity and climate variability. In **XVI INQUA Congress 2003**. (pp 109). Nevada, USA: Geological Society of America.
- Lorsirirat, K. (2007). Effect of forest cover change on sedimentation in Lam Phra Phloeng reservoir, Northeastern Thailand. In Sawada, H., Araki, M., Chappell, N. A., LaFrankie, J.V., and Shimizu, A. (eds.). **Forest Environments in the Mekong River Basin**. (pp 168-178). Springer Japan.
- León, L.F., Soulis, E.D., Kouwen, N., and Farquhar, G.J. (2001). Nonpoint source pollution: a distributed water quality modeling approach. **Water Research**. 35(4): 997-1007.
- Luzio, M.D., Srinivasan, R., and Arnold, J.G. (2004). A GIS-coupled hydrological model system for the watershed assessment of agricultural nonpoint source and point source of pollution. **Transactions in GIS**. 8(1): 113-136.
- Mamillapalli, S., Srinivasan, R., Arnold, J.G., and Engel, B.A. (n.d.) **Effect of spatial variability on basin scale modeling**. [On-line] Available: http://www.ncgia.ucsb.edu/conf/SANTA_FE_CD-ROM/sf_papers/mamillapalli_sudhakar/my_paper.html.
- Novotny, V. (1999). Diffuse pollution from agriculture - a worldwide outlook. **Water Science and Technology**. 39(3): 1-13.

- Ramaswami, A., Milford, J.B., and Small, M.J. (2005). **Integrated environmental modeling: pollutant transport, fate, and risk in the environment**. New Jersey: John Wiley & Sons.
- Srivastava, P., Day, R.L., Robillard, P.D., and Hamlett, J.M. (2001). AnnAGNPS: Integration of GIS and a continuous simulation model for non-point source pollution assessment. **Transactions in GIS**. 5(3): 221-234.
- Thapinta, A., Utarasakul, T., and Thapinta, S. (2009). **Current status on non-point source pollution from agricultural in Thailand**. Established of Knowledge and Network of Researchers on Environment and Climate Change in Thailand and Neighboring Countries (CLMV-T), The Thailand Research Fund, Bangkok.
- Ward, A.D., and Trimble, S.W. (2003). **Environmental hydrology**. 2nd. Boca Raton, FL: Lewis Publishers.
- Simachaya, W. (2002). Water quality monitoring and modeling application in Thailand. In **The Third World Water Forum Session “Water Quality Monitoring and Modeling-The Present Situation and Partnership in the Future”**. Japan: United Nation University Center in Tokyo.
- Simachaya, W. (2003). Lessons learned on integrated watershed and water quality management in the Thachin River basin, Thailand. In **Proceedings First Southeast Asia Water Forum 2003**. Chaing Mai, Thailand: Water Resources Association.
- Yagow, E.R. (1997). **Auxiliary procedures for the AGNPS model in urban fringe watersheds**. Ph.D. Thesis, Virginia Polytechnic Institute and State University.

CHAPTER II

LITERATURE REVIEWS

2.1 Nonpoint source pollution characteristics

Sources of pollution are broadly classified as either point or nonpoint sources. NPS pollution, unlike pollution from point sources such as industrial effluents, comes from many diffuse sources. Polluted runoff is caused by rainfall moving over and through the ground. As the runoff moves, it picks up and carries away natural and human-made pollutions, finally depositing them into watershed through lakes, rivers, wetlands, coastal waters, and groundwater (EPA, 2000). The NPS is intermittent release of pollutants over large areas and difficult to identify and measure directly.

The main characteristics of NPS are that they respond to hydrological condition, are not easily measured or controlled directly. There is correlation between the pollutant loading from a watershed and rainfall volume. NPS pollution is a function of climatic factors and site specific land characteristics such as soil type, land management, and topography (Beven, 2001; Wolfe, 2000; Ongley, 1996). It is possible that there is strong relationship between land use type and the quantity and quality of water (Liu et al., 2005). NPS pollution impacts are typically different in kind, often associated with nutrient enrichment, contamination of sediments (Campbell et al., 2004). Pollutants of primary interest include sediment, nutrients

(particularly nitrogen and phosphorus), pesticides, and pathogens (กรมควบคุมมลพิษ, 2545; Wolfe, 2000).

The most severe concentrations for point source pollutants carried in surface water are during low-flow conditions. In contrast, the highest pollutants loading, and in many cases the highest concentration from diffuse sources, occur during high-flow and flood conditions. Therefore, most of the models used for simulation NPS are linked to models of watershed hydrology. (Leon, 1999; Yagow, 1997).

Control of point sources in several countries having effective control program is carried out by effluent treatment according to regulations, usually under a system of discharge permits. In comparison, control of NPS pollution, especially in agriculture, has been carried out by education, promotion of appropriate management practices and modification of land use (Ongley, 1996).

From the NPS pollution reviews, the main processes of NPS pollution consists of three components 1) runoff processes 2) sediment processes and 3) nutrients processes. The processes of NPS pollution are described as follows.

2.1.1 Runoff processes

NPS pollutants such as sediment, nutrients, pesticides and pathogens are transported across the land surface by runoff and through the soil by percolating water. NPS pollution is intermittent, associated very closely with rainfall runoff. Hydrologic processes are strongly influence NPS pollution (Wolfe, 2000). Spatial representation of hydrological processes is important for watershed planning because restricting potentially pollution activities from runoff source areas is fundamental to controlling NPS pollution (Steenhuis et al., 2003; นิพนธ์ ตั้งจรัสธรรม, 2545).

The simple method most frequently used in the NPS pollution model is the Runoff Curve Number (CN) method of the Natural Resources Conservation Service (NRCS) such as AGNPS (Young et al., 1986), ARM (Donigian and Davis, 1985), CREAMS (Knisel, 1980), GAMES (Dickinson and Rudra, 1999), SWAT (Neitsch et al., 2005), and SWRBB (Williams et al., 1985). However, the models generally have limitations restricting their application. The major limitations are due to the high requirements for handling large amount of input data and analyzing model results. In these regards, GIS provides an effective tool to generate, manipulate and analyze the spatial data for modeling. Integrated GIS with hydrologic modeling has tremendous potential in achieving this goal. Advances in computational power and the growing availability of spatial data have made it possible to accurately describe watershed characteristics for modeling of runoff-NPS pollution.

2.1.2 Sedimentation processes

Sediment *per se* are considered a major pollutant in receiving waters. Although soil erosion is a natural process, it can be greatly accelerated by human activities such as farming. Major sources of sediment include agriculture (cropland), forestry and urban/suburban development. Soil erosion is the major cause of pollution and sediment is the most visible pollutants and also an important vehicle for the transport of soil-bound chemical contaminants from NPS areas to water (Leon, 1999; Nearing et al., 2000). The sediment has a tremendous societal cost associated with it in terms of stream degradation, disturbance to wildlife habitat, and direct costs for dredging and reservoir storage losses. Solutions to NPS pollution problems invariably must address the problem of erosion and sediment control.

Soil erosion depends on particle size, soil texture, and the presence or absence of protective surface cover such as vegetation. Vegetation cover is importance since it provides additional resistance to shear stresses caused by falling and running water. Hydrological erosion processes are classified as overland erosion and stream or channel erosion. Many factors such as distance from source to streams, vegetation covers, slope, and roughness characteristics of the land, depositional area during overland flow, affect the delivery of the sediment to the receiving water (นิพนธ์ ตั้งจรรยา, 2545).

As noted from the reviews, most of NPS models use the Universal Soil Loss Equation (USLE) or its modifications to estimate the soil loss caused by rainfall and runoff. It is still the most widely used. The sediment model used in this research is based on Modified USLE.

Sediment production by erosion, transportation and deposition is extremely variable in both time and space at the watershed scale, and in general only a small portion of the eroded soil from hillslopes leaves a watershed at an event or annual time step. For NPS model views, the studies should be linkages between watershed soil erosion and sediment delivered to the downstream point of interest. Spatial variation in sediment yields are very important since sediment delivery processes vary in space and time.

An approach that may be capable of providing accurate and reliable estimates of the sediment yield at the watershed scale with relative low data requirements is the Sediment Delivery Ratio (SDR) (Saavedra, 2005). In a watershed, part of the soil eroded in an overland region deposits within the watershed before reaching its outlet.

The fraction or portion of sediment that is available for delivery is referred to as the SDR. This ratio is then multiplied by the predicted erosion rate to estimate the percent of eroded material, sediment, pollutant to reach the watershed outlet (Fraser, 1999).

A SDR is not homogenous across a watershed; instead it varies with changes in watershed. Fraser (1999) estimated the SDR for each grid cell as a multiplier of six variable including flow-path slope gradient, flow-path slope shape, flow-path surface roughness, proximity to streams, soil texture, and overland flow index. Ferro and Porto (2000) estimated SDR for each grid cell as a exponent function of the inverse of travel time to streams.

In present study, SDR is calculation of this spatial variation utilizing a GIS. The SDR is multiplied by predicted amount of erosion soil calculated on cell by cell and then totaled for specific watershed. Grid-based soil erosion model and Grid-based sediment delivery model are developed to estimate sediment yield in the watershed. The total soil loss and sediment yield are calculated by summing up individual cells in the specific watershed. This tool would be greatly beneficial to sediment-NPS pollution management.

2.1.3 Nutrients processes

Nutrients provide better plant production rates. Fertilizers rich in nitrogen, phosphorus and potassium are applied on agricultural land. From the water quality point of view and as NPS pollutants, nutrients are transported from the watershed by runoff, erosion and leaching. Nitrogen and phosphorus are two major nutrients from agricultural land that degrade water quality. Soluble forms of nitrogen and phosphorus are transported in the runoff. Insoluble forms and forms adsorbed to the soil are moved by the sediments. Nitrate is the principle nutrient leached to groundwater by

percolation. The concentrations of nutrients and total loads depend on the amount of nutrients available for transport and on the conditions that affect the transport mechanisms (Leon, 1999).

Weather, soils, topography, and land uses all affect the transport capacity. Information about runoff, sediment, and availability of nutrients should be considered as input data for any nutrient model. The quantification results of runoff and sediment should be performed in the watershed in order to predict the nitrogen and phosphorus moving in runoff, with sediment, and by leaching.

In general, chemical exist in two phases: (1) dissolved (solution); and (2) attached (adsorbed) to clay-size particles. Nitrogen and phosphorus are recognized to be exists in both the dissolved and adsorbed state. In natural system, nutrients are commonly derived from the weathering and leaching of nutrients from rocks and soils. However, nutrients inputs to aquatic ecosystems can be greatly accelerated by human activities, resulting in nutrient enrichment and its accompanying interferences with many water uses (Ritter and Bergstrom, 2000).

As part of this research, simple relations to account for enrichment, solubility, adsorption and leaching (Frere et al., 1980) are used. Grid-based approach and nutrient yield algorithm were developed for more spatial variation of nutrient yield estimated. This tool would be greatly beneficial to nutrient-NPS pollution management.

2.2 Modeling environment of NPS

Approaches to model NPS pollution vary widely. The common elements among these models are the processes affecting the entrainment and transport of sediment

and pollutants in surface runoff. The dominant transport vector is runoff. As a result, the majority of NPS models are attached to the ability to model surface runoff (Leon et al., 2000).

The development of geospatial model for NPS pollution assessment should be consideration of the model. In terms of spatial, temporal, and processes consideration, NPS models are distinguished by: a) the precision of the spatial units used in analysis as being *lumped or distributed* b) the precision of the events modeled over time as being a *single event or continuous* time steps and c) the model algorithm describing the NPS processes included *empirical, conceptual, and physically based* models.

2.2.1 Spatial context

2.2.1.1 Lumped model

Lumping is often associated with averaging. The modeling of NPS using lumped approach represents a watershed as a single entity and simulate state variables and fluxes into and out of the watershed as a whole (Beven, 2001). Spatial variation of rainfall, topography, land use, soil types, is assumed to have no influence on the watershed response for a given rainfall event. The whole watershed is assumed to be homogeneous, and all the potential variations are lumped together. Lumped provide a unique output for the whole watershed. They do not provide any information regarding the spatial behavior of the outputs. Lumped models usually use empirical equations and may require historical data for calibration (Bouraoui, 1994).

2.2.1.2 Distributed model

Distributed models take into account the spatial variability of watershed characteristics. Distributed parameter models divide the watershed up into many entities, each representing small parts of the watershed, and the state variables and

fluxes between the entities are determined across the watershed (Beven, 2001). The dynamics of the simulated processes are then described at each cell within the watershed, and the outputs from each cell are routed to the watershed outlet.

A compromise between fully distributed model and lumped model are the semi-distributed models that break a watershed down into a group of sub-watershed or other regions over which the model is applied (Merritt et al., 2003).

Distributed model have several major advantages over lumped model for NPS pollution assessment. Their principal advantages are that they can more accurately represent the effects of spatial variability of watershed features, and that they can estimate pollutant losses at different locations within the watershed. The major disadvantages of distributed model is that their required considerable computer resource, and extensive data collection and preparation. However, with advances in computer technology distributed models are gaining popularity (Merritt et al., 2003; Pullar and Springer, 2000). Validation is desirable at both the watershed and cell level, but data to validation at the cell level is seldom available.

NPS model is concerned with the source and movement of runoff, sediment, and nutrient, as well as pesticide. Distributed models incorporate the variability in landscape features that control hydrologic flow, sediment transport processes, nutrient transport, and thus are potentially more realistic (Wu et al., 2005).

2.2.2 Temporal context

A key consideration in determining an appropriate model for application is the timing of the events or processes that the model user wants to predict. NPS models are further divided into events-based and continuous models (Pullar and Springer, 2000).

2.2.2.1 Event-based model

Event-based models calculate a single storm event and run over a short period that covers the rainfall duration and time for runoff to drain from watershed. Event-based models are used to assess the impact of management practices on water quality for specific storms.

2.2.2.2 Continuous model

Continuous models calculate for longer periods like a year or over the period of a seasonal crop rotation. Continuous models are used to determine the long-term impact of management scenario alternative on water quality.

Both model types are useful and give different types of information. Continuous models do not produce accurate estimates for single storms. Similarly, event-based models may not necessarily provide accurate long term predictions.

2.2.3 Processes context

NPS modeling is based on understanding of the physical laws and landscape processes such as runoff and sediment yield occurring in the natural system. Modeling translates these components into mathematical relationships, describing the fundamental runoff, sediment, and nutrient transport through the watershed.

In general, processes of models fall into three main categories, depending on the physical processes simulated, the model algorithm describing these processes, and the data dependency of the model. These three main categories are the empirical, conceptual and physically based models.

2.2.3.1 Empirical model

Empirical models are generally the simplest of the three model types. They are based on the analysis of field experiments and seek to characterize the

response from these NPS plots using statistical inference. The computational and data requirements for such models are usually less than for conceptual and physically based models (Li et al., 1996). They are particularly useful as a first step in identifying the NPS pollution.

However, empirical models are often criticized for employing unrealistic assumptions about the physicals of the watershed system, for ignoring the heterogeneity of watershed inputs and characteristics, such as rainfall and soil types, and for ignoring inherent nonlinearities in a watershed system (Foster, 1996)

This assumption limits the potential of empirical model for assessing the potential of NPS pollution. Furthermore, empirical models tend not to be event-responsive (Kandel et al., 2004). Nonetheless, empirical models are frequently used in preference to more complex models as they can be implemented in a situation with limited data inputs.

2.2.3.2 Conceptual model

Placed somewhere in between empirical and physically based models, conceptual model aims at reflecting the physical processes governing the system but describe them with empirical relationship (Sivapalan et al., 2002). Conceptual model tend to include a general description of watershed processes, without including the specific details occurring in the complex processes interactions (Arnold, 1996).

Recently developed conceptual models have provided outputs in a spatially distributed manner. Alternative, lumped conceptual model may be applied in the semi-distributed manner by disaggregation a watershed into linked sub-watersheds, to which the model is applied.

Parameter values for conceptual models are typically obtained through calibration against observed data, such runoff, sediment, and nutrient yield measurements. Because parameter values are determined through calibration against observed data, conceptual models tend to suffer from problems associated with identification of the parameter values; notwithstanding, conceptual models play an intermediate role between empirical and physically based models. Though they tend to be aggregated, they still reflect the hypothesis about the processes governing system behavior. This is the main feature that distinguishes conceptual models from empirical models. Empirical models make no inferences as to the processes at work; instead they rely on observed or statistical relationships between the causal variable and model output (Saavedra, 2005).

2.2.3.3 Physically based model

These models are based on an understanding of the physics of the runoff, sediment transport, and nutrient losses processes and describe the NPS system using equation governing the transfer of mass, momentum and energy (Kandel et al., 2004). In principle, they can be applied outside the range of conditions used for calibration and, as their parameters have a physical meaning, they can be evaluated from direct measurements and without need for long hydro-meteorological records (Smith et al., 1995). They are limited only by the relevance of the physical laws on which they are based. Physically based model computes NPS using a mathematical representation of fundamental hydrological, erosion and sediment transport processes, and nutrient losses processes. The physical model did not widely used until the mainframe computers became readily available. Example of the NPS physically based models are

ANSWER (Beasley et al., 1980), CREAMS (Knisel, 1980), and WEPP (Arnold and Fohrer, 2005).

2.3 Tools for NPS pollution model

2.3.1 Existing NPS pollution model

Since the early 1970, a large number of NPS models have been developed. Reviews of the available NPS pollution modeling of agricultural watershed have been prepared by Srivastava et al. (2007). NPS modeling approaches vary in term of simulated processes, spatial and temporal detail, and data requirements. Table 2.1 contains a summary of the features from some of the reviewed recent developed NPS models.

Table 2.1 Summary of the characteristics from some of the reviewed NPS models.

Model	Time context		Spatial context		Processes			
	Single event	Continuous	Lumped model	Distributed model	Surface runoff	Sediment	Nutrients	Pesticides
AGNPS	•	•		•	•	•	•	•
ANSWERS	•			•	•	•	•	
ARM		•	•		•	•	•	•
CREAMS	•	•	•		•	•	•	•
GAMES	•			•	•	•		
SWAT		•	•		•	•	•	
SWRRB		•	•		•	•	•	•

Following is a brief description of the reviewed models with the intention of determining what is already done, what could be improved, and what is still needed.

AGNPS - *Agricultural Nonpoint Source Pollution Model* was developed by the US Department of Agriculture (Young et al., 1986). It can simulate runoff, sediment, nutrient and pesticide loads from agricultural watersheds for a single storm event or for a continuous simulation. The watershed must be divided into uniform square cells where computations are done, and runoff, sediment, nutrients and chemicals are routed from cell to cell from the watershed to the outlet. The hydrology is calculated by runoff curve number approach. Soil erosion is based on the USLE. Simple correlation for extraction of nutrients and pesticides in runoff and sediment forms the water quality component of the model.

The model is useful for assessing large scale NPS pollution problem in agricultural areas. Due to spatial variability of the required data, the model can be linked to a GIS to perform several tasks (storing data, manipulate data, analysis, and displaying results as map).

ANSWERS - *Areal Nonpoint Source Watershed Environment Response Simulation* was developed by the Agricultural Engineering Department of Purdue University (Beasley et al., 1980). It is a distributed parameter and event oriented model. The watershed is divided into uniform square elements ranging from 1 to 4 hectares. Within each element the model simulates processes of interception, infiltration, surface storage, surface flow, sediment detachment and transport. Connectivity of cells and continuity equations are used to route sediment transport and flow. It is primarily a runoff and sediment model; the nutrient simulation is based on simple correlation between chemical concentration, sediment yield, and runoff volume. ANSWERS outputs an event hydrograph, and event sediment graph, and erosion and deposition rates for individual grid cell.

ARM - *Agricultural Runoff Model* is a version of the Hydrologic Simulation Program in Fortran (HSP-F) that was originally developed from the Stanford Watershed Model (Donigian and Davis, 1985). It is large, lumped model and required considerable effort when applied to a watershed. It is capable of simulating a hydrologic time series event, including hydrographs and pollutants. The model uses a basin scale analysis framework that includes fate and transport in one-dimensional stream channels. It integrates the simulation of land runoff processes (runoff curve number method) with in-stream hydraulics, sediment detachment, transport, and nutrients. Beside the complex and large amount of data needed, the model requires extensive calibration and application for large drainage systems is very limited.

CREAMS - *Chemical, Runoff, and Erosion from Agricultural Management Systems* was developed by the US Department of Agriculture (Knisel, 1980). It is a field scale lumped approach model that uses separate hydrology, erosion, and chemistry submodels, connected by shared files. It can simulate continuous series, using the runoff curve number, when daily rainfall data are available or single events with hourly rainfall data using the Green-Ampt equation. The erosion component of the model considers the basic processes of soil detachment, transport, and deposition. The basic concepts for nutrient modeling treat their transport as proceeding separately in adsorbed and dissolved phases where soil nitrogen is modified by nitrification-denitrification processes. The Groundwater Loading Effects of Agricultural Management Systems (GLEAM) module is essentially a vadose zone component for CREAMS.

GAMES - *Guelph model for evaluating effects of Agricultural Management Systems on Erosion and Sedimentation* (Dickinson and Rudra, 1990) was developed

to describe and predict soil loss by fluvial erosion and the delivery of suspended solids from agricultural fields. The analysis erosion is achieved through the use of the USLE with modifications to the rainfall erosion index and to the soil erodibility factor for local and seasonal conditions. The runoff curve number method drives the hydrology model. The discretization of a watershed into field sized elements is done based on homogeneity of land use, soil type and slope.

SWAT - *Soil Water Analysis Tool* developed by the USDA-ARS, to help water resource managers in assessing water supplies, soil erosion, and water and sediment transfers through watersheds (Neitsch et al., 2005). The SWAT model estimates surface runoff volume using the runoff curve number method. Overland sediment yield is computed using the MUSLE. Nutrient yield and nutrient cycling use the algorithms developed for the EPIC model. SWAT allows for simultaneous computations on each sub-basin and routes the water, sediment and nutrients from the sub-basin outlets to the basin outlet.

SWRRB - *Simulator for Water Resources in Rural Basins* was developed for evaluating basin scale quality in rural watersheds (Williams et al., 1985). It operates on a daily time step and simulates hydrology, crop growth, sedimentation, flood plain degradation, and nitrogen, phosphorus, and pesticide movement. The lumped approach model was developed by modifying the CREAMS model for applications to larger rural basins. Surface runoff is calculated using the runoff curve number method and sediment yield is computed using the modified USLE.

2.3.2 Tool selected for the study

As suggested by Bouraoui (1994), the primary goal involved with model selection is the definition of the problem to be addressed, and the determination of the

potential models that could be used to simulate the desired processes. Additional consideration included data availability, accuracy of the output required and the marginal cost of different models. Assumption and limitation should always be taken into consideration during model selection. Previous model validation and study results should play a key role in determining which model is used. Use the simplest model that will satisfy the project objective. Adding complexity means more time, money, and data.

The AGNPS model was chosen for this study due to its cell based capability and the ability to simulate water quantity and quality in different parts of the watershed. The AGNPS model is a well established and applicable for event simulation. Due to its distributed scheme, it is also a good choice for geospatial model integration.

2.4 GIS technology and NPS model

Modeling the NPS pollution in watershed is a complex problem, and one that has troubled natural resource managers for many years. The development of spatially distributed hydrologic models has led to improved model forecasting at the cost of requiring more detailed spatial information. Incorporation of watershed models into GIS has improved matters by streamline data input and providing better interpretation of model outputs (Pullar and Spring, 2000).

GIS is a computer system capable of storing, manipulation, and displaying geographically referenced information. The integration of GIS and NPS models are becoming more attractive due to the capability of GIS to store, retrieve, analysis and present geographically referenced spatial data. They are suited for studying the

processes and impacts of NPS pollution. These tools become interesting to users such as personal at local government officials, regional and national planning authorities and can be very useful for decision support in NPS pollution management.

In the context of NPS pollution modeling, a GIS is a tool used to characterize the information content of the spatially variable data required for NPS pollutants assessment. GIS is characterized by its capability to integrate layers of spatially oriented information.

For the present study we have chosen to use the grid-based GIS approach. The followings are the main advantages of a grid-based system (Burrough and McDonnell, 1998):

- (a) Simple data structures (each grid cell is represented by a single data values).
- (b) Location-specific manipulation of attribute data is easy (each grid cell has a X and Y coordinate that represents its geographical location).
- (c) Many kinds of spatial analysis and filtering may be used.
- (d) Mathematical modeling is easy because all spatial entities have a simple, regular square shape.
- (e) Many forms of data are available and commonly used.

Some of the disadvantages of the grid-based system have been overcome by advances in computing storage capabilities and data processing speeds of today's computers.

The integration of GIS and NPS models also enables users to identify critical areas and to perform various "what...if?" scenarios to better understand the effect of alternative management strategies on pollutant reduction (Srivastava et al., 2001).

However, the current generation of GIS is generally difficult task to use in NPS part because of the wide range and cumbersome nature of user interface. They are lack of sophisticate spatial analysis functions for NPS modeling such as dynamic analytical tools.

2.5 Previous NPS studies

The recent developed technology in NPS modeling has been reviewed, concluded, and discussed accordingly.

Najim et al. (2006) attempts to verify the suitability of the AGNPS model developed for an agricultural watershed, for a mixed forest watershed. The study watershed is Huai Nong Prong in Southern Thailand. The study revealed that the AGNPS model produces satisfactory results regarding runoff volume and soluble nitrogen yields for the watershed. The sediment yield prediction is marginal for selected watershed. The model, however, could not accurately simulate the peak flows, suggesting the peak flow simulating approach in AGNPS is not suitable predict peak flows from mixed forest watersheds.

Reungsang (2007) applied SWAT model, for the Chi River subbasin located in the Northeastern Thailand. Calibration and validation of the SWAT output were performed by comparing predicted runoff and nitrogen losses with corresponding instream measurements from four gauging station within the watershed for five years (2000-2003, 2005). Calibration results gave a reasonable agreement for both coefficient of determination (R^2) and coefficient of efficiency (E) within ranges of 0.77-0.88 and 0.55-0.79, respectively. The validation results was poor with R^2 and E values ranging from 0.23-0.77 and -0.78-0.66. Overall, the evaluation of the SWAT

model demonstrated that this model can be used as a decision support tool for making decisions on sustainable management of water resources.

Grunwald and Frede (1999) modified AGNPS model (AGNPSm) in three different watersheds in Germany. The modifications include the following: replacement of the CN method by the method of Lutz (1984) for calculating runoff volume; replacement of the USLE LS factor algorithm of Wischmeier and Smith (1978) by the algorithm of Moore and Burch (1986) based on stream power theory; linkage of channel erosion by individual categories of particle size to runoff velocity; replacement of uniform precipitation input. The performance of AGNPSm was much more satisfactory than AGNPS, thus demonstrating the value of the modifications to the AGNPS model made in AGNPSm. Further research is necessary to transfer data-grid to model-grid information considering the spatial variability of parameters and to improve algorithm used in simulation models.

Rode and Frede (1999) linked AGNPS model to a GIS and tested in two medium-sized agricultural watersheds in the Germany. Runoff volume for all observed and simulated showed high level of agreement in both watersheds. Only for one of the two watersheds sediment and total phosphorus yield were computed satisfactory. The modified AGNPS model can thus be employed by environmental agencies as a useful planning.

Baginska et al. (2003) applied Annualized AGNPS (AnnAGNPS) to prediction of export of nitrogen and phosphorus from Currency Creek, Australia. Event flows were simulated satisfactorily with AnnAGNPS but only moderate accuracy was achieved for prediction of event-based nitrogen and phosphorus exports. The biggest

deviations from the measured data were observed for daily simulations but trends in the generated nutrients matched observed data.

Yuan et al. (2008) identified critical areas where conservation practices could be implemented and to predict their impact on Beasley Lake water quality in the Mississippi Delta using AnnAGNPS. Model evaluation was performed by comparing the observed runoff and sediment from US Geological Survey gauging station draining 7 ha of Beasley Lake watershed with the simulated runoff and sediment. The model demonstrated satisfactory capability in simulating runoff and sediment at an event scale. Without calibration, the *E* was 0.81 for runoff and 0.54 for sediment. The approach taken in this study could be used elsewhere in applying AnnAGNPS to ungauged watershed.

He (2003) integrated GIS and AGNPS to analyze the effect of land use change on NPS pollution. ArcView GIS and AGNPS integration was developed to facilitate agricultural watershed modeling. It was applied to simulate the impact of land use change on runoff, sediment, and nutrient yield in a watershed. The simulation results showed that expansion of urban land is likely to lead to an increase in surface runoff, peak flow, and soil erosion.

Huang et al. (2008) carried out for control agricultural NPS pollution in a medium sized watershed covering $1.47 \times 10^4 \text{ km}^2$ in Southeast China using quantitative analysis coupled with GIS, USLE, CN method, nutrient loss equation, and AnnAGNPS. This study proved that integrating GIS with NPS model can be adopted to efficiently evaluate major sources and contributors of NPS, and identify the critical source areas of NPS.

Diebel et al. (2009) build a predictive model to estimate the sediment and phosphorus load reduction that should be achievable following the implementation of riparian buffers. The results indicated that these pollutants can be eliminated from streams with buffers. Cumulative frequency distribution of load reduction potential indicates that targeting pollution reduction in the highest 10% of Wisconsin watersheds would reduce total phosphorus and sediment loads in the entire state by approximately 20%.

Liu et al. (2009) studied the NPS pollution loads in the upper reach of Yangtze River Basin in the year 2000. They were estimated using export coefficient model and remote sensing technique. The spatial distributions of the NPS loads within the watershed were displayed using GIS. Important source areas for the nutrients were croplands.

Bhuyan et al. (2003) integrated AGNPS and GIS to estimate the nutrient loadings of different sub-watersheds of the Cheney Reservoir watershed, Kansas, USA. This process was validated by running the calibrated AGNPS model on each sub-watershed. This integrated modeling process was found to be effective for small watersheds that had adequate rainfall data.

Cho et al. (2008) used AGNPS model in two small agricultural watersheds in Korea. The model was calibrated for 412.5 ha located in the Balhan watershed. A validation was performed for 274.1 ha located in the Banwol watershed, with similar land use and soil characteristics as the 412.5 ha in the Balhan watershed. Simulated results from the irregular cell-based scheme (ICS) and the uniform grid scheme (USG) of AGNPS were compared with the observed data. The ICS increased runoff volume and decreased peak flow rate and sediment yields from the watershed

compared to the UGS. The ICS significantly reduced the number of cells in a watershed and provided better agreement for surface runoff and peak flow rate compared to the UGS.

It is evident that the use of models in NPS pollution assessment is increasingly being appreciated throughout the world. However, literatures reveal that for watersheds in Thailand, very few models have been applied for this purpose despite the region being highly prone to pollutants contamination from agricultural activities. This research is therefore necessary as it is likely to make valuable contributions to fulfill the literature gap existing on NPS study in Thailand.

2.6 References

- กรมควบคุมมลพิษ. (2545). รายงานสถานการณ์และการจัดการปัญหามลพิษทางน้ำปี 2544-2545. กรุงเทพฯ: กรมควบคุมมลพิษ.
- นิพนธ์ ตั้งธรรม. (2545). แบบจำลองคณิตศาสตร์การชะล้างพังทลายของดิน และมลพิษตะกอนในพื้นที่ลุ่มน้ำ. กรุงเทพฯ: ภาควิชาอนุรักษ์วิทยา คณะวนศาสตร์ มหาวิทยาลัยเกษตรศาสตร์.
- Arnold, J.G. (1996). **SWAT: Soil and Water Assessment Tool User's Manual**. USDA-ARS.
- Arnold, J.G., and Fohrer, N. (2005). SWAT2000: current capabilities and research opportunities in applied watershed modeling. **Hydrological Processes**. 19(3): 563-572.
- Baginska, B., Milne-Home, W., and Cornish, P.S. (2003). Modelling nutrient transport in Currency Creek, NSW with AnnAGNPS and PEST. **Environmental Modelling & Software**. 18: 801-808.

- Beasley, D.B., Huggins, L.F., and Monke, E.J. (1980). ANSWER: A model for watershed planning. **Transactions of the American Society of Agricultural Engineers**. 23(4): 938-944.
- Beven, K.J. (2001). **Rainfall-Runoff Modelling: the Primer**. Chichester, UK: John Wiley and Sons.
- Bhuyan, S.J., Koelliker, J.K., Marzen, L.J., and Harrington, J.A. (2003). An integrated approach for water quality assessment of a Kansas watershed. **Environmental Modelling & Software**. 18: 473-484.
- Bouraoui, F. (1994). **Development of a continuous, Physically-Based, Distributed parameter, Nonpoint source model**. Ph.D. Dissertation, Virginia Polytechnic Institute and State University.
- Burrough, P.A., and McDonnell, R.A. (1998). **Principles of geographic information systems**. Oxford University Press.
- Campbell, N., D'Arcy, B., Frost, A., Novotny, V., and Sansom, A. (2004). **Diffuse pollution an introduction to thr problems and solutions**. UK: IWA publishing.
- Cho, J., Park, S., and Im, S. (2008). Evaluation of agricultural nonpoint source (AGNPS) model for small watersheds in Korea applying irregular cell delineation. **Agricultural Water Management**. 95: 400-408.
- Dickinson, W.T., and Rudra, R.P. (1990). **GAMES – The Guelph model for evaluating effects of Agricultural Management Systems on Erosion and Sedimentation**. User's Manual, V3.01, Tech. Rep. 126-86, School of Engineering, University of Guelph, Canada.

- Diebel, M.W., Maxted, J.T., Robertson, D.M., Han, S., and Zanden, M.J.V. (2009). Landscape planning for agricultural nonpoint source pollution reduction III: Assessing phosphorus and sediment reduction potential. **Environmental Management**. 43: 69-83.
- Donigian, A.S., and Davis, H.H. (1985). **User Manual for Agricultural Runoff Management (ARM) Model**. EPA 600/3-78-080, U.S. Environmental Protection Agency, Athens, GA.
- Environmental Protection Agency [EPA] (2000). **National management measures for the control of nonpoint pollution from agriculture**. U.S. Environmental Protection Agency, Washington, D.C.
- Ferro, V., and Porto, P. (2000). Sediment delivery distributed (SEDD) model. **Journal of Hydrologic Engineering**. 5(4): 411-422.
- Foster, G.R. (1996). Process-based modelling of soil erosion by water on agricultural land. In Boardman, J., Foster, I.D.L., and Dearing, H.D. (eds.). **Soil erosion on agricultural land**. (pp 429-445). Wiley: Chichester.
- Fraser, R.H. (1999). **A GIS-based delivery model for diffuse source pollutants**. Ph.D. Dissertation, Yale University, USA.
- Frere, M.H., Rose, J.D., and Lane, L.J. (1980). The nutrient submodel. In Knisel, W.G. (ed.). **CREAMS: A field scale model for Chemicals, Runoff, and Erosion from Agricultural Management Systems**. (pp 65-86). USDA, Cons. Research Report No. 26.
- Grunwald, S., and Frede, H.-G. (1999). Using the modified agricultural non-point source pollution model in German watershed. **CATANA**. 37: 319-328.

- He, C. (2003). Integration of geographic information systems and simulation model for watershed management. **Environmental Modelling & Software**. 18: 809-813.
- Huang, J., Hong, H., and Zhang, L. (2008). Control division of agricultural non-point source pollution at medium-sized watershed scale in Southeast China. **Frontiers of Environmental Science & Engineering in China**. 2(3): 333-339.
- Kandel, D.D., Western, A.W., Grayson, R.B., and Turrall, H.N. (2004). Process parameterization and temporal scaling in surface runoff and erosion modeling. **Hydrological Processes**. 18: 1423-1446.
- Kinsel, W.G. (1980). **CREAMS: A Field Scale Model for Chemicals, Runoff, and Erosion from Agricultural Management Systems**. Conservation Research Report No. 26, U.S. Department of Agriculture, Washington, D.C.
- Leon, L.F. (1999). **Integral system for nonpoint source pollution modeling in surface waters**. Ph.D. thesis. University of Waterloo.
- Leon, L.F., Lam, D.C., Swayne, D.A., Farquhar, G.J., and Soulis, E.D. (2000). Integration of a nonpoint source pollution model with a decision support system. **Journal of Environmental Modeling and Software**. 15: 249-255.
- Li, Z., O'Neill, A.L., and Lacey, S. (1996). Modelling approaches to the prediction of soil erosion in catchments. **Environmental Software**. 11(1-3): 123-133.
- Liu, J., Zhang, L., and Hong, H. (2005). An inexact system programming for agricultural land utilization based on nonpoint source pollution control in Wuchuang watershed. **Environmental Informatics Archives**. 3: 391-397.

- Liu, R., Yang, Z., Shen, Z., Yu, S.L., Ding, X., Wu, X., and Liu, F. (2009). Estimating nonpoint source pollution in the upper Yangtze river using the export coefficient model, remote sensing, and geographical information system. **Journal of Hydraulic Engineering**. 135(9): 698-704.
- Merritt, W.S., Letcher, R.A., and Jakeman, A.J. (2003). A review of erosion and sediment transport models. **Environmental Modelling & Software**. 18(2003): 761-799.
- Najim, M.M.M., Bable, M.S., and Loof, R. (2006). AGNPS model assessment for a mixed forest watershed in Thailand. **Science Asia**. 32: 53-61.
- Nearing, M.A., Norton, L.D., and Zhang, X. (2000). Soil erosion and sedimentation. In Ritter, W.E. and Shirmohammadi, A. (eds). **Agricultural nonpoint source pollution: Watershed management and hydrology**. (pp 29-58). United States: Lewis Publishers.
- Neithsch, S.L., Arnold, J.G., Kiniry, J.R., and Williams, J.R. (2005). **Soil and Water Assessment Tools Theoretical Documentation version 2005**. Agricultural Research Service, Temple, Texas, USA.
- Ongley, E.D. (1996). **Control of water pollution from agriculture**. Rome: Food and Agriculture Organization of the United Nations.
- Pullar, D., and Springer, D. (2000). Towards integrating GIS and catchment models. **Environmental modelling and software**. 15(5): 451-495.
- Reungsang, P. (2007). **Application of SWAT model in predicting water quantity and quality for U.S. and Thailand watersheds**. Ph.D. Dissertation. Iowa State University.

- Ritter, W.F., and Bergstorm, L. (2000). Nitrogen and water quality. In Ritter, W.E. and Shirmohammadi, A. (eds). **Agricultural nonpoint source pollution: Watershed management and hydrology**. (pp 59-90). United States: Lewis Publishers.
- Rode, M., and Frede, H.-G. (1999). Testing AGNPS for soil erosion and water quality modeling in agricultural catchments in Hesse (Germany). **Physics and Chemistry of the Earth, Part B : Hydrology, Oceans and Atmosphere**. 24(4): 297-301.
- Saavedra, C. (2005). **Estimating spatial patterns of soil erosion and deposition in the Andean region using geo-information techniques**. Ph.D. Dissertation, Wageningen University, Netherlands.
- Sivapalan, M., Jothiyangkoon, C., and Menabde, M. (2002). Linearity and non linearity of basin response as a function of scale: discussion of alternative definitions. **Water Resources Research**. 38(2): 4.1-4.5.
- Smith, R.E., Goodrich, D.C., Woolhiser, D.A., and Unkrich, C.L. (1995). KINEROS: a kinematic runoff and erosion model. In Singh, V.P. (ed.) **Computer models of watershed hydrology**. (pp 697-732). Water Resources Publications: Colorado.
- Srivastava, P., Day, R.L., Robillard, P.D., and Hamlett, J.M. (2001). AnnGIS: Integration of GIS and a continuous simulation model for non-point source pollution assessment. **Transactions in GIS**. 5(3): 221-234.

- Srivastava, P., Migliaccio, K.W., and Simunek, J. (2007). Landscape models for simulating water quality at point, field, and watershed scales. **Transaction of the American Society of Agricultural and Biological Engineers**. 50(5): 1683-1693.
- Steenhuis, T.M., Mendoza, G., Lyon, S.W., Gerard-Marchant, P., Walter, M.T., and Scheiderman, E. (2003). Distributed GIS based runoff predictions for variable source watersheds using the SCS-Curve Number. **Geophysical Research Abstract**. 5(01628).
- Wolfe, M.L. (2000). Hydrology. In Ritter, W.E. and Shirmohammadi, A. (eds). **Agricultural nonpoint source pollution: Watershed management and hydrology**. (pp 1-28). United States: Lewis Publishers.
- Wu, S., Li, J., and Huang, G. (2005). GIS application to agricultural non-point source pollution modeling: A status review. **Environmental Informatics Archives**. 3: 202-206.
- Yagow, E.R. (1997). **Auxiliary procedures for the AGNPS model in urban fringe watersheds**. Ph.D. Thesis, Virginia Polytechnic Institute and State University.
- Young, R., Onstad, C., Bosch, D., and Anderson, W. (1986). **Agricultural Nonpoint Source Pollution Model: A Watershed Analysis Tool, Model document**. Agricultural Research Service, U.S. Department of Agricultural, Morris. MN.
- Yuan, Y., Locke, M.A., and Bingner, R.L. (2008). Annualized agricultural non-point source model application for Mississippi Delta Beasley Lake watershed conservation practices assessment. **Journal of Soil and Water Conservation**. 63(6): 542-551.

CHAPTER III

SURFACE RUNOFF SIMULATION USING GRID-BASED CURVE NUMBER METHOD

3.1 Abstract

This chapter employed grid-based Curve Number (CN) method through the GIS drainage analysis operating on DEM to estimate surface runoff depth for each grid cell in the watershed. The total depths of runoff in grid cells were accumulated from upstream to downstream along the flow path. Eighteen storm events in rainy season of the year 2008 were observed. Surface runoff data measured at two observation stations (M.171 and M.145) of ten events were used for the model calibration. Data of other eight events were for model validation. The calibration results show that the coefficient of efficiency (E) is 0.94 and the coefficient of determination (R^2) is 0.95 at the M.171 station. While E is 0.87 and R^2 is 0.91 at the M.145 station. The validation results show that E is 0.87 and 0.68 and R^2 is 0.89 and 0.75 at the M.171 and M.145 stations, respectively. This indicates that the calibrated grid-based CN method working under GIS can be applied with satisfactory accuracy to the surface runoff estimation.

3.2 Introduction

NPS pollution is an important environmental and water quality management problem. It is intermittent, associated very closely with hydrological phenomenon. Surface runoff estimation is essential for assessment of water yield potential of a watershed, because restricting potential pollution activities from runoff source areas is fundamental to controlling NPS pollution (Steenhuis et al., 2003). The in situ measurement of runoff is considered more accurate but cannot be operated anytime and anywhere as required. This conventional measurement is also expensive, time-consuming and difficult. Therefore, the accurate surface runoff modeling developed can serve this purpose with more convenient and less time consuming.

In terms of spatial domain, the model can be classified as lumped or distributed model. Lumped model is typically assumed that rainfall and hydrologic factors are uniform over the watershed. It might miss some local process that affects the overall response of the system. To overcome this deficiency, spatial distributed model, in which the watershed is divided into grid cells with spatially specific hydrologic parameters, has been developed (Olivera and Maidment, 1999).

GIS is a useful tool to assist with this task. It provides a generic tool to derive the result from primary data collected over watershed. The use of this advanced tool, along with process-based hydrological models and empirical model, results in more accurate surface runoff simulation and more leading to spatial variability for watershed management purpose.

The objective of this chapter is to simulate the surface runoff volume of the Upper Lam Phra Phloeng watershed using grid-based Curve Number (CN) method. In this method, watershed characteristics are considered to be spatial heterogeneity. The

model outputs from selected storm events in rainy season of the year 2008 were calibrated and validated with results measured from the field.

3.3 Materials and methods

3.3.1 Curve Number (CN) method

The CN method was developed to estimate total storm runoff from total storm rainfall. This method estimates direct runoff, which consists of channel runoff, surface runoff, and unknown proportion subsurface runoff. The CN method is based on the water balance equation and two fundamental hypotheses (NRCS, 2004). The first hypothesis equates the total rainfall (P ; or maximum potential surface runoff) to the actual amount of direct surface runoff (Q), the amount of actual infiltration (F), and the initial abstraction (I_a). The second hypothesis shows relationships among I_a , the amount of the potential maximum retention (S). Thus, the CN method consists of the following equations (Mishra and Singh, 2003):

(a) Water balance equation

$$P = I_a + F + Q \quad (3.1)$$

(b) Proportional equality hypothesis

$$\frac{Q}{P - I_a} = \frac{F}{S} \quad (3.2)$$

(c) I_a - S hypothesis

$$I_a = \lambda S \quad (3.3)$$

where, P is total rainfall; I_a is initial abstraction; F is cumulative infiltration excluding I_a ; Q is direct surface runoff; S is potential maximum retention; λ is regional parameter dependent on geologic and climate factors ($0.1 \leq \lambda \leq 0.3$). The I_a consists mainly of interception, infiltration, antecedent soil moisture and depression storage, all of which occur before surface runoff begins (Grunwald and Norton, 2000). The relation between I_a and S was developed by analyzing the rainfall runoff data from experiments in small watersheds and expressed as, $I_a = 0.2S$. Combining the water balance equation and proportional equality hypothesis, the CN equation is presented as:

$$Q = \frac{(P - I_a)^2}{P + S - I_a} \quad (3.4)$$

Eq. (3.4) is valid for $P > I_a$, otherwise, $Q = 0$. The parameter S in Eq. (3.4) is defined as:

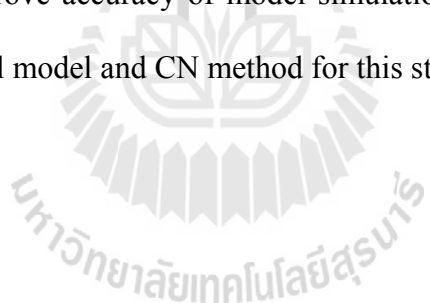
$$S = \frac{25400}{CN} - 254 \quad (3.5)$$

where S is in mm and CN is curve number values, which varies based on a function of land use, land treatment, hydrologic soil group, and antecedent moisture condition of watershed. Mohammed et al. (2004) suggested that the CN values is the most

sensitive parameter, should be carefully determined through field assessment based on local conditions such as cultural practices, land use, and topography.

Generally, the CN method is well suited for small watershed (Tekeli et al., 2007). In contrast, it is not restricted to use for only small watersheds. It can be applied equally well to other large areas if the geographic variations of storm rainfall, soil, and land use are taken into account. So that with increasing availability of finer spatial resolution information from remote sensing data on land use, it is possible to use CN method for large areas with better accuracy (Chatterjee et al., 2001).

Many hydrological models were developed based on the CN method, because of its simplicity, relative ease of use, and availability of information for the estimation of the *CN* values (Garen et al., 1999). The challenge of spatial model integrated with CN method is to improve accuracy of model simulation. The schematic diagram of processes in the spatial model and CN method for this study are shown in Figure 3.1.



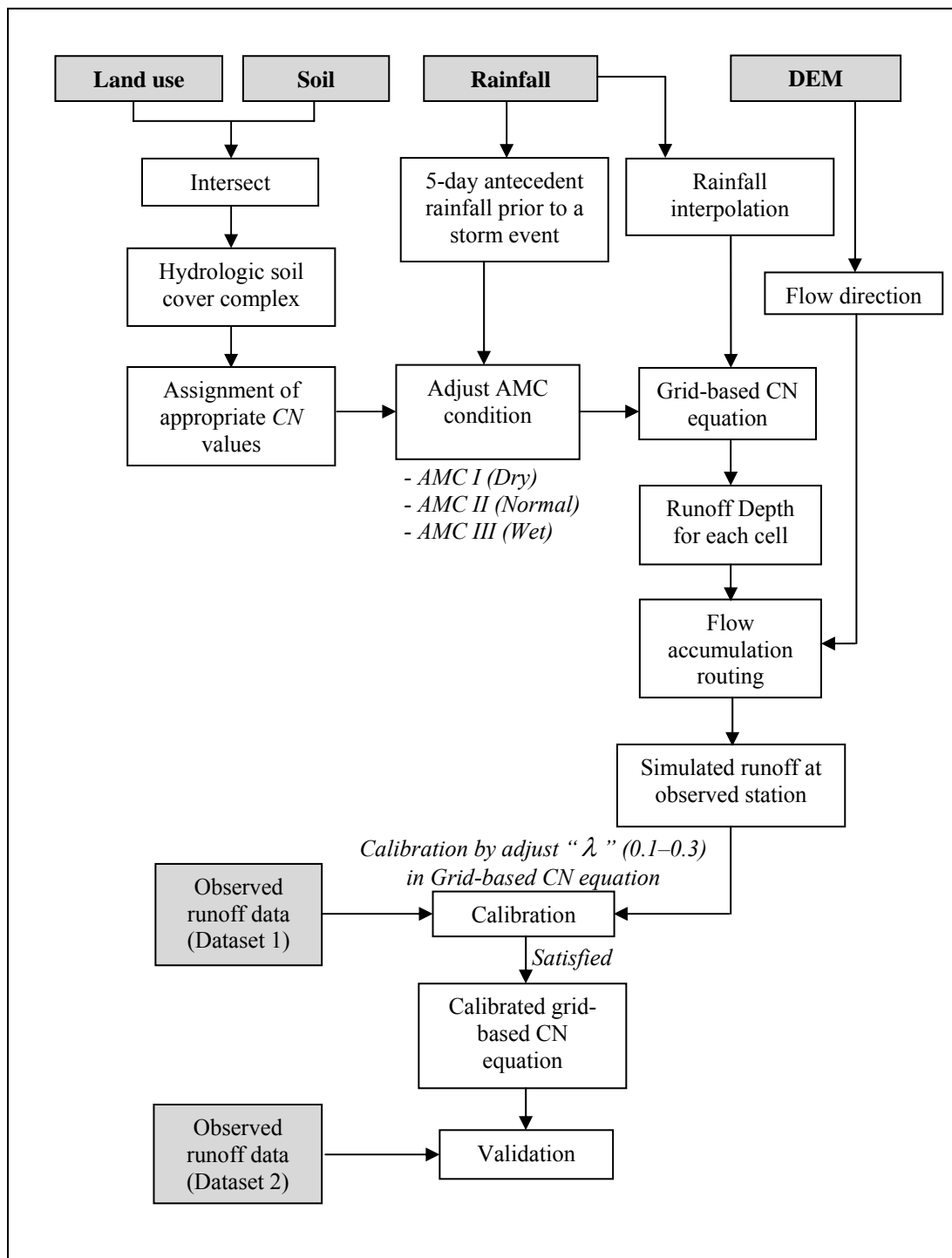


Figure 3.1 Flow diagrams of the grid-based curve number method.

3.3.2 Data Collection

The present study aims at developing a grid-based GIS processes. To prepare spatial as input of the model, the watershed is discretized into cell or grid areas. Spatially distributed information of each cell in the watershed includes rainfall data, soil, land use, etc. and is prepared through a GIS.

3.3.2.1 Rainfall data

The Hydrology and Water Center Management for Lower Northeastern Region, RID provided rainfall data with 11 manual rain gauges, located within and near the watershed (Table 3.1). Spatial variation of rainfall event was computed using the IDW interpolation method, instead of assuming a uniform rainfall event over the entire watershed. It creates a grid of spatially distributed values extracted from attribute table of rain gauge points.

Table 3.1 Rainfall station (The rainfall station map is shown in Figure 1.1).

Station name	Station Code	UTM WGS 1984 Zone 47 Coordinate	
		Easting	Northing
M.145	25751	789281	1603890
RM.146	25771	793890	1588840
RM.147	25781	785739	1602060
Huai Krok De	25930	779296	1601040
Ban Bu Ta Ko	25960	809958	1597670
Ban Sub Sai Tong	25950	803890	1601850
Ban Din U-Dom	25970	804375	1591620
M.33	25511	805775	1614360
Chok Chai 4 Farm	25651	767536	1614160
Ban Nong Jok	25981	772766	1606540
Ban Sub Sai Tai	251A1	784935	1618720

Eighteen storm events in rainy season of the year 2008 were observed. Ten events were used for the model calibration events (Figure 3.2). Other eight events were for model validation (Figure 3.3).

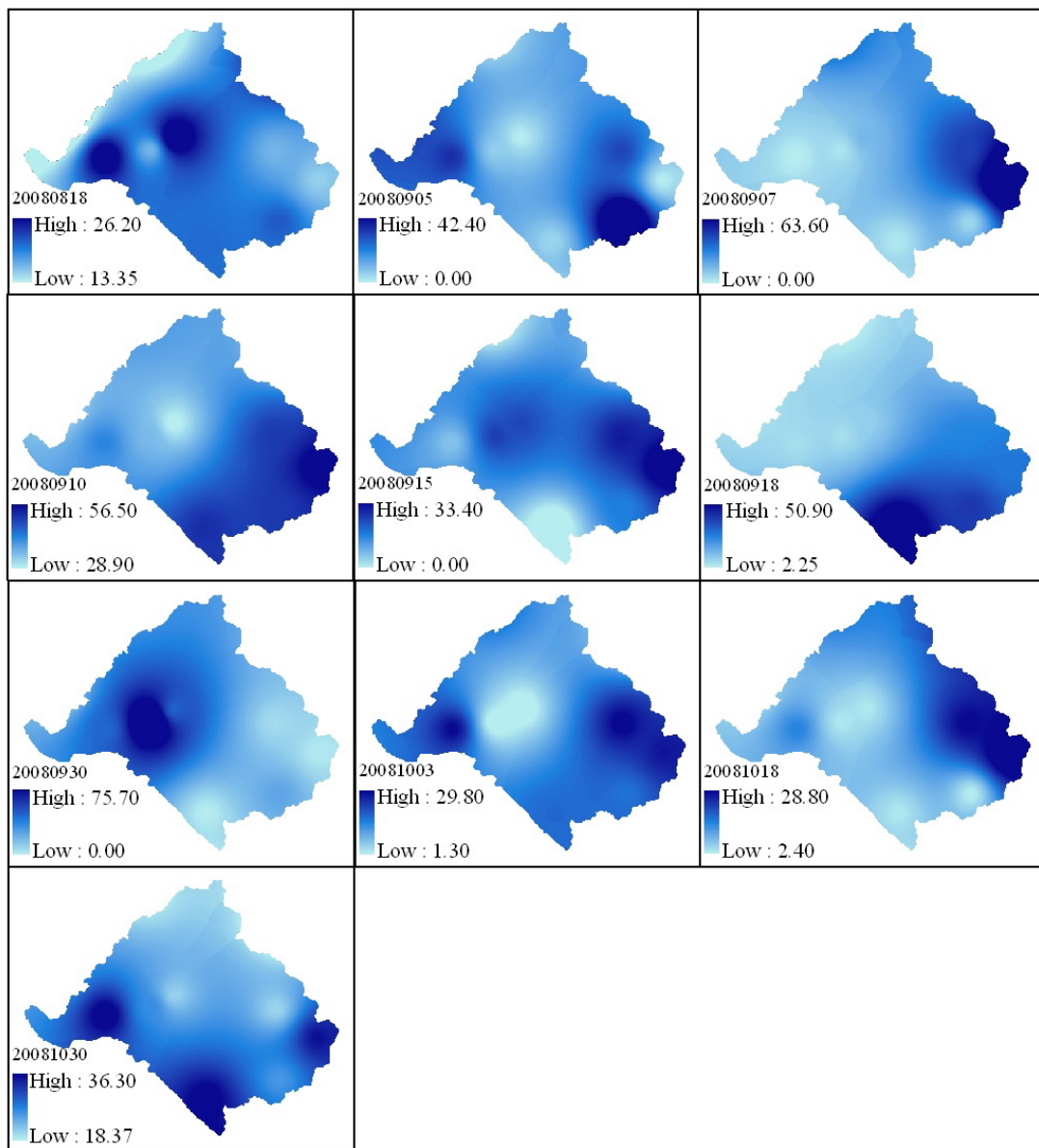


Figure 3.2 Rainfall data (mm) for calibration events.

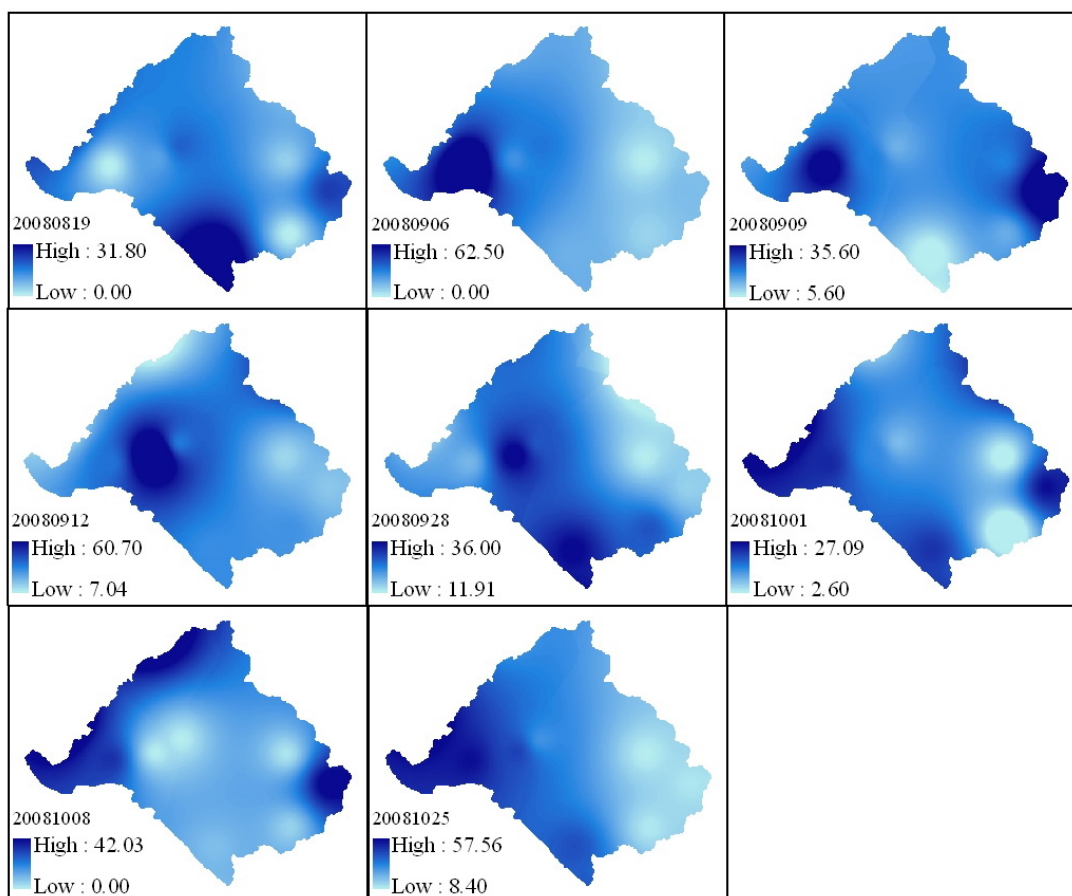


Figure 3.3 Rainfall data (mm) for validation events.

3.3.2.2 Hydrologic soil group (HSG) data

Hydrologic soil groups (Figure 3.4) are assigned to soil series using the criteria found in the (NRCS, 2007) (Appendix A). To account for the infiltration characteristics of soils, the CN method has divided soils into four hydrologic soil group including A - Low runoff potential, B - Moderately low runoff potential, C - Moderately high runoff potential, D - High runoff potential.

The soil properties and soil map at scale 1:25,000 were obtained from LDD (2004). Fifteen soil series with soil texture class and quantitative particle size distribution analysis by LDD were transformed to hydrologic soil group. The soil series is related to hydrologic soil group as shown in Table 3.2.

Table 3.2 Soil series properties for hydrologic soil group determination.

Soil series	Particle size analysis (LDD, 2004)			Texture	HSG
	%clay	%silt	%sand		
Ban Chong series (Bg)	47.7	20.2	32.1	clay	D
Bo Thai series (Bo)	7.9	17.2	74.9	sandy loam	B
Chiang Khong series (Cg)	59.2	31.7	9.1	clay	D
Chan Thuek series (Cu)	6.2	7.8	86	loamy sand	B
Dan Sai series (Ds)	23.1	20.5	56.4	sandy clay loam	C
Li series (Li)	43.5	46.4	10.1	silty clay	C
Muak Lek series (Ml)	58.3	26	15.7	clay	D
Pak Chong series (Pc)	74.5	21.5	4	clay	D
Phon Ngam series (Png)	11.9	16.1	72	sandy loam	B
Pak Thong Chai series (Ptc)	-	-	-	loamy sand	B
Si Thon series (St)	15.3	33.7	51	loam	C
Takhli series (Tk)	25.5	44.8	29.7	loam	C
Wang Hai series (Wi)	34.4	43	22.6	clay loam	C
Wang Nam Khieo series (Wk)	-	-	-	loamy sand	B
Wang Saphung seires (Ws)	40.4	27.3	32.3	clay	D
ES, RL, SC*					D

* There as soil information in areas of slope complex (SC), escarpment (ES), and rocky land (RL) considered with geological data also.

* For this study, the ES, RL, and SC area were not considered for nonpoint source pollution management purpose

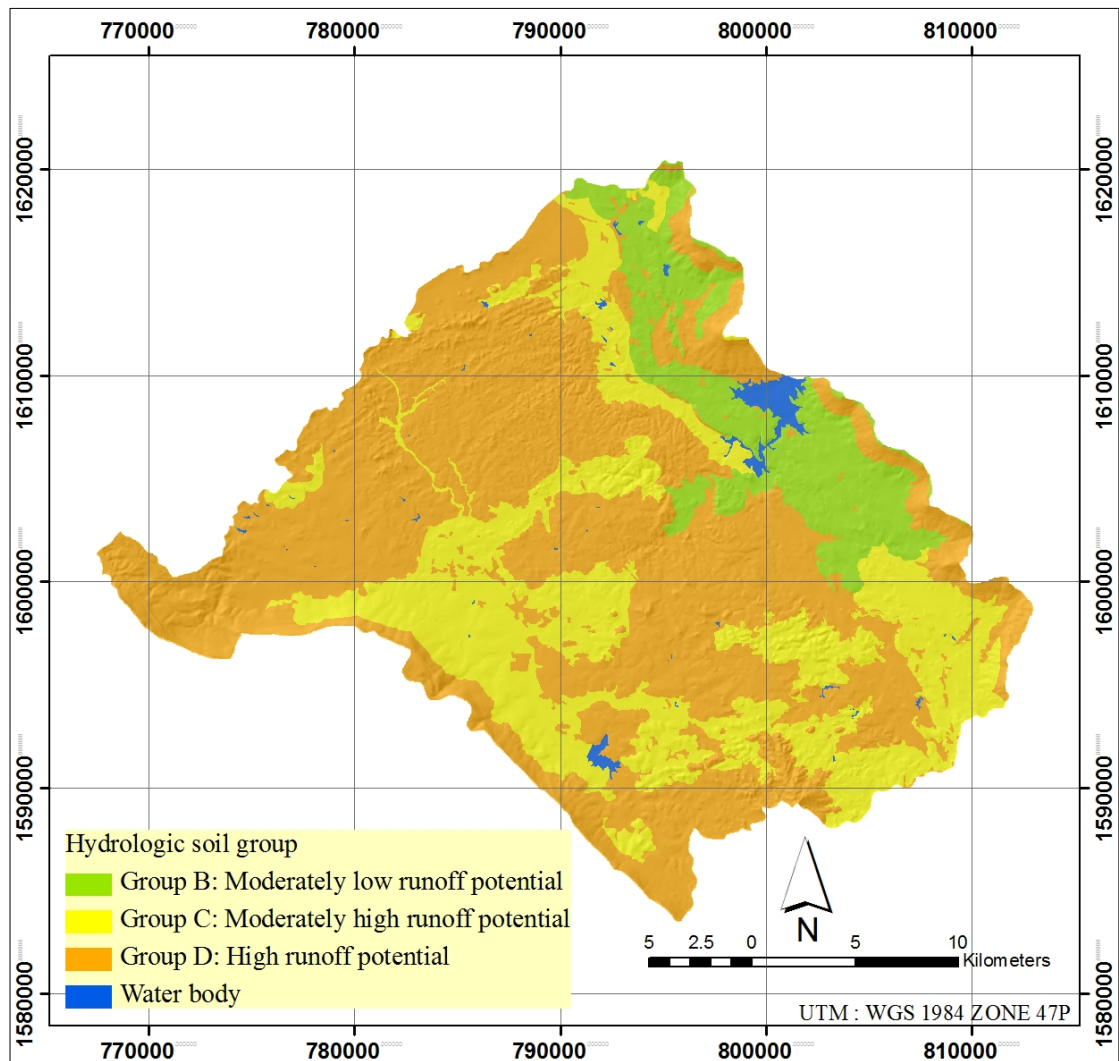


Figure 3.4 Hydrologic soil group data.

3.3.2.3 Land use data

The digital land use data (Figure 3.5) at scale 1:25,000 were obtained from LDD, which were updated to the year 2007. The land treatment obtained from field observation during June - October 2008 and previous study by Cho and Zoebisch (2003) showed mostly poor treatment especially on field crops. In this study, the treatment of all agricultural areas was assumed to be poor.

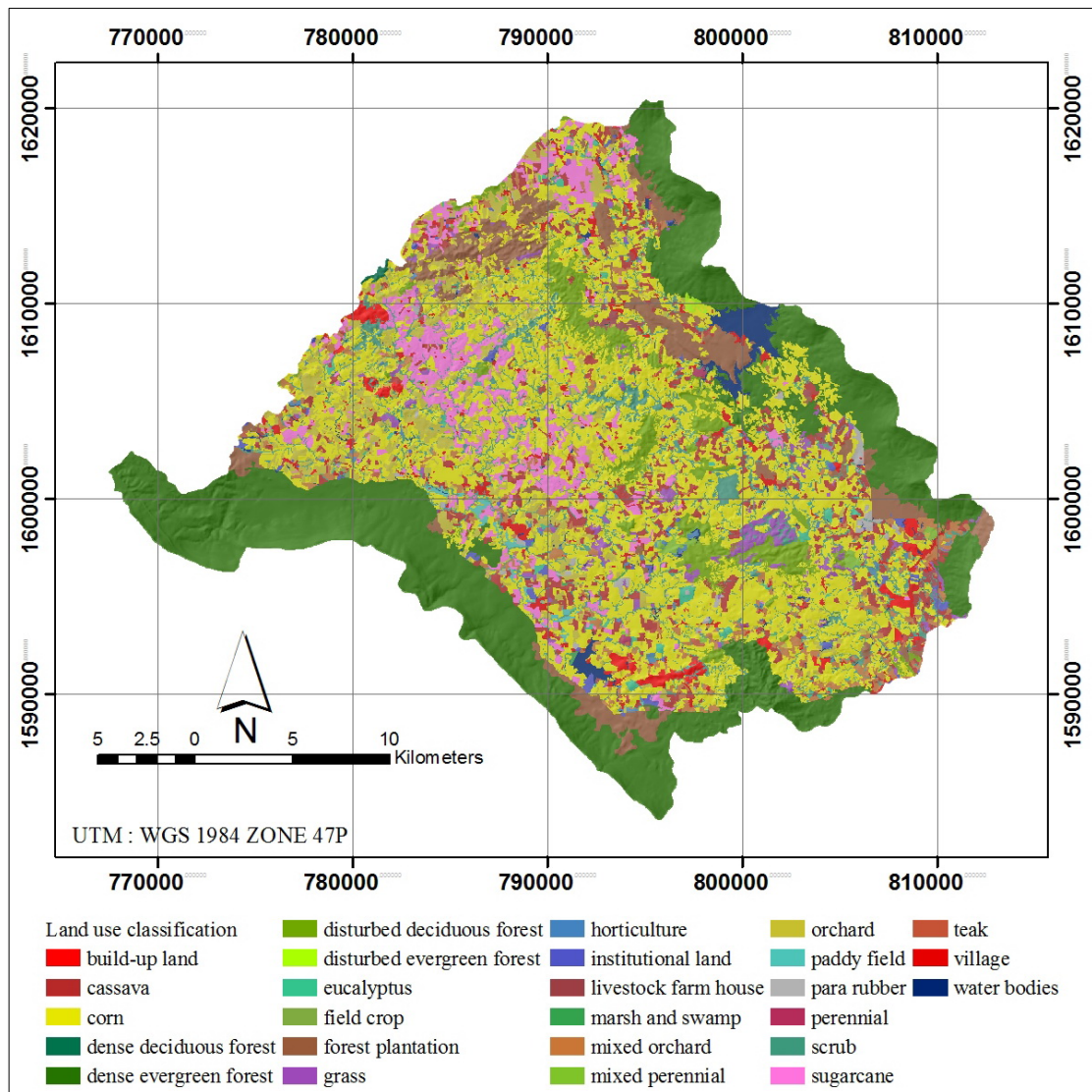


Figure 3.5 Land use data (Level 3 Classification).

3.3.3 Assignment of appropriate curve number values

The curve number value (Figure 3.6) is dependent on HSG, land use, and land treatment. A combination of these is a hydrological soil cover complex. The curve number values were assigned to each grid cell to such complex to indicate their specific runoff potential.

Modified curve number values matching to specific terrain characteristics mentioned above were rearranged from conventional ones (NRCS, 2004) to be appropriate to the study area. The modified curve number values are summarized in the Table 3.3.



Table 3.3 Modified curve number values of Upper Lam Phra Phloeng watershed.

Land cover	Treatment	Hydrologic condition ¹	Appropriate assumption to land use in study area	Curve numbers for hydrologic soil group			
				A	B	C	D
Row crop	Straight row	Poor	Cassava, corn, field crop	72	81	88	91
	Straight row	Partial cover ²	Sugarcane	49	69	79	84
Small grain	Straight row	Poor	Paddy field, horticulture	65	76	84	88
Pasture, grassland		Poor	Grass	68	79	86	89
Brush-grass mixture with brush the major element			Scrub	48	67	77	83
Woods-grass combination (orchard or tree farm)		Fair ³	Perennial, mixed perennial, orchard, mixed orchard, para rubber, teak, eucalyptus	43	65	76	82
Forest ⁴		Poor	Forest plantation	45	66	77	83
		Fair	Disturbed deciduous forest, disturbed evergreen forest	36	60	73	79
		Good	Dense evergreen, Dense deciduous forest	30	55	70	77
Impervious and water surface			Water body, marsh, swamp	98	98	98	98
Farmstead-building			livestock farm house	59	74	82	86
Urban districts		85% of average impervious area	Build-up land, institutional land, village	89	92	94	95

¹ Hydrologic condition is based on combinations of factors that affect infiltration and runoff, including (a) density and canopy of vegetative areas, (b) amount of year-round cover, (c) amount of grass or close-seeded legumes, (d) percent of residue cover on the land surface, and (e) degree of surface toughness.

Poor: Factors impair infiltration and tend to increase runoff

Good: Factors encourage average and better than average infiltration and tend to decrease runoff.

² Sugarcane degrees of cover

Partial cover-Cane in transition period between limited and completed cover; canopy over half to nearly the entire field area.

³ Pasture, grassland

Fair: 50 to 70% ground cover and not heavily grazed.

⁴ Forest conditions

Poor: forest litter, small trees, and brush are destroyed by heavy grazing or regular burning.

Fair: Woods are grazed, but not burned, and some forest litter covers the soil.

Good: Woods are protected from grazing, and litter and brush adequately cover the soil.

Sources: adapted from (NRCS, 2004).

The curve number values were adjusted based on Antecedent Soil Moisture Condition (AMC) (Appendix B). AMC is an indicator of watershed wetness and availability of soil storage prior to a storm. Three levels of AMC were used: AMC-I for dry, AMC-II for normal, and AMC-III for wet conditions. The curve numbers should be adjusted based on the season and 5-day antecedent precipitation (Ward and Trimble, 2003). Mathematically, adjustments to runoff curve number values for the cases of AMC-I, AMC-III, the following equations were used (Chow et al., 1988).

$$CN_I = \frac{4.2CN_{II}}{10 - 0.058CN_{II}} \quad (3.6)$$

$$CN_{III} = \frac{23CN_{II}}{10 + 0.13CN_{II}} \quad (3.7)$$

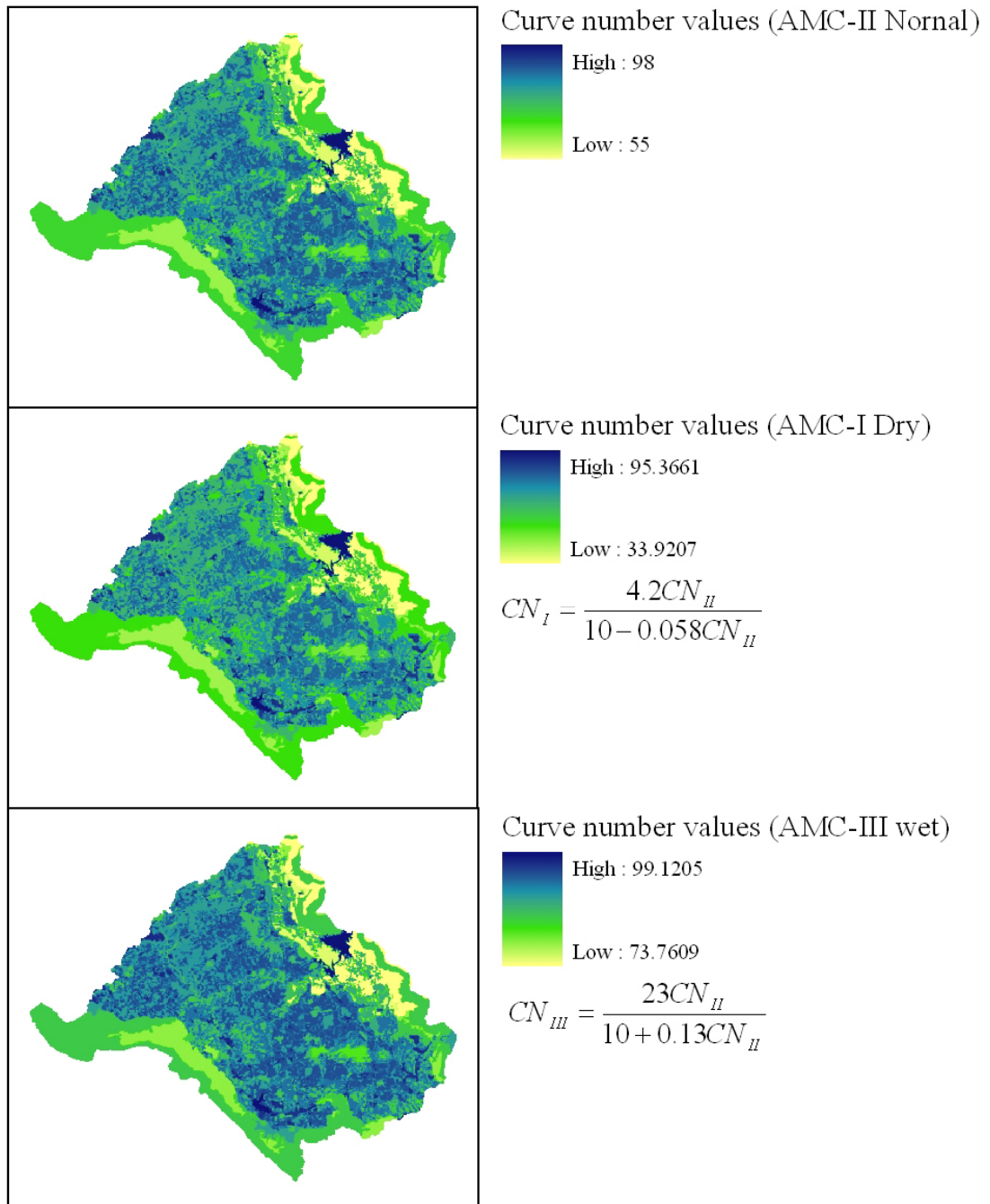


Figure 3.6 Curve number values according to antecedent soil moisture condition.

3.3.4 Model development of grid-based approach

Each GIS layer of hydrologic parameters was prepared in raster format with grid cell size of 30×30 meters. Each cell homogenously represents characteristics of the hydrological factors. The computer program ModelBuilderTM of ArcGISTM was used to develop the model toolbox (Appendix C) with required sets of spatial analyses. The surface runoff depth in each grid cell was computed using the CN method, and then routed through the watershed based on flow direction and flow accumulation from one grid cell to the next until it reaches the watershed outlet. The simulated runoff values were picked up from cells located at M.171 and M.145 stations. The outputs of model simulations (Q_{sim}) and field observations (Q_{obs}) of all events at these two cells were tabulated in an ExcelTM spreadsheet to estimate the statistical parameters for model evaluation.

An overview of the grid-based approach is shown in Figure 3.7. It is a grid-based spatial analysis applying all the mathematic equations present in the CN method algorithm.

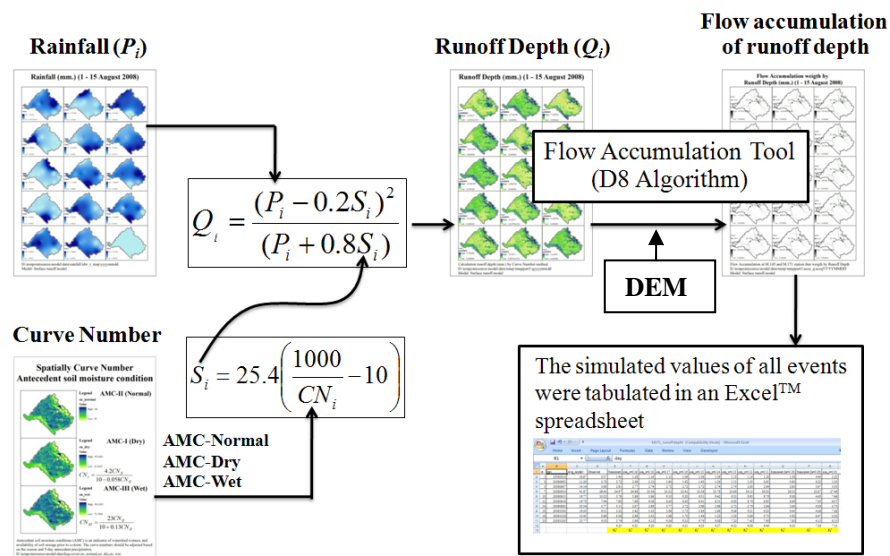


Figure 3.7 Simulated surface runoff from grid-based Curve Number method.

3.3.5 Model Evaluation

The model evaluation procedure included both calibration and validation processes. Performance of the model was based on qualitative (graphical displays) and quantitative (statistical measurement) assessment. Statistical parameters namely Nash and Sutcliffe's coefficient of efficiency (E), coefficient of determination (R^2), Deviation (D_v), Root Mean Square Error ($RMSE$) were used to validate the model simulated results. The reason of such extensive evaluation was to eliminate the bias and limitation of each measurement stated above. The simulated runoff was compared with the observed runoff values recorded at the M.171 and M.145 gauge station for selected rainfall events in the rainy season of 2008. The numerical performance criteria are briefly described below.

The Nash-Sutcliffe's coefficient of efficiency (E) (Nash and Sutcliffe, 1970) is used to assess the simulated power of hydrological model. It is defined as:

$$E = 1 - \frac{\sum_{i=1}^n (Obs - Sim)^2}{\sum_{i=1}^n (Obs - \overline{Obs})^2} \quad (3.8)$$

where Obs is the observed runoff; Sim is the simulated runoff; and \overline{Obs} is the mean of the observed values. The values for E can be varied from $-\infty$ to 1, with 1 indicating a perfect fit.

The coefficient of determination (R^2) ranges from 0.0 (poor model) to 1.0 (perfect model) is given as:

$$R^2 = \left\{ \frac{\sum_{i=1}^n (Obs_i - \overline{Obs})(Obs_i - Sim_i)}{\left[\sum_{i=1}^n (Obs_i - \overline{Obs})^2 \right]^{0.5} \left[\sum_{i=1}^n (Sim_i - \overline{Sim})^2 \right]^{0.5}} \right\} \quad (3.9)$$

where Obs is observed data, Sim is the corresponding simulated data, \overline{Obs} is the mean of observed data set, \overline{Sim} is the mean of simulated data set, i is the event, and n is the total count of data pair.

The Root Mean Square Error ($RMSE$) is frequently-used measurement of the differences between simulated values and the observed values. The $RMSE$ is determined by calculating the square of deviations of simulated data from their observed data, summing up the deviations, and then taking the square root of the sum. These individual differences are also called residuals, and the $RMSE$ serves to aggregate them into a single measurement of predictive power. According to the evaluation the closer this value is to zero the better the model is. It is defined as:

$$RMSE = \sqrt{\frac{1}{n} \times \sum_{i=1}^n (Obs - Sim)^2} \quad (3.10)$$

Another criterion for goodness-of-fit is the deviation of runoff values, Dv is given by the following equation:

$$Dv(\%) = \frac{Obs - Sim}{Obs} \times 100 \quad (3.11)$$

The closer this value is to zero the better the model is. Dv would equal to zero for a perfect model.

3.4 Results and Discussion

3.4.1 Model Calibration

The ratio of initial abstraction (I_a) to maximum potential retention (S) was assumed in its original development to be equal to 0.2 in CN method. The constant initial abstraction ratio is the most ambiguous assumption and required considerable refinement (Shi et al., 2009). Ten selected events were used for model calibration. A part of calibration procedure was done by adjusting “ λ ” values in the Eq. 3.3 in such manner that the calculated coefficient of efficiency (E) for all calibration events would be highest.

The calibration results show that the model provides the best simulation results with $E = 0.94$, $R^2 = 0.95$ when adjusting $I_a = 0.1S$ for M.171 station (Figure 3.8) and $E = 0.87$, $R^2 = 0.91$ when adjusting $I_a = 0.2S$ for M.145 station (Figure 3.9). The varying “ λ ” (from 0.1, 0.2, and 0.3) can improve accuracy of their relationship as shown in Table 3.4.

Table 3.4 Data comparison of model simulations (Q_{sim}) and field observations (Q_{obs}) of ten events for model calibration.

Calibration events	Antecedent soil moisture condition (AMC)	Runoff Depth (mm)							
		M.171 station				M.145 station			
		Rainfall (mm)	Q_{obs}	Q_{sim}	Dv (%)	Rainfall (mm)	Q_{obs}	Q_{sim}	Dv (%)
20080818	Dry	20.34	0.07	1.38	-1851.78	20.35	0.45	1.46	-226.07
20080905	Dry	12.00	0.78	0.90	-15.81	10.56	0.94	2.86	-202.70
20080907	Normal	11.96	0.99	2.90	-193.07	5.50	0.80	1.22	-51.84
20080910	Wet	42.39	29.40	26.52	9.81	40.47	19.49	22.15	-13.63
20080915	Wet	16.69	10.52	6.88	34.61	13.49	3.70	3.64	1.81
20080918	Wet	18.89	7.44	8.96	-20.43	17.33	3.83	7.15	-86.40
20080930	Dry	21.82	5.77	2.93	49.18	26.08	4.79	3.48	27.29
20081003	Wet	16.42	6.51	6.45	0.84	15.42	5.76	4.32	25.07
20081018	Dry	8.89	0.96	0.62	34.79	6.53	0.67	3.81	-466.95
20081030	Normal	27.47	6.50	7.90	-21.45	28.66	6.34	5.76	9.16
Total			68.94	65.45			46.79	55.84	
Coefficient of efficiency (E)				0.94				0.87	
Coefficient of determination (R^2)				0.95				0.91	
Average deviation (%)				-197.33				-98.43	
Root Mean Squared Error ($RMSE$)				1.98				1.92	

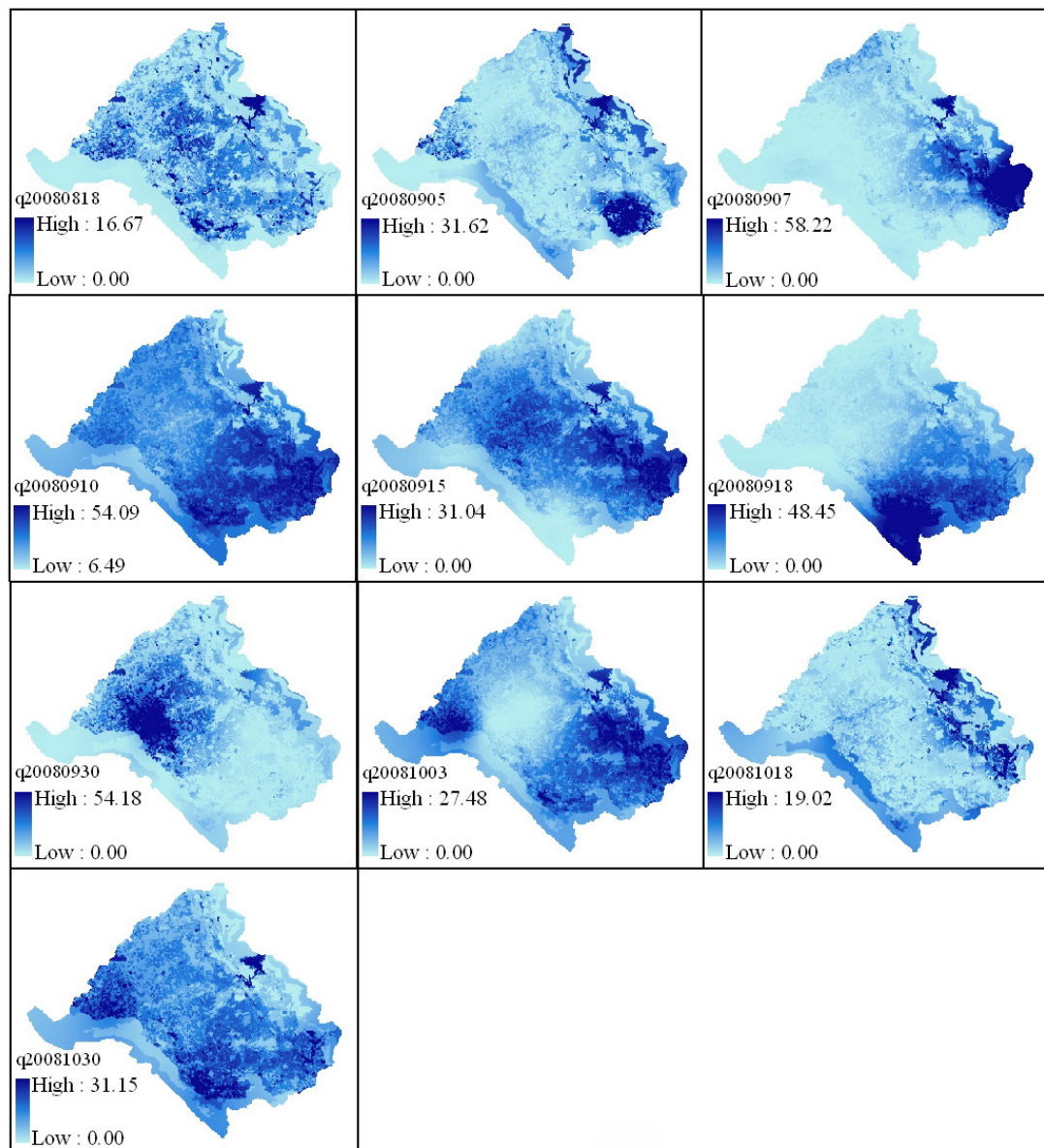


Figure 3.8 Runoff depth (mm) for calibration events (M.171).

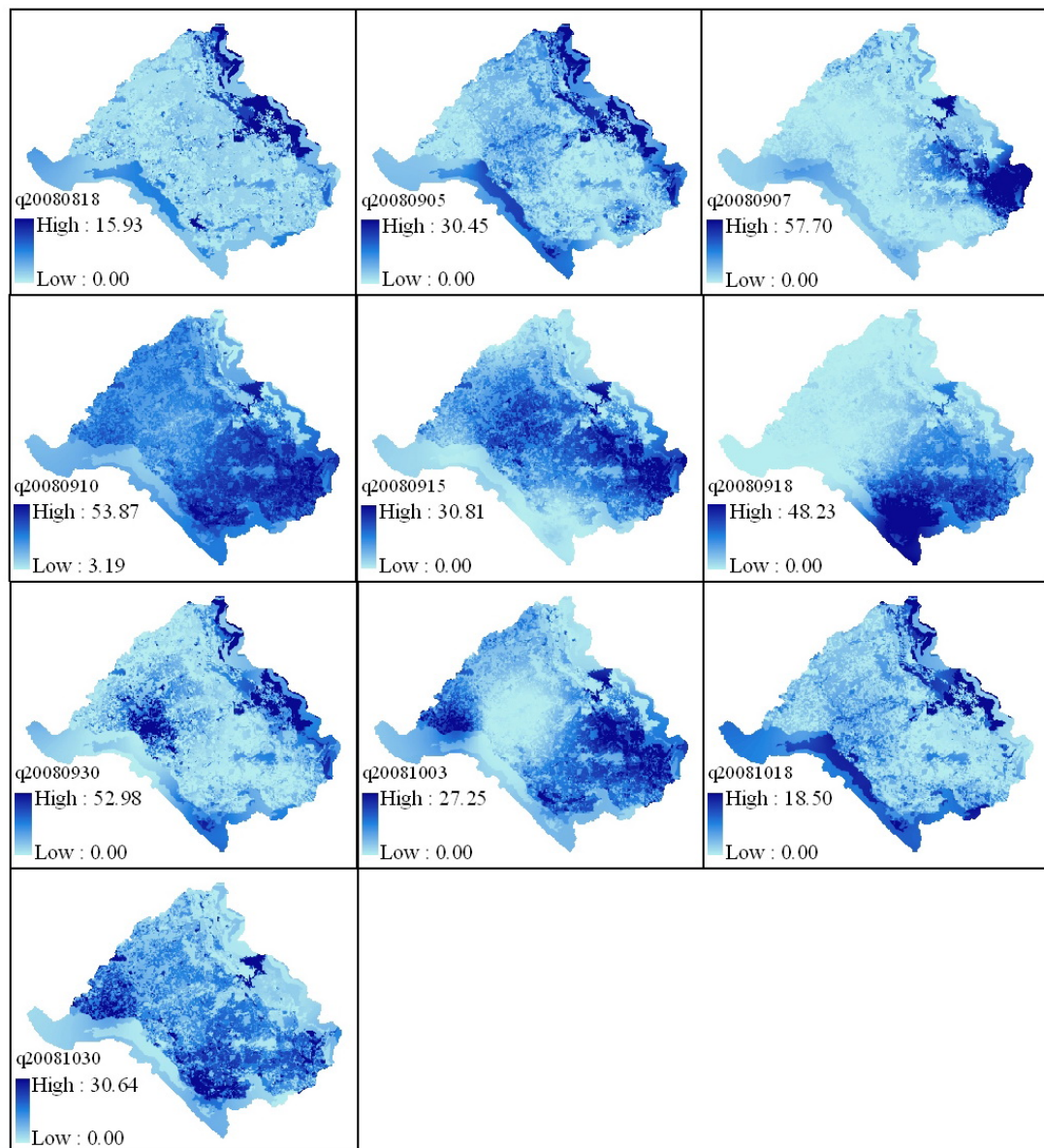
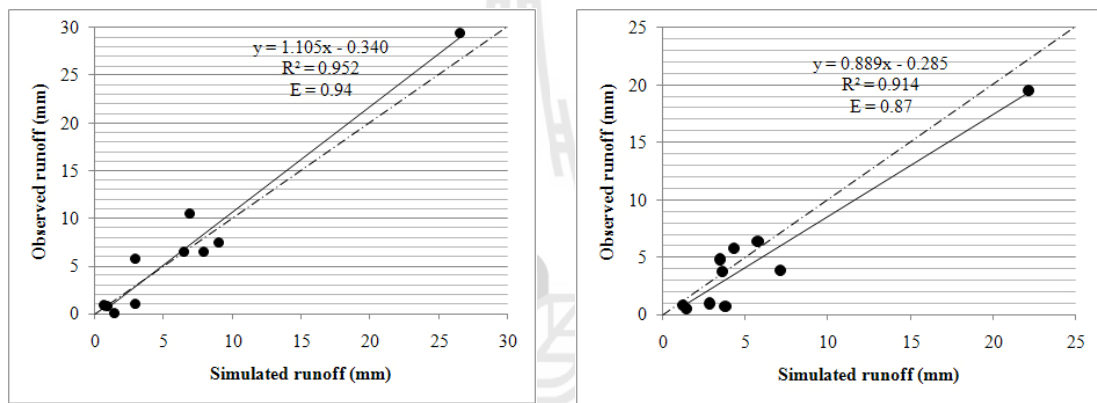


Figure 3.9 Runoff depth (mm) for calibration events (M.145).

The scatter plot of observed and simulated runoffs for calibration events at the station M.171 and M.145 along with 1:1 line (dash line) are shown in Figure 3.10. It is observable that the M.171 simulated runoff values are slightly above the 1:1 line, indicating that the model is slightly underestimation. Meanwhile, it is observed that the M.145 simulated runoff values are slightly below the 1:1 line, indicating that the model is slightly overestimation, whereas both M.171 and M.145 well distributed of scatter plot quite satisfactory.



(a) M.171 station

(b) M.145 station

Figure 3.10 Comparison of observed and simulated runoffs at M.171 and M.145 stations.

3.4.2 Model validation

Other eight events were used for the model validation. The validation results show that $E = 0.87$ and $R^2 = 0.89$ are for M.171 station (Figure 3.11) and $E = 0.68$ and $R^2 = 0.75$ are for M.145 station (Figure 3.12). The validation results for simulated runoffs are presented in Table 3.5.

Table 3.5 Data comparison of calibrated model simulations (Q_{sim}) and field observations (Q_{obs}) of eight events for model validation.

Validation events	Antecedent soil moisture condition (AMC)	Runoff Depth (mm)							
		M.171 station				M.145 station			
		Rainfall (mm)	Q_{obs}	Q_{sim}	Dv (%)	Rainfall (mm)	Q_{obs}	Q_{sim}	Dv (%)
20080819	Dry	12.38	0.11	0.71	-550.90	13.74	1.19	2.58	-117.88
20080906	Dry	17.23	1.63	1.50	8.39	22.26	2.47	2.16	12.64
20080909	Normal	16.86	1.16	3.15	-170.94	15.93	1.53	1.59	-3.73
20080912	Wet	25.72	12.08	13.02	-7.74	28.36	10.80	12.87	-19.20
20080928	Dry	25.56	2.20	2.55	-15.78	27.18	1.59	1.81	-14.26
20081001	Normal	15.91	3.84	5.85	-52.55	17.97	3.55	5.44	-53.48
20081008	Normal	13.32	3.85	2.30	40.22	14.35	3.51	1.90	45.67
20081025	Dry	31.51	5.54	4.54	18.14	39.80	7.23	3.64	49.59
Total			30.42	33.62			31.86	32.02	
Coefficient of efficiency (E)				0.87				0.68	
Coefficient of determination (R^2)				0.89				0.75	
Average deviation (%)				-91.40				-12.58	
Root Mean Squared Error ($RMSE$)				1.27				1.78	

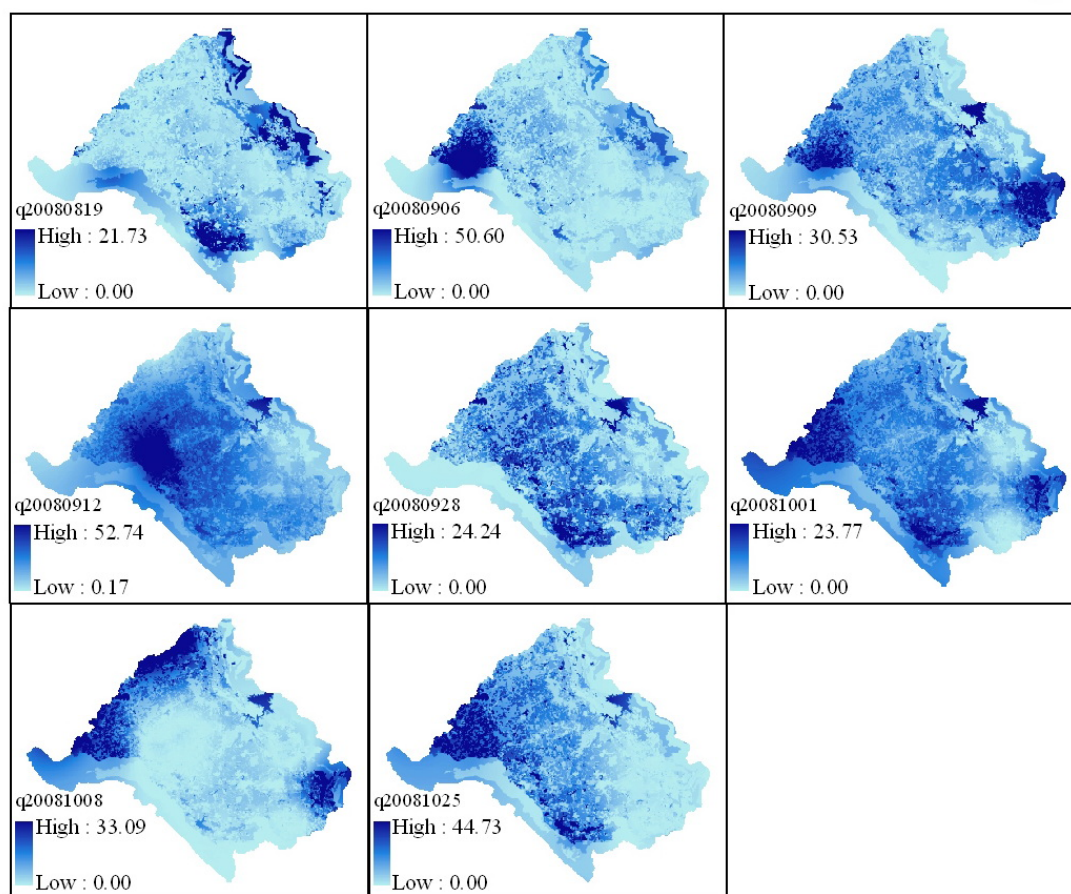


Figure 3.11 Runoff depth (mm) for validation events (M.171).

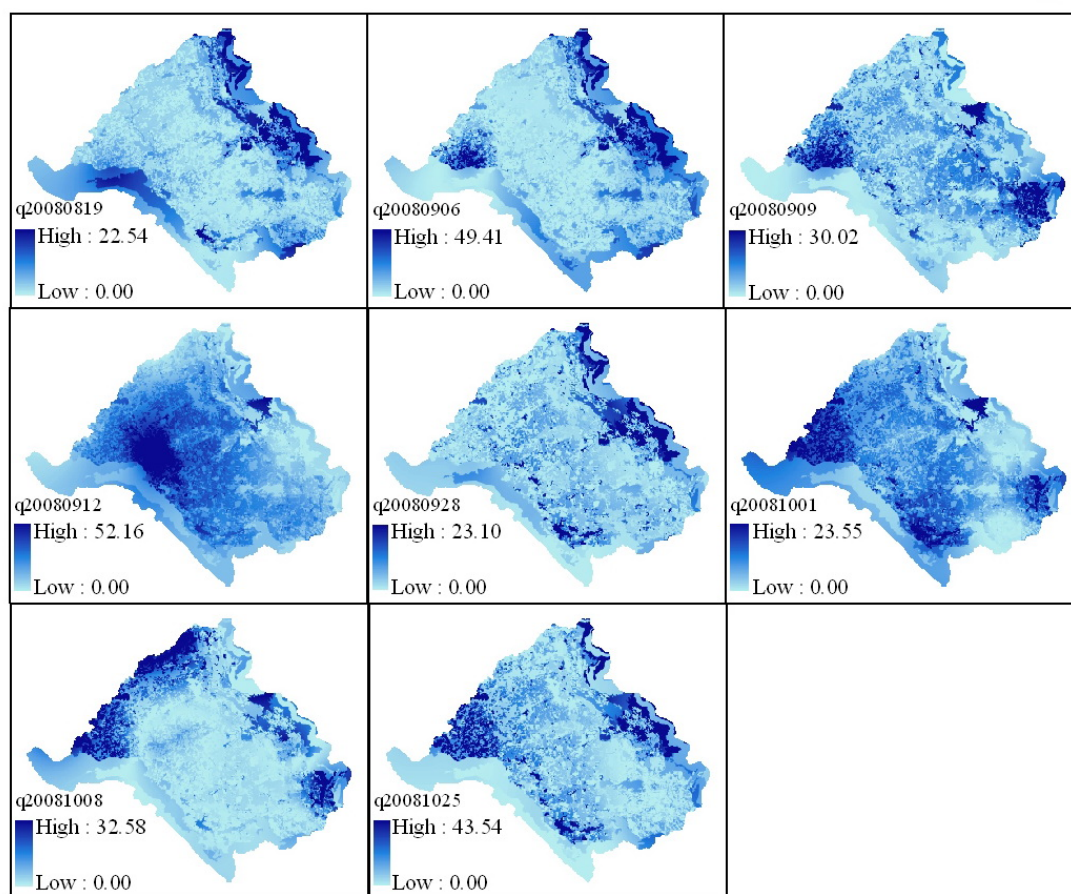


Figure 3.12 Runoff depth (mm) for validation events (M.145).

The scatter plots of observed and calibrated-simulated runoffs for event validations at the station M.171 and M.145 along with 1:1 line are shown in Figure 3.13. It is observable that the M.171 relation line is almost identical to the 1:1 line. The M.145 relation line is slightly below the 1:1 line when the runoff is approximately higher than 4.5 mm., indicating that the model is slightly overestimation in heavier events. However, the scatter plot of M.171 is better distribution than of M.145.

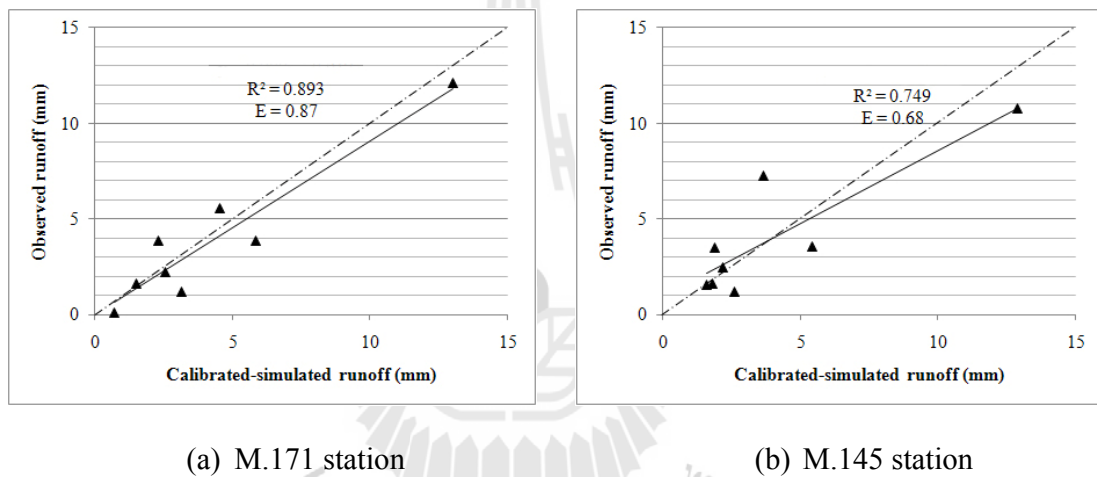


Figure 3.13 Relationships of observed and calibrated-simulated runoffs for model validation at the M.171 and M.145 stations.

3.5 Conclusion

From the study, the calibrated results of the modified CN method with spatial modeling can be applied to runoff simulations with acceptable accuracy. Not only the satisfied quantitative results provided but the model is also able to estimate varying runoff depth over the watershed spatially. As the result of the case study at the Upper Lam Phra Phloeng watershed, it can be confirmed that grid-based modified CN method is applicable

to surface runoff estimation effectively. The curve number values used in CN method was used to develop the NPS pollution potential index in Chapter VI, because it indicate to their specific runoff potential.

3.6 References

- Chatterjee, C., Jha, R., Lohani, A.K., Kumar, R., and Singh, R. (2001). Run-off curve number estimation for a basin using remote sensing and GIS. **Asian-Pacific Remote Sensing and GIS Journal**. 14: 1-8.
- Cho, K.M., and Zoebisch, M.A. (2003). Land-use change in the Upper Lam Phra Phloeng watershed, Northeastern Thailand: characteristics and driving forces. **Journal of Agriculture and Rural Development in the Tropics and Subtropics**. 104(1): 15-29.
- Chow, V.T., Maidment, D.R., and Mays, L.W. (1988). **Applied hydrology**. New York: McGraw-Hill.
- Garen, D., Woodward, D., and Geter, F. (1999). A user agency's view of hydrology, soil erosion and water quality modeling. **CATENA**. 37(3-4): 277-289.
- Grunwald, S., and Norton, L.D. (2000). Calibration and validation of nonpoint source pollution model. **Agricultural Water Management**. 45: 17-39.
- Han, H., Daniel, G., and Allan, L. (2008). Textural averages of saturated soil hydraulic conductivity predicted from water retention data. **Geoderma**. 146(1-2): 121-128.

- Land Development Department (LDD). (2004). **Characterization of established soil series in the Northeast region of Thailand reclassified according to soil taxonomy 2003**. Bangkok: Office of Soil Survey and Land Use Planning, Land Development Department, Ministry of Agriculture and Cooperatives.
- Mishra, S.K., and Singh, V.P. (2003). **Soil conservation service curve number (SCS-CN) methodology**. Dordrecht, Netherlands: Kluwer Academic Publishers.
- Mohammed, H., Yohannes, F., and Zeleke, G. (2004). Validation of agricultural nonpoint source (AGNPS) pollution model in Kari water, South Wollo, Ethiopia. **International Journal of Applied Earth Observation and Geoinformatics**. 6: 97-109.
- Nash, J.E., and Sutcliffe, J.V. (1970). River flow forecasting through conceptual models part I-A, Discussion of principles. **Journal of Hydrology**. 10(3): 282-290.
- National Resources Conservation Service (NRCS). (2004). **Estimation of direct runoff from storm rainfall: Part 630 hydrology national engineering handbook**. United States Department of Agriculture.
- National Resources Conservation Service (NRCS). (2007). **Hydrologic soil groups: Part 630 hydrology national engineering handbook**. United States Department of Agriculture.
- Olivera, F., and Maidment, D. (1999). Geographic information systems (GIS)-based spatially distributed model for runoff routing. **Water Resources Research**. 35(4): 1155-1164.

- Salazar, O., Wesstrom, I., and Joel, A. (2008). Evaluation of DRAINMOD using saturated hydraulic conductivity estimated by a pedotransfer function model. **Agricultural Water Management**. 95(10): 1135-1143.
- Shi, Z.H., Chen, L.D., Fang, N.F., Qin, D.F., and Cai, C.F. (2009). Research on the SCS-CN initial abstraction ratio using rainfall-runoff event analysis in the Three Gorges Area, China. **CATENA**. 77: 1-7.
- Steenhuis, T.S., Mendoza, G, Lyon, S.W., Marchant, P.G., Walter, M.T., and Schneiderman, E. (2003). Distributed GIS based runoff predictions for variable source watersheds using the SCS-curve number. **Geophysical Research Abstracts**. 5 (01628).
- Tekeli, T.I., Akgul, S., Dengiz, O., and Akuzum, T. (2007). Estimation of flood discharge for small watershed using SCS curve number and geographic information system. In **International Congress on River Basin Management 2007**. (pp 527-538). Antalya, Turkey.
- Ward, A.D., and Trimble, S.W. (2003). **Environmantal hydrology**. 2nd. Boca Raton, FL: Lewis Publishers.

CHAPTER IV

SEDIMENT YIELD ESTIMATION USING MODIFIED UNIVERSAL SOIL LOSS EQUATION AND SEDIMENT DELIVERY DISTRIBUTED MODEL

4.1 Abstract

The grid-based approach has been applied for the estimation of sediment yield in Upper Lam Phra Phloeng watershed. The approach involves spatial disintegration of the watershed into homogenous grid cell to capture the watershed heterogeneity. The gross soil erosion in each cell was calculated using modified universal soil loss equation (MUSLE). The sediment delivery distributed model (SEDD) is used to route surface erosion from each of the grid cells to the watershed outlet. Sixteen sediment yield events in rainy season of the year 2008 were observed. Eight events were used for model calibration with sediment yield data measured at two observed stations (M.171 and M.145). Other eight were for the model validation. The calibration results show that the coefficient of efficient (E) is 0.85 and the coefficient of determination (R^2) is 0.89. The validation results show that E is 0.79 and R^2 is 0.92. This indicates that the calibrated-MUSLE and SEDD working under GIS can be applied with satisfactory accuracy to the sediment yield estimation.

4.2 Introduction

Soil erosion includes the processes of detachment of soil particles from the soil mass and subsequent transport and deposition of those sediment particles on land surface and water bodies. This sediment has a tremendous societal cost associated with it in terms of stream degradation, disturbance to wildlife habitat, and direct costs for dredging, levees, and reservoir storage losses. Sediment is also an important vehicle for the transport of soil-bound chemical contaminants from NPS areas to waterways. (Nearing et al., 2000; นิพนธ์ ตั้งธรรม, 2545). Soil erosion can pose a great concern to the environment because cultivated areas can act as a pathway for transport nutrients, pesticides, especially phosphorus attached to sediment particles of water systems (Ouyang and Bartholic, 1997).

Pollution by sediment has two major dimensions (Ongley, 1996). Physical dimension – top soil loss and land degradation by gully and sheet erosion and which leads both to excessive levels of turbidity in receiving waters, and to off-site ecological and physical impacts from deposition in river and water bodies beds. Chemical dimension – the clay fraction is primary carrier of adsorbed chemicals, especially phosphorus, and most metals, which are transported by sediment into the aquatic system.

Lam Phra Phloeng reservoir is the highest reservoir sedimentation in the Northeastern Thailand (Tangtham and Lorsirirat, 1993). Solutions to NPS pollution problems must address the problem of erosion and sediment control. Therefore, it becomes necessary to quantify soil erosion and sediment yield, with the aim of providing a tool for nonpoint source management on watershed basis.

The objective of this chapter, spatial model was applied with MUSLE and SEDD for sediment yield simulation where heterogeneity of watershed characteristics was considered to simulate the sediment yield of Upper Lam Phra Phloeng watershed. Finally, the accuracy of the output from the model was evaluated by comparing calibrated-simulated sediment yield with the observed sediment yield.

4.3 Materials and methods

In the application of sediment yield model on GIS environment, sediment yield was estimated within the grid-based GIS. The factors required for MUSLE and SEDD were derived using GIS technique. A GIS technique was used for derivation and spatial discretization of the watershed was prepared physical factors related to sediment yield in the grid cell. All variables are based on cell unit area. The flow diagram of the MUSLE, SEDD, and geospatial model for sediment yield estimation are shown in Figure 4.1.

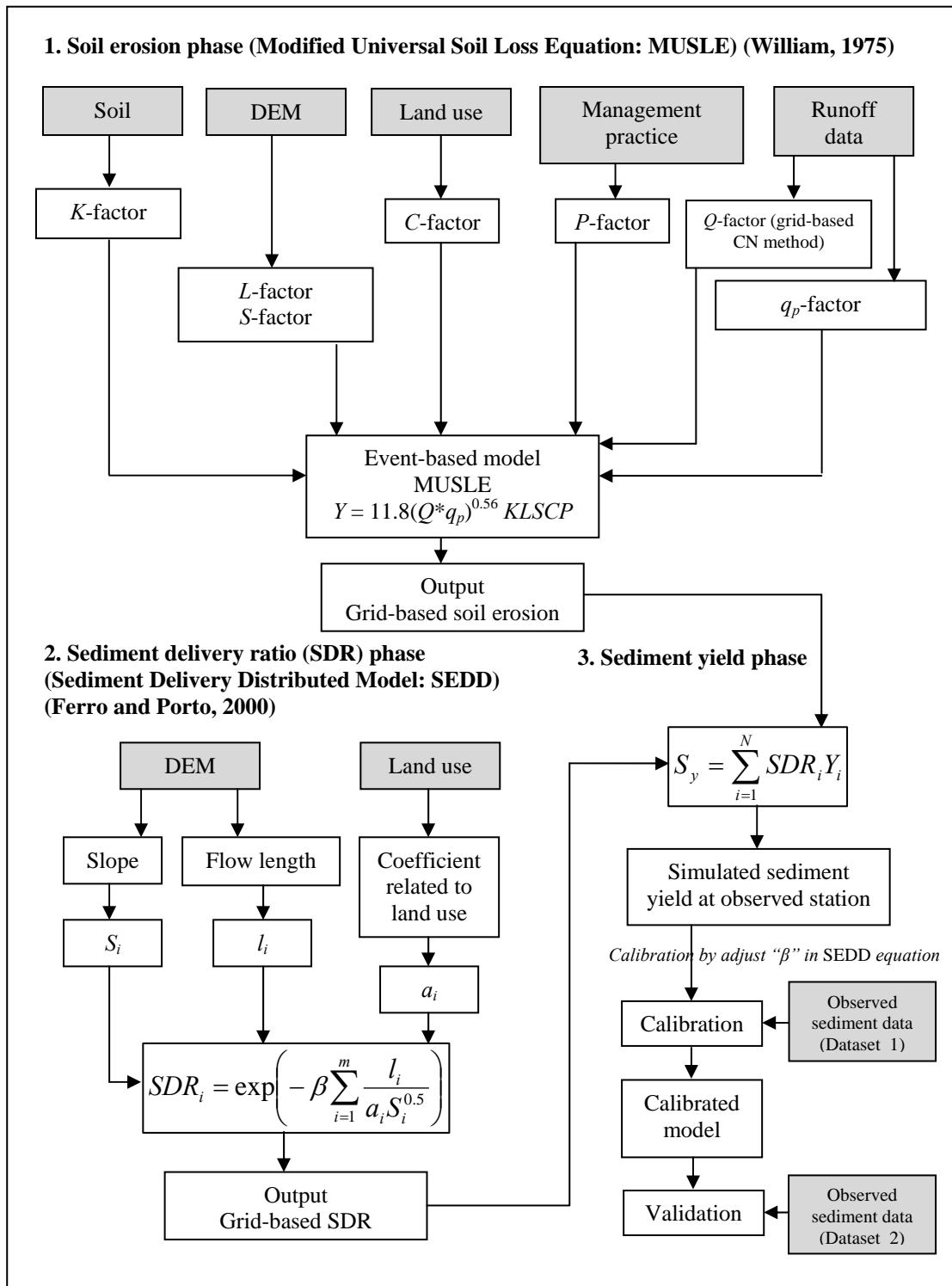


Figure 4.1 Flow diagrams of the sediment yield estimation.

4.3.1 Modified Universal Soil Loss Equation (MUSLE)

Soil erosion is a hydrological driven process and it depends on sediment being discharged with runoff (Kinnell, 2005). By including the runoff as an independent factor in modeling erosion, MUSLE has an improved accuracy of soil erosion prediction over USLE and Revised USLE, which do not include runoff factor. In general, MUSLE can be expressed as follows (William, 1975):

$$Y = a(Q \times q_p)^b K \times LS \times C \times P \quad (4.1)$$

where Y is the sediment yield to the stream network in metric tons, Q is the runoff volume from a given rainfall event in m^3 , q_p is peak flow rate in $\text{m}^3 \text{s}^{-1}$, K is the soil erodibility factor, LS is the slope length and slope steepness factor, C is the cover management factor derived from land use data, and P is the erosion control practice factor which is a field specific value, and a and b are location coefficients. For the area where the equation was developed, a and b were 11.8 and 0.56, respectively. Sadeghi (2004) suggests that the model need to be calibrated before application on other area. To reduce error in the analysis, sufficient number of storms occurring during the different conditions with a wide range of variation should be considered for calibration and new equation development.

4.3.2 Data collection for MUSLE

The present study aims at developing a grid-based GIS processes. To prepare spatial parameters as input of the model, the watershed is discretized into cell or grid areas. Spatially distributed information of each cell in the watershed includes runoff factor, q_p factor, K factor, LS factor, C factor, P factor is prepared through a GIS. Runoff factor, which is a major input to MUSLE was computed using the grid-based CN method mentioned in chapter 3. The graphical peak discharge method is used to q_p factor (NRCS, 1986; Zhang et al., 2009). The following describes the collecting and estimating of the runoff factor and watershed parameters including K factor, LS factor, C factor, and P factor.

4.3.2.1 Runoff factor

i) Runoff volume (Q)

Runoff volume was computed using the grid-based CN method mentioned in the previous chapter. The spatial distribution of the runoff volume maps of eight events for model development are shown in Figure 4.2.

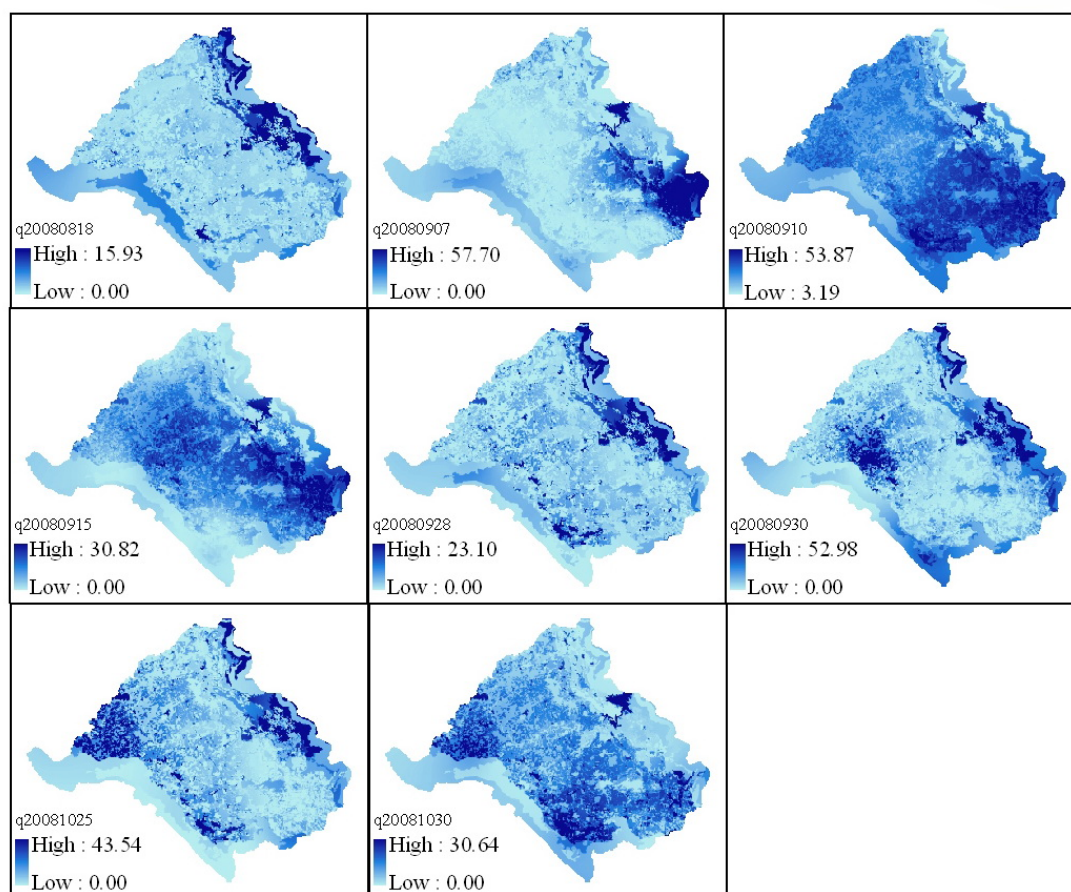


Figure 4.2 Runoff factor.

ii) Peak discharge (q_p)

The graphical peak discharge method (NRCS, 1986; Zhang et al., 2009) used to compute peak discharge q_p ($\text{m}^3 \text{s}^{-1}$) is expressed as:

$$q_p = q_u A Q_d F_p \quad (4.2)$$

where q_u is the unit peak discharge in $\text{m}^3 \text{s}^{-1} \text{km}^{-2} \text{mm}^{-1}$, A is the drainage area in km^2 (grid-cell), Q_d is the runoff depth in mm, and F_p is the pond and swamp adjustment factor which is the percentage of pond and swamp area over the unit area. The time of concentration T is required for the calculation of q_u and is developed by calculating a travel time for sheet flow and a travel time for shallow concentrated flow. Sheet flow is flow over plane surface and usually occurs in the headwater area of stream. The time of travel for sheet flow (T_{sheet}) of less than 91.4 meters (NRCS, 1986) is calculated using Manning's kinematic solution.

$$T_{sheet} = \frac{0.091(nL)^{0.8}}{J^{0.5} s^{0.4}} \quad (4.3)$$

where travel time is in hours, n is the Manning's roughness coefficient (Appendix D) (Vieux, 2004), L is the flow path length in meters, s is the slope in percentage and J is the 2-year 24-h rainfall (typical 24-h duration precipitation with a 2-year return period) in mm which was evaluated by RID (Appendix E). After a maximum of 91.4 meters, sheet flow usually becomes shallow concentrated flow and the time of travel for shallow concentrated flow ($T_{shallow}$) is calculated using the following equation for the remainder of the flow path until it flows into a defined channel.

$$T_{i,shallow} = \frac{3.281 \times L}{3600 \times 16.1345 \times s^{0.5}} \quad (4.4)$$

where L is the flow path length in meter. This equation is based on Manning's equation and two assumptions for Manning's roughness coefficient (0.05) and hydraulic radius (0.4) (NRCS, 1986). Now the two times of travel calculated can be added together to come up with the time of concentration (T) where each drainage way discharge into a stream.

The unit peak discharge can then be calculated using the following equation:

$$q_u = 10^{(C_0 + C_1 \log T + C_2 (\log T)^2)} \quad (4.5)$$

Coefficients C_0 , C_1 , and C_2 are available from NRCS (1986). They are determined by rainfall type, the ratio of initial abstraction (I_a) and 2-year 24-h rainfall. The peak discharge can then be calculated using Equation (4.2). The spatial distribution (grid-based) of the peak discharge maps of eight events are shown in Figure 4.3.

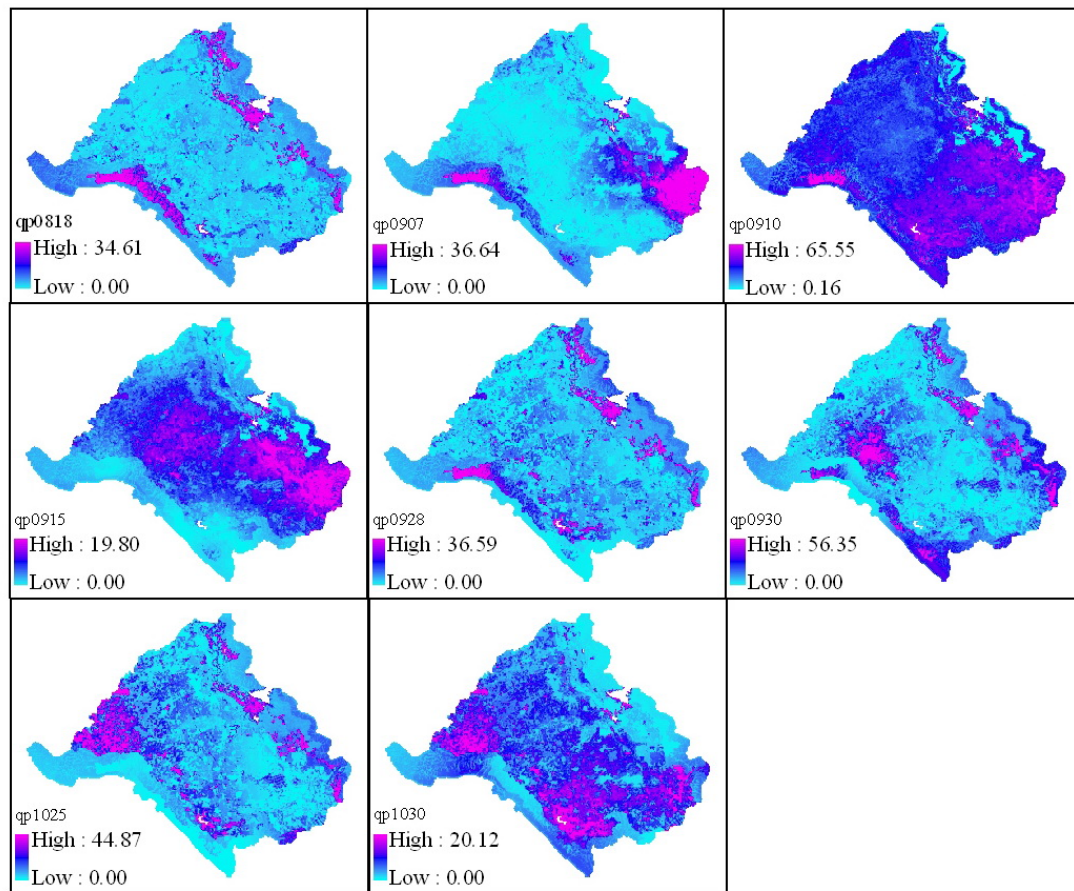


Figure 4.3 Spatial distribution of peak discharge ($\text{m}^3 \text{s}^{-1}$) of eight events.

4.3.2.2 Soil erodibility factor (K factor)

The K factor is an empirical measure of soil erodibility as affected by intrinsic soil properties. The main soil properties affecting K are soil texture, organic matter, structure, and permeability of the soil profile (Fu et al., 2006). Normally soil sampling were done in the field and laboratory tests for determining the percentages of fine sand, silt, and clay and organic matter etc. After which the erodibility value for each soil unit can be estimated using the soil erodibility nomograph method (Wischmeier and Smith, 1978). The nomograph is also based on the following equation, which can estimate K . It is shown below (Lal, 1994):

$$K = 2.8 \times 10^{-7} M^{1.14} (12 - a) + 4.3 \times 10^{-3} (b - 2) + 3.3 \times 10^{-3} (c - 3) \quad (4.6)$$

where K = soil erodibility factor; M = particle size parameter [(%silt + %VFS)(100-%clay)]; a = organic matter (%); b = soil structure code (very fine granular = 1; fine granular = 2; medium or coarse granular = 3; blocky, platy or massive = 4); and c = profile permeability class (rapid = 1; moderate to rapid = 2; moderate = 3; slow to moderate = 4; slow = 5 and very slow = 6). The K factor was estimated using digital soil maps available from LDD at the scale of 1:25,000 and K values for each soil series are available from the LDD literature (กรมพัฒนาที่ดิน, 2543). In the slope-complex area where soil information is missing K values set were from geological formations (obtained from the Department of Mineral Resources at the scale of 1:50,000) and used as the soil erodibility values (กรมพัฒนาที่ดิน, 2543; Thinley, 2008)

(Appendix F). The spatial distribution of soil erodibility values is displayed in Figure 4.4.

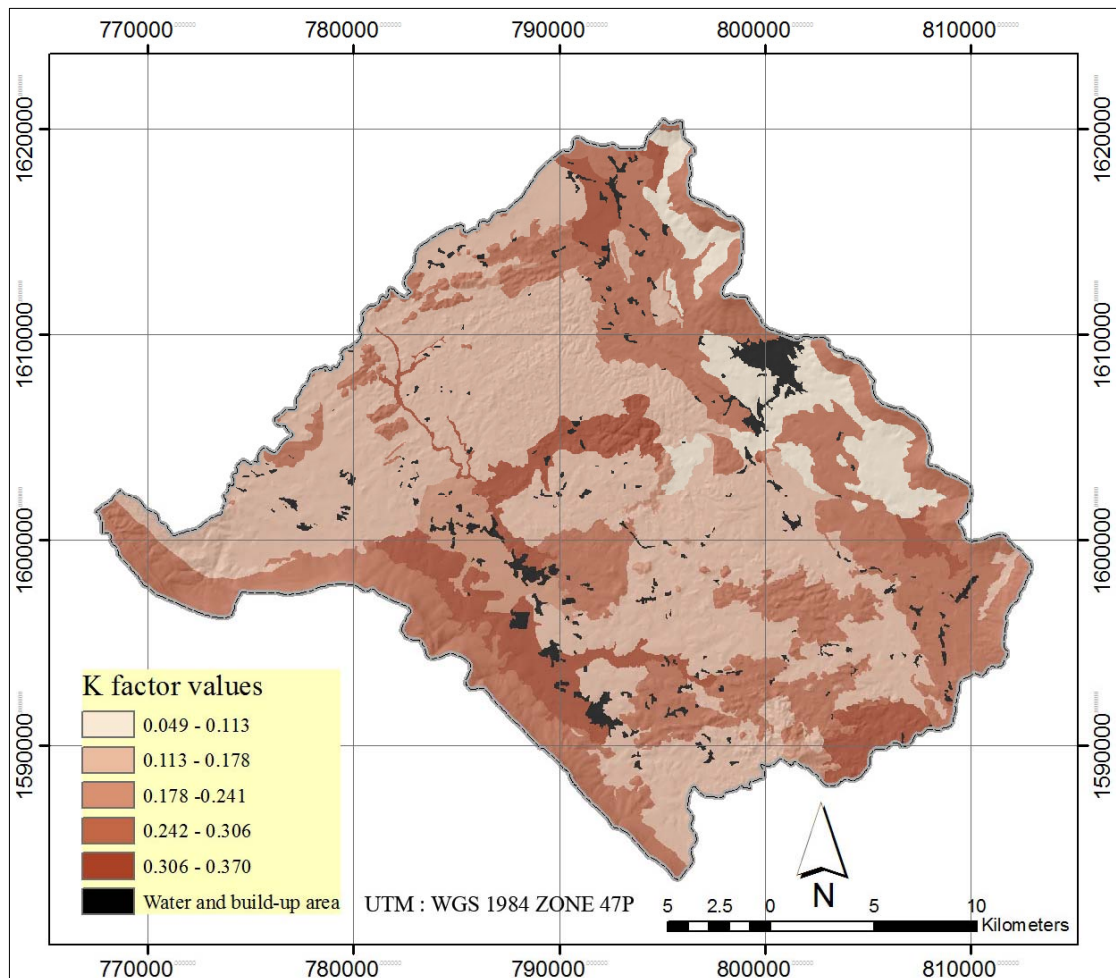


Figure 4.4 Spatial distribution of *K* factor in the study area.

4.3.2.3 Slope-length (*L*) and slope steepness (*S*) factors

Although the *LS* factor is usually either estimated or manually calculated from actual field measurements of slope length and steepness for local conservation planning purposes, labor-intensive field measurements are generally not feasible for model soil erosion at significantly larger spatial scales. Nowadays with new

developed procedures of GIS, user can generate raster grids of the *LS* factor for various site characterizations. The *LS* factor can be estimated from the DEM.

Generally as hill slope length or hill slope gradient increases, soil loss increases. As hill slope length increase, total soil loss and soil loss per unit area increase due to the progressive accumulation of runoff in the down slope direction. As the hill slope gradient increase, the velocity and erosivity of runoff increases.

The digital contours with 20 meter interval initially obtained from RTSD at scale 1:50,000 have been utilized. Digital contours were then interpolated into raster DEM using topo to raster interpolation function of ArcGIS after which slope in degree unit and slope length in meter unit were calculated using ArcGIS. For preparing the *LS* factor layer from DEM, the equation was used for the study as follows.

The slope length factor is calculated by applying equation developed by Wischmeier and Smith (1978):

$$L = \left(\frac{\lambda}{22.13} \right)^m \quad (4.7)$$

where λ is the horizontal projection of the slope length (in meter), m = variable slope length exponent.

The slope length exponent m is related to the ratio β of rill erosion (cause by flow) to inter-rill erosion (principally caused by raindrop impact) by following equation:

$$m = \beta / (1 + \beta) \quad (4.8)$$

For moderately susceptible soil in both rill and inter-rill erosion, McCool et al. (1987) suggested the equation:

$$\beta = \frac{(\sin \theta / 0.0896)}{3.0(\sin \theta)^{0.8} + 0.56} \quad (4.9)$$

where θ is the slope angle (degrees). In this case, slope angle of each cell was taken into account for its β estimation.

The slope steepness (S) reflects the effect of slope gradient on soil erosion. The slope steepness factor S is evaluated from this expression (McCool et al., 1987):

$$S = \begin{cases} 10.8 \sin(\theta) + 0.03 & \text{for } \text{Slope} < 9\% \\ 16.8 \sin(\theta) - 0.50 & \text{for } \text{Slope} \geq 9\% \end{cases} \quad (4.10)$$

where θ is the slope angle (degrees).

The spatial distribution of the derived L and S factor maps is shown in Figures 4.5 and 4.6, respectively.

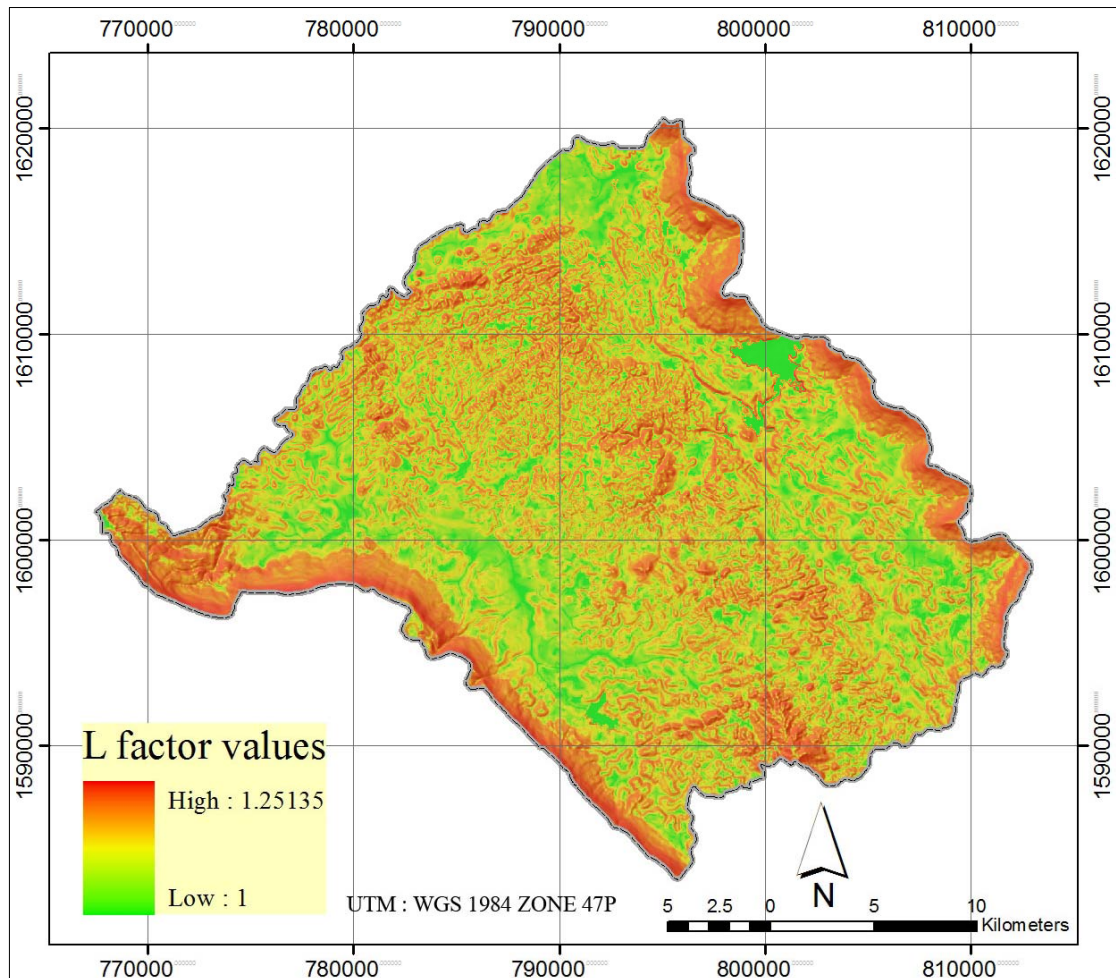


Figure 4.5 Spatial distribution of L factor.

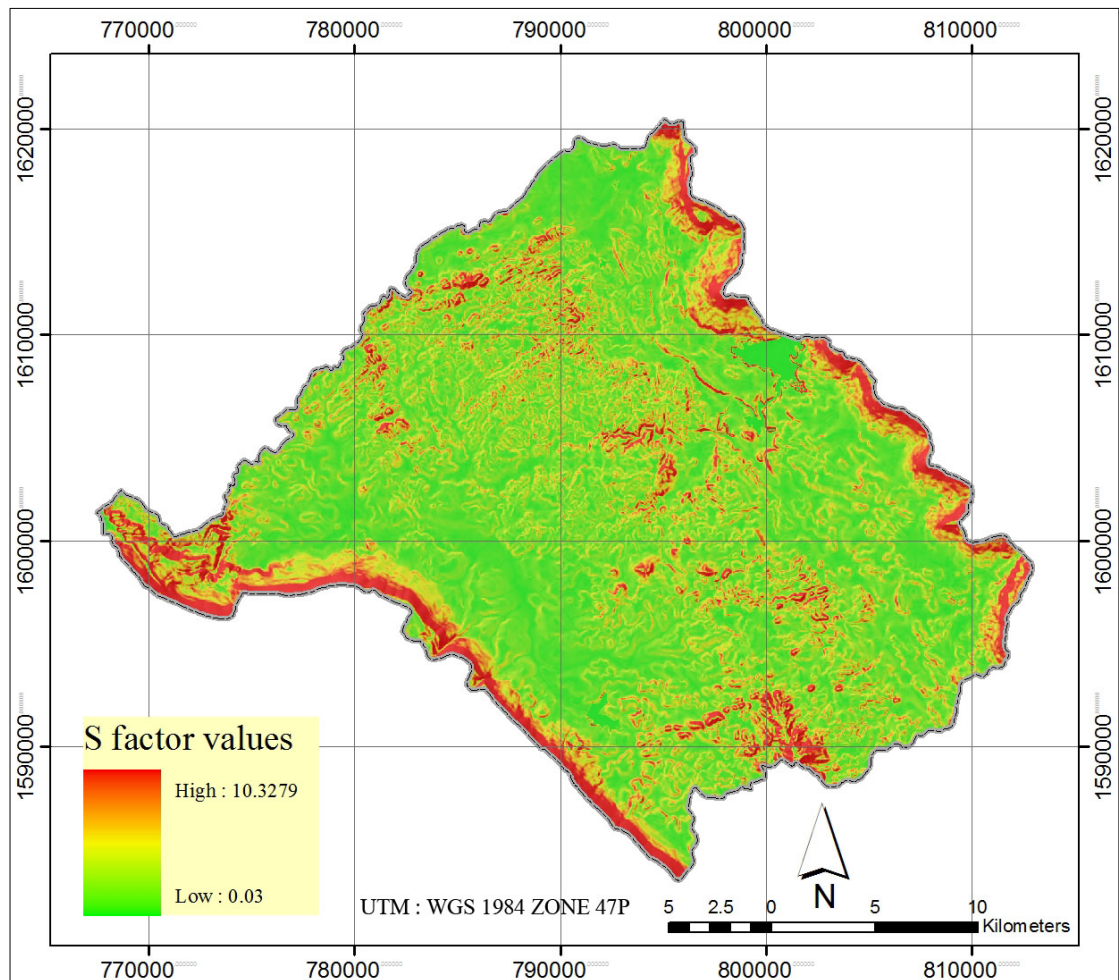


Figure 4.6 Spatial distribution of *S* factor.

4.3.2.4 Cover management factor (*C* factor)

The *C* factor reflects the effect of cropping and management practice on erosion rate, and is the factor used most often to compare the relative impacts of management option on conservation plans (Renard et al., 1997). The *C* factor has a close linkage to land use types. The more the vegetation cover increases, the soil loss decreases. In the MUSLE, the vegetation cover *C* factor is derived based on empirical equation with measurements of ground cover, aerial cover, and minimum drip height (Wischmeier and Smith, 1978). This study, *C* factor estimated using digital land use

database at scale 1:25,000 which were updated to the year 2007. Values of the C factor for land uses are available from the LDD literature (กรมพัฒนาที่ดิน, 2543) (Appendix G). The spatial distribution of crop management factor is given in Figure 4.7.

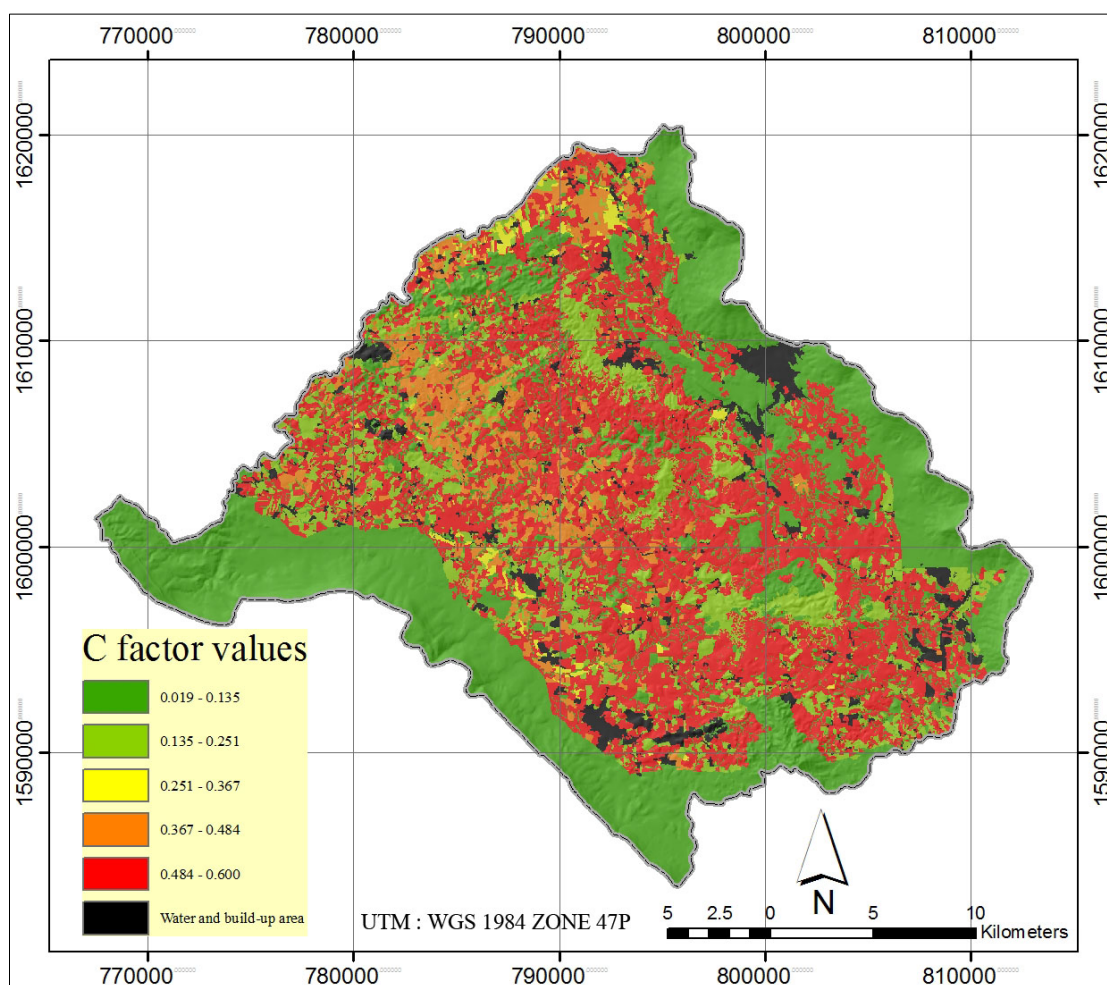
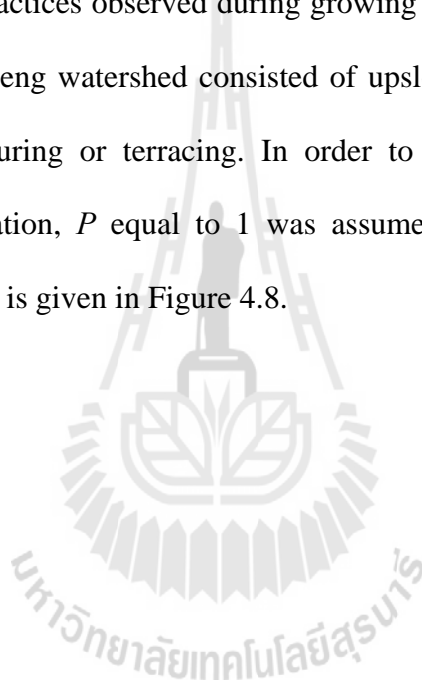


Figure 4.7 Spatial distribution of C factor.

4.3.2.5 Support practice factor (P factor)

The P factor is the ratio between soil loss with a specific support practice and the corresponding loss with upslope and downslope tillage. These practices principally affect erosion by modifying the flow pattern, grade, or direction of surface runoff and by reducing the amount and rate of runoff. For cropland, the support practices considered included contouring, strip-cropping, terracing (Renard et al., 1997). Agricultural practices observed during growing season of the year 2008 in the Upper Lam Phra Phloeng watershed consisted of upslope-downslope tillage without any significant contouring or terracing. In order to avoid the P factor from the sediment yield estimation, P equal to 1 was assumed. The spatial distribution of support practice factor is given in Figure 4.8.



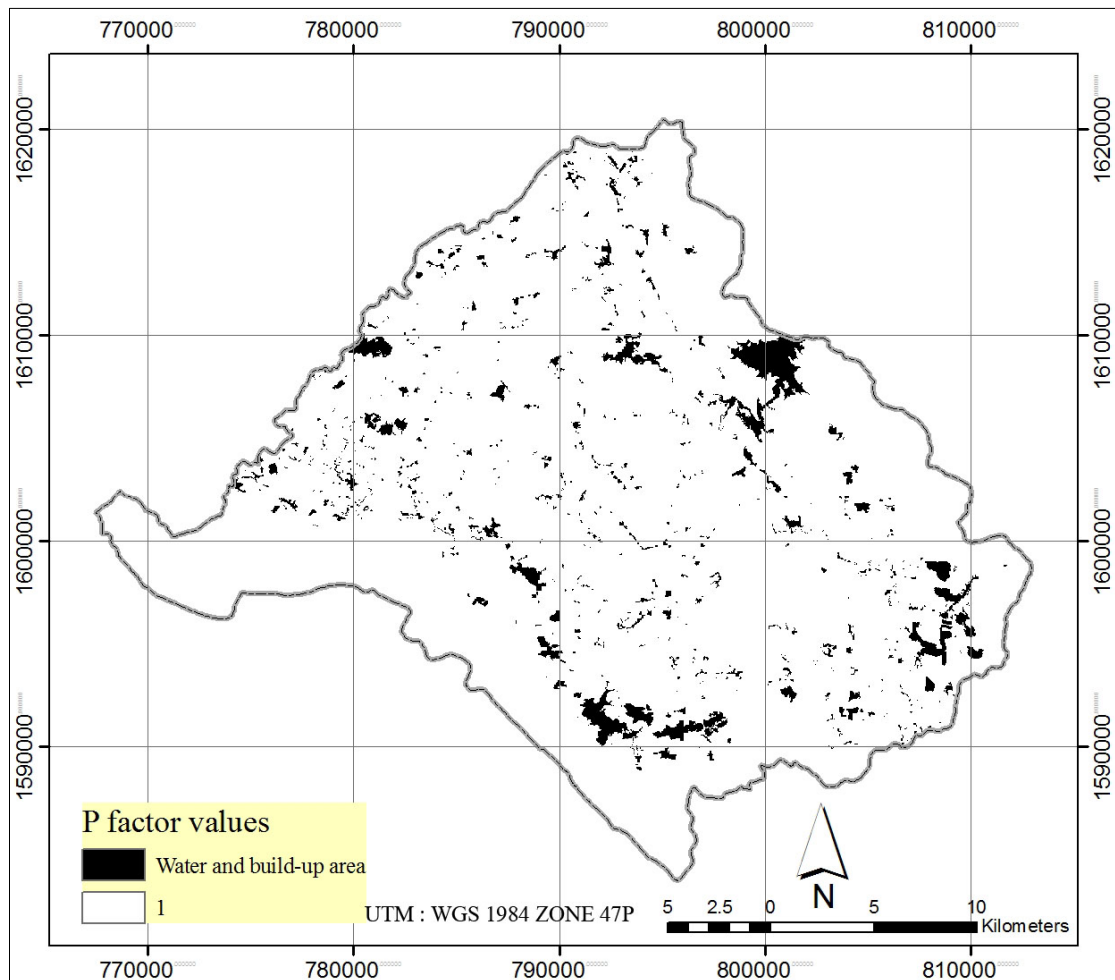


Figure 4.8 Spatial distribution of P factor.

The MUSLE was then applied for the selected storm events and using those corresponding information. The results for event-based MUSLE simulation are presents in Figure 4.9.

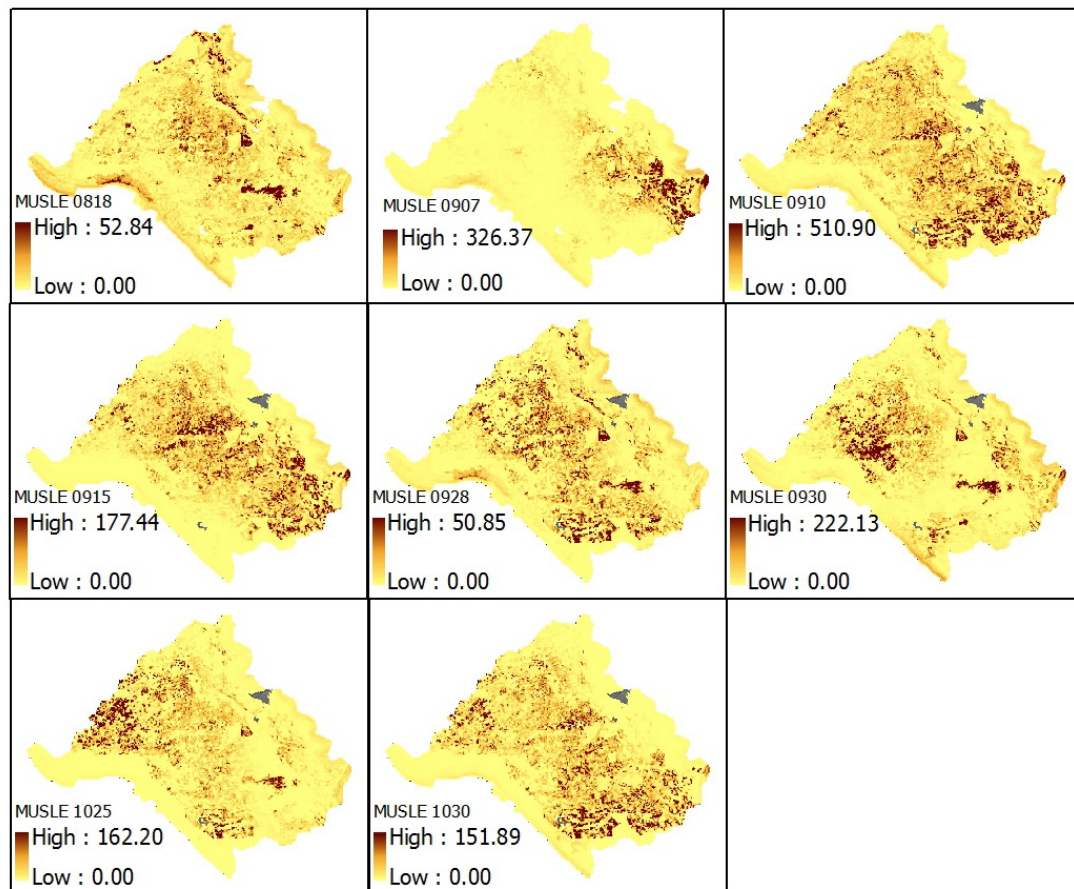


Figure 4.9 Spatial variation of event-based MUSLE simulated.

4.3.3 Sediment delivery distributed model (SEDD)

The ratio of sediment delivered to the stream channel to total soil erosion within the watershed was used in this study. The channel erosion and delivery process were not included in this study. The magnitude of the sediment delivery ratio (SDR) for particular watershed will be influenced by a wide range of geomorphological, hydrological, and watershed factors (Fu et al., 2006).

Ferro and Porto (2000) proposed to model the variability of the sediment delivery process within a watershed by calculating the SDR per cell (SDR_i) using the sediment delivery distributed model (SEDD). The SDR in grid cells is strong function

of the travel time of overland flow within the cell. The travel time is strongly dependent on the topographic and land cover characteristics of an area and therefore its relationship with SDR is justified. A SDR is not homogeneous across a watershed. Instead it varies with changes in topographic and land use. According to Stefano et al. (2000), that SDR_i indicates the probability that eroded particles mobilized from an individual cell will be transported to the nearest stream pixel and can be derived according to:

$$SDR_i = \exp(-\beta t_i) \quad (4.11)$$

where t_i is the travel time (hour) of overland flow from the i th overland grid to the nearest channel grid down the drainage path and β is a coefficient considered as constant for a given watershed.

The travel time for grid cells located in a flow path to the nearest channel can be estimated if one knows the lengths and velocities for the flow path. In raster-based GIS analysis, the direction of flow from one cell to a neighboring cell is ascertained by using an eight direction pour point algorithm. This algorithm chooses the direction of steepest descent among the eight permitted choices. Once the pour point algorithm identifies the flow direction in each cell, a cell to cell flow path is determined to the nearest stream channel and thus to the watershed outlet (Maidment, 1993). If the flow path from cell i to the nearest channel cell traverses m cells and the flow length of the i th cell is l_i (which can be equal to the length of square side or to a diagonal depending on the direction of flow in the i th cell) and the velocity of flow in cell i is

v_i , the travel time t_i from cell i to the nearest channel can be estimated by summing the time through each of m cells located in that flow path:

$$t_i = \sum_{i=1}^m \frac{l_i}{v_i} \quad (4.12)$$

The flow velocity is considered to be a function of the land surface slope and the land cover characteristics:

$$v_i = a_i \cdot S_i^b \quad (4.13)$$

where b is a numerical constant equal to 0.5 (Ferro and Minacapilli, 1995), S_i is the slope of the i th cell (m/m) and a_i is a coefficient related to land use (Haan et al., 1994) (Appendix H). Introducing equations (4.12) and (4.13) into equation (4.11) gives:

$$SDR_i = \exp\left(-\beta \sum_{i=1}^m \frac{l_i}{a_i S_i^{0.5}}\right) \quad (4.14)$$

The watershed specific parameter β depends primarily on the watershed morphological characteristics and was modeling until acceptable sediment yield predictions were obtained, using an inverse modeling approach (Saavedra, 2005). Jain and Kothiyari (2000) tested the β between 0.1 and 1.6 with an increment of 0.1 and found sediment yield is not very sensitive to the value of β used. However, Fu et al. (2006) tested β between 0.5 and 2.0 with an increment of 0.1 and found that the

sediment delivery ratio was very sensitive to the values of β vary from 0.60 ($\beta = 0.5$) to 0.27 ($\beta = 2.0$).

If Y is the amount of soil erosion produced within the i th cell of the watershed estimated using MUSLE model, the sediment yield for the watershed, S_y , during a storm event was obtained as below:

$$S_y = \sum_{i=1}^N SDR_i Y_i \quad (4.15)$$

where N is the total number of cells over the watershed and the term SDR_i is the fraction of Y_i that ultimately reached the nearest channel. Since the SDR_i of a cell is hypothesized as a function of travel time to the nearest channel, it implies that the gross erosion in that cell multiplied by the SDR_i value of the cell becomes the sediment yield contribute of that cell to nearest stream channel. This hypothesis is accurate at event scale only while it is applicable at the mean annual scale in other cases.

The SDR spatial distribution (Figure 4.10) is very important for identifying the critical sediment source and delivery areas as well as soil erosion control. The SDR average for all grid cells in the Upper Lam Phra Phloeng watershed was 0.007. (Maximum is 0.26).

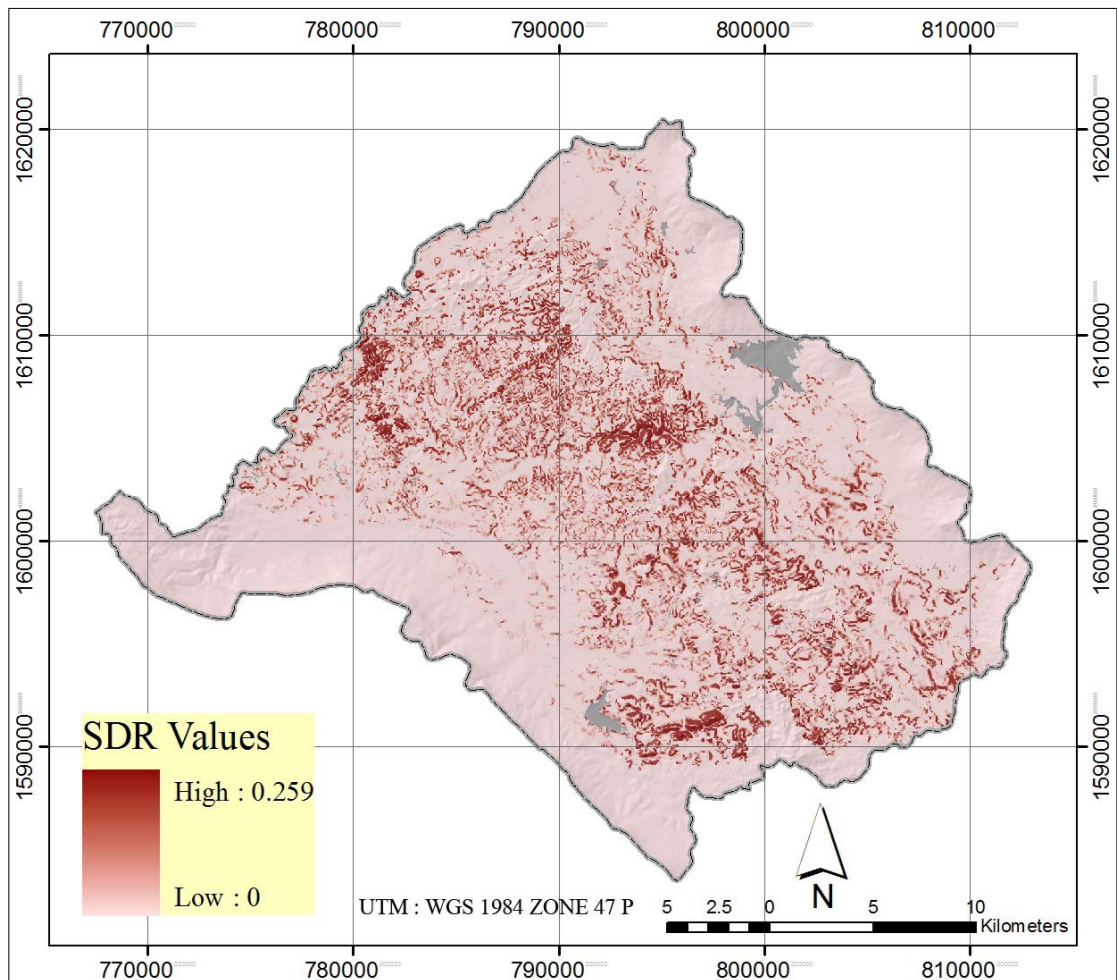


Figure 4.10 Spatial distribution of SDR.

4.3.4 Model development of grid-based approach

Each GIS layer of MUSLE and SEDD parameters was prepared in raster format with grid cell size of 30×30 meter. Each cell homogenously represents characteristics of the sedimentation factors. The computer program ModelBuilderTM of ArcGISTM was used to develop the model toolbox (Appendix I) with required sets of spatial analyses. It is a grid-based spatial analysis applying all the mathematic equations present in the MUSLE and SEDD algorithm. The soil erosion in each grid cell was computed using the MUSLE, and the routed though the watershed based on

sediment delivery ratio using SEDD model. The simulated sediment yield values were picked up from cells located at M.171 and M.145 stations. The outputs of model simulation (SY_{sim}) and field observation (SY_{obs}) of all events at these two cells were tabulated in an ExcelTM spreadsheet to estimate the statistical parameters for model evaluation.

4.3.5 Event-based sediment yield measurement

Event-based suspended sediments sampling conducted by depth integrating method. Subsamples were taken at various depths or distances from the stream bank, and integrated into a single sample. The collection of sediment samples was attempted to conduct coincides with the runoff peaks, and also temporally over the rising and descending portion of the hydrograph curve. Prior to collecting a sample, measurement of the stream velocity was conducted. The instrument used is US.DH 59-40P (from RID). The instrument was winch operated from a bridge (M.171) and a cable-way (M.145). The suspended sediment concentration samples were then analyzed after drying at 103°C and necessary calculations were consequently conducted. The amount of total sediment yield was then calculated based on the sediment concentration and runoff volume (RID). These steps are shown in Figure 4.11.

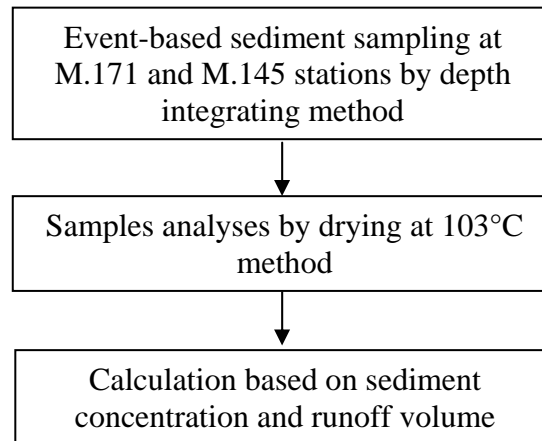


Figure 4.11 Flow diagrams of event-based sediment yield measurement.

Although an attempt was made to collect samples for every storm event, some storm events were not sampled due to unforeseen circumstances, such as equipment malfunctions. Therefore, comparison between model simulation and observed results were made only sixteen samples at two stations.

The observed data was used for model evaluation as shown in Table 4.1.

Table 4.1 Observed sediment yield data at M.171 and M.145 stations.

Observed date	M.171 station			M.145 station		
	River Discharge (Million cubic meters)	Sediment concentration (mg/kg)	Sediment yield (tons)	River Discharge (Million cubic meters)	Sediment concentration (mg/kg)	Sediment yield (tons)
20080818	0.04	3,753.33	149.17	0.15	1,107.78	166.54
20080907	0.55	2,050.00	1,128.25	0.27	998.00	269.03
20080910	16.35	2,312.00	37,797.98	3.23	932.00	3,006.80
20080915	5.85	1,690.00	9,883.82	1.24	878.00	1,089.34
20080928	1.23	160.00	196.02	0.53	186.00	98.99
20080930	3.21	980.00	3,143.87	1.60	764.00	1,225.80
20081025	3.08	188.00	579.39	2.42	175.00	423.81
20081030	3.62	156.00	564.07	2.13	145.00	308.19

4.4 Results and discussion

4.4.1 Model calibration

The grid-based watershed parameters and the runoff factor collected for 16 storm events occurring in 2008 rainy season were used to apply the MUSLE and SEDD models. Eight selected events were used for model calibration. A part of calibration procedure was done by adjusting “ β ” values in the Eq. 4.14 in such manner that the calculated coefficient of efficiency (E) for all calibration events would be highest.

The sediment yield calibration results show that the model provides the best simulation results with $E = 0.85$, $R^2 = 0.89$ when adjusting β (watershed specific parameter in Eq. 4.14) = 0.2. The calibration results for simulated sediment yield are presented in Table 4.2.

Table 4.2 Data comparison of sediment yield simulation (SY_{sim}) and observation (SY_{obs}) of eight events for sediment yield model calibration.

Calibration events	Antecedent soil moisture condition (AMC)	Sediment yield (metric tons)		
		Observed (SY_{obs})	Simulated (SY_{sim})	$Dv(\%)$
M171_20081030	Normal	564.06	6,285.71	- 1,014.35
M171_20080930	Dry	3,143.87	1,563.78	50.26
M171_20080818	Dry	149.17	406.55	- 172.54
M171_20080910	Wet	37,797.98	28,470.30	24.68
M145_20081030	Normal	308.19	2,854.50	- 826.22
M145_20080930	Dry	1,225.80	988.92	19.32
M145_20080818	Dry	166.54	135.92	18.39
M145_20080910	Wet	3,006.80	10,305.40	- 242.74
Total		46,362.42	51,011.08	
Coefficient of efficiency (E)			0.85	
Coefficient of determination (R^2)			0.89	
Average deviation (%)			- 267.90	
Root Mean Square Error ($RMSE$)			4,771.22	

The scatter plot of observed and simulated sediment yield for calibration events along with 1:1 line (dash line) are shown in Figure 4.12. It is observable that the relation line is slightly above the 1:1 line when the sediment yield is approximately higher than 8,000 metric tons, indicating that the model slightly underestimates in heavier events. However, the number of events is too small. The result is not well distributed of scatter plot.

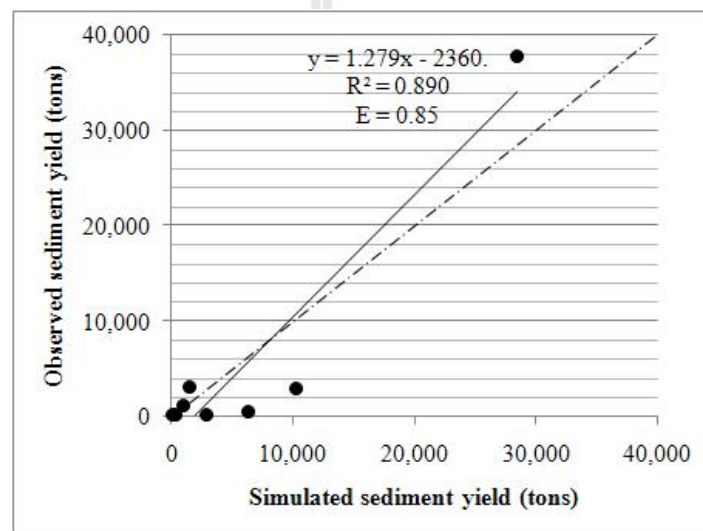


Figure 4.12 Scatter plot of results of observed and simulated sediment yield.

4.4.2 Model validation

Other eight events were for the model validation. The validation results show that $E = 0.79$ and $R^2 = 0.92$. The validation results for simulated sediment yield are presented in Table 4.3 and Figure 4.13.

Table 4.3 Data comparison of calibrated-sediment yield simulation (SY_{sim}) and observation (SY_{obs}) of eight events for sediment yield model validation.

Validation events	Antecedent soil moisture condition (AMC)	Sediment yield (metric tons)		
		Observed (SY_{obs})	Simulated (SY_{sim})	Dv(%)
M171_20081025	Dry	579.39	2,242.69	- 287.07
M171_20080928	Dry	196.02	1,159.69	- 491.61
M171_20080907	Normal	1,128.25	1,803.25	- 59.83
M171_20080915	Wet	9,883.82	6,703.69	32.18
M145_20081025	Dry	423.81	1,682.77	- 297.05
M145_20080928	Dry	98.99	592.35	- 498.37
M145_20080907	Normal	269.03	93.60	65.21
M145_20080915	Wet	1,089.34	1,586.53	- 45.64
Total		13,668.67	15,864.56	
Coefficient of efficiency (E)			0.79	
Coefficient of determination (R^2)			0.92	
Average deviation (%)			- 197.77	
Root Mean Square Error ($RMSE$)			1,430.49	

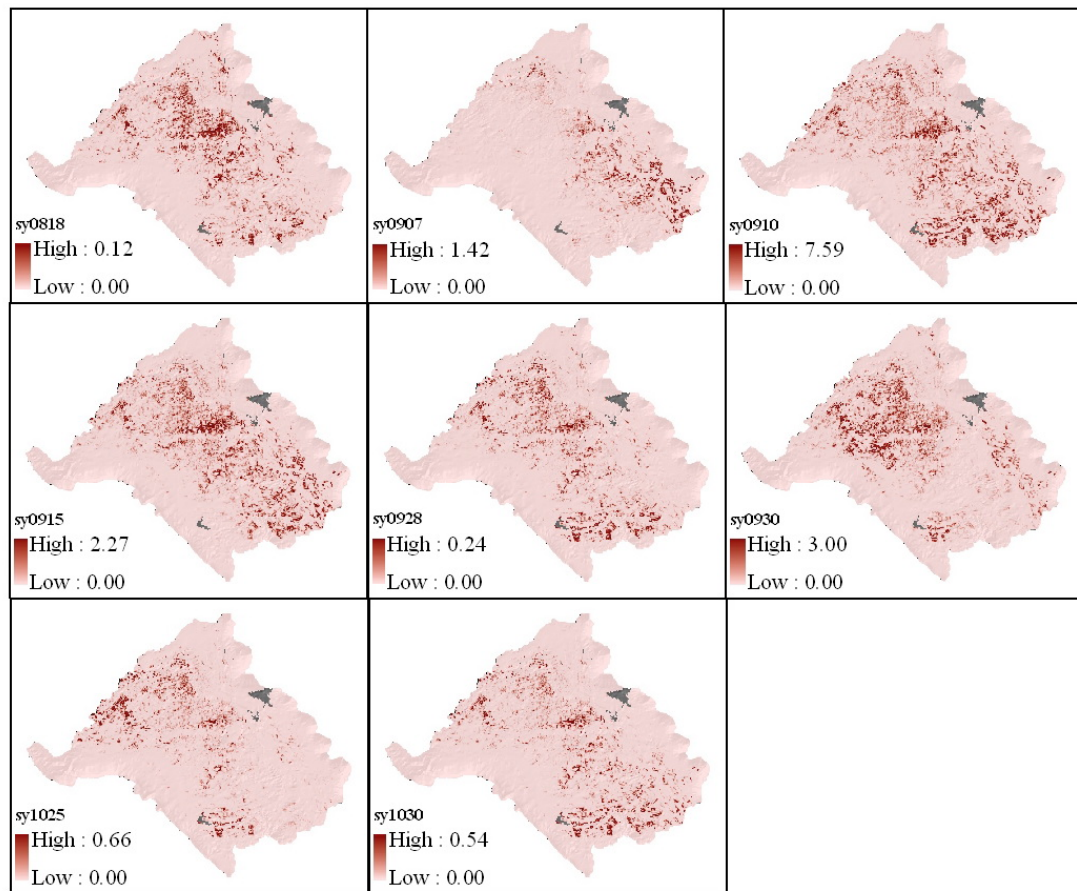


Figure 4.13 Spatial variation of event-based simulated sediment yields.

The scatter plots of observed and calibrated-simulated sediment yields for event validation along with 1:1 line are shown in Figure 4.14. It is observable that the relation line is slightly above the 1:1 line when the sediment yield is approximately higher than 2,500 metric tons, indicating that the model slightly underestimates in heavier events.

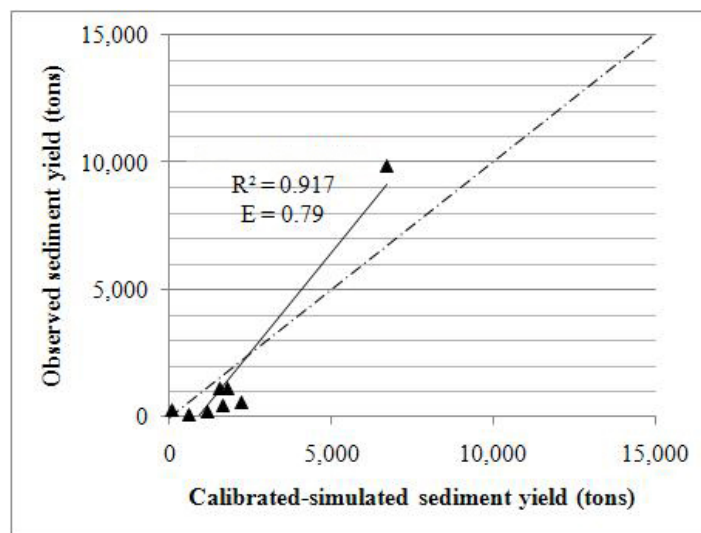


Figure 4.14 Relationships of observed and calibrated-simulated sediment yield for model validation.

Similar results of high deviation for sediment yield model was found in the Najim et al. (2006), Shamshad et al. (2008), Cho et al. (2008), Shrestha et al. (2006), and Haregeweyn and Yohannes (2003). Accordingly the studies on NPS model concluded that the model is good in simulation runoff while other outputs such as sediment yield are only of moderate accuracy. For the low rainfall events, the model simulation is overestimated and for the high rainfall events the model simulation is underestimated. In reality, the heavier events cause the erosion of river stream banks

which in this study was ignored. Normally, the larger runoff has the bigger sediment transport capacity and thus can delivery more sediment to the outlet.

The higher error in sediment yield, compared to the runoff simulation, can be explained by the selected sampling method. An appropriate sampling method is necessary in order to obtain a representative sediment yield for each storm event. The concentration of suspended solids can be affected by flow rate and sampling time. In this study, depth integrating was operated manually during storm event with limitation of labor and time. Therefore, the sediment data may not be completely representative of the watershed conditions.

The obvious error encountered in events measured at M.171 and M.175 stations could be explained that the models really provide every cell simulation and accumulate them from upstream to the cells at the stations while the observations were hardly possible to represent all activities and results from those cells even though samples were collected at the instant time of expected peak of the flow. This could be because of too high spatial and temporal variations of dynamic variables such as rainfall and erosion process. Additionally, time-series manual sampling when peak of flows are not practically and instantly realized in the field investigation are hard to perform.

Although, event-based sediment yield estimations are in the range of moderate accuracy. Comparison of individual events may not agree as well as observed values. However, the performance of the model estimation the sediment yield can be increased by improving the input parameters for both MUSLE and SEDD. These can done by developing suitable methodologies to estimate the peak discharge factor, better seasonal change of crop growth period in the watershed. This chapter therefore

revealed that, in general, the MUSLE and SEDD model can be acceptably used in simulating sediment yield in the Upper Lam Phra Phloeng watershed.

4.5 Conclusion

As researcher mention above, the results of MUSLE and SEDD with geospatial modeling can be applied to sediment yield simulations with acceptable accuracy with E is 0.79 and R^2 is 0.92. Not only the satisfied quantitative results provided but the model is also able to estimate varying sediment yield over the watershed spatially. Although, the biggest deviation for event-based simulation and observed data but trends in the sediment simulated matched observed data. However, though the results were not very good, it was still able to represent a certain portion of variability in the observed data. For annual estimation, accumulation of all events obtained by this model simulation should be acceptable. As the result of the case study at the Upper Lam Phra Phloeng watershed, it can be confirmed that MUSLE and SEDD with geospatial modeling is applicable to sediment yield estimation effectively, however, with lower accuracy than the runoff model. The system parameters used in sediment yield model such as K factor, L factor, and S factor were used to develop the NPS potential index in Chapter VI.

4.6 References

กรมพัฒนาที่ดิน. (2543). การชะล้างพังทลายของดินในประเทศไทย. กรุงเทพฯ: กรมพัฒนาที่ดิน
กระทรวงเกษตรและสหกรณ์.

นิพนธ์ ตั้งจจธรณ. (2545). แบบจำลองคณิตศาสตร์การชะล้างพังทลายของดิน และมลพิษตะกอนใน

พื้นที่ลุ่มน้ำ. กรุงเทพฯ: ภาควิชาอนุรักษ์วิทยา คณะวนศาสตร์ มหาวิทยาลัยเกษตรศาสตร์.

Cho, J., Park, S., and Im, S. (2008). Evaluation of Agricultural Nonpoint Source (AGNPS) model for small watersheds in Korea applying irregular cell delineation. **Agricultural Water Management**. 95: 400-408.

Ferro, V., and Minacapilli, M. (1995). Sediment delivery processes at basin scale. **Hydrological Sciences**. 40(6): 703-717.

Ferro, V., and Porto, P. (2000). Sediment delivery distributed (SEDD) model. **Journal of Hydrologic Engineering**. 5(4): 411-422.

Fu, G., Chen, S., and McCool, D.K. (2006). Modeling the impacts of no-till practice on soil erosion and sediment yield with RUSLE, SEDD, and ArcView GIS. **Soil & Tillage Research**. 85: 38-49.

Haan, C.T., Barfield, B.J., and Hayes, J.C. (1994). **Design hydrology and sedimentology for small catchments**. Academic Press.

Haregeweyn, N., and Yohannes, F. (2003). Testing and evaluation of the agricultural non-point source pollution model (AGNPS) on Augucho catchment, western Hararghe, Ethiopia. **Agricultural, Ecosystems and Environment**. 99: 201-212.

Jain, M.K., and Kothiyari, U.C. (2000). Estimation of soil erosion and sediment yield using GIS. **Hydrological Science Journal**. 45: 771-786.

Kinnell, P.I.A. (2005). Why the universal soil loss equation and the revised version of it do not predict event erosion well. **Hydrological Processes**. 19: 851-854.

Lal, R. (1994). **Soil erosion research methods**. 2nd. Delray Beach, FL: St. Lucie Press.

- Maidment, D.R. (1993). Developing a spatially distributed unit hydrograph by using GIS. In **Proceeding of International Conference of HydroGIS 1993**. (pp 181-192). Vienna, Austria: International Association of Hydrological Sciences.
- McCool, D.K., Brown, L.C., Foster, G.R., Mutchler, C.K., and Meyer, L.D. (1987). Revised slope steepness factor for the universal soil loss equation. **Transaction of the American Society of Agricultural and Biological Engineers**. 30(5): 1387-1396.
- Najim, M.M.M., Babel, M.S., and Loof, R. (2006). AGNPS model assessment for a mixed forest watershed in Thailand. **Science Asia**. 32: 53-61.
- Natural Resources Conservation Service [NRCS] (1986). **Urban hydrology for small watersheds TR-55**. The U.S. Department of Agriculture.
- Nearing, M.A., Norton, L.D., and Zhang, X. (2000). Soil erosion and sedimentation. In Ritter, W.F., and Shirmohammadi, A. (Eds.). **Agricultural nonpoint source pollution: Watershed management and hydrology**. United States: Lewis Publishers.
- Ongley, E.D. (1996). **Control of water pollution from agriculture**. FAO irrigation and drainage paper 55.
- Ouyang, D., and Bartholic, J. (1997). Predicting sediment delivery ratio in Saginaw Bay watershed. In **The 22nd National Association of Environmental Professionals Conference Proceedings 1997**. (pp 659-671). Orlando, FL: National Association of Environmental Professionals.

- Renard, K.G., Foster, G.R., Weesies, G.A., McCool, D.K., and Yoder, D.C. (1997). **Predicting soil erosion by water: A guide to conservation planning with the Revised Universal Soil Loss Equation (RUSLE)**. USDA – Agricultural Handbook No. 703.
- Saavedra, C. (2005). **Estimating spatial patterns of soil erosion and deposition in the Andean region using geo-information techniques**. Ph.D. Dissertation, Wageningen University, Netherlands.
- Sadeghi, S.H. (2004). Application of MUSLE in prediction of sediment yield in Iranian conditions. In **13th International Soil Conservation Organization Conference 2004**. Brisbane, Australia.
- Shrestha, S., Babel., Gupta, A.D., and Kazama, F. (2006). Evaluation of annualized agricultural nonpoint source model for a watershed in the Siwalik Hills of Nepal. **Environmental Modelling & Software**. 21: 961-975.
- Stefano, C.D., Ferro, V., Palazzolo, E., and Panno, M. (2000). Sediment delivery processes and agricultural non-point pollution in a Sicilian basin. **Journal of Agricultural Engineering Research**. 77(1): 103-112.
- Tangtham, N., and Lorsirirat, K. (1993). Prediction models of the effect of the basin characteristics and forest cover on reservoir sedimentation in Northeastern Thailand. **Kasetsart Journal (Natural Science)**. 27: 230-235.
- Thinley, U. (2008). **Spatial modeling for soil erosion assessment in Upper Lam Phra Phloeng watershed, Nakhon Ratchasima, Thailand**. M.Sc. Thesis, Suranaree University of Technology.
- Vieux, B.E. (2004). **Distributed hydrologic modeling using GIS**. 2nd. Dordrecht: Kluwer Academic Publishers.

Williams, J.R. (1975). Sediment-yield prediction with universal equation using runoff energy factor. In **Present and perspective technology for predicting sediment yield and sources**. (pp 244-252). Washington: U.S. Government Printing Office.

Wischmeier, W.H., and Smith, D.D. (1978). **Predicting rainfall erosion losses**. USDA Agricultural Research Services Handbook 537: Washington.

Zhang, Y., Degroote, J., Wolter, C., and Sugumaran, R. (2009). Intergration of modified universal soil loss equation (MUSLE) into a GIS framework to assess soil erosion risk. **Land Degradation & Development**. 20: 84-91.



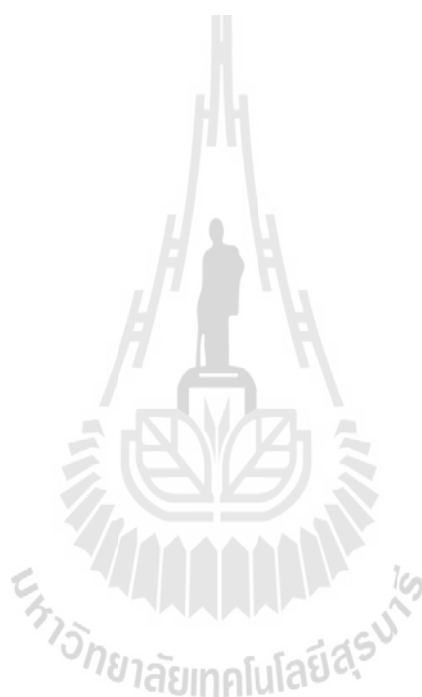
CHAPTER V

NUTRIENT YIELD ESTIMATION USING GRID-BASED AGNPS MODEL

5.1 Abstract

This chapter employed grid-based nutrient yield model for estimation of nutrient yield which are nitrogen and phosphorus in the Upper Lam Phra Phloeng watershed. Nutrient yield portion is subdivided into soluble form and sediment-attachment form. The method used in AGNPS model is selected to simulate the nutrient processes. The AGNPS algorithm integrated with geospatial model was developed. Eight events were used for the model calibration with nutrient yield data observed at two stations (M.171 and M.145). Other eight were for the model validation. The calibration was performed by adjusting nitrogen and phosphorus extraction coefficient. The calibration results show that nitrogen and phosphorus yields in runoff simulation were obtained with $E = 0.82$, $R^2 = 0.91$ and $E = 0.92$, $R^2 = 0.96$, respectively, and nitrogen and phosphorus yields in sediments produced same results with $E = 0.90$, $R^2 = 0.93$. The validation results show that nitrogen and phosphorus yields in runoff simulation produced slightly good results with $E = 0.63$, $R^2 = 0.89$ and $E = 0.52$, $R^2 = 0.78$, respectively, and nitrogen yield in sediment produced good results with $E = 0.70$ and $R^2 = 0.93$ while phosphorus yield in sediment produced poor results with $E = 0.13$ and $R^2 = 0.87$. Overall, the evaluation

of the grid-based nutrient yield model demonstrated that this model can be used as a NPS management tool within the Upper Lam Phra Phloeng watershed. Results of this study also indicated that more studies are needed to improve accuracy for each storm event. In addition to improve model performance, detailed of input data are needed for further analyses. However, for annual estimation, accumulation of all events obtained by this model simulation should be acceptable.



5.2 Introduction

Rainfall – runoff event is a phenomenon that impacts NPS pollution on surface water quality. It produced both excessive runoff and sediment. Nutrient yield loss associated with rainfall-runoff events is due to surface flow, erosion, and leaching. Soluble nutrients are transported by surface flow. Nutrients adsorbed to sediment particles are transported by erosion. Nutrients leaching by percolating water to groundwater are not considered in this study. Phosphorus and nitrogen deal with in this study are the two plants nutrients most frequently associated with water quality.

The high potential pollution, due to erosion from tillage processes as well as excessive nutrients from agricultural activities, has degraded the quality of water.

Data on nutrient yield with runoff and sediment are essential for accurate evaluating impact of NPS pollution, and for assessing the environmental impact including deterioration on surface water quality (Hussein et al., 1999). The *in situ* measurement of nutrient yield is considered more accurate but cannot be operated anytime and anywhere as required. Therefore, the accurate nutrient yield modeling developed can serve this purpose with more convenient and less time consuming.

The objective of this chapter is to estimation nutrient yield both soluble and sediment-attached forms by using grid-based nutrient yield model in which heterogeneous watershed characteristics were considered. Finally, the output from model was evaluated by comparing with the observed nutrient yield.

5.3 Materials and methods

The nutrient yield model estimates yield of nitrogen and phosphorus throughout the watershed. The nutrient yield portion is subdivided into one part handling soluble fractions and another part handling sediment-attached pollutants.

The method selected to simulate the nutrient processes for geospatial model are based on AGNPS (Agricultural Non-Point Source Pollution Model) (Young et al., 1986) developed from earlier CREAMS (Chemicals, Runoff and Erosion from Agricultural Management Systems) model (Frere et al., 1980). The model considers soluble and sediment-attached nutrients separately. These algorithms are the most widely used and accepted. Further details can be found in the technical documentation on nutrient information from AGNPS model. Understanding the technical processes of the model is essential as the study attempts to modify input parameters that best suit the local watershed conditions.

This section described the models from the geospatial integration perspective. The algorithms and equations were coded in ModelBuilder™ of ArcGIS™ with required sets of spatial analyses (Appendix J). The nutrient yield in each grid cell was computed using the AGNPS algorithm, and then routed through the watershed based on flow accumulation algorithm. The simulated nutrient yield values were picked up from cells located at M.171 and M.145 stations. The outputs of the model simulations and field observations of all events at these two cells were tabulated in an Excel™ spreadsheet to estimate the statistical parameters for model evaluation.

5.3.1 Nitrogen yield in runoff simulation model

For the soluble part, the general assumption is that the rate of change in concentration of soluble nutrients in the surface is proportion to the difference between existing concentrations and concentration in rainfall. The available nitrogen content in the surface is a result of combining the residual nitrogen in the surface with amount from the fertilizer application. The available nitrogen due to rainfall is estimated with the nitrogen concentration in rainfall and given as input data. The movement rates are evaluated using nitrogen leaching and runoff extraction coefficients given as input data for the model.

The soluble nitrogen concentration in the runoff is calculated with (Young et al., 1986):

$$C_{RON} = \frac{(N_{AVS} - N_{AVR})}{F_{POR}} \left[e^{(-N_{DMV}I_{EFF})} - e^{(-N_{DMV}I_{EFF} - N_{RMV}R_{OFF})} \right] + \frac{N_{RNC}R_{OFF}}{P_{EFF}} \quad (5.1)$$

where C_{RON} is the soluble nitrogen concentration in runoff (kg/cell), N_{AVS} is the available nitrogen content in the surface (kg/cell), N_{AVR} is the available nitrogen in rainfall (kg/cell), N_{DMV} is the rate for downward movement of nitrogen into the soil, N_{RMV} is the rate for nitrogen movement into the runoff, I_{EFF} is the effective or total infiltration (mm), R_{OFF} is the total runoff (mm), F_{POR} is a porosity factor, N_{RNC} is the nitrogen contribute due to rain (kg/cell), and P_{EFF} is the effective precipitation (mm).

The available nitrogen content in the surface is a result of combining the residual nitrogen in the surface with the amount from the fertilizer application:

$$N_{AVS} = [Sol_N + (N_{FER}N_{fa})]F_{POR} \quad (5.2)$$

where Sol_N is the soluble nitrogen in the surface centimeter of the soil (kg/cell), N_{FER} is the nitrogen fertilizer application (kg/cell) given as a input data for the model, N_{fa} is the fraction of nitrogen availability for the fertilizer application also given as input data.

The soluble nitrogen in the surface top of the soil is estimated by:

$$Sol_N = 0.10N_{CPW}Por \quad (5.3)$$

where N_{CPW} is the nitrogen concentration in the pore water of the top centimeter of surface soil varying with soil series obtained from LDD and field investigation, Por is the soil porosity.

The porosity and porosity factor are calculated with the bulk density, σ , values for the soil as:

$$Por = 1 - (\sigma / 2.65); \quad F_{POR} = 0.00001 / Por \quad (5.4)$$

The available nitrogen due to rainfall is:

$$N_{AVR} = N_{CRN} \times 10^{-6} \quad (5.5)$$

where N_{CRN} is the nitrogen concentration in the rainfall (ppm) and is given as input data. The movement rates are evaluated using:

$$N_{DMV} = \frac{N_{LEC}}{10Por}; \quad N_{RMV} = \frac{N_{REC}}{10Por} \quad (5.6)$$

where N_{LEC} is the nitrogen leaching extraction coefficient and N_{REC} is the nitrogen runoff extraction coefficient, both given as input data for model. The 10 in the equation is the depth of soil interaction in millimeters, giving to the movement rates units of (mm^{-1}) that will cancel with the (mm) from infiltration and runoff in equation (5.1). In the model the infiltration is calculated simply by subtracting the runoff from amount of rainfall, while the runoff is calculated with the grid-based curve number method.

For the nitrogen contribution due to rain, N_{RNC} , the following expression is used:

$$N_{RNC} = 0.01(N_{CRN})P \quad (5.7)$$

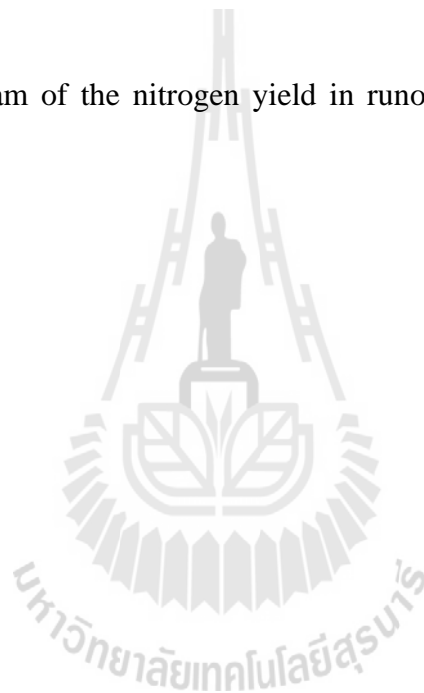
where P is the storm precipitation (mm) and the 0.01 is a unit conversion factor.

The effective precipitation is related to the precipitation and soil porosity by:

$$P_{EFF} = P - (10Por) \quad (5.8)$$

The 10 in the equation is the top 1 cm in millimeters of soil interaction. The precipitation values will be taken from the rain gauge by interpolation technique as rainfall in a cell.

The flow diagram of the nitrogen yield in runoff estimation for this study is shown in Figure 5.1.



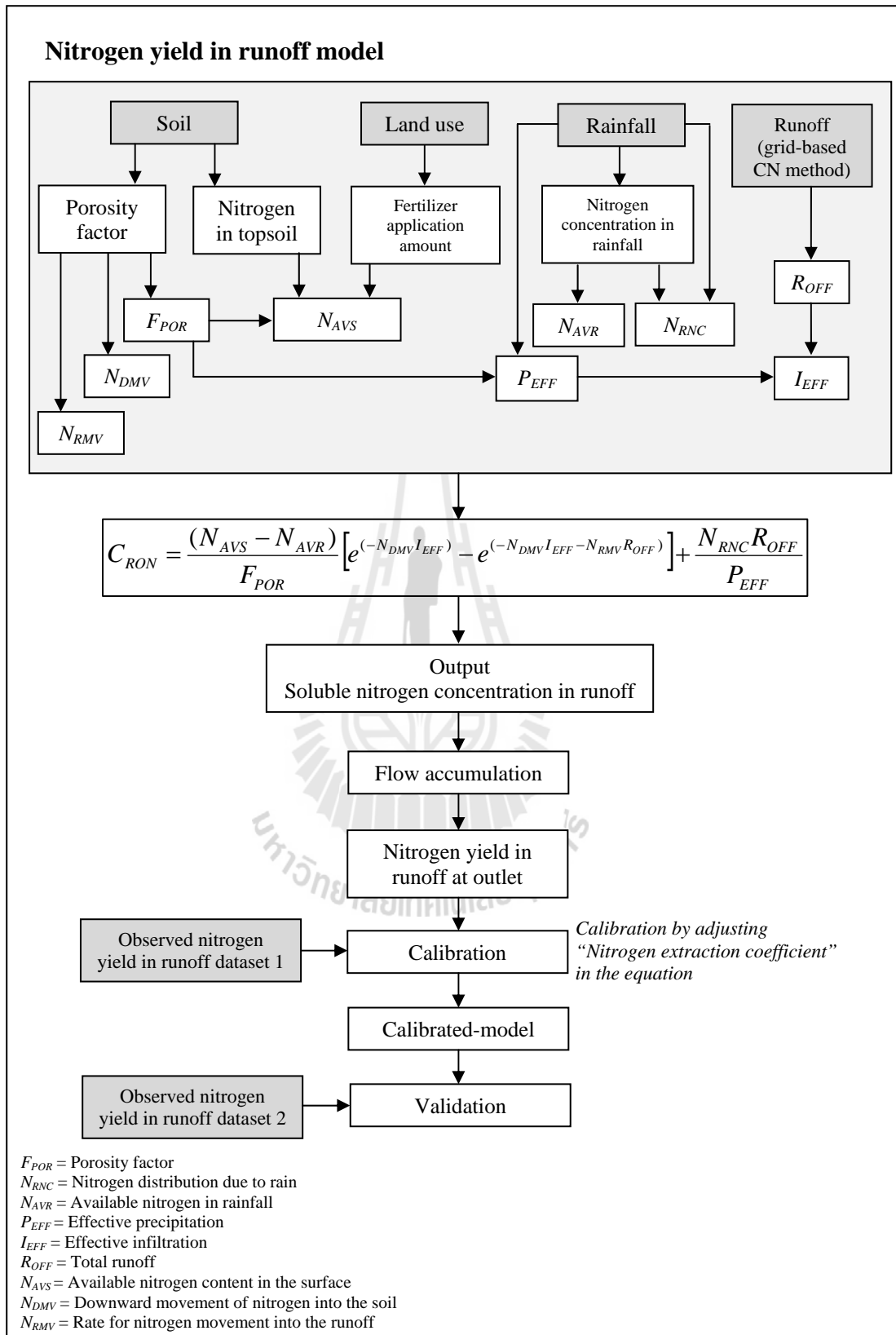


Figure 5.1 Flow diagrams of the nitrogen yield in runoff estimation.

5.3.2 Phosphorus yield in runoff simulation model

The sequence of phosphorus yield estimation is similar to the one of nitrogen except that the effects of rainfall are omitted. This is due to the fact that very little soluble phosphorus is found in rainfall. The equation used to predict soluble phosphorus in the runoff is (Young et al., 1986):

$$C_{ROP} = \frac{(P_{AVS} - P_{AVR})}{F_{POR}} [e^{(-P_{DMV}I_{EFF})} - e^{(-P_{DMV}I_{EFF} - P_{RMV}R_{OFF})}] + \frac{P_{AVR}P_{RMV}R_{OFF}}{F_{POR}} \quad (5.9)$$

where C_{ROP} is the soluble phosphorus concentration in runoff (kg/cell), P_{AVS} is the available phosphorus in the surface due to fertilizer application (kg/cell), P_{AVR} is the available phosphorus due to residual levels in the soil (kg/cell), P_{DMV} and P_{RMV} are the movement rates for leaching and runoff respectively. The rest of the terms are the same as in the nitrogen calculations:

$$P_{AVS} = [Sol_p + (P_{FER}P_{fa})]F_{POR} \quad (5.10)$$

where Sol_p is the soluble phosphorus in the surface centimeter of the soil (kg/cell), P_{FER} is the phosphorus fertilizer application (kg/cell), P_{fa} is the fraction of phosphorus availability for the fertilizer application. The soluble phosphorus in the surface top of the soil is estimated by:

$$Sol_p = 0.10P_{CPW}Por \quad (5.11)$$

where P_{CPW} is the phosphorus concentration in the pore water of the top centimeter of surface soil varying with soil series obtained from LDD and field investigation.

The available phosphorus due to initial soil residuals is solved using the equation:

$$P_{AVR} = Sol_p F_{POR} \quad (5.12)$$

The movement rates are evaluated using:

$$P_{DMV} = \frac{P_{LEC}}{10P_{or}}; \quad P_{RMV} = \frac{P_{REC}}{10P_{or}} \quad (5.13)$$

where P_{LEC} is the phosphorus leaching extraction coefficient and P_{REC} is the phosphorus runoff extraction coefficient, both given as input data for the model. The rest of the terms are the same as in the nitrogen calculations.

The flow diagram of the phosphorus yield in runoff estimation for this study is shown in Figure 5.2.

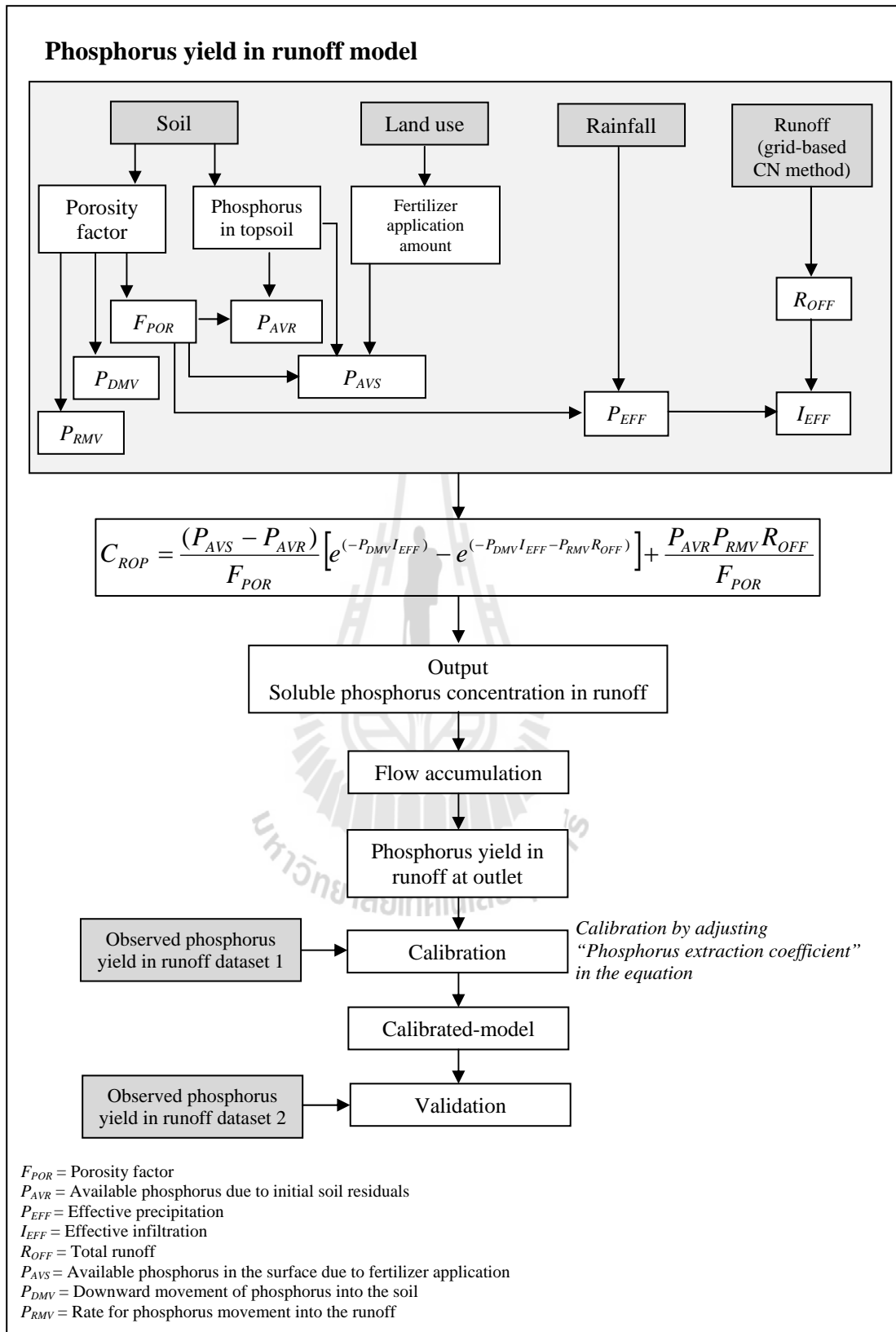


Figure 5.2 Flow diagrams of the phosphorus yield in runoff estimation.

5.3.3 Nitrogen yield in sediment simulation model

The nitrogen yield in the sediment is calculated using total sediment yield from a cell as following equation (Young et al., 1986):

$$N_{SED} = N_{SCN} Y_{SED} ER \quad (5.14)$$

where N_{SED} is the overland nitrogen transported by the sediment (kg/cell), N_{SCN} is the soil nitrogen concentration (g N/g soil), Y_{SED} is the total sediment yield (kg/cell), and ER is the nutrient enrichment ratio calculated with:

$$ER = aY_{SED}^b T_f \quad (5.15)$$

where a and b are experiment constants with values of 7.4 and -0.20 respectively. T_f is a correction factor for soil texture and has values of 0.85 for sand, 1.0 for silt, 1.15 for clay and 1.50 for peat. The flow diagram of the nitrogen yield in sediment estimation for this study is shown in Figure 5.3.

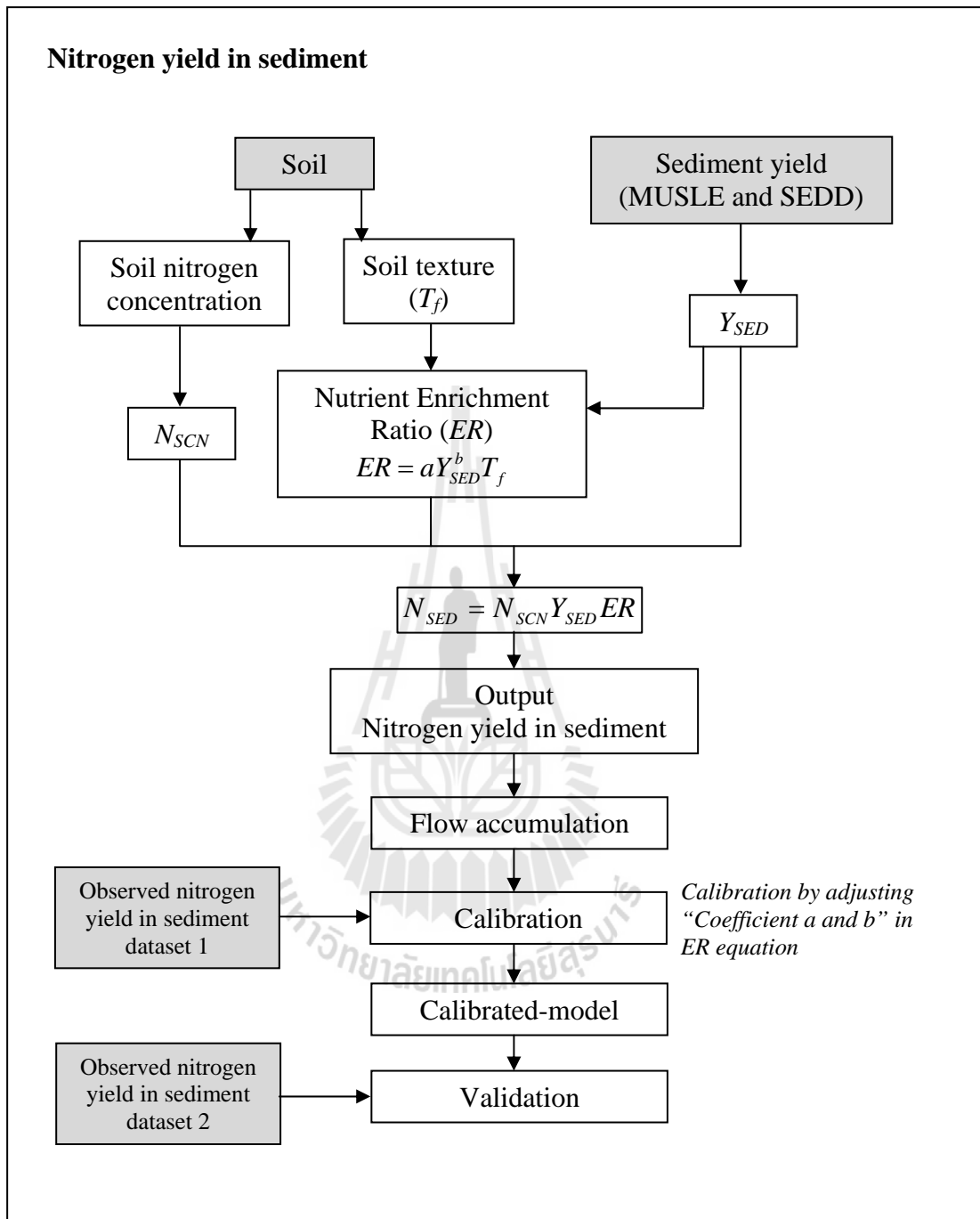


Figure 5.3 Flow diagrams of the nitrogen yield in sediment estimation.

5.3.4 Phosphorus yield in sediment simulation model

Phosphorus pollutant is closely correlated with soil erosion. The phosphorus exported from each cell unit can be roughly estimated on the basis of the product of phosphorus content in the surface soil layers, the sediment yield, and the phosphorus enrichment ratio (which is dependent on soil texture) (Krysanova et al., 2000).

To estimate phosphorus yield in the sediment is calculated using total sediment yield from a cell as following equation (Young et al., 1986):

$$P_{SED} = P_{SCN} Y_{SED} ER \quad (5.16)$$

where P_{SED} is the overland phosphorus transported by the sediment (kg/cell), P_{SCN} is the soil phosphorus concentration (g P/g soil). The rest of the terms are the same as in the nitrogen yield in sediment calculations. The flow diagram of the phosphorus yield in sediment estimation for this study is shown in Figure 5.4.

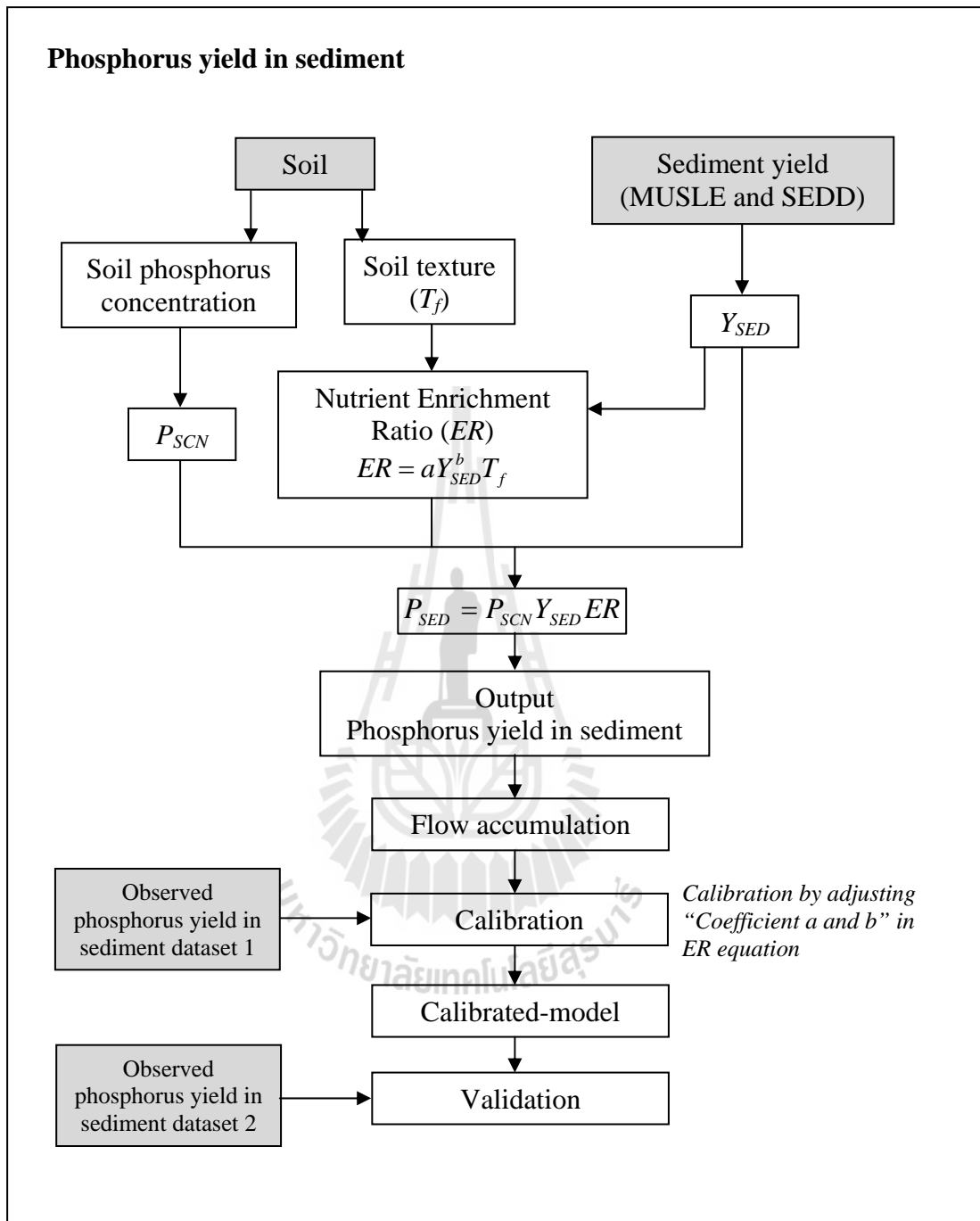


Figure 5.4 Flow diagrams of the phosphorus yield in sediment estimation.

5.3.5 Nutrient observation and analysis

The field observations were conducted on rainstorm events during July-October 2008. The purpose of the field observations was collecting soluble nutrients and sediment-attached nutrients.

Water samples were collected in grass bottles and frozen until analyzing. The samples returned to the laboratory for analysis as soon as possible after each rainfall event (within 24 hours). The methods of water sampling and analysis procedures were followed the standard method for the examination of and wastewater (American Public Health Association, 1998).

The analytical results of nitrogen and phosphorus concentrations in runoff events were shown in Table 5.1 and Figures 5.5 and 5.6, respectively.

Table 5.1 Observed nutrient concentration in runoff at M.171 and M.145 stations.

Observed Date	M.171			M.145		
	River discharge (Million cubic meters)	Nitrogen concentration in runoff (mg/liter)	Phosphorus concentration in runoff (mg/liter)	River discharge (Million cubic meters)	Nitrogen concentration in runoff (mg/liter)	Phosphorus concentration in runoff (mg/liter)
20080818	0.04	5.60	1.99	0.15	10.27	1.73
20080907	0.55	21.01	0.47	0.27	24.22	0.84
20080910	16.35	21.01	0.32	3.23	13.35	0.54
20080915	5.85	16.34	0.19	1.24	10.51	0.62
20080928	1.23	14.01	0.31	0.53	7.00	0.28
20080930	3.21	14.01	0.18	1.60	3.50	0.19
20081025	3.08	13.01	0.21	2.42	4.01	0.23
20081030	3.62	12.33	0.24	2.13	3.67	0.41

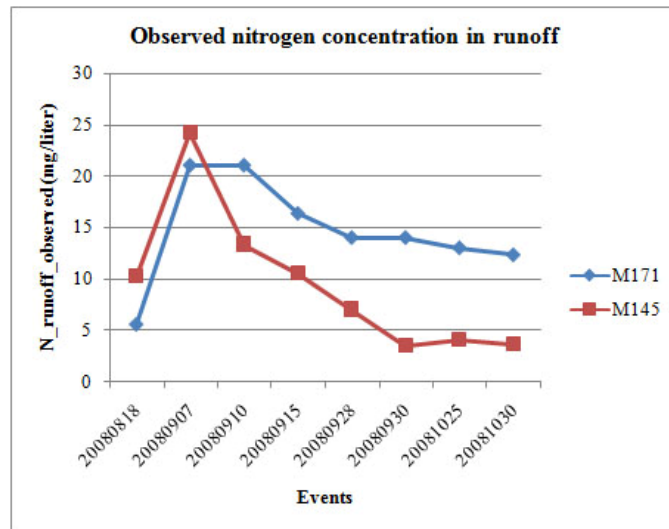


Figure 5.5 Observed nitrogen concentration in runoff at M.171 and M.145.

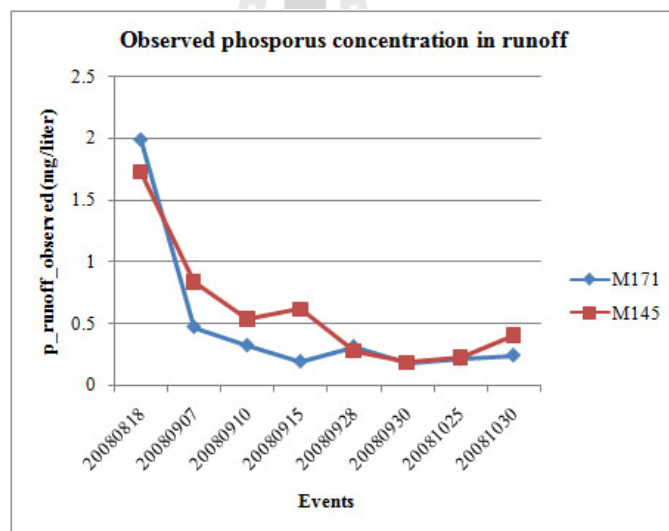


Figure 5.6 Observed phosphorus concentration in runoff at M.171 and M.145.

The analytical results of nitrogen and phosphorus attached in sediment were shown in Table 5.2 and Figures 5.7 and 5.8, respectively.

Table 5.2 Observed nutrient attached in sediment at M.171 and M.145 stations.

Observed date	M.171			M.145		
	Sediment yield (tons)	Nitrogen concentration in sediment (mg/kg)	Phosphorus concentration in sediment (mg/kg)	Sediment yield (tons)	Nitrogen concentration in sediment (mg/kg)	Phosphorus concentration in sediment (mg/kg)
20080818	149.17	2,300.00	6.85	166.54	1,800.00	12.22
20080907	1,128.25	2,000.00	10.20	269.03	2,400.00	15.70
20080910	37,797.98	1,200.00	12.58	3,006.80	1,500.00	14.30
20080915	9,883.82	1,200.00	15.20	1,089.34	1,800.00	18.40
20080928	196.02	1,300.00	15.40	98.99	1,800.00	17.40
20080930	3,143.87	1,600.00	17.70	1,225.80	1,900.00	18.44
20081025	579.39	1,200.00	18.40	423.81	1,600.00	17.40
20081030	564.07	1,000.00	18.20	308.19	1,200.00	17.80

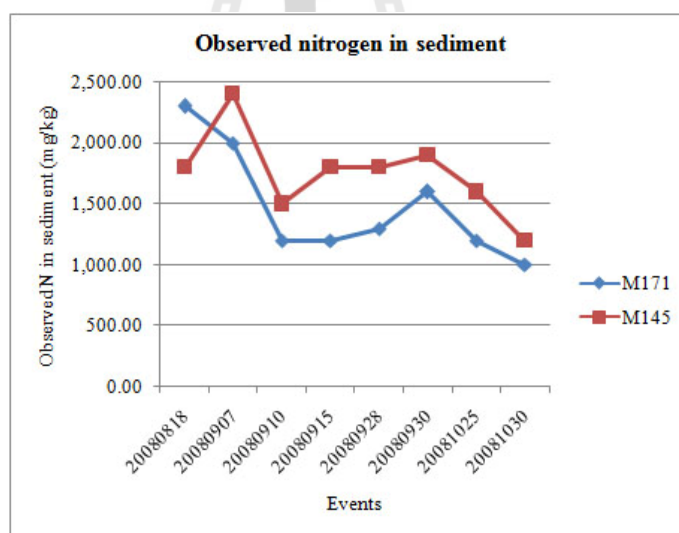


Figure 5.7 Observed nitrogen attached in sediment at M.171 and M.145.

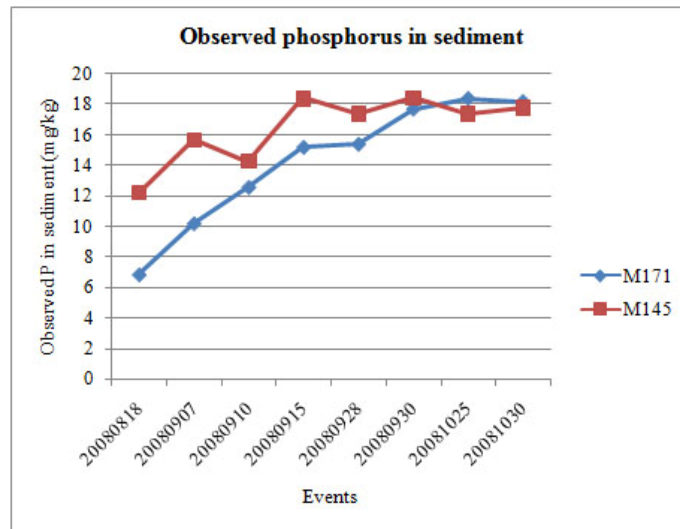


Figure 5.8 Observed phosphorus attached in sediment at M.171 and M.145.

5.4 Results and discussion

5.4.1 Results of nitrogen yield in runoff

5.4.1.1 Calibration of nitrogen yield in runoff simulation model

The calibration was carried out by adjusting nitrogen leaching extraction coefficient (N_{LEC}) and nitrogen runoff extraction coefficient (N_{REC}) in the Eq. 5.6 in such a manner that the calculated coefficient of efficiency (E) for all calibration events would be highest. Eight selected events were used for model calibration.

The calibration results of nitrogen yields in runoff show that the model produced good results with $E = 0.82$, $R^2 = 0.91$ when adjusting $N_{LEC} = 0.002$ and $N_{REC} = 0.0002$. The varying “ N_{LEC} and N_{REC} ” can improve accuracy of their relationship as shown in Table 5.3.

Table 5.3 Data comparison of nitrogen yield in runoff simulation and observation of eight events for model calibration.

Calibration events	Nitrogen yield in runoff (kg)		
	Observed	Simulated	$Dv(\%)$
M171_20081030	44,538.72	52,748.56	-18.43
M171_20080930	44,898.58	29,344.30	34.64
M171_20080910	343,149.84	226,478.00	34.00
M171_20080818	220.33	12,556.89	-5,599.13
M145_20081030	7,791.24	33,575.20	-330.94
M145_20080930	5,610.20	19,533.54	-248.18
M145_20080910	87,076.85	129,036.00	-48.19
M145_20080818	1,538.34	7,832.65	-409.16
Total	534,824.11	511,105.14	
Coefficient of efficiency (E)		0.82	
Coefficient of determination (R^2)		0.91	
Average deviation (%)		-823.17	
Root Mean Squared Error ($RMSE$)		45,733.88	

The regression line with 1:1 line as plot of observed and simulated nitrogen yield in runoff for calibration events are shown in Figure 5.9. It is observable that the simulated values are slightly above the 1:1 line, indicating that the model is slightly underestimation.

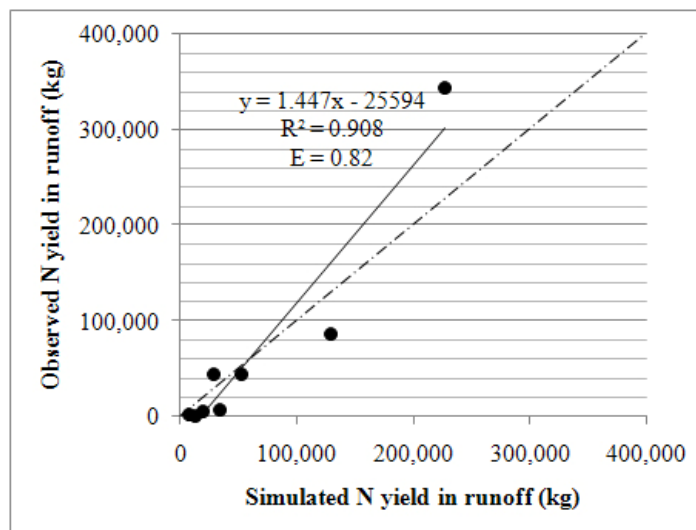


Figure 5.9 Calibration results of observed and simulated nitrogen yield in runoff.

In general, the result obtained confirmed that the model was good for simulation the watershed in term of nitrogen yield in runoff. After calibration, the calibrated-model was then validated with other independent events.

5.4.1.2 Validation of nitrogen yield in runoff simulation model

Other eight events were for the model validation. The validation results of nitrogen yield in runoff show that the model produced good results with $E = 0.63$, $R^2 = 0.89$. These statistical values suggested that the model was applicable for the study area. The validation results for simulated nitrogen yield in runoff are presented in Table 5.4.

Table 5.4 Data comparison of nitrogen yield in runoff simulation and observation of eight events for model validation.

Validation events	Nitrogen yield in runoff (kg)		
	Observed	Simulated	$Dv(\%)$
M171_20081025	40,051.52	25,138.04	37.24
M171_20080928	17,151.25	16,202.50	5.53
M171_20080915	95,464.03	51,764.95	45.78
M171_20080907	11,545.62	24,388.05	- 111.23
M145_20081025	9,701.39	18,097.76	-86.55
M145_20080928	3,719.58	10,521.50	-182.87
M145_20080915	13,025.25	20,626.98	-58.36
M145_20080907	6,513.70	8,498.21	-30.47
Total	197,172.33	175,237.99	
Coefficient of efficiency (E)		0.82	
Coefficient of determination (R^2)		0.91	
Average deviation (%)		-47.62	
Root Mean Squared Error ($RMSE$)		17,593.82	

The regression line with 1:1 line as plot of observed and simulated nitrogen yield in runoff for validation events are shown in Figure 5.10. It is observable that the regression line is above the 1:1 line when the nitrogen yield is

approximately higher than 20,000 kg, indicating that the model is underestimation in heavier events.

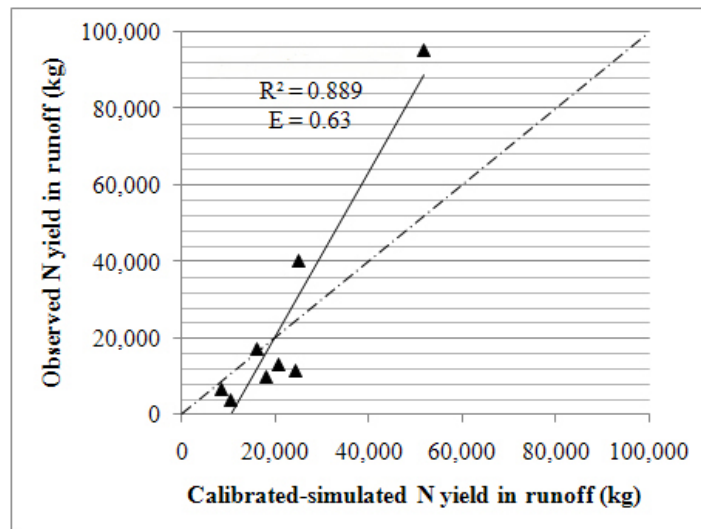


Figure 5.10 Relationships of observed and calibrated-simulated nitrogen yield in runoff.

The results of nitrogen yield in runoff are displayed in Figure 5.11.

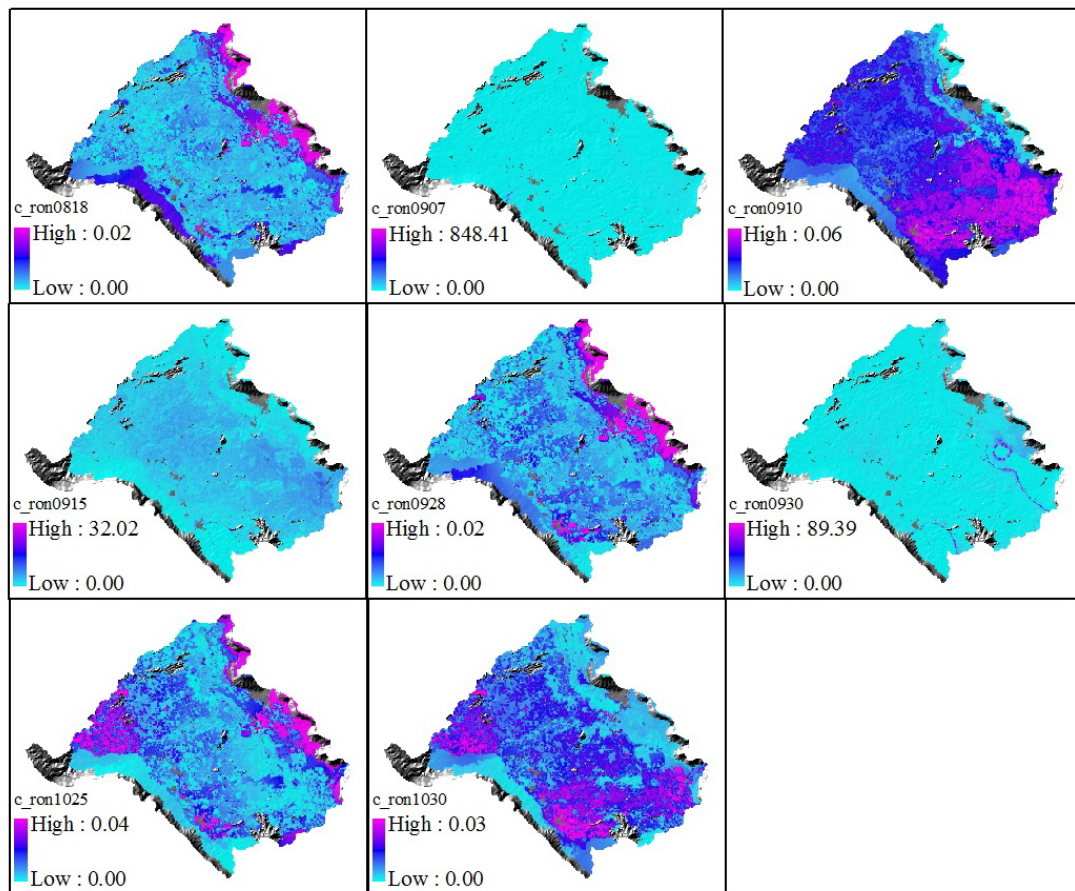


Figure 5.11 Spatial variation of event-based simulated nitrogen yield in runoff.

5.4.2 Results of phosphorus yield in runoff

5.4.2.1 Calibration of phosphorus yield in runoff simulation model

The calibration was carried out by adjusting phosphorus leaching extraction coefficient (P_{LEC}) and phosphorus runoff extraction coefficient (P_{REC}) in the Eq. 5.13 in such a manner that the coefficient of efficient (E) for all calibration events would be highest. Eight selected events were used for model calibration.

The calibration results of phosphorus yields in runoff show that the model produced excellent results with $E = 0.92$, $R^2 = 0.96$ when adjusting $P_{LEC} =$

0.015 and $P_{REC} = 0.0015$. The calibration results for simulated phosphorus yield in runoff are presented in Table 5.5.

Table 5.5 Data comparison of phosphorus yield in runoff simulation and observation of eight events for model calibration.

Calibration events	Phosphorus yield in runoff (kg)		
	Observed	Simulated	$Dv(\%)$
M171_20080818	78.30	122.42	-56.36
M171_20080910	5,226.46	4,809.19	7.98
M171_20080930	576.86	458.44	20.53
M171_20081025	646.49	553.71	14.35
M145_20080818	259.14	57.62	77.76
M145_20080910	3,522.21	2,236.52	36.50
M145_20080930	304.55	343.47	-12.78
M145_20081025	556.44	446.01	19.85
Total	11,170.44	9,027.39	
Coefficient of efficiency (E)		0.92	
Coefficient of determination (R^2)		0.96	
Average deviation (%)		13.48	
Root Mean Squared Error ($RMSE$)		488.11	

The regression line with 1:1 line as plot of observed and simulated phosphorus yield in runoff for calibration events are shown in Figure 5.12. It is observable that the simulated values are slightly above 1:1 line, indicating that the model is slightly underestimation.

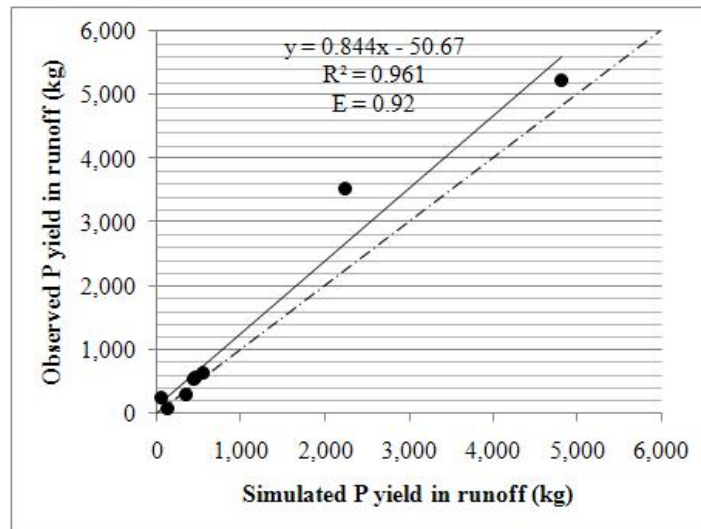


Figure 5.12 Calibration results of observed and simulated phosphorus yield in runoff.

After calibration, the calibrated-model was then validated with other independent events.

5.4.2.2 Validation of phosphorus yield in runoff simulation model

Other eight events were for the model validation. The validation results of phosphorus yield in runoff show that the model produced good results with $E = 0.52$, $R^2 = 0.78$. These statistical values suggested that the model was applicable for the study area. The validation results for simulated phosphorus yield in runoff are presented in the Table 5.6.

Table 5.6 Data comparison of phosphorus yield in runoff simulation and observation of eight events for model validation.

Validation events	Phosphorus yield in runoff (kg)		
	Observed	Simulated	$Dv(\%)$
M171_20080907	258.28	444.91	-72.26
M171_20081030	866.93	1,313.38	-51.50
M171_20080928	379.51	286.48	24.51
M171_20080915	1,110.05	1,403.96	-26.48
M145_20080907	225.91	41.22	81.75
M145_20081030	870.41	708.21	18.64
M145_20080928	148.78	170.92	-14.88
M145_20080915	768.38	514.04	33.10
Total	4,628.25	4,883.10	
Coefficient of efficiency (E)		0.52	
Coefficient of determination (R^2)		0.78	
Average deviation (%)		-0.89	
Root Mean Squared Error ($RMSE$)		238.43	

The regression line with 1:1 line as plot of observed and simulated phosphorus yield in runoff for validation events are shown in Figure 5.13. It is observable that the regression line is slightly below the 1:1 line when phosphorus yield is approximately higher than 500 kg, indicating that the model is slightly overestimation in heavier events.

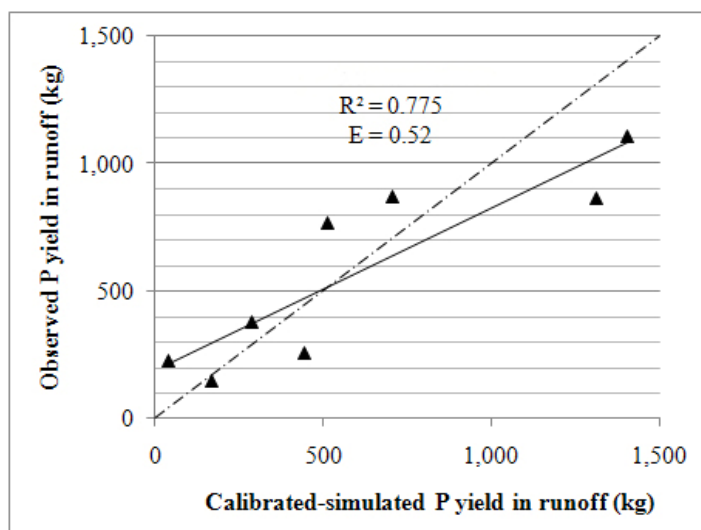
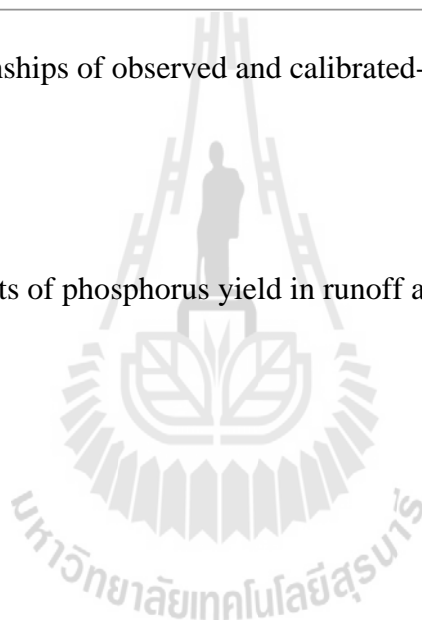


Figure 5.13 Relationships of observed and calibrated-simulated phosphorus yield in runoff.

The results of phosphorus yield in runoff are displayed in Figure 5.14.



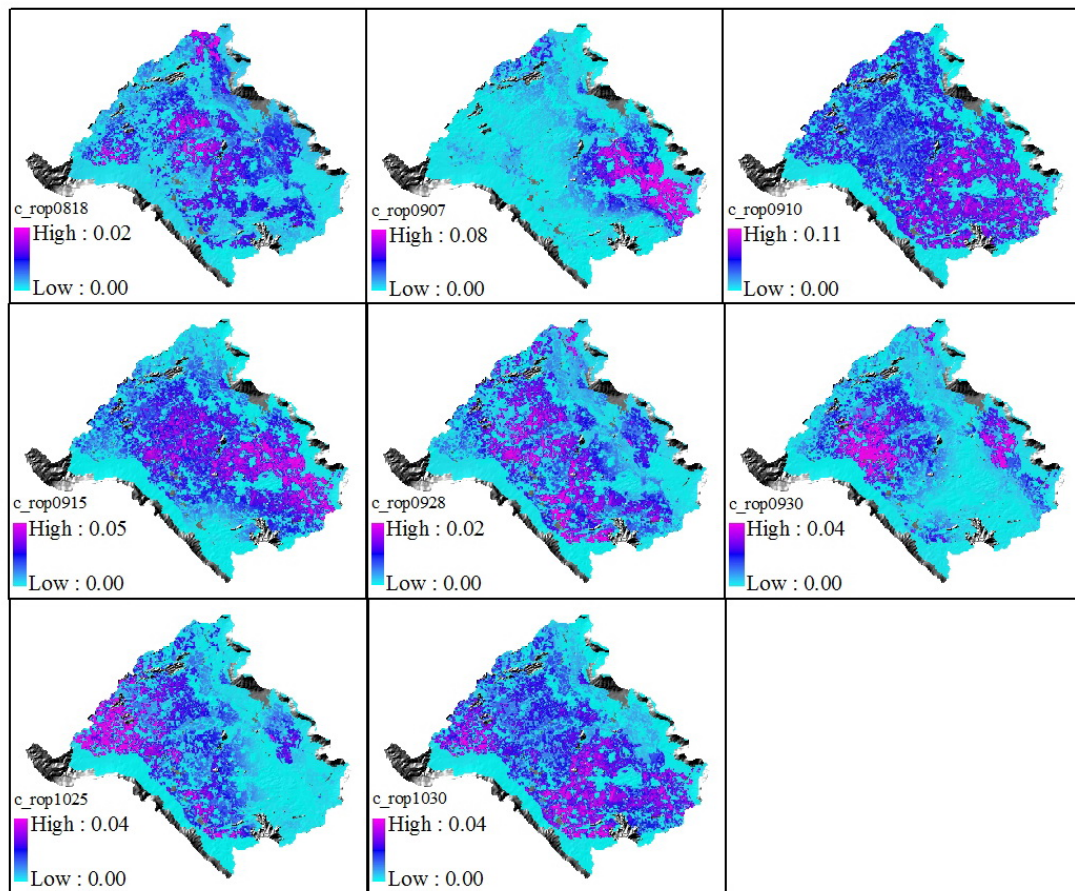


Figure 5.14 Spatial variation of event-based simulated phosphorus yield in runoff.

5.4.3 Results of nitrogen yield in sediment

5.4.3.1 Calibration of nitrogen yield in sediment simulation model

The calibration was carried out by adjusting a and b coefficient in the Eq. 5.15 in such a manner that the coefficient of efficient (E) for all calibration events would be highest. Eight selected events were used for model calibration.

The calibration results of nitrogen yield in sediment show that the model produced excellent results with $E = 0.90$, $R^2 = 0.93$ when adjusting $a = 0.01$ and $b = -0.35$. The calibration results for simulated nitrogen yield in sediment are presented in Table 5.7.

Table 5.7 Data comparison of nitrogen yield in sediment simulation and observation of eight events for model calibration.

Calibration events	Nitrogen yield in sediment (kg)		
	Observed	Simulated	$Dv(\%)$
M171_20080818	343.09	1,120.24	- 26.51
M171_20080910	45,357.58	36,105.19	20.40
M171_20080928	254.83	1,310.07	-414.10
M171_20081025	695.27	1,778.99	-155.87
M145_20080818	299.77	409.86	-36.72
M145_20080910	4,510.20	13,766.85	-205.24
M145_20080928	178.18	638.86	-258.55
M145_20081025	678.10	1,144.92	-68.84
Total	52,317.02	56,274.98	
Coefficient of efficiency (E)		0.90	
Coefficient of determination (R^2)		0.93	
Average deviation (%)		-168.18	
Root Mean Squared Error ($RMSE$)		4,672.28	

The regression line with 1:1 line as plot of observed and simulated nitrogen yield in sediment for calibration events are shown in Figure 5.15. It is observable that the simulated values are slightly above 1:1 line when nitrogen yield in sediment is approximately higher than 10,000 kg, indicating that the model is slightly underestimation in heavier events.

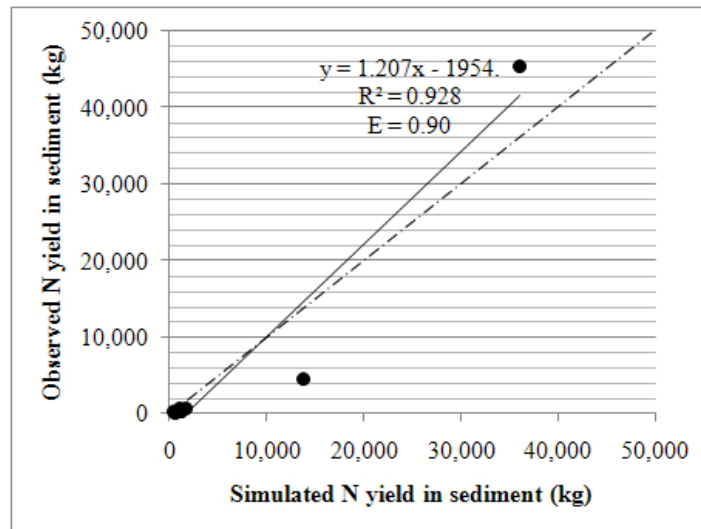


Figure 5.15 Calibration results of observed and simulated nitrogen yield in sediment.

After calibration, the calibrated-model was then validated with other independent events.

5.4.3.2 Validation of nitrogen yield in sediment simulation model

Other eight events were for the model validation. The validation results of nitrogen yield in sediment show that the model produced very good results with $E = 0.70$, $R^2 = 0.93$. These statistical values suggested that the model was applicable for the study area. However, the result may change if more data events were involved in the analysis. The validation results for simulated nitrogen yield in sediment are presented in the Table 5.8.

Table 5.8 Data comparison of nitrogen yield in sediment simulation and observation of eight events for model validation.

Validation events	Nitrogen yield in sediment (kg)		
	Observed	Simulated	$Dv(\%)$
M171_20080907	2,256.50	2,767.11	-22.63
M171_20080915	11,860.58	13,717.04	-15.65
M171_20080930	5,030.19	8,642.38	-71.81
M171_20081030	564.07	2,579.97	-357.39
M145_20080907	645.67	319.59	50.50
M145_20080915	1,960.81	3,845.78	-96.13
M145_20080930	2,329.02	4,794.49	- 05.86
M145_20081030	369.83	1,103.87	-198.48
Total	25,016.67	37,770.23	
Coefficient of efficiency (E)		0.70	
Coefficient of determination (R^2)		0.93	
Average deviation (%)		-102.18	
Root Mean Squared Error ($RMSE$)		1,971.54	

The regression line with 1:1 line as plot of observed and simulated nitrogen yield in sediment for validation events are shown in Figure 5.16. It is observable that the simulated values are slightly below the 1:1 line, indicating that the model is slightly overestimation.

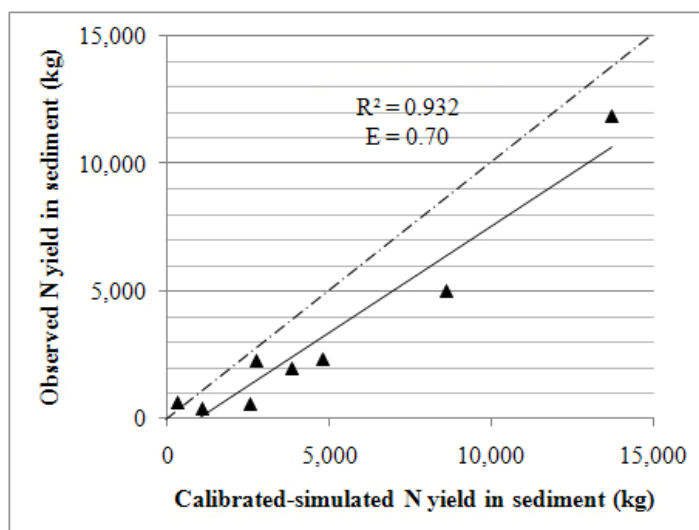
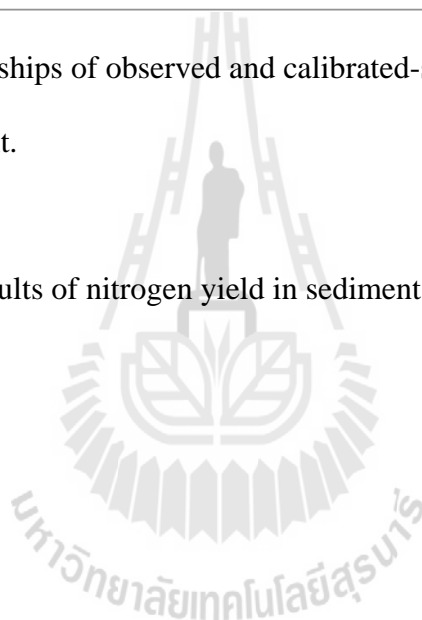


Figure 5.16 Relationships of observed and calibrated-simulated nitrogen yield in sediment.

The results of nitrogen yield in sediment are displayed in Figure 5.17.



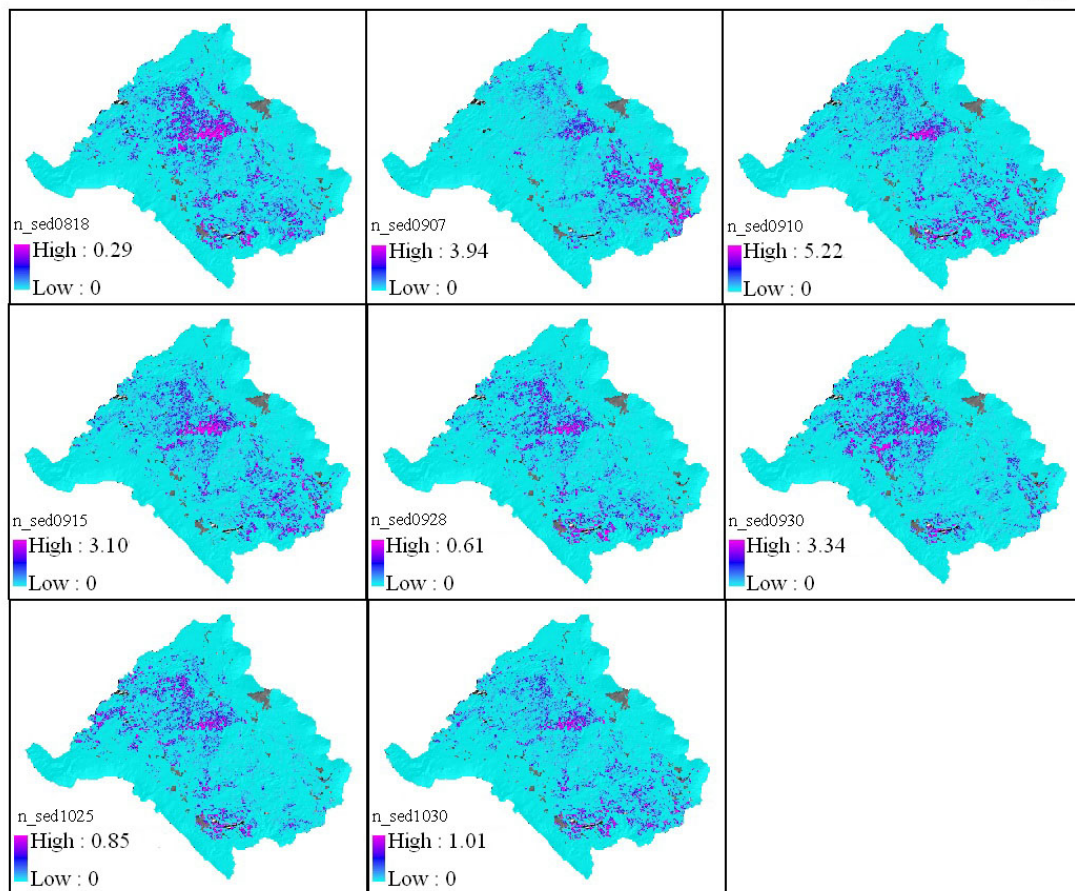


Figure 5.17 Spatial variation of event-based simulated nitrogen yield in sediment.

5.4.4 Results of phosphorus yield in sediment

5.4.4.1 Calibration of phosphorus yield in sediment simulation model

The calibration was carried out by adjusting a and b coefficient in the Eq. 5.15 in such a manner that the coefficient of efficient (E) for all calibration events would be highest. Eight selected events were used for model calibration.

The calibration results of phosphorus yield in sediment show that the model produced excellent results with $E = 0.90$, $R^2 = 0.93$ when adjusting $a = 0.01$ and $b = -0.45$. The calibration results for simulated phosphorus yield in sediment are presented in Table 5.9.

Table 5.9 Data comparison of phosphorus yield in sediment simulation and observation of eight events for model calibration.

Calibration events	Phosphorus yield in sediment (kg)		
	Observed	Simulated	$Dv(\%)$
M171_20080818	1.02	24.53	-2,300.87
M171_20080910	475.50	399.29	16.03
M171_20080928	3.02	24.52	-712.33
M171_20081025	10.66	33.35	-212.86
M145_20080818	2.04	8.31	-308.39
M145_20080910	43.00	148.25	-244.78
M145_20080928	1.72	10.34	-500.51
M145_20081025	7.37	20.17	-173.46
Total	544.33	668.76	
Coefficient of efficiency (E)		0.90	
Coefficient of determination (R^2)		0.93	
Average deviation (%)		-554.64	
Root Mean Squared Error ($RMSE$)		48.34	

The regression line with 1:1 line as plot of observed and simulated phosphorus yield in sediment for calibration events are shown in Figure 5.18. It is observable that the simulated values are slightly above 1:1 line when phosphorus yield in sediment is approximately higher than 170 kg, indicating that the model is slightly underestimation in heavier events.

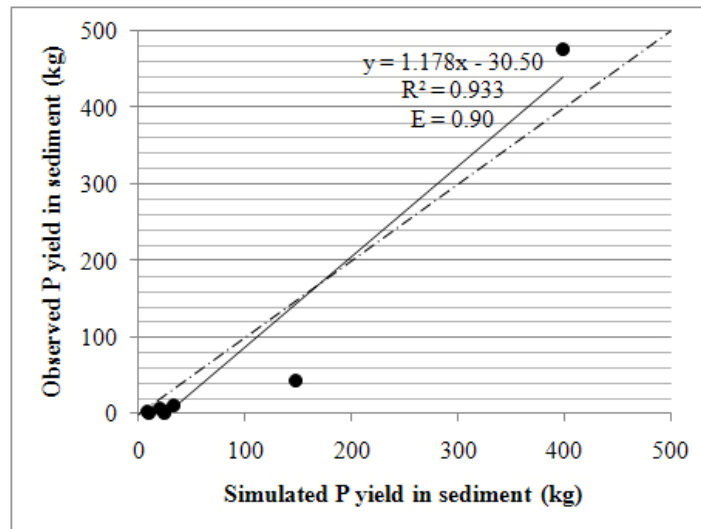


Figure 5.18 Calibration results of observed and simulated phosphorus yield in sediment.

After calibration, the calibrated-model was then validated with other independent events.

5.4.4.2 Validation of phosphorus yield in sediment simulation model

Other eight events were for the model validation. The validation results of phosphorus yield in sediment show that the model produced poor results with $E = 0.13$, $R^2 = 0.87$. The validation results for simulated phosphorus yield in sediment are presented in the Table 5.10.

Table 5.10 Data comparison of phosphorus yield in sediment simulation and observation of eight events for model validation.

Validation events	Phosphorus yield in sediment (kg)		
	Observed	Simulated	$Dv(\%)$
M171_20080907	11.51	40.79	-254.44
M171_20080915	150.23	193.28	-28.65
M171_20080930	55.65	135.77	-143.98
M171_20081030	10.27	39.81	-287.78
M145_20080907	4.22	5.62	-33.08
M145_20080915	20.04	63.10	-214.80
M145_20080930	22.60	76.60	-238.87
M145_20081030	5.49	15.83	-188.65
Total	280.01	570.79	
Coefficient of efficiency (E)		0.13	
Coefficient of determination (R^2)		0.87	
Average deviation (%)		-173.78	
Root Mean Squared Error ($RMSE$)		43.13	

The regression line with 1:1 line as plot of observed and simulated phosphorus yield in sediment for validation events are shown in Figure 5.19. It is observable that the simulated values are slightly below 1:1 line, indicating that the model is slightly overestimation.

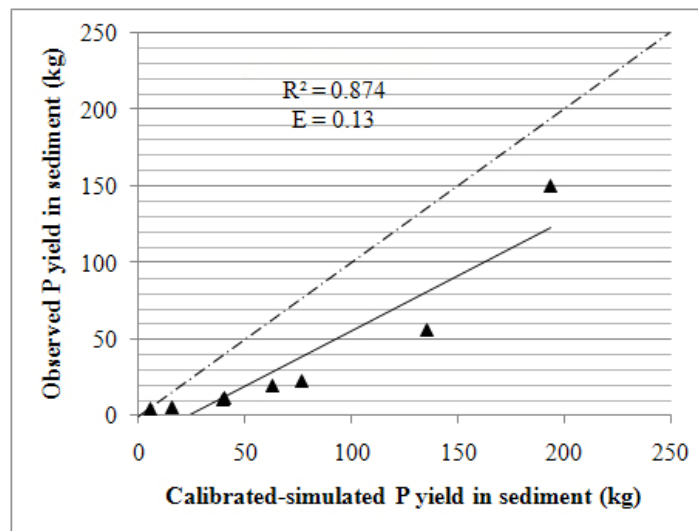
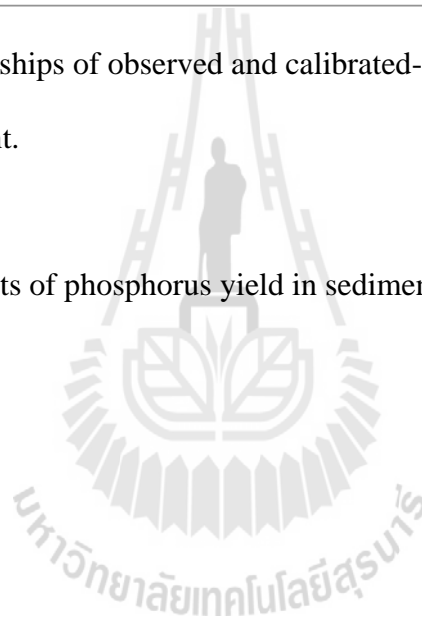


Figure 5.19 Relationships of observed and calibrated-simulated phosphorus yield in sediment.

The results of phosphorus yield in sediment are displayed in Figure 5.20.



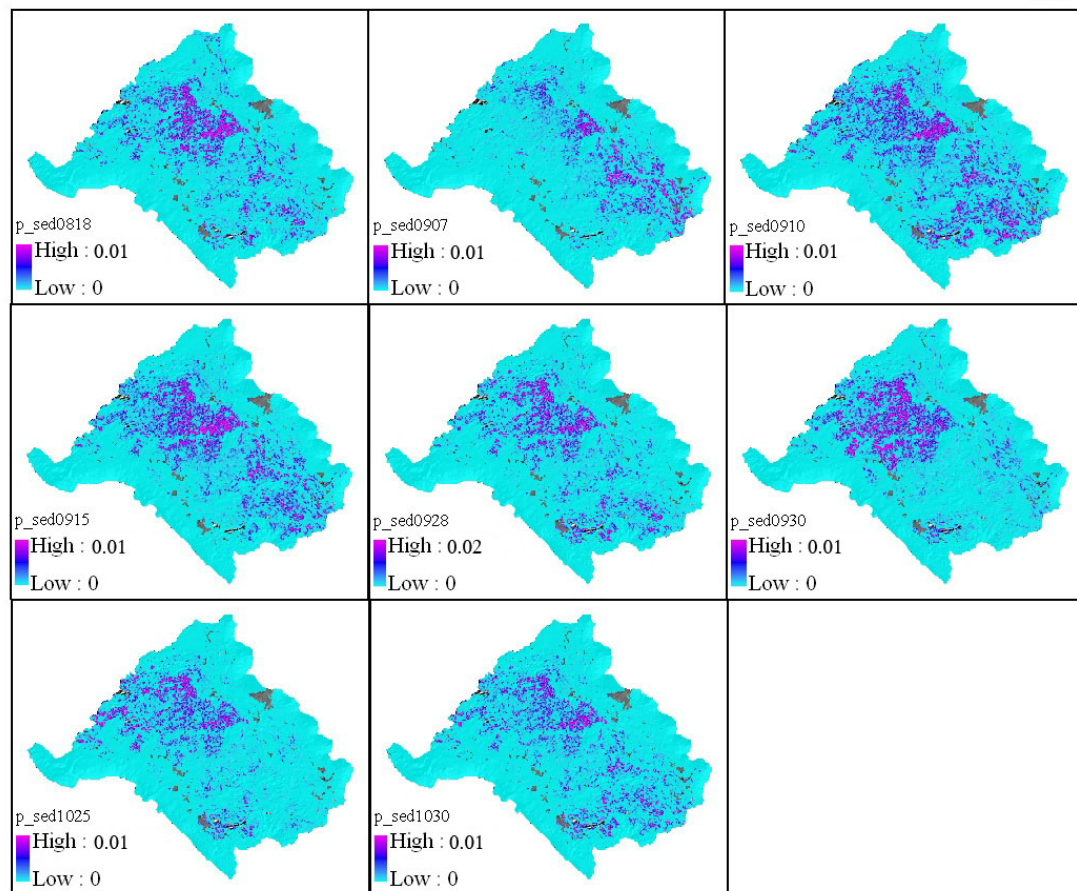


Figure 5.20 Spatial variation of event-based simulated phosphorus yield in sediment.

Poor performance of nutrient yield model in prediction of nutrient loading was also highlighted by Rode and Frede (1999), Shamshed et al. (2008), Bakinska et al. (2003), and Reungsang et al. (2007). The biggest deviation for event-based simulation and observed data but trends in the nutrients simulated matched observed data. Due to the fact that nutrient loading is based on mass conservation, any missing input or output information of nutrients in watershed will affect the results considerably. Few of sample events may be the cause for poor model performance. However, though the results were not very good, it was still able to represent a certain portion of variability in the observed data.

5.5 Conclusion

The overall results of the model simulation in this chapter indicated that the model performance was good with E and R^2 values range from 0.52-0.70 and 0.78-0.93, respectively. However phosphorus in sediment shows exceptionally poor model performance. In general, it can be concluded that grid-based nutrient yield model has the adequate capability to estimate nitrogen and phosphorus in runoff and nitrogen in sediment within the desired range. Overall, the validation of the grid-based nutrient yield model demonstrated that this model can be used as a NPS management tool within the Upper Lam Phra Phloeng watershed. In addition to improve model performance, a bigger number of events including more detailed input data are needed for analyses. However, for annual estimation, accumulation of all events obtained by this model simulation should be acceptable.

5.6 References

- American Public Health Association. [APHA] (1998). **Standard Methods for the Examination of Water and Wastewater**. 18th American Public Health Association, Washington.
- Baginska, B., Milne-Home, W., and Cornish, P.S. (2003). Modelling nutrient transport in Currency Creek, NSW with AnnAGNPS and PEST. **Environmental Modelling & Software**. 18: 801-808.
- Frere, M.H., Rose, J.D., and Lane, L.J. (1980). The nutrient submodel. In Knisel, W.G. (ed.). **CREAMS: A field scale model for Chemicals, Runoff, and Erosion from Agricultural Management Systems**. (pp 65-86). USDA, Cons. Research Report No.26.

- Hussein, M.H., Hussein, A.J., and Awad, M.M. (1999). Phosphorus and nitrogen losses associated with runoff and erosion on an Aridisol in northern Iraq. **Hydrological Sciences Journal**. 44(5): 657-664.
- Krysanova, V., Muller-Wohlfeil, D.I., Cramer, W., and Becker, A. (2000). Spatial analysis of soil-moisture deficit and potential soil loss in the Elbe river basin. In Wilson, J.P., and Gallant, J.C. (2000). **Terrain analysis: principles and applications**. USA: John Wiley & Sons.
- Reungsang, P. (2007). **Application of SWAT model in predicting water quantity and quality for United States and Thailand watersheds**. Ph.D. Thesis, Iowa State University.
- Rode, M., and Frede, H.G. (1999). Testing AGNPS for soil erosion and water quality modeling in agricultural catchments in Hesse (Germany). **Physics and Chemistry of the Earth, Part B : Hydrology, Oceans and Atmosphere**. 24(4): 297-301.
- Shamshad, A., Leow, C.S., Ramlah, A., Wan Hussin, W.M.A., and Mohd.Sanusi, S.A. (2008). Applications of AnnAGNPS model for soil loss estimation and nutrient loading for Malaysian conditions. **International Journal of Applied Earth Observation and Geoinformation**. 10: 239-252.
- Young, R., Onstad, C., Bosch, D., and Anderson, W. (1986). **Agricultural nonpoint source pollution model: a watershed analysis tool**. Model documentation, Agricultural Research Services, U.S. Department of Agriculture, Morris, MN.

CHAPTER VI

DEVELOPMENT OF NONPOINT SOURCE POLLUTION POTENTIAL INDEX

6.1 Abstract

The main objective of this study is to develop nonpoint source pollution potential index (NPSI) to evaluate NPS potential area. The NPSI for identifying and prioritizing critical areas was established using GIS and Multi-Criteria Decision Analysis (MCDA) technique. Quantification of the factors which relate to the NPS pollution was carried out as follows: runoff potential index, sediment potential index and nutrients potential index. The weight factor of each index was evaluated according to the results of quantification. The method was successfully applied for evaluating NPS pollution potential in Upper Lam Phra Phloeng watershed. Results from the model showed the critical areas for NPS pollution control in study area. The map of NPSI was helpful for examining the pattern of diffuse pollution and could facilitate the decision on NPS pollution management at local level.

6.2 Introduction

Assessment of the NPS pollution is complicating and time consuming task. NPS has specifics which distinguish it from point source pollution by being spatially distributed, and varying in magnitude on the basis of complex interaction between environment and the agricultural system (Giupponi and Rosato, 1995). To reduce NPS pollution in the most cost effective way, it is important to have knowledge of contributions to water from different sources especially the main source. To resolve the complexity of NPS it is most efficient to control NPS in the critical area. But where the critical area for NPS control of the Upper Lam Phra Phloeng watershed is and how to identify. Local Administration does not have a useful tool to identify and prioritize where remedial measures should be taken to control NPS pollution.

Agricultural pollution potential index (APPI) was developed for identifying and ranking the NPS pollution potential of 104 watersheds in Pennsylvania, USA (Hamlett et al., 1992). This ranking index, consisting of four components – 1) a runoff index, 2) a sediment production index, 3) an animal loading index, and 4) chemical use index, was used to predict the relative potentials for agricultural nonpoint source pollution in the watershed. Li and Yeh (2004) developed nonpoint source pollution potential index, composed of six sub-indices – 1) runoff volume, 2) specific peak runoff rate, 3) soluble nitrogen, 4) soluble phosphorus, 5) chemical oxygen demand in the runoff and 6) specific sediment yield, each with relative importance weighting. Guo et al. (2004) applied APPI system to identifying and ranking critical areas of NPS with GIS. Quantification of factors in nonpoint source pollution was carried out the following: 1) sediment production index, 2) runoff index, 3) people and animal loading index and 4) chemical use index. Zhang and Huang (2011) assessed the NPS

pollution using a spatial multi-criteria analysis approach. Four criteria were formulated to characterize the source capacity of nitrogen export, the flow path to surface water, the efficiency of runoff generation, and climatic driving force. Monafo et al. (2005) also developed a potential nonpoint pollution index to assess the pressure on water bodies by different land management scenarios.

Previous studies emphasized that the proposed NPS pollution indices of watersheds were restricted to study area, and specific to local condition. Small amount of researches have applied the NPS pollution potential index in Thailand. The NPSI which can be applied to Upper Lam Phra Phloeng watershed conditions should be studied.

This chapter aims to develop a NPS pollution potential assessment system in terms of a potential index which suites to represent the NPS pollution characteristics of the Upper Lam Phra Phloeng watershed. The approach in this chapter may be applicable for other watersheds with the same geographic and practical conditions.

6.3 Materials and methods

6.3.1 GIS and Multi-criteria decision analysis (MCDA)

Geospatial model is a powerful tool for targeting NPS pollution and watershed management. However, model output (from Chapter III, IV, and V) can be voluminous and confusing. Thus, the complex information should be derived into an index. The index has served as valuable aids to communicating information and in evolving surface water quality policy. An index value, which increases with increasing nonpoint source pollution potential, is universal accepted. The NPSI was developed as a means of synthesizing quantification model outputs for impact

assessment of NPS to surface water quality in the Upper Lam Phra Phloeng watershed. NPSI is a GIS-based, watershed scale tool designed to inform decision makers and public about the potential of NPS pollution.

In multi-criteria analysis, a criterion can be defined as a standard of judging, i.e., a way to express the degree of achievement of an objective (Geneletti, 2007). Criteria have crucial influence on the results of evaluation. They should be complete on the one hand to make sure that the whole problem is encompassed; on the other hand the set of criteria should be kept minimal to reduce the complexity of the evaluation process. Three criteria were developed in this study to assess the potential of NPS from land to surface water within the Upper Lam Phra Phloeng watershed. The criteria are composed of the three sub-indices: runoff potential index, sediment potential index, nutrient potential index. The runoff potential index is developed for characterizing the generation of runoff. The sediment potential index is developed for characterizing the generation of sediment. The nutrient potential index is developed for characterizing the generation of sediment. All of them, higher value of the grid cell indicates a higher NPS potential generation. Calculation of these indexes required information of hydrologic soil group, land use (runoff potential generation), K factor, LS factor, C factor, P factor, SEDD factor (sediment potential generation), fertilizer application rate and land use (nutrient potential generation).

Calculating a NPSI consists of two fundamental steps – first, calculation of the sub-indices of factors that contribute to the overall index, and second, aggregation of the sub-indices into an overall index, called the NPSI. A subindex I_i ranges from 0 to 1. The subindex I_i for the i^{th} potential factor is determined using the MCDA techniques (Malczewski, 1999).

MCDA techniques were incorporated into GIS to allow the development of the model that produced standardized commensurate map layers. The score range procedure (benefit criteria) was used for linear scale transformation. It was introduced to transform input data into commensurate criterion maps. The procedure uses the following:

$$X'_{ij} = \frac{X_{ij} - X_j^{\min}}{X_j^{\max} - X_j^{\min}} \quad (6.1)$$

where X'_{ij} is the standardized score for the i^{th} object and the j^{th} attribute, X_{ij} is the raw score, and X_j^{\max} is the maximum score for the j^{th} attribute. X_j^{\min} is the minimum score for the j^{th} attribute. The value of standardized score can range from 0 to 1. The higher the value of the score, the more potential the criteria value is. The advantage of this method is that it is a proportional (linear) transformation of the raw data.

Once the sub-indices are calculated, they are aggregated in a second step to generate the overall index. The overall index can be calculated using the following expression:

$$NPSI = \sum_{i=1}^n W_i I_i \quad (6.2)$$

where I_i is subindex of the i^{th} potential factor, n is the number of potential factor, W_i is the weight of the i^{th} potential factor. The output of the calculation is presented in the form of maps that highlight areas critical to produce NPS pollution.

In the formulation of the NPSI, the potential factors responsible for NPS pollution must be selected and their relative weights determined. In this study, potential factors including (1) runoff potential factor; (2) sediment potential factor; and (3) nutrient potential factor were determined from quantification results of the previous models in Chapters III, IV, and V, respectively. The rank sum method (Stillwell et al., 1981) was used to determine the criteria weights. The simplest method for assessing the importance of weights is to arrange them in rank order; that is, every criterion under consideration is ranked in the order of the decision maker's preference. The weight (W_i) of each potential factor to the NPS pollution were 0.50 for runoff potential index (W_1), 0.33 for sediment potential index (W_2), and 0.17 for nutrient index (W_3).

Both spatial analysis and multi-criteria analysis were conducted using ArcGISTM with the extension of Spatial AnalystTM. The flow diagrams of the NPSI development for this study are shown in Figure 6.1.

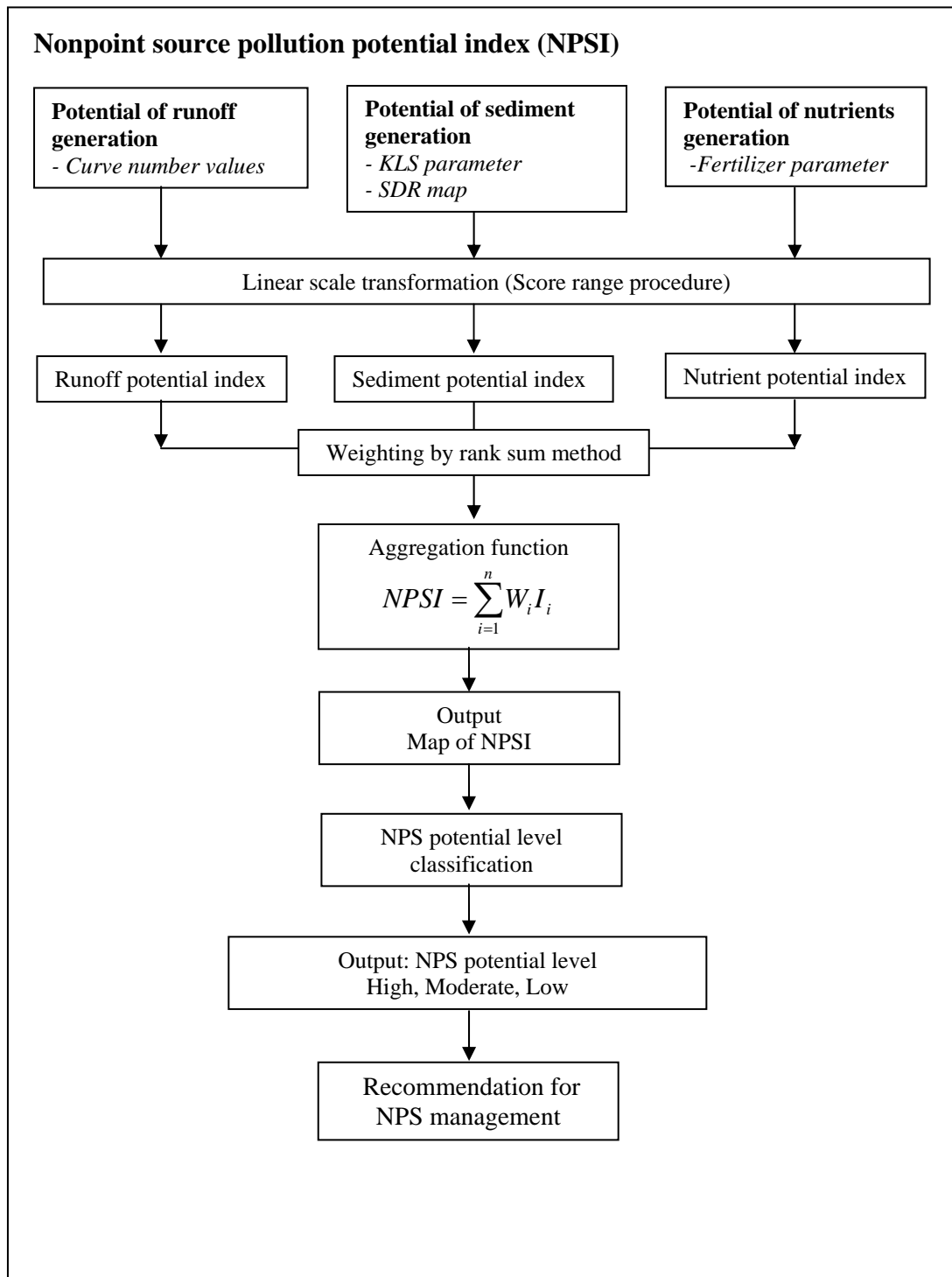


Figure 6.1 Flow diagram of the NPSI development.

6.3.2 Runoff potential index

Runoff is an important factor that controls the movement of sediment and nutrients from land surface to stream network (Zhang and Huang, 2011). The relationship of total nutrients export and runoff have been reported in many researches, most of which indicated that high runoff rate was favorable to the removal of nutrients from soil (Edwards and Withers, 2008; Drewry et al., 2009; Pathak et al., 2004; Wallin, 2005; Reginato and Piechota, 2004). The runoff potential index was developed to evaluate the potential runoff generated through grid-based Curve Number method mentioned in chapter III. This study emphasized on potential assessment. Therefore, only temporally static parameters during the study period were considered. The value of the runoff potential index was calculated based on the curve number value which has been widely adopted in NPS pollution models. The curve number values indicate their specific runoff potential. The flow diagram of the runoff potential index development for this study is shown in Figure 6.2.

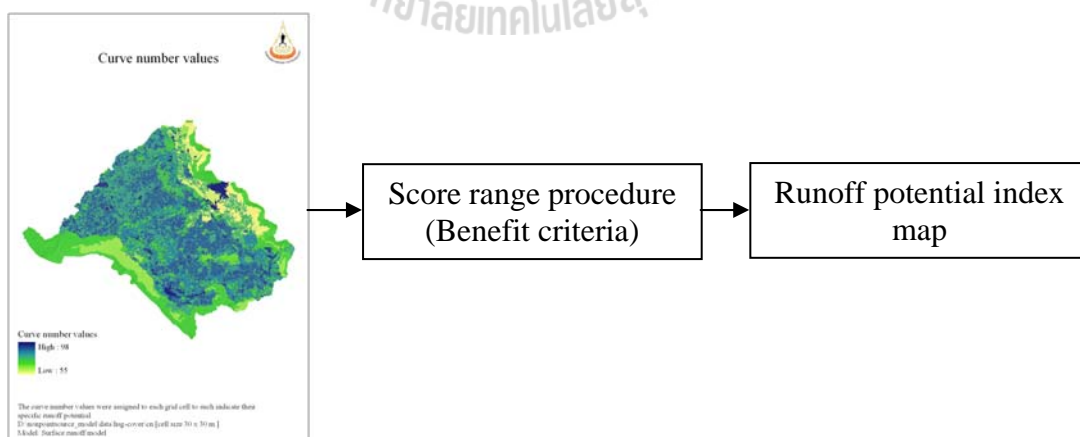


Figure 6.2 Flow diagram of the runoff potential index development.

The distribution of normalized runoff potential index is exhibited in Figure 6.3. Areas of high values are found in the central of watershed with undulating topographic and field crop is the dominant land use, especially maize, sugarcane, and cassava. Mountainous areas are assigned with relative low value due to the distribution of forest land.

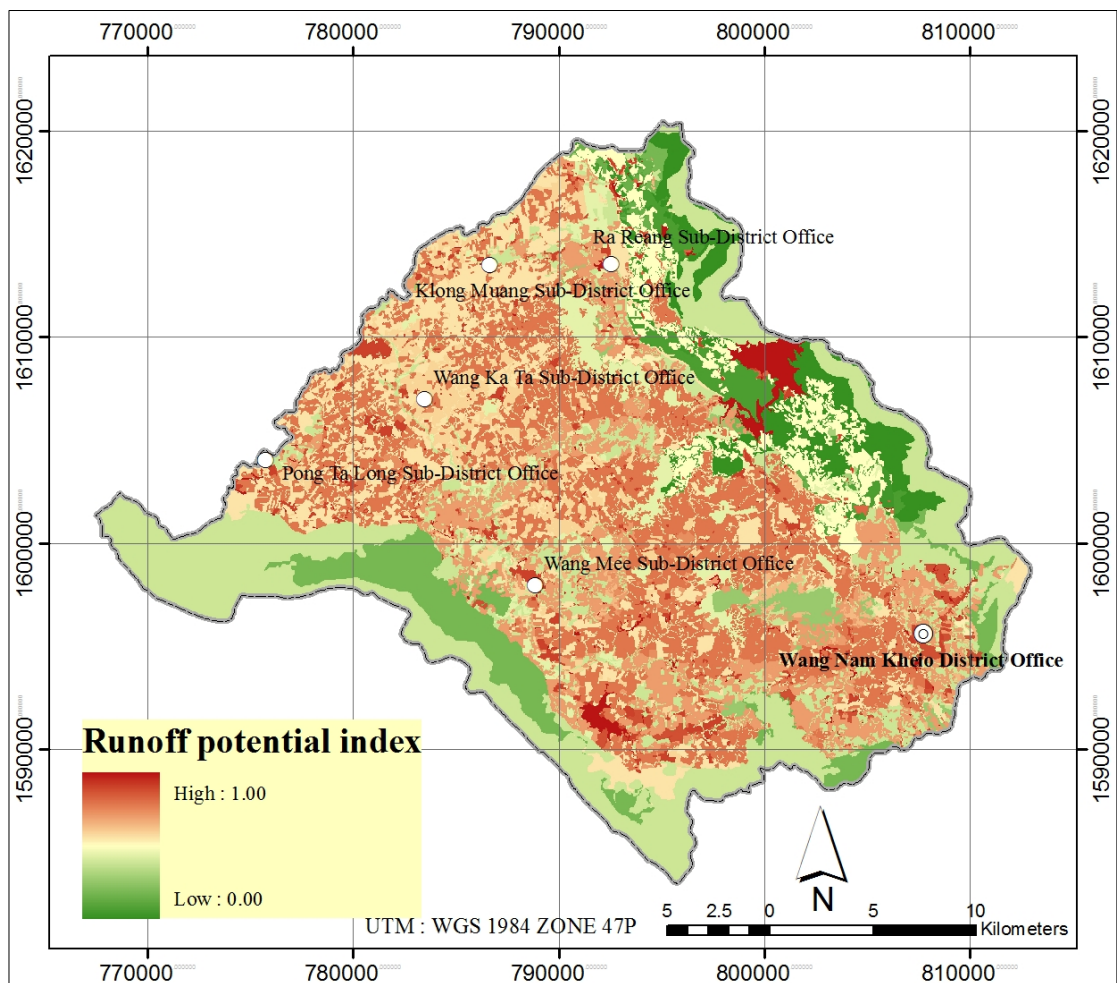


Figure 6.3 Distribution of the runoff potential index.

6.3.3 Sediment potential index

The sediment potential index was developed using a combination of the sediment yield potential calculation (*KLS* factors in Chapter IV) for each cell and

sediment delivery ratio potential for each cell. This study emphasized on potential assessment. Therefore, only temporally static parameters during the study period were considered. The driving force parameters such as runoff factor, *C* factor, and *P* factor were not included in sediment potential index assessment because they are regarded as temporally dynamic parameters. The temporally static parameters used for this case were *K*, *L*, *S*, and SDR. The flow diagram of the sediment potential index development for this study is shown in Figure 6.4.

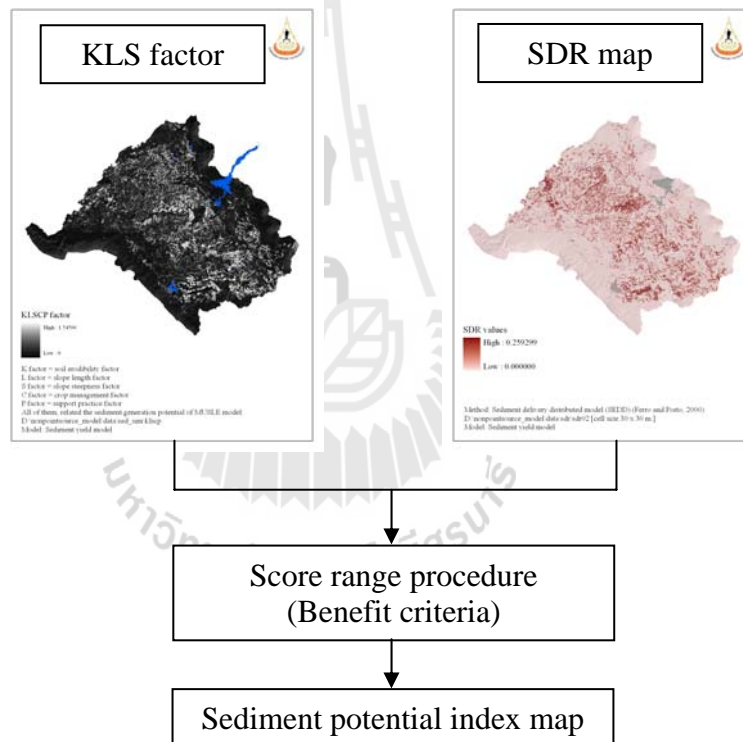


Figure 6.4 Flow diagram of the sediment potential index development.

The distribution of normalized sediment potential index is exhibited in Figure 6.5. Areas of high values are found in the steep slope closed to the stream network. However, mountainous areas are assigned with relative low values due to the

distribution of forest land which has good ground cover and low sediment generation potential.

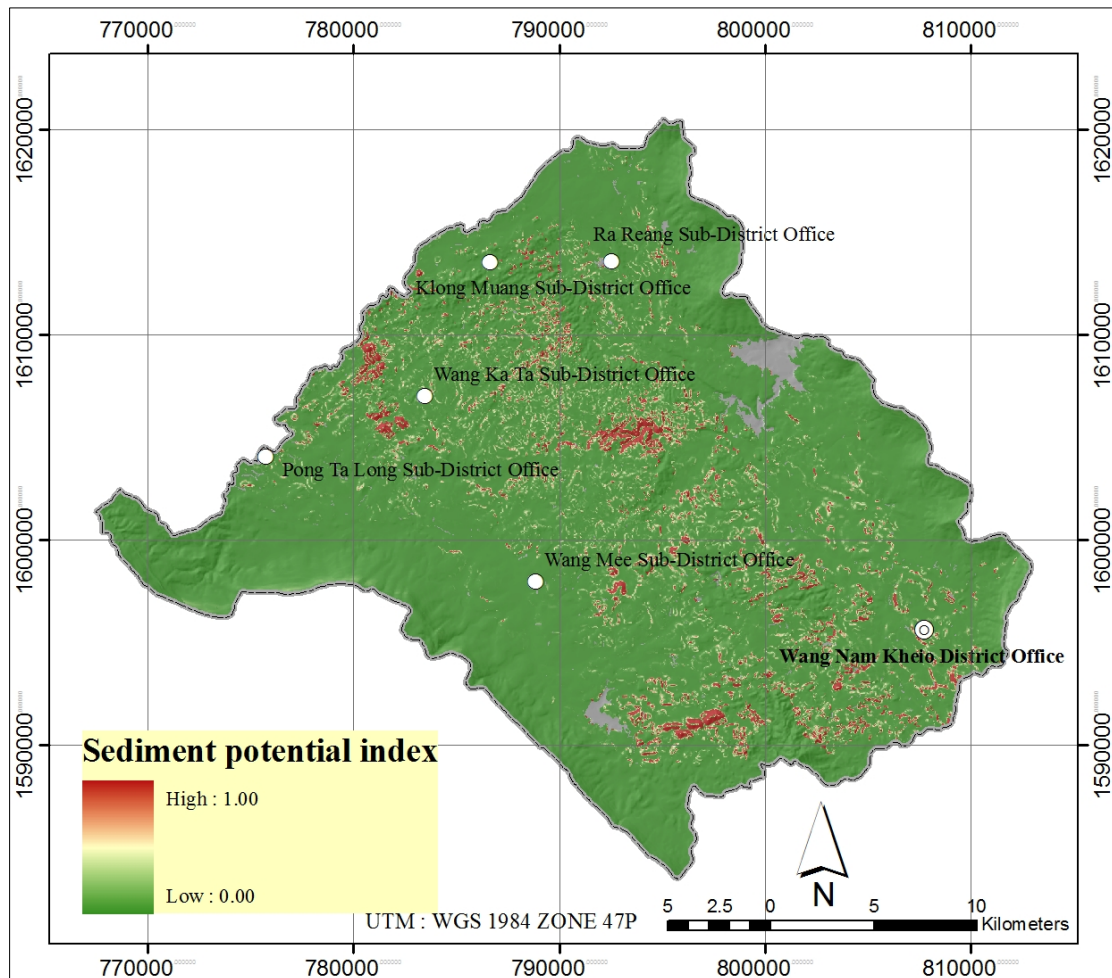


Figure 6.5 Distribution of the sediment potential index.

6.3.4 Nutrient potential index

The potential generation of agricultural pollutants results from land application of fertilizers. Nutrient potential index ranks the potential for fertilizer application to the various agricultural lands. Due to the limited time of this study it was not possible to conduct field survey to individual area. Therefore, an approximation was made of

the relative fertilizer use for different agricultural land uses. The potential loading of agricultural fertilizer for each type of land use was rated as high, medium, low, and not applicable based on the potential for each type of land use to receive fertilizer (Guo et al., 2004). These potential loading categories were assigned numerical values 4, 3, 2, and 1 for the high, medium, low and not applicable rating, respectively. Table 6.1 presents the associated potential loading value for fertilizer used for various main land uses. The data were obtained through survey on the farmers in 2008. Once the land use was determined for each grid cell, the relative fertilizer used potential was assigned to the grid cell. The flow diagram of the nutrient potential index development for this study is shown in Figure 6.6.

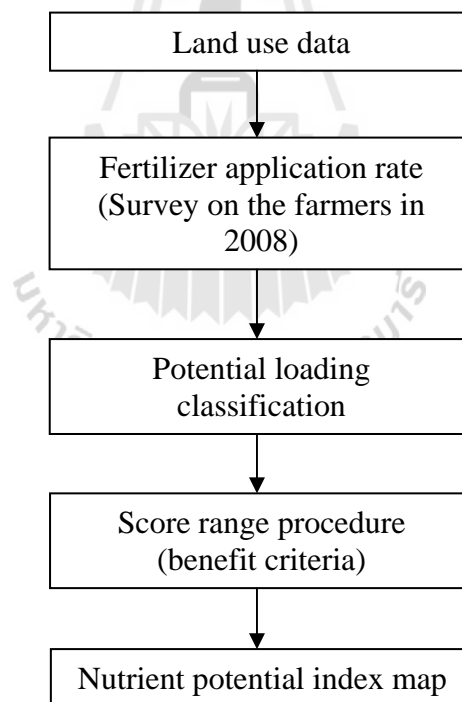


Figure 6.6 Flow diagram of the nutrient potential index development.

Table 6.1 Potential loading values of fertilizer for different main land uses in the Upper Lam Phra Phloeng watershed during year 2008.

Potential loading (Value)	Fertilizer application rate	Land uses
High (4)	>100 Kg/Rai/Year	Cassava, Maize, Sugarcane, Field crop
Medium (3)	75-100 Kg/Rai/Year	Paddy field, Horticulture
Low (2)	<75 Kg/Rai/Year	Grass, Orchard, Mixed orchard, Para rubber, Perennial, Mixed Perennial
Not applicable (1)		Scrub, Teak, Eucalyptus, Build-up land, institutional land, village, Forest plantation, Disturbed deciduous forest, Disturbed evergreen forest, Dense evergreen, Dense deciduous forest, Water body, Marsh, Swamp, Livestock farm house.

The distribution of normalized nutrient potential index is exhibited in Figure 6.7. Areas of high values are found in the main cash crop such as cassava, maize, and sugarcane.

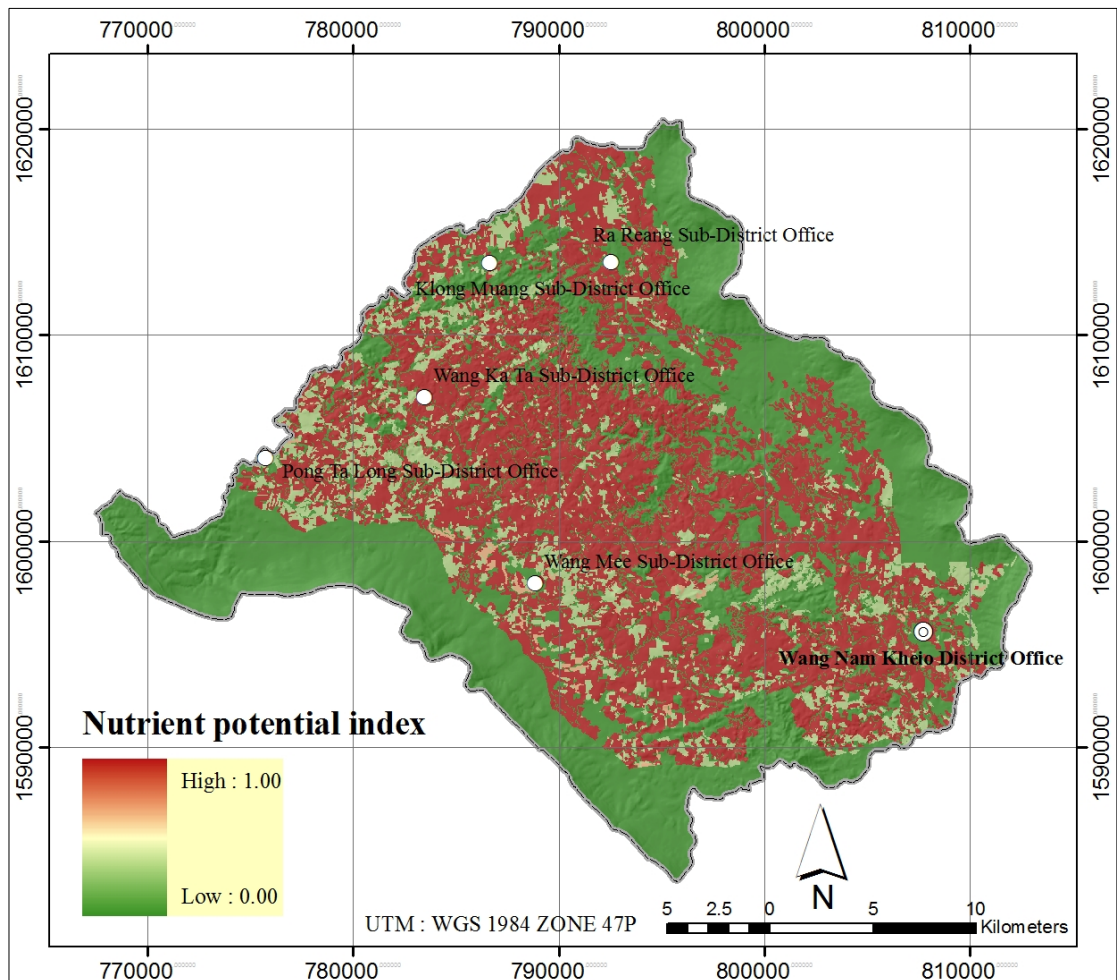


Figure 6.7 Distribution of the nutrient potential index.

6.4 Results and Discussion

The result of the NPSI map is depicted in Figure 6.8 and the classes of NPS potential are as follows:

a) High NPS potential area

251.12 km² (32.42%) of the total watershed area is high NPS potential and found in the central part of the watershed. Most area is high slope terrain used mainly for maize crop.

b) Moderate NPS potential area

270.04 km² (34.87%) of the total watershed area is moderate NPS potential and found in the central part of watershed. Most area is undulating-rolling topography used for cassava, sugarcane, and other field crops.

c) Low NPS potential area

253.36 km² (32.71%) of the total watershed area is low NPS potential and mainly distributed in the southern part and northern part of watershed characterized by the mountainous topography and forest land.

In order to provide an applicable understanding of the results, the map of NPSI was zonal based on the boundaries of local administration at village level as shown in Figure 6.9. This map should be useful for supporting decision of NPS pollution management at the watershed scale or local administrative scale. NPSI can be used to identify areas within watershed that potentially contribute more significantly to NPS by spatial analysis.



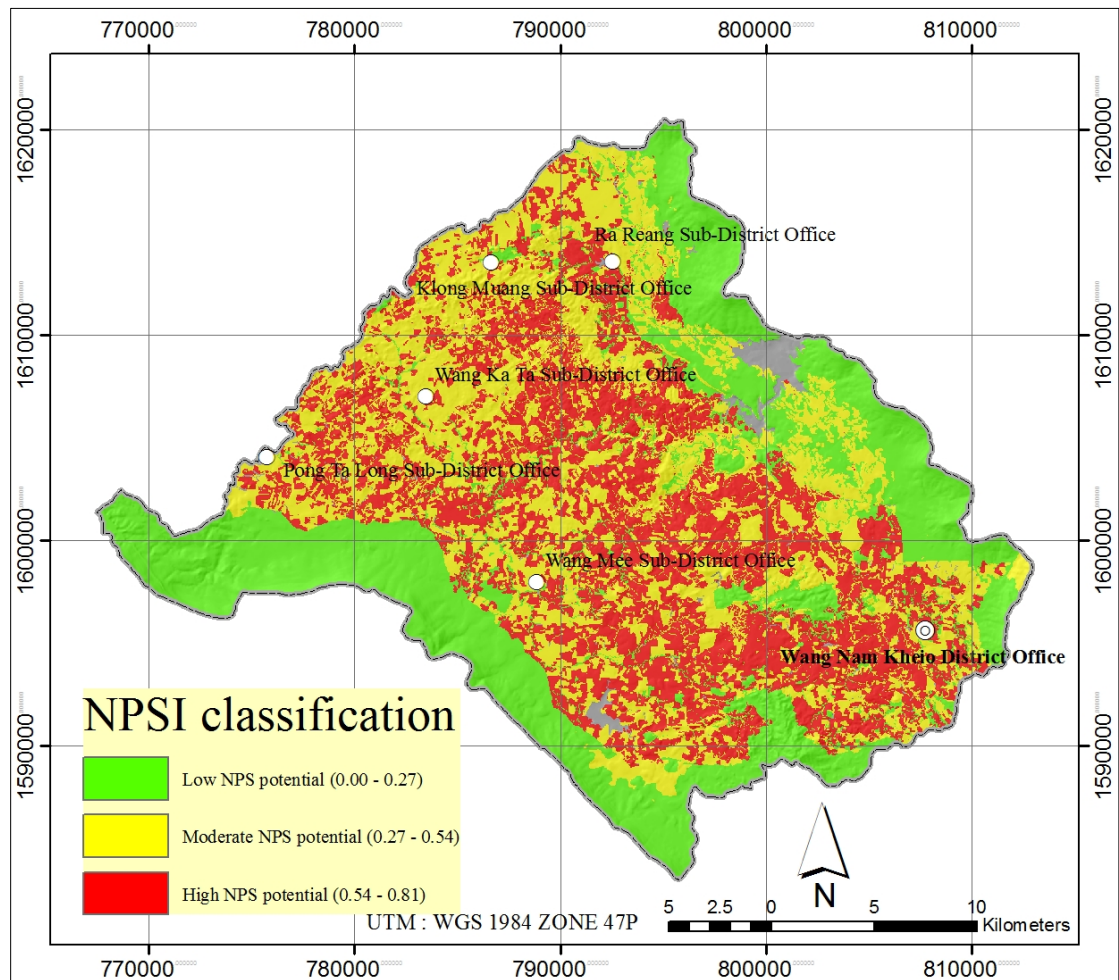


Figure 6.8 The NPSI distribution in the study area.

The study developed a NPSI by GIS-MCDA to support the evaluation of NPS pollutants at the watershed level and local administrative level. The criteria were developed from quantification results of three previous models - runoff model, sediment model, and nutrient model. Being implemented in GIS environment, this method generated maps that could be easily interpreted to support decision making process.

The validation of a NPSI is not an easy task. NPSI does not aim at absolutely describing the variation of the quantitative concentration of pollutants. However, it can be acceptably used to prioritize the areas that are required to monitoring and plan for better condition.

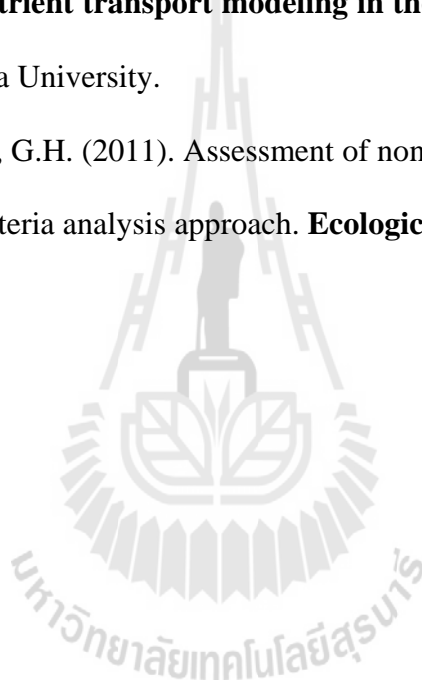
The NPSI map aim at facilitating the cell-by-cell comparison, however, village-by-village is also applied to orient local administration decision makers. It is useful for a variety decision making such as identifying high-priority areas of runoff, sediment, nutrients or overall NPSI for watershed management.

6.6 References

- Drewry, J.J., Newham, L.T.H., and Croke, B.F.W. (2009). Suspended sediment, nitrogen and phosphorus concentrations and exports during storm-events to the Tuross estuary, Australia. **Journal of Environmental Management**. 90(2): 879-887.
- Edwards, A.C., and Withers, P.J.A. (2008). Transport and delivery of suspended solids, nitrogen and phosphorus from various sources to freshwaters in the UK. **Journal of Hydrology**. 350: 144-153.

- Geneletti, D. (2007). An approach based on spatial multicriteria analysis to map the natural conservation value of agricultural land. **Journal of Environmental Management**. 83: 228-235.
- Giupponi, C., and Rosato, P. (1995). Simulating impacts of agricultural policy on nitrogen losses from a watershed on Northern Italy. **Environment International**. 21(5): 577-582.
- Guo, H.Y., Wang, X.R., and Zhu, J.G. (2004). Quantification and index of non-point pollution in Taihu Lake region with GIS. **Environmental Geochemistry and Health**. 26: 147-156.
- Hamlett, J.M., Miller, D.A., Day, R.L., Peterson, G.W., Baumer, G.M., and Russo, J. (1992). Statewide GIS-based ranking of watersheds for agricultural pollution prevention. **Journal of Soil and Water Conservation**. 47(5): 399-404.
- Li, K.C., and Yeh, M.C. (2004). Nonpoint source pollution potential index: A case study of the Feitsui reservoir watershed, Taiwan. **Journal of the Chinese Institute of Engineers**. 27(2): 253-259.
- Malczewski, J. (1999). **GIS and multicriteria decision analysis**. John Wiley & Sons: New York.
- Munafo, M., Cecchi, G., Baiocco, F., and Mancini, L. (2005). River pollution from non-point sources: a new simplified method of assessment. **Journal of Environmental Management**. 77: 93-98.
- Pathak, B.K., Kazama, F., and Toshiaki, I. (2004). **Monitoring of nitrogen leaching from a Tropical Paddy in Thailand**. Agricultural Engineering International: The CIGR Journal of Scientific Research and Development.

- Reginato, M., and Piechota, T.C. (2004). Nutrient contribution of nonpoint source runoff in the Las Vegas valley. **Journal of the American Water Resource Association**. 1537-1551.
- Stillwell, W.G., Seaver, D.A., and Edwards, W. (1981). A comparison of weight approximation techniques in multiattribute utility decision making. **Organizational Behavior and Human Performance**. 28(1): 62-77.
- Wallin, A. (2005). **Nutrient transport modeling in the Daugava river basin**. M.Sc. Thesis. Uppsala University.
- Zhang, H., and Huang, G.H. (2011). Assessment of non-point source pollution using a spatial multicriteria analysis approach. **Ecological Modelling**. 222: 313-321.



CHAPTER VII

GENERAL CONCLUSION AND RECOMMENDATION

The main contribution of this research is to develop the decent geospatial models for NPS pollution assessment in the agricultural watershed which is located at the Upper Lam Phra Phloeng. Instead of using conventional lump-based analysis in the model, grid-based GIS with advanced analysis was offered to perform the NPS models. The results achieved from events are appropriate for a year round planning and management for planner. They provided information on the critical areas of NPS where management on reducing runoff, sediment, and nutrient yield potential from agricultural watershed urgently required.

These models consist of the three components of event-based spatial modeling. The first component is for generating events of runoff for each grid cell using CN method. In the second component, sediment yield was estimated by MUSLE and sediment delivery ratio by SEDD model. In the third component, nutrient yield was estimated by AGNPS model. All results were validated. The estimated spatial impact conditions from three components were used to formulate NPSI.

A set of model operations was developed under the ModelBuilder™ of ArcGIS™ environment requiring grid-based input data. The model performances were incorporation of GIS data with functions for effective data acquisition and manipulation as well as input/output presentation.

In this study, an integration of GIS and NPS models demonstrates an effective approach for conducting complicated and large scale watershed modeling. The system allows users to manage vast amounts of inputs and outputs, and present them graphically.

In pre-calibration, the NPS models did not simulate satisfied runoff, sediment, and nutrient yields, largely due to the empiricism involved in model equations. However, the present calibrated-model results could be of use in NPS simulation in the study area. The developed system was applied to simulate NPS pollutants from agricultural watershed, Upper Lam Phra Phloeng watershed. Herein, the developed system covers the geospatial model and NPS algorithm. The modeling outputs were verified through measuring data, demonstrated reasonable simulation accuracy for an acceptable $E \geq 0.5$. The result indicated that the model provides an effective means for simulating the NPS from agricultural watershed.

There are four main results which were reported in this study including (1) surface runoff estimation using grid-based CN method (Chapter III), (2) sediment yield estimation using MUSLE and SEDD (Chapter IV), (3) nutrient yield estimation using grid-based AGNPS model (Chapter V), and (4) development of NPSI for NPS management (Chapter VI). From results obtained from each work, the overall conclusion and some recommendations can be presented as follows.

7.1 General conclusion

7.1.1 Surface runoff model development

In this work, the development system was based on surface runoff algorithm implemented in a grid-based GIS that represents distributed runoff processes. The

process worked on spatial variation of features which are land use, hydrologic soil group, rainfall, topographic characteristics, leading to runoff potential assessment. Inclusion of the distributed spatial characteristics provided significant advantage modeling compared with lumped model.

The surface runoff depth in each grid cell was computed using the CN method, and then routed through the watershed based on flow direction and flow accumulation from one grid cell to the next until it reached the watershed outlet. Runoff depth for each grid cell was examined. For model evaluation, the statistical parameters were calculated from the outputs of model simulation (Q_{sim}) and field observation (Q_{obs}) of all events.

From the study, the calibrated results of the spatial modeling using modified CN method can be applied to runoff simulations with acceptable accuracy. Not only the satisfied quantitative results provided but the model is also able to estimate varying runoff depth over the watershed spatially. As the result of the case study at the Upper Lam Phra Phloeng watershed, it can be confirmed that grid-based modified CN method is applicable to surface runoff estimation effectively. The curve number values used in CN method was used as a part to develop the NPS pollution potential index, because it indicated specific runoff potential spatially.

7.1.2 Sediment yield model development

The sediment yield estimation based on MUSLE and SEDD models implemented in a grid-based GIS that represents distributed sediment yield processes. Such features included the spatial variation of runoff depth, peak discharge, K factor, LS factor, C factor, P factor, flow length, slope factor, leading to sediment yield processes and sediment generation potential.

Each GIS layer of MUSLE and SEDD parameters was prepared in raster format. Each cell homogeneously represents characteristics of the sedimentation factors. It is a grid-based spatial analysis applying all the mathematic equations present in the MUSLE and SEDD algorithm. The soil erosion in each grid cell was computed using the MUSLE, and the routed through the watershed based on sediment delivery ratio using SEDD model. The statistical parameters for model evaluation were calculated from the outputs of model simulation (SY_{sim}) and field observation (SY_{obs}) of all events.

The results of MUSLE and SEDD operated on geospatial modeling can be applied to sediment yield simulations with acceptable accuracy referring to 0.79 and 0.92 of E and R^2 , respectively. Not only the satisfied quantitative results provided but the model is also able to estimate varying sediment yield over the watershed spatially. Although the bigger deviation of individual event-based simulation and observed data exist but for overall consideration the sediment simulated and observed data are not much different as confirmed by statistical parameters. For annual estimation, accumulation of all events obtained by this model simulation should be acceptable. As the result of the case study at the Upper Lam Phra Phloeng watershed, it can be confirmed that geospatial modeling using MUSLE and SEDD is applicable to sediment yield estimation effectively, however, with lower accuracy than the runoff model. The present results could be of use in sediment yield potential prioritization in the study area.

However, the performance of the model estimation the sediment yield can be increased by improving the input parameters for both MUSLE and SEDD. These can

be done by developing suitable methodologies to estimate the peak discharge factor, and better detect different characteristics of crop growth in different season.

The present study applied the MUSLE and SEDD to estimation of event-based sediment yield. The results validation show low capability of the original model in providing accurate estimates, while its calibrated version developed during the study significantly improved the performance of the model. Therefore, it is recommended that application of the MUSLE and SEDD in the new study area with different geographical characteristics requires calibration of certain parameters for better accuracy.

7.1.3 Nutrient yield model development

This work employed grid-based model for estimation of nutrient yield which are nitrogen and phosphorus in the Upper Lam Phra Phloeng watershed. Nutrient yield portions are subdivided into soluble form and sediment-attachment form. The method used AGNPS model is selected for simulation. The AGNPS algorithm integrated with geospatial model was developed.

Modeling results showed that significant pollution problems exist in the study area with the major pollutants being sediments and nutrients in surface runoff. Most pollutants have been generated from agricultural activities.

The overall results of the model simulation indicated that the model performance was good with E and R^2 values range from 0.52-0.70 and 0.78-0.93, respectively. However, phosphorus in sediment shows exceptionally poor model performance. In general, it can be concluded that the grid-based nutrient yield model has adequate capability to estimate nitrogen and phosphorus in runoff and nitrogen in sediment within the desired range. Overall, the validation of the grid-based nutrient

yield model demonstrated that this model can be used as a NPS management tool within the Upper Lam Phra Phloeng watershed. In addition, to improve model performance, a bigger number of events including more detailed input data are needed for analyses. However, for annual estimation, accumulation of all events obtained by this model simulation should be acceptable.

7.1.4 NPSI development

The main objective of this work is to develop NPSI to evaluate NPS potential area. The NPSI for identifying and prioritizing critical areas was established using GIS and MCDA technique. Quantification of the factors which relate to the NPS pollution was carried out and resulted in runoff potential index, sediment potential index and nutrients potential index.

The method was successfully applied for evaluating NPS pollution potential in Upper Lam Phra Phloeng watershed. Results from the model showed the critical areas for NPS pollution control in study area. The map of NPSI was helpful for examining the pattern of diffused pollution and could facilitate the decision on NPS pollution management at local level.

The NPSI map aims at facilitating the cell-by-cell comparison. Moreover, comparison of village-by-village can also be applied to orient decision makers of local administration. It is useful for a variety decision making such as identifying high-priority areas of runoff, sediment, nutrients or overall NPSI for watershed management.

Critical source areas or hot spots of NPS potential pollution were identified by the NPSI. They were generally located where potential of surface runoff, sediment yield, and nutrient yield are considerable high. The intersection of these areas within a

watershed generally indicated the critical NPS areas. Thus, the efficient management should focus primarily on reducing or controlling level of NPS potential at critical NPS areas.

The calibrated-grid based NPS model can successfully be used for prioritization of critical NPS areas in order to develop event-based management plan to reduce the runoff, sediment and nutrient yield from agricultural watershed.

For better result expectation, while developing such tools to address the NPS problem at the watershed scale. This can be assured the sustainable NPS management at the watershed scale it could be better idea if each individual type of farming system can be brought into consideration. This expectation can become true in case of no limitation of the database required.

7.2 Recommendation for further research

The research revealed some limitations in working with geospatial model to assessment NPS potential. Some improvements in the NPS model can still be made. Thus, the following recommendations are made for future research to improve the NPS model and further advance the status of NPS modeling.

1. The NPS model uses many empirical and quasi-physically based algorithms that might not be appropriate for tropical condition like Thailand. Therefore, one possible future effort is to modify those various equations to be more suitable for local conditions.
2. Due to the complex nature of the NPS system, the data required for the study was extensive. Although most data are relatively accurate, some are still less and uncertain. Therefore, increasing the certainty of the data sets through

reinvestigation and verification would help increase the accuracy of the simulating results.

3. The developed modeling system should be applicable to other watershed in the similar conditions. Therefore, the NPS model should be tested and validated in other watersheds for extensive use of the model.

4. Higher error in simulation of sediment and nutrient yield by the model may be because of the effect of small reservoirs, which act as sediment traps. Therefore, one possible future effort is to modify equation to cover sediment trap effect.

5. New algorithm for computing sediment should be investigated. The present study model does not take channel erosion into account, it could be a part of contributor to total sediment yield in study area.

6. There are possibilities for further research on the integrating NPS algorithm as the embedded GIS with user friendly interface.

7. Further work on validating the model capabilities to simulate runoff, sediment, and nutrient has to be done more seriously by addition adequate amount of field sampling. This field sampling should cover a wide range of field conditions, climate, topography, and land use.

8. In this study, nitrogen and phosphorus were the target pollutants since they are the most commonly used as fertilizer in study area. In fact, the developed modeling can also be used to simulate the other substances such as pesticides with some modified algorithm.



APPENDICES

APPENDIX A

CRITERIA FOR HYDROLOGIC SOIL GROUP

Table A-1 Criteria for hydrologic soil group determination.

Hydrologic soil group	Runoff potential	Percent of clay and sand	Soil texture	Saturated hydraulic conductivity (mm/h)
A	low runoff potential	%clay<10 and %sand>90	gravel or sand textures	> 36
B	moderately low runoff potential	%clay10-20 and %sand50-90	loamy sand or sandy loam textures	≤36 to >14.48
C	moderately high runoff potential	%clay20-40 and %sand<50	loam, silt loam, sandy clay loam, clay loam, and silty clay loam textures	≤14.48 to >1.52
D	high runoff potential	%clay>40 and %sand<50	clayey textures	≤1.52

The U.S. Natural Resource Conservation Service (NRCS) classified soil into four hydrologic groups based on infiltration characteristics of the soil. NRCS defines a hydrologic group as a group of soils having similar runoff potential under similar storm and cover conditions. Soil properties that influence runoff potential are those that impact the minimum rate of infiltration for a bare soil after prolonged wetting and when not frozen. These properties are depth to seasonally high water table, saturated hydraulic conductivity, and depth to a very slowly permeable layer. Soil may be placed in one of four groups, A, B, C, and D, or three dual classes, A/D, B/D, and C/D.

Definitions of the classes are:

Group A Soils: High infiltration (Low runoff potential). The soils have a high infiltration rate even when thoroughly wetted. They chiefly consist of deep, well drained to excessively drained sands or gravels. They have a high rate of water transmission. Sand, loamy sand, or sandy loam. Infiltration rate >0.3 in/hr when wet.

Group B Soils: Moderate infiltration (Moderately low runoff potential). The soils have a moderate infiltration rate when thoroughly wetted. They chiefly are moderately deep to deep, moderately well-drained to well-drained soils that have moderately fine to moderately coarse textures. They have a moderate rate of water transmission. Silt loam or loam. Infiltration rate 0.15 to 0.3 in/hr when wet.

Group C Soils: Low infiltration (Moderately high runoff potential). The soils have a slow infiltration rate when thoroughly wetted. They chiefly have a layer that impedes downward movement of water or have moderately fine to fine texture. They have a slow rate of water transmission. Sandy clay loam. Infiltration rate 0.05 to 0.15 in/hr when wet.

Group D Soils: Very low infiltration (High runoff potential). The soils have a very slow infiltration rate when thoroughly wetted. They chiefly consist of clay soils that have a high swelling potential, soils that have a permanent water table, soils that have clay pan or clay layer at or near the surface, and shallow soils over nearly impervious material. They have a very slow rate of water transmission. Clay loam, silty clay loam, sandy clay, silty clay, or clay. Infiltration rate 0 to 0.05 in/hr when wet.

APPENDIX B

ANTECEDENT SOIL MOISTURE CONDITION (AMC)

Table B-1 AMC for this study.

Events*	Rainfall (mm)	Total rainfall (mm) 5-day prior	AMC
18 Aug 08	19.97	15.19	AMC-I
19 Aug 08	11.53	26.52	AMC-I
5 Sep 08	11.26	22.04	AMC-I
6 Sep 08	15.19	24.92	AMC-I
7 Sep 08	14.14	37.85	AMC-II
9 Sep 08	16.73	51.71	AMC-II
10 Sep 08	41.87	63.50	AMC-III
12 Sep 08	24.27	163.60	AMC-III
15 Sep 08	16.77	159.39	AMC-III
18 Sep 08	16.73	63.65	AMC-III
28 Sep 08	24.14	2.45	AMC-I
30 Sep 08	20.54	32.96	AMC-I
1 Oct 08	15.43	53.50	AMC-III
3 Oct 08	16.30	70.05	AMC-III
8 Oct 08	14.50	36.37	AMC-II
18 Oct 08	10.45	6.29	AMC-I
25 Oct 08	29.09	24.93	AMC-I
30 Oct 08	25.77	40.28	AMC-II

*AMC-I 8 events, AMC-II 4 events, and AMC-III 6 event.

Table B-2 Criteria for AMC classification.

AMC conditions	Total 5-day antecedent rainfall (mm)	
	Dormant season	Growing season
AMC-I (Dry)	<12.7	<35.56
AMC-II (Normal)	12.7-27.94	35.56-53.34
AMC-III (Wet)	>27.94	>53.34

APPENDIX C

SOURCE CODE OF RUNOFF MODEL

Source code (VBScript)

```
'-----  
' Runoff.vbs  
' (generated by ArcGIS/ModelBuilder)  
'-----  
  
' Create the Geoprocessor object  
set gp = WScript.CreateObject("esriGeoprocessing.GPDispatch.1")  
  
' Check out any necessary licenses  
gp.CheckOutExtension "spatial"  
  
' Load required toolboxes...  
gp.AddToolbox "C:/Program Files/ArcGIS/ArcToolbox/Toolboxes/Spatial Analyst Tools.tbx"  
gp.AddToolbox "C:/Program Files/ArcGIS/ArcToolbox/Toolboxes/Conversion Tools.tbx"  
  
' Local variables...  
v20080818 = "D:\nonpointsource_model\data\rainfall\idw_r_map\20080818"  
v20080819 = "D:\nonpointsource_model\data\rainfall\idw_r_map\20080819"  
v20080905 = "D:\nonpointsource_model\data\rainfall\idw_r_map\20080905"  
v20080906 = "D:\nonpointsource_model\data\rainfall\idw_r_map\20080906"  
v20080907 = "D:\nonpointsource_model\data\rainfall\idw_r_map\20080907"  
v20080910 = "D:\nonpointsource_model\data\rainfall\idw_r_map\20080910"  
v20080911 = "D:\nonpointsource_model\data\rainfall\idw_r_map\20080911"  
v20080912 = "D:\nonpointsource_model\data\rainfall\idw_r_map\20080912"  
v20080915 = "D:\nonpointsource_model\data\rainfall\idw_r_map\20080915"  
v20080916 = "D:\nonpointsource_model\data\rainfall\idw_r_map\20080916"  
v20080918 = "D:\nonpointsource_model\data\rainfall\idw_r_map\20080918"  
v20080928 = "D:\nonpointsource_model\data\rainfall\idw_r_map\20080928"  
v20080930 = "D:\nonpointsource_model\data\rainfall\idw_r_map\20080930"  
v20081001 = "D:\nonpointsource_model\data\rainfall\idw_r_map\20081001"  
v20081003 = "D:\nonpointsource_model\data\rainfall\idw_r_map\20081003"  
v20081008 = "D:\nonpointsource_model\data\rainfall\idw_r_map\20081008"  
v20081018 = "D:\nonpointsource_model\data\rainfall\idw_r_map\20081018"  
v20081025 = "D:\nonpointsource_model\data\rainfall\idw_r_map\20081025"  
v20081030 = "D:\nonpointsource_model\data\rainfall\idw_r_map\20081030"  
v20081031 = "D:\nonpointsource_model\data\rainfall\idw_r_map\20081031"  
q20081031 = "D:\nonpointsource_model\data\runoff_sim\cal2\q\q20081031"  
accq1031 = "D:\nonpointsource_model\data\runoff_sim\cal2\accq\accq1031"  
flowdirection = "D:\nonpointsource_model\data\dem\flowdirection"  
s_dry = "D:\nonpointsource_model\data\hsg-cover\s_dry"  
s_normal = "D:\nonpointsource_model\data\hsg-cover\s_normal"  
s_wet = "D:\nonpointsource_model\data\hsg-cover\s_wet"  
q20081030 = "D:\nonpointsource_model\data\runoff_sim\cal2\q\q20081030"  
accq1030 = "D:\nonpointsource_model\data\runoff_sim\cal2\accq\accq1030"  
accq1025 = "D:\nonpointsource_model\data\runoff_sim\cal2\accq\accq1025"  
q20081025 = "D:\nonpointsource_model\data\runoff_sim\cal2\q\q20081025"  
accq1018 = "D:\nonpointsource_model\data\runoff_sim\cal2\accq\accq1018"  
q20081018 = "D:\nonpointsource_model\data\runoff_sim\cal2\q\q20081018"  
accq1008 = "D:\nonpointsource_model\data\runoff_sim\cal2\accq\accq1008"  
q20081008 = "D:\nonpointsource_model\data\runoff_sim\cal2\q\q20081008"  
accq1003 = "D:\nonpointsource_model\data\runoff_sim\cal2\accq\accq1003"  
q20081003 = "D:\nonpointsource_model\data\runoff_sim\cal2\q\q20081003"  
accq1001 = "D:\nonpointsource_model\data\runoff_sim\cal2\accq\accq1001"  
q20081001 = "D:\nonpointsource_model\data\runoff_sim\cal2\q\q20081001"  
accq0930 = "D:\nonpointsource_model\data\runoff_sim\cal2\accq\accq0930"  
q20080930 = "D:\nonpointsource_model\data\runoff_sim\cal2\q\q20080930"  
accq0928 = "D:\nonpointsource_model\data\runoff_sim\cal2\accq\accq0928"  
q20080928 = "D:\nonpointsource_model\data\runoff_sim\cal2\q\q20080928"
```

```

accq0918 = "D:\nonpointsource_model\data\runoff_sim\cal2\accq\accq0918"
q20080918 = "D:\nonpointsource_model\data\runoff_sim\cal2\q\q20080918"
accq0916 = "D:\nonpointsource_model\data\runoff_sim\cal2\accq\accq0916"
q20080916 = "D:\nonpointsource_model\data\runoff_sim\cal2\q\q20080916"
accq0915 = "D:\nonpointsource_model\data\runoff_sim\cal2\accq\accq0915"
q20080915 = "D:\nonpointsource_model\data\runoff_sim\cal2\q\q20080915"
accq0912 = "D:\nonpointsource_model\data\runoff_sim\cal2\accq\accq0912"
q20080912 = "D:\nonpointsource_model\data\runoff_sim\cal2\q\q20080912"
accq0911 = "D:\nonpointsource_model\data\runoff_sim\cal2\accq\accq0911"
q20080911 = "D:\nonpointsource_model\data\runoff_sim\cal2\q\q20080911"
accq0910 = "D:\nonpointsource_model\data\runoff_sim\cal2\accq\accq0910"
q20080910 = "D:\nonpointsource_model\data\runoff_sim\cal2\q\q20080910"
accq0819 = "D:\nonpointsource_model\data\runoff_sim\cal2\accq\accq0819"
q20080819 = "D:\nonpointsource_model\data\runoff_sim\cal2\q\q20080819"
accq0905 = "D:\nonpointsource_model\data\runoff_sim\cal2\accq\accq0905"
q20080905 = "D:\nonpointsource_model\data\runoff_sim\cal2\q\q20080905"
accq0906 = "D:\nonpointsource_model\data\runoff_sim\cal2\accq\accq0906"
q20080906 = "D:\nonpointsource_model\data\runoff_sim\cal2\q\q20080906"
accq0907 = "D:\nonpointsource_model\data\runoff_sim\cal2\accq\accq0907"
q20080907 = "D:\nonpointsource_model\data\runoff_sim\cal2\q\q20080907"
accq0818 = "D:\nonpointsource_model\data\runoff_sim\cal2\accq\accq0818"
q20080818 = "D:\nonpointsource_model\data\runoff_sim\cal2\q\q20080818"
v20080909 = "D:\nonpointsource_model\data\rainfall\idw_r_map\20080909"
q20080909 = "D:\nonpointsource_model\data\runoff_sim\cal2\q\q20080909"
accq0909 = "D:\nonpointsource_model\data\runoff_sim\cal2\accq\accq0909"
runoff_sim2 = "D:\nonpointsource_model\data\runoff_sim\cal2\runoff_sim2"
runoff_get_values_shp =
"D:\nonpointsource_model\data\runoff_measured\runoff_get_values.shp"
cal2 = "D:\nonpointsource_model\data\runoff_sim\cal2"
cal2_2_ = "D:\nonpointsource_model\data\runoff_sim\cal2"

' Process: CN (1031)...
gp.SingleOutputMapAlgebra_sa "POW ((([20081031] - 0.2 * [s_normal]) , [2]) /
([20081031] + 0.8 * [s_normal]))", q20081031,
"D:\nonpointsource_model\data\rainfall\idw_r_map\20081031;D:\nonpointsource_model\data\
hsg-cover\s_normal"

' Process: Flow Accumulation (1031)...
gp.FlowAccumulation_sa flowdirection, accq1031, q20081031, "FLOAT"

' Process: CN (1030)...
gp.SingleOutputMapAlgebra_sa "POW ((([20081030] - 0.2 * [s_normal]) , [2]) /
([20081030] + 0.8 * [s_normal]))", q20081030, "D:\nonpointsource_model\data\hsg-
cover\s_normal;D:\nonpointsource_model\data\rainfall\idw_r_map\20081030"

' Process: Flow Accumulation (1030)...
gp.FlowAccumulation_sa flowdirection, accq1030, q20081030, "FLOAT"

' Process: CN (1025)...
gp.SingleOutputMapAlgebra_sa "POW ((([20081025] - 0.2 * [s_dry]) , [2]) / ([20081025] +
0.8 * [s_dry]))", q20081025,
"D:\nonpointsource_model\data\rainfall\idw_r_map\20081025;D:\nonpointsource_model\data\
hsg-cover\s_dry"

' Process: Flow Accumulation (1025)...
gp.FlowAccumulation_sa flowdirection, accq1025, q20081025, "FLOAT"

' Process: CN (1018)...
gp.SingleOutputMapAlgebra_sa "POW ((([20081018] - 0.2 * [s_dry]) , [2]) / ([20081018] +
0.8 * [s_dry]))", q20081018,
"D:\nonpointsource_model\data\rainfall\idw_r_map\20081018;D:\nonpointsource_model\data\
hsg-cover\s_dry"

' Process: Flow Accumulation (1018)...
gp.FlowAccumulation_sa flowdirection, accq1018, q20081018, "FLOAT"

' Process: CN (1008)...
gp.SingleOutputMapAlgebra_sa "POW ((([20081008] - 0.2 * [s_normal]) , [2]) /
([20081008] + 0.8 * [s_normal]))", q20081008, "D:\nonpointsource_model\data\hsg-
cover\s_normal;D:\nonpointsource_model\data\rainfall\idw_r_map\20081008"

' Process: Flow Accumulation (1008)...
gp.FlowAccumulation_sa flowdirection, accq1008, q20081008, "FLOAT"

```

```

' Process: CN (1003)...
gp.SingleOutputMapAlgebra_sa "POW ((([20081003] - 0.2 * [s_wet]) , [2]) / ([20081003] +
0.8 * [s_wet]))", q20081003,
"D:\nonpointsource_model\data\rainfall\idw_r_map\20081003;D:\nonpointsource_model\data
\hsg-cover\s_wet"

' Process: Flow Accumulation (1003)...
gp.FlowAccumulation_sa flowdirection, accq1003, q20081003, "FLOAT"

' Process: CN (1001)...
gp.SingleOutputMapAlgebra_sa "POW ((([20081001] - 0.2 * [s_wet]) , [2]) / ([20081001] +
0.8 * [s_wet]))", q20081001,
"D:\nonpointsource_model\data\rainfall\idw_r_map\20081001;D:\nonpointsource_model\data
\hsg-cover\s_wet"

' Process: Flow Accumulation (1001)...
gp.FlowAccumulation_sa flowdirection, accq1001, q20081001, "FLOAT"

' Process: CN (0930)...
gp.SingleOutputMapAlgebra_sa "POW ((([20080930] - 0.2 * [s_dry]) , [2]) / ([20080930] +
0.8 * [s_dry]))", q20080930,
"D:\nonpointsource_model\data\rainfall\idw_r_map\20080930;D:\nonpointsource_model\data
\hsg-cover\s_dry"

' Process: Flow Accumulation (0930)...
gp.FlowAccumulation_sa flowdirection, accq0930, q20080930, "FLOAT"

' Process: CN (0928)...
gp.SingleOutputMapAlgebra_sa "POW ((([20080928] - 0.2 * [s_dry]) , [2]) / ([20080928] +
0.8 * [s_dry]))", q20080928,
"D:\nonpointsource_model\data\rainfall\idw_r_map\20080928;D:\nonpointsource_model\data
\hsg-cover\s_dry"

' Process: Flow Accumulation (0928)...
gp.FlowAccumulation_sa flowdirection, accq0928, q20080928, "FLOAT"

' Process: CN (0918)...
gp.SingleOutputMapAlgebra_sa "POW ((([20080918] - 0.2 * [s_wet]) , [2]) / ([20080918] +
0.8 * [s_wet]))", q20080918,
"D:\nonpointsource_model\data\rainfall\idw_r_map\20080918;D:\nonpointsource_model\data
\hsg-cover\s_wet"

' Process: Flow Accumulation (0918)...
gp.FlowAccumulation_sa flowdirection, accq0918, q20080918, "FLOAT"

' Process: CN (0916)...
gp.SingleOutputMapAlgebra_sa "POW ((([20080916] - 0.2 * [s_wet]) , [2]) / ([20080916] +
0.8 * [s_wet]))", q20080916,
"D:\nonpointsource_model\data\rainfall\idw_r_map\20080916;D:\nonpointsource_model\data
\hsg-cover\s_wet"

' Process: Flow Accumulation (0916)...
gp.FlowAccumulation_sa flowdirection, accq0916, q20080916, "FLOAT"

' Process: CN (0915)...
gp.SingleOutputMapAlgebra_sa "POW ((([20080915] - 0.2 * [s_wet]) , [2]) / ([20080915] +
0.8 * [s_wet]))", q20080915,
"D:\nonpointsource_model\data\rainfall\idw_r_map\20080915;D:\nonpointsource_model\data
\hsg-cover\s_wet"

' Process: Flow Accumulation (0915)...
gp.FlowAccumulation_sa flowdirection, accq0915, q20080915, "FLOAT"

' Process: CN (0912)...
gp.SingleOutputMapAlgebra_sa "POW ((([20080912] - 0.2 * [s_wet]) , [2]) / ([20080912] +
0.8 * [s_wet]))", q20080912,
"D:\nonpointsource_model\data\rainfall\idw_r_map\20080912;D:\nonpointsource_model\data
\hsg-cover\s_wet"

' Process: Flow Accumulation (0912)...
gp.FlowAccumulation_sa flowdirection, accq0912, q20080912, "FLOAT"

```

```

' Process: CN (0911)...
gp.SingleOutputMapAlgebra_sa "POW ((([20080911] - 0.2 * [s_wet]) , [2]) / ([20080911] + 0.8 * [s_wet]))", q20080911,
"D:\nonpointsource_model\data\rainfall\idw_r_map\20080911;D:\nonpointsource_model\data\hsg-cover\s_wet"

' Process: Flow Accumulation (0911)...
gp.FlowAccumulation_sa flowdirection, accq0911, q20080911, "FLOAT"

' Process: CN (0910)...
gp.SingleOutputMapAlgebra_sa "POW ((([20080910] - 0.2 * [s_wet]) , [2]) / ([20080910] + 0.8 * [s_wet]))", q20080910,
"D:\nonpointsource_model\data\rainfall\idw_r_map\20080910;D:\nonpointsource_model\data\hsg-cover\s_wet"

' Process: Flow Accumulation (0910)...
gp.FlowAccumulation_sa flowdirection, accq0910, q20080910, "FLOAT"

' Process: CN (0819)...
gp.SingleOutputMapAlgebra_sa "POW ((([20080819] - 0.2 * [s_dry]) , [2]) / ([20080819] + 0.8 * [s_dry]))", q20080819,
"D:\nonpointsource_model\data\rainfall\idw_r_map\20080819;D:\nonpointsource_model\data\hsg-cover\s_dry"

' Process: Flow Accumulation (0819)...
gp.FlowAccumulation_sa flowdirection, accq0819, q20080819, "FLOAT"

' Process: CN (0905)...
gp.SingleOutputMapAlgebra_sa "POW ((([20080905] - 0.2 * [s_dry]) , [2]) / ([20080905] + 0.8 * [s_dry]))", q20080905,
"D:\nonpointsource_model\data\rainfall\idw_r_map\20080905;D:\nonpointsource_model\data\hsg-cover\s_dry"

' Process: Flow Accumulation (0905)...
gp.FlowAccumulation_sa flowdirection, accq0905, q20080905, "FLOAT"

' Process: CN (0906)...
gp.SingleOutputMapAlgebra_sa "POW ((([20080906] - 0.2 * [s_dry]) , [2]) / ([20080906] + 0.8 * [s_dry]))", q20080906,
"D:\nonpointsource_model\data\rainfall\idw_r_map\20080906;D:\nonpointsource_model\data\hsg-cover\s_dry"

' Process: Flow Accumulation (0906)...
gp.FlowAccumulation_sa flowdirection, accq0906, q20080906, "FLOAT"

' Process: CN (0907)...
gp.SingleOutputMapAlgebra_sa "POW ((([20080907] - 0.2 * [s_normal]) , [2]) / ([20080907] + 0.8 * [s_normal]))", q20080907, "D:\nonpointsource_model\data\hsg-cover\s_normal;D:\nonpointsource_model\data\rainfall\idw_r_map\20080907"

' Process: Flow Accumulation (0907)...
gp.FlowAccumulation_sa flowdirection, accq0907, q20080907, "FLOAT"

' Process: CN (0818)...
gp.SingleOutputMapAlgebra_sa "POW ((([20080818] - 0.2 * [s_dry]) , [2]) / ([20080818] + 0.8 * [s_dry]))", q20080818,
"D:\nonpointsource_model\data\rainfall\idw_r_map\20080818;D:\nonpointsource_model\data\hsg-cover\s_dry"

' Process: Flow Accumulation (0818)...
gp.FlowAccumulation_sa flowdirection, accq0818, q20080818, "FLOAT"

' Process: CN (0909)...
gp.SingleOutputMapAlgebra_sa "POW ((([20080909] - 0.2 * [s_normal]) , [2]) / ([20080909] + 0.8 * [s_normal]))", q20080909, "D:\nonpointsource_model\data\hsg-cover\s_normal;D:\nonpointsource_model\data\rainfall\idw_r_map\20080909"

' Process: Flow Accumulation (0909)...
gp.FlowAccumulation_sa flowdirection, accq0909, q20080909, "FLOAT"

' Process: Sample...
gp.Sample_sa
"D:\nonpointsource_model\data\runoff_sim\cal2\accq\accq1031;D:\nonpointsource_model\da

```

```

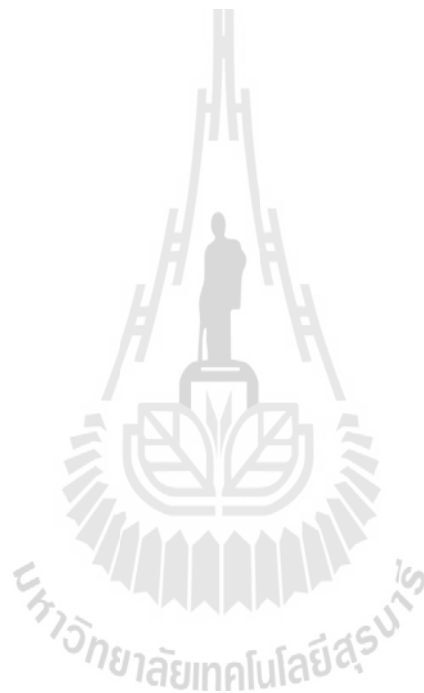
ta\runoff_sim\cal2\accq\accq1030;D:\nonpointsource_model\data\runoff_sim\cal2\accq\acc
q1025;D:\nonpointsource_model\data\runoff_sim\cal2\accq\accq1018;D:\nonpointsource_mod
el\data\runoff_sim\cal2\accq\accq1008;D:\nonpointsource_model\data\runoff_sim\cal2\acc
q\accq1003;D:\nonpointsource_model\data\runoff_sim\cal2\accq\accq1001;D:\nonpointsourc
e_model\data\runoff_sim\cal2\accq\accq0930;D:\nonpointsource_model\data\runoff_sim\cal
2\accq\accq0928;D:\nonpointsource_model\data\runoff_sim\cal2\accq\accq0918;D:\nonpoint
source_model\data\runoff_sim\cal2\accq\accq0916;D:\nonpointsource_model\data\runoff_si
m\cal2\accq\accq0915;D:\nonpointsource_model\data\runoff_sim\cal2\accq\accq0912;D:\non
pointsource_model\data\runoff_sim\cal2\accq\accq0911;D:\nonpointsource_model\data\runo
ff_sim\cal2\accq\accq0910;D:\nonpointsource_model\data\runoff_sim\cal2\accq\accq0819;D
:\nonpointsource_model\data\runoff_sim\cal2\accq\accq0905;D:\nonpointsource_model\data
\runoff_sim\cal2\accq\accq0906;D:\nonpointsource_model\data\runoff_sim\cal2\accq\accq0
907;D:\nonpointsource_model\data\runoff_sim\cal2\accq\accq0818;D:\nonpointsource_model
\data\runoff_sim\cal2\accq\accq0909", runoff_get_values_shp, runoff_sim2, "NEAREST"

```

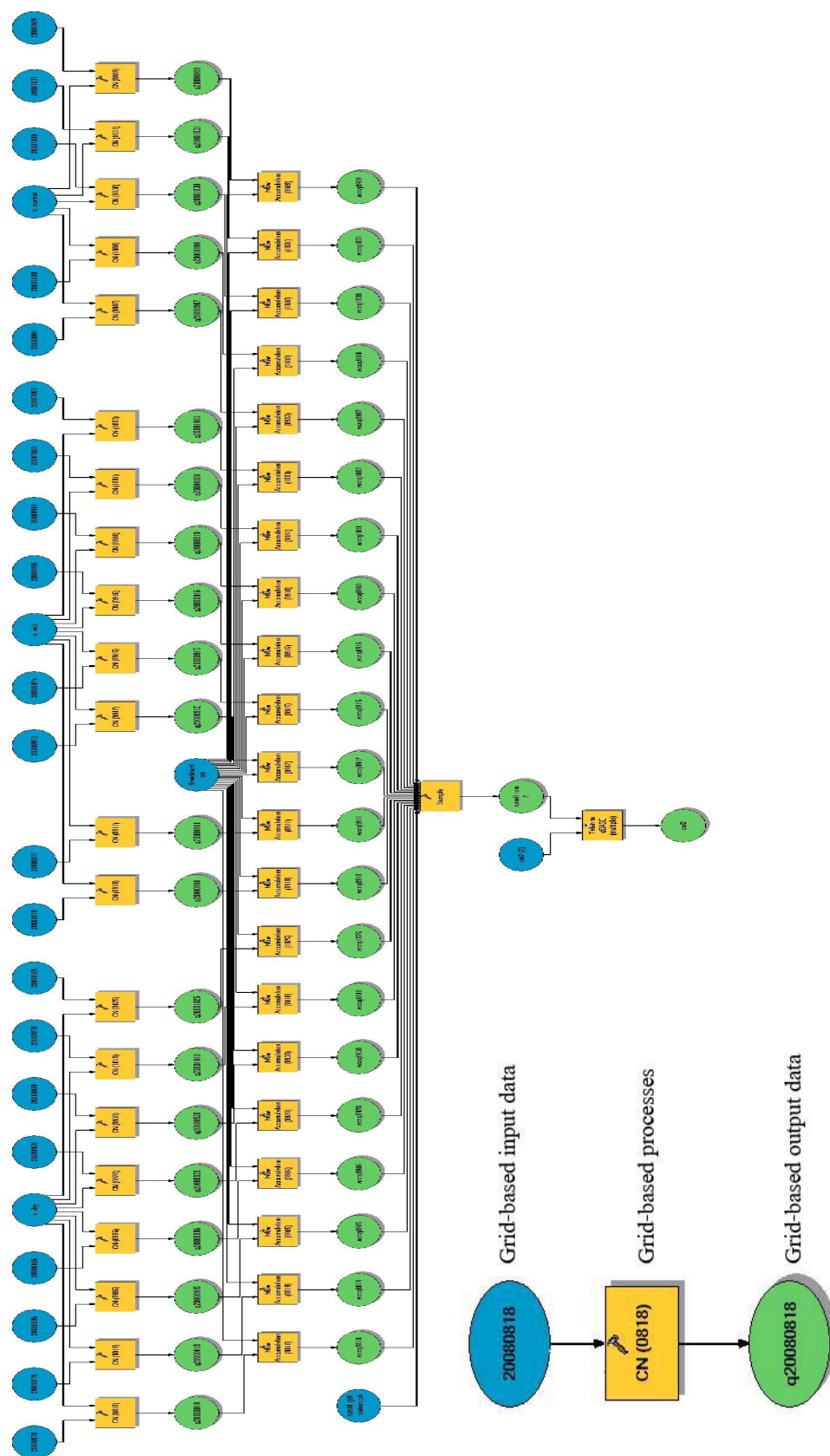
```

' Process: Table to dBASE (multiple)...
gp.TableToDBASE_conversion "D:\nonpointsource_model\data\runoff_sim\cal2\runoff_sim2",
cal2__2_

```



Model Diagram



APPENDIX D

MANNING’S ROUGHNESS COEFFICIENTS FOR CERTAIN TYPES OF LAND USE FOR THIS STUDY

Table D-1 Manning’s roughness coefficients for certain types of land use for this study.

Land use classification	Appropriate assumption to land use in study area	Manning <i>n</i>
Residential		0.015
Commercial and service		0.012
Industrial		0.012
Other urban and build-up land	Build-up land, institutional land, village, livestock farm house	0.015
Cropland and pasture	Cassava, corn, sugarcane, field crop, grass, horticulture, paddy field	0.035
Confined feeding operations		0.05
Other agricultural land	Scrub	0.035
Deciduous forest land	Dense deciduous forest, disturbed deciduous forest	0.1
Evergreen forest land	Dense evergreen forest, disturbed evergreen forest	0.1
Mixed forest land	Forest plantation,	0.1
Stream and canals		0.03
Forested wetlands	Marsh, swamp	0.07
Non-forested wetlands		0.05
Transitional areas		0.05
	eucalyptus, mixed orchard, mixed perennial, orchard, para rubber, perennial, teak (assumption for this study)	0.08

(Vieux, 2004)

APPENDIX E

24-HOUR DURATION PRECIPITATION WITH A 2-YAER RETURN PERIOD DATA

Table E-1 24-hour duration precipitation with a 2-year return period.

Station name	Station code	2-Year return period (mm.)
M.145	25751	74.8
RM.146	25771	82.6
RM.147	25781	75.8
Huai Krok De	25930	67.4
Ban Bu Ta Ko	25960	83.4
Ban Sub Sai Tong	25950	80.1
Ban Din U-Dom	25970	98.2
M.33	25511	67.1
Chok Chai 4 Farm	25651	82.6
Ban Nong Jok	25981	80.9
Ban Sub Sai Tai	251A1	66.7

APPENDIX F

K-VALUES BASED ON GEOLOGICAL DATA

Table F-1 K values based on major rock types of each of the geological formations.

Symbol	Formation	K	Major rocks	Remarks
Jpw	Phra Wihan	0.29	Sedimentary	Some formations were unnamed as the database was not formally published.
Jpk	Phu Kradung	0.29	Sedimentary	
P	*	0.29	Sedimentary and metamorphic	
P2	*	0.29	Sedimentary and metamorphic	
P3	*	0.29	Sedimentary and metamorphic	
PTRan	*	0.13	Igneous, andesite	
PTRrh	*	0.13	Igneous, rhyolite	
Qa	Quaternary	0.37	Alluvial deposit, gravel, sand, silt, and clay	
TRgr	*	0.13	Igneous, granite	
TRgr1	*	0.13	Igneous, granite	
TRgr2	*	0.13	Igneous, granite	
TRgr3	*	0.13	Igneous, granite	
Trhl	Huai Hin Lat	0.29	Sedimentary and metamorphic	

* No name for this unit.

APPENDIX G

C-VALUES BASED ON LAND USE DATA

Table G-1 C values based on land use data in the study area.

Land use	C values	Land use	C values
Abandoned paddy field crop	0.100	Longan	0.150
Acacia	0.088	Magosa	0.088
Agalloch	0.150	Mango	0.150
Bamboo	0.150	Mixed orchard	0.150
Banana	0.150	Mixed perennial	0.150
Betel palm/Chili	0.400	Oil palm	0.300
Cashew	0.400	Orange	0.300
Cassava	0.600	Paddy field	0.280
Chili	0.600	Papaya	0.600
Coconut	0.400	Para rubber	0.150
Corn	0.502	Paradise garden	0.600
Cotton	0.500	Pasture	0.100
Custard apple	0.300	Plummango	0.150
Dense deciduous forest	0.020	Pomelo	0.150
Dense evergreen forest	0.019	Pterocarpus sp.	0.088
Disturbed deciduous forest	0.250	Rose apple	0.150
Disturbed evergreen forest	0.040	Santol	0.150
Dragon fruit	0.600	Sapodilla	0.150
Eucalyptus	0.150	Scrub	0.048
Floricultural	0.386	Sugarcane	0.400
Forest plantation	0.088	Tamarind	0.150
Grass	0.100	Teak	0.088
Integrated farm/Diversified farm	0.225	Track crop	0.600
Jackfruit	0.150	Vine	0.600
Jujube	0.300		

APPENDIX H

COEFFICIENT RELATED TO LAND USE FOR SEDD

MODEL

Table H-1 Coefficient (a_i) related to land use for SEDD model.

Land use	a_i	Land use	a_i
build-up land	5.80	dense evergreen forest	1.20
institutional land	5.80	disturbed evergreen forest	1.20
village	5.80	forest plantation	1.20
livestock farm house	5.80	marsh and swamp	1.20
cassava	4.90	eucalyptus	1.20
corn	4.90	mixed orchard	1.20
sugarcane	4.90	mixed perennial	1.20
field crop	4.90	orchard	1.20
grass	4.90	paddy field	4.90
horticulture	4.90	para rubber	1.20
scrub	5.50	perennial	1.20
dense deciduous forest	1.20	teak	1.20
disturbed deciduous forest	1.20	water bodies	0.00

APPENDIX I

SOURCE CODE OF SEDIMENT YIELD MODEL

Source code (VBScript)

```
' -----  
' sed.vbs  
' (generated by ArcGIS/ModelBuilder)  
' Usage: sed <sdr>  
' -----  
  
' Create the Geoprocessor object  
set gp = WScript.CreateObject("esriGeoprocessing.GPDispatch.1")  
  
' Check out any necessary licenses  
gp.CheckOutExtension "spatial"  
  
' Load required toolboxes...  
gp.AddToolbox "D:/nonpointsource_model/modelbuilder/tbx/Grid-based Sediment Yield.tbx"  
gp.AddToolbox "C:/Program Files/ArcGIS/ArcToolbox/Toolboxes/Spatial Analyst Tools.tbx"  
gp.AddToolbox "C:/Program Files/ArcGIS/ArcToolbox/Toolboxes/Conversion Tools.tbx"  
  
' Script arguments...  
sdr = wscript.arguments.item(0)  
if sdr = "#" then  
    sdr = "D:\nonpointsource_model\data\sdr\sdr025" ' provide a default value if  
unspecified  
end if  
  
' Local variables...  
qp0818 = "D:\nonpointsource_model\data\sed_sim\m_usle\qp0818"  
qp0907 = "D:\nonpointsource_model\data\sed_sim\m_usle\qp0907"  
qp0910 = "D:\nonpointsource_model\data\sed_sim\m_usle\qp0910"  
qp0915 = "D:\nonpointsource_model\data\sed_sim\m_usle\qp0915"  
qp0928 = "D:\nonpointsource_model\data\sed_sim\m_usle\qp0928"  
qp0930 = "D:\nonpointsource_model\data\sed_sim\m_usle\qp0930"  
qp1025 = "D:\nonpointsource_model\data\sed_sim\m_usle\qp1025"  
qp1030 = "D:\nonpointsource_model\data\sed_sim\m_usle\qp1030"  
klscp = "D:\nonpointsource_model\data\sed_sim\klscp"  
q20080818 = "D:\nonpointsource_model\data\runoff_sim\cal2\q\q20080818"  
q20080907 = "D:\nonpointsource_model\data\runoff_sim\cal2\q\q20080907"  
q20080910 = "D:\nonpointsource_model\data\runoff_sim\cal2\q\q20080910"  
q20080915 = "D:\nonpointsource_model\data\runoff_sim\cal2\q\q20080915"  
q20080928 = "D:\nonpointsource_model\data\runoff_sim\cal2\q\q20080928"  
q20080930 = "D:\nonpointsource_model\data\runoff_sim\cal2\q\q20080930"  
q20081025 = "D:\nonpointsource_model\data\runoff_sim\cal2\q\q20081025"  
q20081030 = "D:\nonpointsource_model\data\runoff_sim\cal2\q\q20081030"  
sy0818 = "D:\nonpointsource_model\data\sed_sim\m_usle\sy0818"  
musle_exp_ab_shp = "D:\nonpointsource_model\data\sed_sim\musle_exp_ab.shp"  
a_coef = "D:\nonpointsource_model\data\sed_sim\a_coef"  
b_coef = "D:\nonpointsource_model\data\sed_sim\b_coef"  
sy0907 = "D:\nonpointsource_model\data\sed_sim\m_usle\sy0907"  
sy1030 = "D:\nonpointsource_model\data\sed_sim\m_usle\sy1030"  
sy0910 = "D:\nonpointsource_model\data\sed_sim\m_usle\sy0910"  
sy1025 = "D:\nonpointsource_model\data\sed_sim\m_usle\sy1025"  
sy0915 = "D:\nonpointsource_model\data\sed_sim\m_usle\sy0915"  
sy0930 = "D:\nonpointsource_model\data\sed_sim\m_usle\sy0930"  
sy0928 = "D:\nonpointsource_model\data\sed_sim\m_usle\sy0928"  
flowdirection = "D:\nonpointsource_model\data\dem\flowdirection"  
y1030 = "D:\nonpointsource_model\data\sed_sim\m_usle\y1030"  
y1025 = "D:\nonpointsource_model\data\sed_sim\m_usle\y1025"
```

```

y0930 = "D:\nonpointsource_model\data\sed_sim\m_usle\y0930"
y0928 = "D:\nonpointsource_model\data\sed_sim\m_usle\y0928"
y0818 = "D:\nonpointsource_model\data\sed_sim\m_usle\y0818"
y0907 = "D:\nonpointsource_model\data\sed_sim\m_usle\y0907"
y0910 = "D:\nonpointsource_model\data\sed_sim\m_usle\y0910"
y0915 = "D:\nonpointsource_model\data\sed_sim\m_usle\y0915"
y = "D:\nonpointsource_model\data\sed_sim\table_sediment\y"
runoff_get_values_shp =
"D:\nonpointsource_model\data\runoff_measured\runoff_get_values.shp"
table_sediment = "D:\nonpointsource_model\data\sed_sim\table_sediment"
table_sediment__2_ = "D:\nonpointsource_model\data\sed_sim\table_sediment"

' Process: Convert a_coef...
gp.FeatureToRaster_conversion musle_exp_ab_shp, "a_coef", a_coef, "30"

' Process: Convert b_coef...
gp.FeatureToRaster_conversion musle_exp_ab_shp, "b_coef", b_coef, "30"

' Process: MUSLE (1030)...
gp.toolbox = "D:/nonpointsource_model/modelbuilder/tbx/Grid-based Sediment Yield.tbx"
gp.SingleOutputMapAlgebra "pow (([q20081030] * [qp1030]) , [b_coef]) * [a_coef] *
[klscp] * 0.09 * [sdr]", sy1030,
"D:\nonpointsource_model\data\sed_sim\klscp;D:\nonpointsource_model\data\sed_sim\m_usle\qp1030;D:\nonpointsource_model\data\sed_sim\klscp;D:\nonpointsource_model\data\sed_sim\m_usle\qp1030;D:\nonpointsource_model\data\runoff_sim\cal2\q\q20081030;D:\nonpointsource_model\data\sdr\sdr025"

' Process: Flow Accumulation (sy1030)...
gp.FlowAccumulation_sa flowdirection, y1030, sy1030, "FLOAT"

' Process: MUSLE (1025)...
gp.toolbox = "D:/nonpointsource_model/modelbuilder/tbx/Grid-based Sediment Yield.tbx"
gp.SingleOutputMapAlgebra "pow (([q20081025] * [qp1025]) , [b_coef]) * [a_coef] *
[klscp] * 0.09 * [sdr]", sy1025,
"D:\nonpointsource_model\data\sed_sim\klscp;D:\nonpointsource_model\data\sed_sim\m_usle\qp1025;D:\nonpointsource_model\data\sed_sim\klscp;D:\nonpointsource_model\data\sed_sim\m_usle\qp1025;D:\nonpointsource_model\data\runoff_sim\cal2\q\q20081025;D:\nonpointsource_model\data\sdr\sdr025"

' Process: Flow Accumulation (sy1025)...
gp.FlowAccumulation_sa flowdirection, y1025, sy1025, "FLOAT"

' Process: MUSLE (0930)...
gp.toolbox = "D:/nonpointsource_model/modelbuilder/tbx/Grid-based Sediment Yield.tbx"
gp.SingleOutputMapAlgebra "pow (([q20080930] * [qp0930]) , [b_coef]) * [a_coef] *
[klscp] * 0.09 * [sdr]", sy0930,
"D:\nonpointsource_model\data\sed_sim\klscp;D:\nonpointsource_model\data\sed_sim\m_usle\qp0930;D:\nonpointsource_model\data\sed_sim\klscp;D:\nonpointsource_model\data\sed_sim\m_usle\qp0930;D:\nonpointsource_model\data\runoff_sim\cal2\q\q20080930;D:\nonpointsource_model\data\sdr\sdr025"

' Process: Flow Accumulation (sy0930)...
gp.FlowAccumulation_sa flowdirection, y0930, sy0930, "FLOAT"

' Process: MUSLE (0928)...
gp.toolbox = "D:/nonpointsource_model/modelbuilder/tbx/Grid-based Sediment Yield.tbx"
gp.SingleOutputMapAlgebra "pow (([q20080928] * [qp0928]) , [b_coef]) * [a_coef] *
[klscp] * 0.09 * [sdr]", sy0928,
"D:\nonpointsource_model\data\sed_sim\klscp;D:\nonpointsource_model\data\sed_sim\m_usle\qp0928;D:\nonpointsource_model\data\sed_sim\klscp;D:\nonpointsource_model\data\sed_sim\m_usle\qp0928;D:\nonpointsource_model\data\runoff_sim\cal2\q\q20080928;D:\nonpointsource_model\data\sdr\sdr025"

' Process: Flow Accumulation (sy0928)...
gp.FlowAccumulation_sa flowdirection, y0928, sy0928, "FLOAT"

' Process: MUSLE (0818)...
gp.toolbox = "D:/nonpointsource_model/modelbuilder/tbx/Grid-based Sediment Yield.tbx"
gp.SingleOutputMapAlgebra "pow (([q20080818] * [qp0818]) , [b_coef]) * [a_coef] *
[klscp] * 0.09 * [sdr]", sy0818,
"D:\nonpointsource_model\data\sed_sim\m_usle\qp0818;D:\nonpointsource_model\data\runoff_sim\cal2\q\q20080818;D:\nonpointsource_model\data\sed_sim\klscp;D:\nonpointsource_model\data\sdr\sdr025"

```

```

del\data\sed_sim\a_coef;D:\nonpointsource_model\data\sed_sim\b_coef;D:\nonpointsource_
model\data\sdr\sdr025"

' Process: Flow Accumulation (sy0818)...
gp.FlowAccumulation_sa flowdirection, y0818, sy0818, "FLOAT"

' Process: MUSLE (0907)...
gp.toolbox = "D:/nonpointsource_model/modelbuilder/tbx/Grid-based Sediment Yield.tbx"
gp.SingleOutputMapAlgebra "pow (([q20080907] * [qp0907]) , [b_coef]) * [a_coef] *
[klscp] * 0.09 * [sdr]", sy0907,
"D:\nonpointsource_model\data\sed_sim\klscp;D:\nonpointsource_model\data\sed_sim\a_coe
f;D:\nonpointsource_model\data\sed_sim\b_coef;D:\nonpointsource_model\data\sed_sim\m_u
sle\qp0907;D:\nonpointsource_model\data\runoff_sim\cal2\q\q20080907;D:\nonpointsource_
model\data\sdr\sdr025"

' Process: Flow Accumulation (sy0907) ...
gp.FlowAccumulation_sa flowdirection, y0907, sy0907, "FLOAT"

' Process: MUSLE (0910)...
gp.toolbox = "D:/nonpointsource_model/modelbuilder/tbx/Grid-based Sediment Yield.tbx"
gp.SingleOutputMapAlgebra "pow (([q20080910] * [qp0910]) , [b_coef]) * [a_coef] *
[klscp] * 0.09 * [sdr]", sy0910,
"D:\nonpointsource_model\data\sed_sim\klscp;D:\nonpointsource_model\data\sed_sim\a_coe
f;D:\nonpointsource_model\data\sed_sim\b_coef;D:\nonpointsource_model\data\sed_sim\m_u
sle\qp0910;D:\nonpointsource_model\data\runoff_sim\cal2\q\q20080910;D:\nonpointsource_
model\data\sdr\sdr025"

' Process: Flow Accumulation (sy0910)...
gp.FlowAccumulation_sa flowdirection, y0910, sy0910, "FLOAT"

' Process: MUSLE (0915)...
gp.toolbox = "D:/nonpointsource_model/modelbuilder/tbx/Grid-based Sediment Yield.tbx"
gp.SingleOutputMapAlgebra "pow (([q20080915] * [qp0915]) , [b_coef]) * [a_coef] *
[klscp] * 0.09 * [sdr]", sy0915,
"D:\nonpointsource_model\data\sed_sim\klscp;D:\nonpointsource_model\data\sed_sim\a_coe
f;D:\nonpointsource_model\data\sed_sim\b_coef;D:\nonpointsource_model\data\sed_sim\m_u
sle\qp0915;D:\nonpointsource_model\data\runoff_sim\cal2\q\q20080915;D:\nonpointsource_
model\data\sdr\sdr025"

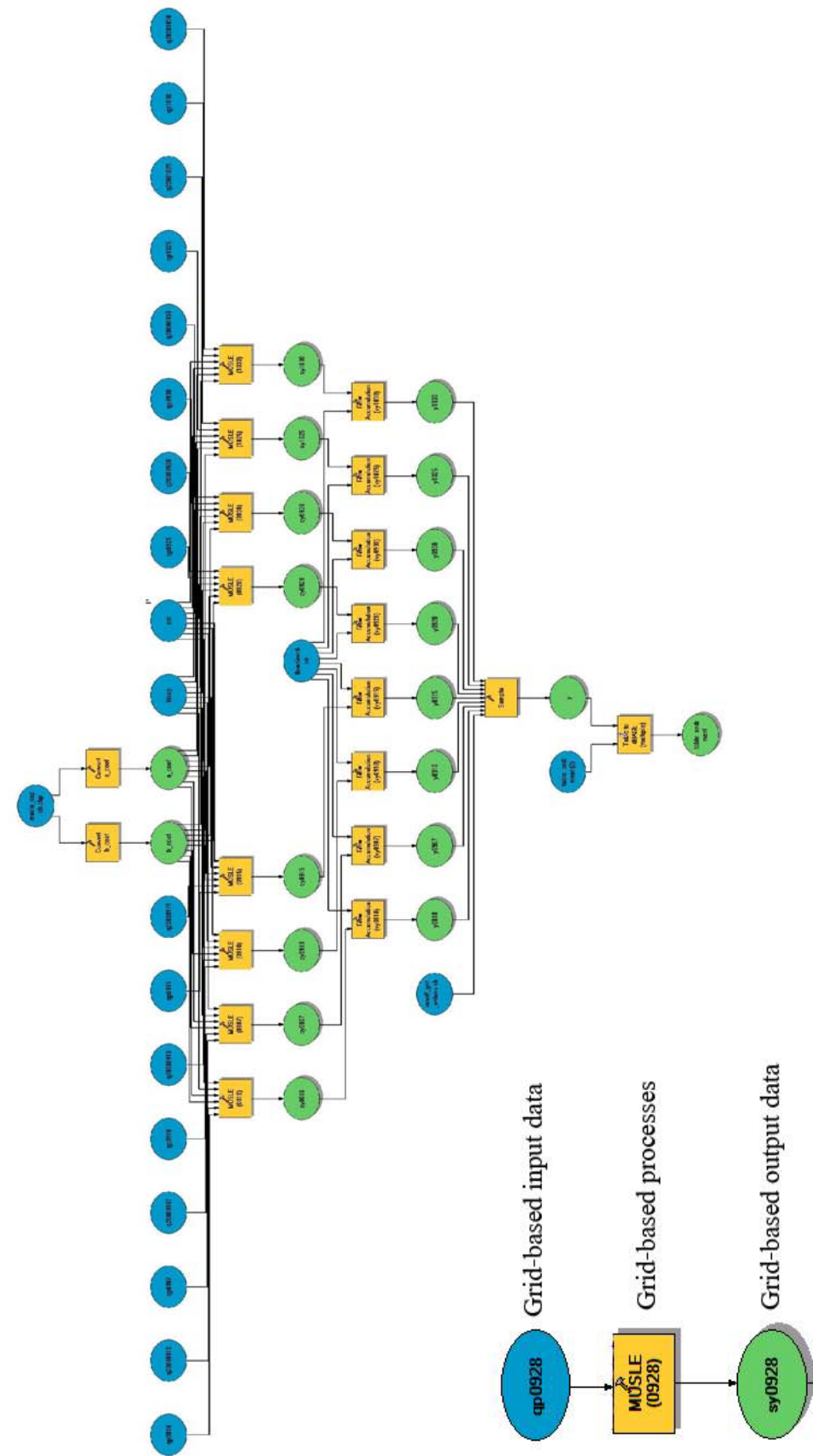
' Process: Flow Accumulation (sy0915)...
gp.FlowAccumulation_sa flowdirection, y0915, sy0915, "FLOAT"

' Process: Sample...
gp.Sample_sa
"D:\nonpointsource_model\data\sed_sim\m_usle\y1030;D:\nonpointsource_model\data\sed_si
m\m_usle\y1025;D:\nonpointsource_model\data\sed_sim\m_usle\y0930;D:\nonpointsource_mod
el\data\sed_sim\m_usle\y0928;D:\nonpointsource_model\data\sed_sim\m_usle\y0818;D:\nonp
ointsource_model\data\sed_sim\m_usle\y0907;D:\nonpointsource_model\data\sed_sim\m_usle
\y0910;D:\nonpointsource_model\data\sed_sim\m_usle\y0915", runoff_get_values_shp, y,
"NEAREST"

' Process: Table to dBASE (multiple)...
gp.TableToDBASE_conversion "D:\nonpointsource_model\data\sed_sim\table_sediment\y",
table_sediment__2_

```


Model Diagram



APPENDIX J

SOURCE CODE OF NUTRIENT YIELD MODEL

Source code (VBScript)

```
'-----  
' nutrient_n.vbs  
' (generated by ArcGIS/ModelBuilder)  
'-----  
  
' Create the Geoprocessor object  
set gp = WScript.CreateObject("esriGeoprocessing.GPDispatch.1")  
  
' Check out any necessary licenses  
gp.CheckOutExtension "spatial"  
  
' Load required toolboxes...  
gp.AddToolbox "C:/Program Files/ArcGIS/ArcToolbox/Toolboxes/Spatial Analyst Tools.tbx"  
gp.AddToolbox "C:/Program Files/ArcGIS/ArcToolbox/Toolboxes/Conversion Tools.tbx"  
gp.AddToolbox "C:/Documents and Settings/Administrator/Application  
Data/ESRI/ArcToolbox/My Toolboxes/Grid-based Nutrient Yield Model.tbx"  
  
' Set the Geoprocessing environment...  
gp.cellSize = "MAXOF"  
gp.mask = ""  
  
' Local variables...  
porosity = "D:\nonpointsource_model\data\soil\grid-soil-chem\porosity"  
soluble_n = "D:\nonpointsource_model\data\nutrient\soluble_n"  
total_por = "D:\nonpointsource_model\data\soil\grid-soil-chem\total_por"  
p_eff0818 = "D:\nonpointsource_model\data\nutrient\p_eff0818"  
v20080818 = "D:\nonpointsource_model\data\rainfall\idw_r_map\20080818"  
v20080907 = "D:\nonpointsource_model\data\rainfall\idw_r_map\20080907"  
v20080910 = "D:\nonpointsource_model\data\rainfall\idw_r_map\20080910"  
v20080915 = "D:\nonpointsource_model\data\rainfall\idw_r_map\20080915"  
v20080928 = "D:\nonpointsource_model\data\rainfall\idw_r_map\20080928"  
v20080930 = "D:\nonpointsource_model\data\rainfall\idw_r_map\20080930"  
v20081025 = "D:\nonpointsource_model\data\rainfall\idw_r_map\20081025"  
v20081030 = "D:\nonpointsource_model\data\rainfall\idw_r_map\20081030"  
N_RNC1030 = "D:\nonpointsource_model\data\nutrient\N_RNC1030"  
N_RNC1025 = "D:\nonpointsource_model\data\nutrient\N_RNC1025"  
N_RNC0930 = "D:\nonpointsource_model\data\nutrient\N_RNC0930"  
N_RNC0928 = "D:\nonpointsource_model\data\nutrient\N_RNC0928"  
N_RNC0915 = "D:\nonpointsource_model\data\nutrient\N_RNC0915"  
N_RNC0910 = "D:\nonpointsource_model\data\nutrient\N_RNC0910"  
N_RNC0907 = "D:\nonpointsource_model\data\nutrient\N_RNC0907"  
N_RNC0818 = "D:\nonpointsource_model\data\nutrient\N_RNC0818"  
p_eff0907 = "D:\nonpointsource_model\data\nutrient\p_eff0907"  
p_eff1030 = "D:\nonpointsource_model\data\nutrient\p_eff1030"  
p_eff0910 = "D:\nonpointsource_model\data\nutrient\p_eff0910"  
p_eff1025 = "D:\nonpointsource_model\data\nutrient\p_eff1025"  
p_eff0915 = "D:\nonpointsource_model\data\nutrient\p_eff0915"  
p_eff0930 = "D:\nonpointsource_model\data\nutrient\p_eff0930"  
p_eff0928 = "D:\nonpointsource_model\data\nutrient\p_eff0928"  
q20081030 = "D:\nonpointsource_model\data\runoff_sim\cal2\q\q20081030"  
q20081025 = "D:\nonpointsource_model\data\runoff_sim\cal2\q\q20081025"  
q20080930 = "D:\nonpointsource_model\data\runoff_sim\cal2\q\q20080930"  
q20080928 = "D:\nonpointsource_model\data\runoff_sim\cal2\q\q20080928"  
q20080915 = "D:\nonpointsource_model\data\runoff_sim\cal2\q\q20080915"  
q20080910 = "D:\nonpointsource_model\data\runoff_sim\cal2\q\q20080910"  
q20080907 = "D:\nonpointsource_model\data\runoff_sim\cal2\q\q20080907"  
q20080818 = "D:\nonpointsource_model\data\runoff_sim\cal2\q\q20080818"
```

```

i_eff0818 = "D:\nonpointsource_model\data\nutrient\i_eff0818"
i_eff0907 = "D:\nonpointsource_model\data\nutrient\i_eff0907"
i_eff0910 = "D:\nonpointsource_model\data\nutrient\i_eff0910"
i_eff0915 = "D:\nonpointsource_model\data\nutrient\i_eff0915"
i_eff0928 = "D:\nonpointsource_model\data\nutrient\i_eff0928"
i_eff0930 = "D:\nonpointsource_model\data\nutrient\i_eff0930"
i_eff1025 = "D:\nonpointsource_model\data\nutrient\i_eff1025"
i_eff1030 = "D:\nonpointsource_model\data\nutrient\i_eff1030"
n_fer_nfa = "D:\nonpointsource_model\data\nutrient\n_fer_nfa"
f_por = "D:\nonpointsource_model\data\soil\grid-soil-chem\f_por"
n_avs = "D:\nonpointsource_model\data\nutrient\n_avs"
n_dmv = "D:\nonpointsource_model\data\nutrient\n_dmv"
n_rmv = "D:\nonpointsource_model\data\nutrient\n_rmv"
expl_0818 = "D:\nonpointsource_model\data\nutrient\expl_0818"
expl_0930 = "D:\nonpointsource_model\data\nutrient\expl_0930"
expl_0910 = "D:\nonpointsource_model\data\nutrient\expl_0910"
expl_1030 = "D:\nonpointsource_model\data\nutrient\expl_1030"
expl_0915 = "D:\nonpointsource_model\data\nutrient\expl_0915"
expl_1025 = "D:\nonpointsource_model\data\nutrient\expl_1025"
expl_0928 = "D:\nonpointsource_model\data\nutrient\expl_0928"
expl_0907 = "D:\nonpointsource_model\data\nutrient\expl_0970"
exp2_1030 = "D:\nonpointsource_model\data\nutrient\exp2_1030"
exp2_1025 = "D:\nonpointsource_model\data\nutrient\exp2_1025"
exp2_0928 = "D:\nonpointsource_model\data\nutrient\exp2_0928"
exp2_0907 = "D:\nonpointsource_model\data\nutrient\exp2_0907"
exp2_0915 = "D:\nonpointsource_model\data\nutrient\exp2_0915"
exp2_0930 = "D:\nonpointsource_model\data\nutrient\exp2_0930"
exp2_0818 = "D:\nonpointsource_model\data\nutrient\exp2_0818"
exp2_0910 = "D:\nonpointsource_model\data\nutrient\exp2_0910"
c_ron0907 = "D:\nonpointsource_model\data\nutrient\c_ron0907"
c_ron1030 = "D:\nonpointsource_model\data\nutrient\c_ron1030"
c_ron1025 = "D:\nonpointsource_model\data\nutrient\c_ron1025"
c_ron0930 = "D:\nonpointsource_model\data\nutrient\c_ron0930"
c_ron0928 = "D:\nonpointsource_model\data\nutrient\c_ron0928"
c_ron0915 = "D:\nonpointsource_model\data\nutrient\c_ron0915"
c_ron0910 = "D:\nonpointsource_model\data\nutrient\c_ron0910"
c_ron0818 = "D:\nonpointsource_model\data\nutrient\c_ron0818"
flowdirection = "D:\nonpointsource_model\data\dem\flowdirection"
ac_ron1025 = "D:\nonpointsource_model\data\nutrient\ac_ron1025"
ac_ron0907 = "D:\nonpointsource_model\data\nutrient\ac_ron0907"
ac_ron1030 = "D:\nonpointsource_model\data\nutrient\ac_ron1030"
ac_ron0930 = "D:\nonpointsource_model\data\nutrient\ac_ron0930"
ac_ron0928 = "D:\nonpointsource_model\data\nutrient\ac_ron0928"
ac_ron0915 = "D:\nonpointsource_model\data\nutrient\ac_ron0915"
ac_ron0910 = "D:\nonpointsource_model\data\nutrient\ac_ron0910"
ac_ron0818 = "D:\nonpointsource_model\data\nutrient\ac_ron0818"
Sample_ac_ron = "D:\nonpointsource_model\data\nutrient\Sample_ac_ron"
runoff_get_values_shp =
"D:\nonpointsource_model\data\runoff_measured\runoff_get_values.shp"
nutrient = "D:\nonpointsource_model\data\nutrient"
nutrient__2_ = "D:\nonpointsource_model\data\nutrient"
soil_chem_shp = "D:\nonpointsource_model\data\soil\soil_chem.shp"
n_cpw = "D:\nonpointsource_model\data\nutrient\n_cpw"
n_cpw_ppm = "D:\nonpointsource_model\data\nutrient\n_cpw_ppm"
n_fer = "D:\nonpointsource_model\data\nutrient\n_fer"

' Process: N_FER * N_fa...
gp.SingleOutputMapAlgebra_sa "[n_fer] * 0.45", n_fer_nfa,
"D:\nonpointsource_model\data\nutrient\n_fer"

' Process: N_CPW V-to-R...
gp.FeatureToRaster_conversion soil_chem_shp, "SOILSYM", n_cpw, "147.94692"

' Process: % to ppm...
gp.toolbox = "C:/Documents and Settings/Administrator/Application
Data/ESRI/ArcToolbox/My Toolboxes/Grid-based Nutrient Yield Model.tbx"
gp.SingleOutputMapAlgebra "[n_cpw] * 10000", n_cpw_ppm,
"D:\nonpointsource_model\data\nutrient\n_cpw"

' Process: Sol_n...
gp.SingleOutputMapAlgebra_sa "0.1 * [n_cpw_ppm] * [porosity]", soluble_n,
"D:\nonpointsource_model\data\soil\grid-soil-
chem\porosity:D:\nonpointsource_model\data\nutrient\n_cpw_ppm"

```

```

' Process: N_AVS equation...
gp.toolbox = "C:/Documents and Settings/Administrator/Application
Data/ESRI/ArcToolbox/My Toolboxes/Grid-based Nutrient Yield Model.tbx"
gp.SingleOutputMapAlgebra "([soluble_n] + [n_fer_nfa]) * [f_por]", n_avs,
"D:\nonpointsource_model\data\soil\grid-soil-
chem\f_por;D:\nonpointsource_model\data\nutrient\n_fer_nfa;D:\nonpointsource_model\data\nutrient\soluble_n"

' Process: N-RNC (1025)...
gp.SingleOutputMapAlgebra_sa "[20081025] * [0.01] * [0.8]", N_RNC1025,
"D:\nonpointsource_model\data\rainfall\idw_r_map\20081025"

' Process: total_porosity...
gp.SingleOutputMapAlgebra_sa "[porosity] * 10", total_por,
"D:\nonpointsource_model\data\soil\grid-soil-chem\porosity"

' Process: P_EFF (1025)...
gp.SingleOutputMapAlgebra_sa "[20081025] - [total_por]", p_eff1025,
"D:\nonpointsource_model\data\soil\grid-soil-
chem\total_por;D:\nonpointsource_model\data\rainfall\idw_r_map\20081025"

' Process: N_DMV equation...
gp.toolbox = "C:/Documents and Settings/Administrator/Application
Data/ESRI/ArcToolbox/My Toolboxes/Grid-based Nutrient Yield Model.tbx"
gp.SingleOutputMapAlgebra "0.25 / [total_por]", n_dmv,
"D:\nonpointsource_model\data\soil\grid-soil-chem\total_por"

' Process: P_EFF-runoff (1025)...
gp.SingleOutputMapAlgebra_sa "[p_eff1025] - [q20081025]", i_eff1025,
"D:\nonpointsource_model\data\runoff_sim\cal2\q\q20081025;D:\nonpointsource_model\data\nutrient\p_eff1025"

' Process: Exp_1 (1025)...
gp.toolbox = "C:/Documents and Settings/Administrator/Application
Data/ESRI/ArcToolbox/My Toolboxes/Grid-based Nutrient Yield Model.tbx"
gp.SingleOutputMapAlgebra "EXP (-[n_dmv] * [i_eff1025])", exp1_1025,
"D:\nonpointsource_model\data\nutrient\n_dmv;D:\nonpointsource_model\data\nutrient\i_eff1025"

' Process: N_RMV equation...
gp.toolbox = "C:/Documents and Settings/Administrator/Application
Data/ESRI/ArcToolbox/My Toolboxes/Grid-based Nutrient Yield Model.tbx"
gp.SingleOutputMapAlgebra "0.05 / [total_por]", n_rmv,
"D:\nonpointsource_model\data\soil\grid-soil-chem\total_por"

' Process: Exp_2 (1025)...
gp.toolbox = "C:/Documents and Settings/Administrator/Application
Data/ESRI/ArcToolbox/My Toolboxes/Grid-based Nutrient Yield Model.tbx"
gp.SingleOutputMapAlgebra "exp (-[n_dmv] * [i_eff1025] - [n_rmv] * [q20081025])",
exp2_1025,
"D:\nonpointsource_model\data\nutrient\n_dmv;D:\nonpointsource_model\data\nutrient\n_rmv;D:\nonpointsource_model\data\runoff_sim\cal2\q\q20081025;D:\nonpointsource_model\data\nutrient\i_eff1025"

' Process: C_RON (1025)...
gp.toolbox = "C:/Documents and Settings/Administrator/Application
Data/ESRI/ArcToolbox/My Toolboxes/Grid-based Nutrient Yield Model.tbx"
gp.SingleOutputMapAlgebra "con ([p_eff1025] > 0 , ((([n_avs] - 0.0000008) *
[exp1_1025]) - (([n_avs] - 0.0000008) * [exp2_1025])) / [f_por]) + ((([N_RNC1025] *
[q20081025]) / [p_eff1025]) , [p_eff1025] < 0 , ((([n_avs] - 0.0000008) *
[exp1_1025]) - (([n_avs] - 0.0000008) * [exp2_1025])) / [f_por]))", c_ron1025,
"D:\nonpointsource_model\data\nutrient\n_avs;D:\nonpointsource_model\data\soil\grid-soil-
chem\f_por;D:\nonpointsource_model\data\nutrient\N_RNC1025;D:\nonpointsource_model\data\nutrient\p_eff1025;D:\nonpointsource_model\data\runoff_sim\cal2\q\q20081025;D:\nonpointsource_model\data\nutrient\exp1_1025;D:\nonpointsource_model\data\nutrient\exp2_1025"

' Process: Flow Accumulation (1025)...
gp.FlowAccumulation_sa flowdirection, ac_ron1025, c_ron1025, "FLOAT"

' Process: N-RNC (0907)...

```

```

gp.SingleOutputMapAlgebra_sa "[20080907] * [0.01] * [0.8]", N_RNC0907,
"D:\nonpointsource_model\data\rainfall\idw_r_map\20080907"

' Process: P_EFF (0907)...
gp.SingleOutputMapAlgebra_sa "[20080907] - [total_por]", p_eff0907,
"D:\nonpointsource_model\data\soil\grid-soil-
chem\total_por;D:\nonpointsource_model\data\rainfall\idw_r_map\20080907"

' Process: P_EFF-runoff (0907)...
gp.SingleOutputMapAlgebra_sa "[p_eff0907] - [q20080907]", i_eff0907,
"D:\nonpointsource_model\data\runoff_sim\cal2\q\q20080907;D:\nonpointsource_model\data
\nutrient\p_eff0907"

' Process: Exp_2 (0907)...
gp.toolbox = "C:/Documents and Settings/Administrator/Application
Data/ESRI/ArcToolbox/My Toolboxes/Grid-based Nutrient Yield Model.tbx"
gp.SingleOutputMapAlgebra "exp (-[n_dmv] * [i_eff0907] - [n_rmv] * [q20080907])",
exp2_0907,
"D:\nonpointsource_model\data\nutrient\n_dmv;D:\nonpointsource_model\data\nutrient\n_r
mv;D:\nonpointsource_model\data\runoff_sim\cal2\q\q20080907;D:\nonpointsource_model\da
ta\nutrient\i_eff0907"

' Process: Exp_1 (0907)...
gp.toolbox = "C:/Documents and Settings/Administrator/Application
Data/ESRI/ArcToolbox/My Toolboxes/Grid-based Nutrient Yield Model.tbx"
gp.SingleOutputMapAlgebra "EXP (-[n_dmv] * [i_eff0907])", expl_0907,
"D:\nonpointsource_model\data\nutrient\n_dmv;D:\nonpointsource_model\data\nutrient\i_e
ff0907"

' Process: C_RON (0907)...
gp.toolbox = "C:/Documents and Settings/Administrator/Application
Data/ESRI/ArcToolbox/My Toolboxes/Grid-based Nutrient Yield Model.tbx"
gp.SingleOutputMapAlgebra "(con ([p_eff0907] > 0 , ((([n_avs] - 0.0000008) *
[expl_0907]) - ([n_avs] - 0.0000008) * [exp2_0907])) / [f_por]) + ((([N_RNC0907] *
[q20080907]) / [p_eff0907]) , [p_eff0907] < 0 , ((([n_avs] - 0.0000008) *
[expl_0907]) - ([n_avs] - 0.0000008) * [exp2_0907])) / [f_por])) * 0.09", c_ron0907,
"D:\nonpointsource_model\data\nutrient\n_avs;D:\nonpointsource_model\data\soil\grid-
soil-
chem\f_por;D:\nonpointsource_model\data\nutrient\N_RNC0907;D:\nonpointsource_model\dat
a\nutrient\p_eff0907;D:\nonpointsource_model\data\runoff_sim\cal2\q\q20080907;D:\nonpo
intsource_model\data\nutrient\exp2_0907;D:\nonpointsource_model\data\nutrient\expl_097
0"

' Process: Flow Accumulation (0907)...
gp.FlowAccumulation_sa flowdirection, ac_ron0907, c_ron0907, "FLOAT"

' Process: N-RNC (1030)...
gp.SingleOutputMapAlgebra_sa "[20081030] * [0.01] * [0.8]", N_RNC1030,
"D:\nonpointsource_model\data\rainfall\idw_r_map\20081030"

' Process: P_EFF (1030)...
gp.SingleOutputMapAlgebra_sa "[20081030] - [total_por]", p_eff1030,
"D:\nonpointsource_model\data\soil\grid-soil-
chem\total_por;D:\nonpointsource_model\data\rainfall\idw_r_map\20081030"

' Process: P_EFF-runoff (1030)...
gp.SingleOutputMapAlgebra_sa "[p_eff1030] - [q20081030]", i_eff1030,
"D:\nonpointsource_model\data\runoff_sim\cal2\q\q20081030;D:\nonpointsource_model\data
\nutrient\p_eff1030"

' Process: Exp_1 (1030)...
gp.toolbox = "C:/Documents and Settings/Administrator/Application
Data/ESRI/ArcToolbox/My Toolboxes/Grid-based Nutrient Yield Model.tbx"
gp.SingleOutputMapAlgebra "EXP (-[n_dmv] * [i_eff1030])", expl_1030,
"D:\nonpointsource_model\data\nutrient\n_dmv;D:\nonpointsource_model\data\nutrient\i_e
ff1030"

' Process: Exp_2 (1030)...
gp.toolbox = "C:/Documents and Settings/Administrator/Application
Data/ESRI/ArcToolbox/My Toolboxes/Grid-based Nutrient Yield Model.tbx"
gp.SingleOutputMapAlgebra "exp (-[n_dmv] * [i_eff1030] - [n_rmv] * [q20081030])",
exp2_1030,
"D:\nonpointsource_model\data\runoff_sim\cal2\q\q20081030;D:\nonpointsource_model\data

```

```
\nutrient\n_dmv;D:\nonpointsource_model\data\nutrient\n_rmv;D:\nonpointsource_model\data\nutrient\i_eff1030"
```

```
' Process: C_RON (1030)...
gp.toolbox = "C:/Documents and Settings/Administrator/Application
Data/ESRI/ArcToolbox/My Toolboxes/Grid-based Nutrient Yield Model.tbx"
gp.SingleOutputMapAlgebra "(con ([p_eff1030] > 0 , ((([n_avs] - 0.0000008) *
[exp1_1030]) - (([n_avs] - 0.0000008) * [exp2_1030])) / [f_por]) + (([N_RNC1030] *
[q20081030]) / [p_eff1030]) , [p_eff1030] < 0 , ((([n_avs] - 0.0000008) *
[exp1_1030]) - (([n_avs] - 0.0000008) * [exp2_1030])) / [f_por])) * 0.09", c_ron1030,
"D:\nonpointsource_model\data\nutrient\n_avs;D:\nonpointsource_model\data\soil\grid-
soil-
chem\f_por;D:\nonpointsource_model\data\nutrient\N_RNC1030;D:\nonpointsource_model\data\nutrient\p_eff1030;D:\nonpointsource_model\data\runoff_sim\cal2\q\q20081030;D:\nonpointsource_model\data\nutrient\exp1_1030;D:\nonpointsource_model\data\nutrient\exp2_1030"
```

```
' Process: Flow Accumulation (1030)...
gp.FlowAccumulation_sa flowdirection, ac_ron1030, c_ron1030, "FLOAT"
```

```
' Process: N-RNC (0930)...
gp.SingleOutputMapAlgebra_sa "[20080930] * [0.01] * [0.8]", N_RNC0930,
"D:\nonpointsource_model\data\rainfall\idw_r_map\20080930"
```

```
' Process: P_EFF (0930)...
gp.SingleOutputMapAlgebra_sa "[20080930] - [total_por]", p_eff0930,
"D:\nonpointsource_model\data\soil\grid-soil-
chem\total_por;D:\nonpointsource_model\data\rainfall\idw_r_map\20080930"
```

```
' Process: P_EFF-runoff (0930)...
gp.SingleOutputMapAlgebra_sa "[p_eff0930] - [q20080930]", i_eff0930,
"D:\nonpointsource_model\data\runoff_sim\cal2\q\q20080930;D:\nonpointsource_model\data\nutrient\p_eff0930"
```

```
' Process: Exp_2 (0930)...
gp.toolbox = "C:/Documents and Settings/Administrator/Application
Data/ESRI/ArcToolbox/My Toolboxes/Grid-based Nutrient Yield Model.tbx"
gp.SingleOutputMapAlgebra "exp (-[n_dmv] * [i_eff0930] - [n_rmv] * [q20080930])",
exp2_0930,
"D:\nonpointsource_model\data\nutrient\n_dmv;D:\nonpointsource_model\data\nutrient\n_rmv;D:\nonpointsource_model\data\runoff_sim\cal2\q\q20080930;D:\nonpointsource_model\data\nutrient\i_eff0930"
```

```
' Process: Exp_1 (0930)...
gp.toolbox = "C:/Documents and Settings/Administrator/Application
Data/ESRI/ArcToolbox/My Toolboxes/Grid-based Nutrient Yield Model.tbx"
gp.SingleOutputMapAlgebra "EXP (-[n_dmv] * [i_eff0930])", exp1_0930,
"D:\nonpointsource_model\data\nutrient\n_dmv;D:\nonpointsource_model\data\nutrient\i_eff0930"
```

```
' Process: C_RON (0930)...
gp.toolbox = "C:/Documents and Settings/Administrator/Application
Data/ESRI/ArcToolbox/My Toolboxes/Grid-based Nutrient Yield Model.tbx"
gp.SingleOutputMapAlgebra "(con ([p_eff0930] > 0 , ((([n_avs] - 0.0000008) *
[exp1_0930]) - (([n_avs] - 0.0000008) * [exp2_0930])) / [f_por]) + (([N_RNC0930] *
[q20080930]) / [p_eff0930]) , [p_eff0930] < 0 , ((([n_avs] - 0.0000008) *
[exp1_0930]) - (([n_avs] - 0.0000008) * [exp2_0930])) / [f_por])) * 0.09", c_ron0930,
"D:\nonpointsource_model\data\nutrient\n_avs;D:\nonpointsource_model\data\soil\grid-
soil-
chem\f_por;D:\nonpointsource_model\data\nutrient\N_RNC0930;D:\nonpointsource_model\data\nutrient\p_eff0930;D:\nonpointsource_model\data\runoff_sim\cal2\q\q20080930;D:\nonpointsource_model\data\nutrient\exp2_0930;D:\nonpointsource_model\data\nutrient\exp1_0930"
```

```
' Process: Flow Accumulation (0930)...
gp.FlowAccumulation_sa flowdirection, ac_ron0930, c_ron0930, "FLOAT"
```

```
' Process: N-RNC (0928)...
gp.SingleOutputMapAlgebra_sa "[20080928] * [0.01] * [0.8]", N_RNC0928,
"D:\nonpointsource_model\data\rainfall\idw_r_map\20080928"
```

```
' Process: P_EFF (0928)...
```

```

gp.SingleOutputMapAlgebra_sa "[20080928] - [total_por]", p_eff0928,
"D:\nonpointsource_model\data\soil\grid-soil-
chem\total_por;D:\nonpointsource_model\data\rainfall\idw_r_map\20080928"

' Process: P_EFF-runoff (0928)...
gp.SingleOutputMapAlgebra_sa "[p_eff0928] - [q20080928]", i_eff0928,
"D:\nonpointsource_model\data\runoff_sim\cal2\q\q20080928;D:\nonpointsource_model\data
\nutrient\p_eff0928"

' Process: Exp_1 (0928)...
gp.toolbox = "C:/Documents and Settings/Administrator/Application
Data/ESRI/ArcToolbox/My Toolboxes/Grid-based Nutrient Yield Model.tbx"
gp.SingleOutputMapAlgebra "EXP (-[n_dmv] * [i_eff0928])", exp1_0928,
"D:\nonpointsource_model\data\nutrient\n_dmv;D:\nonpointsource_model\data\nutrient\i_e
ff0928"

' Process: Exp_2 (0928)...
gp.toolbox = "C:/Documents and Settings/Administrator/Application
Data/ESRI/ArcToolbox/My Toolboxes/Grid-based Nutrient Yield Model.tbx"
gp.SingleOutputMapAlgebra "exp (-[n_dmv] * [i_eff0928] - [n_rmv] * [q20080928])",
exp2_0928,
"D:\nonpointsource_model\data\nutrient\n_dmv;D:\nonpointsource_model\data\nutrient\n_r
mv;D:\nonpointsource_model\data\runoff_sim\cal2\q\q20080928;D:\nonpointsource_model\da
ta\nutrient\i_eff0928"

' Process: C_RON (0928)...
gp.toolbox = "C:/Documents and Settings/Administrator/Application
Data/ESRI/ArcToolbox/My Toolboxes/Grid-based Nutrient Yield Model.tbx"
gp.SingleOutputMapAlgebra "(con ([p_eff0928] > 0 , ((([n_avs] - 0.0000008) *
[exp1_0928]) - (([n_avs] - 0.0000008) * [exp2_0928])) / [f_por]) + (([N_RNC0928] *
[q20080928]) / [p_eff0928]) , [p_eff0928] < 0 , ((([n_avs] - 0.0000008) *
[exp1_0928]) - (([n_avs] - 0.0000008) * [exp2_0928])) / [f_por])) * 0.09", c_ron0928,
"D:\nonpointsource_model\data\nutrient\n_avs;D:\nonpointsource_model\data\soil\grid-
soil-
chem\f_por;D:\nonpointsource_model\data\nutrient\N_RNC0928;D:\nonpointsource_model\dat
a\nutrient\p_eff0928;D:\nonpointsource_model\data\runoff_sim\cal2\q\q20080928;D:\nonpo
intsource_model\data\nutrient\exp1_0928;D:\nonpointsource_model\data\nutrient\exp2_092
8"

' Process: Flow Accumulation (0928)...
gp.FlowAccumulation_sa flowdirection, ac_ron0928, c_ron0928, "FLOAT"

' Process: N-RNC (0915)...
gp.SingleOutputMapAlgebra_sa "[20080915] * [0.01] * [0.8]", N_RNC0915,
"D:\nonpointsource_model\data\rainfall\idw_r_map\20080915"

' Process: P_EFF (0915)...
gp.SingleOutputMapAlgebra_sa "[20080915] - [total_por]", p_eff0915,
"D:\nonpointsource_model\data\soil\grid-soil-
chem\total_por;D:\nonpointsource_model\data\rainfall\idw_r_map\20080915"

' Process: P_EFF-runoff (0915)...
gp.SingleOutputMapAlgebra_sa "[p_eff0915] - [q20080915]", i_eff0915,
"D:\nonpointsource_model\data\runoff_sim\cal2\q\q20080915;D:\nonpointsource_model\data
\nutrient\p_eff0915"

' Process: Exp_2 (0915)...
gp.toolbox = "C:/Documents and Settings/Administrator/Application
Data/ESRI/ArcToolbox/My Toolboxes/Grid-based Nutrient Yield Model.tbx"
gp.SingleOutputMapAlgebra "exp (-[n_dmv] * [i_eff0915] - [n_rmv] * [q20080915])",
exp2_0915,
"D:\nonpointsource_model\data\nutrient\n_dmv;D:\nonpointsource_model\data\nutrient\n_r
mv;D:\nonpointsource_model\data\runoff_sim\cal2\q\q20080915;D:\nonpointsource_model\da
ta\nutrient\i_eff0915"

' Process: Exp_1 (0915)...
gp.toolbox = "C:/Documents and Settings/Administrator/Application
Data/ESRI/ArcToolbox/My Toolboxes/Grid-based Nutrient Yield Model.tbx"
gp.SingleOutputMapAlgebra "EXP (-[n_dmv] * [i_eff0915])", exp1_0915,
"D:\nonpointsource_model\data\nutrient\n_dmv;D:\nonpointsource_model\data\nutrient\i_e
ff0915"

' Process: C_RON (0915)...

```

```

gp.toolbox = "C:/Documents and Settings/Administrator/Application
Data/ESRI/ArcToolbox/My Toolboxes/Grid-based Nutrient Yield Model.tbx"
gp.SingleOutputMapAlgebra "(con ([p_eff0915] > 0 , ((([n_avs] - 0.0000008) *
[exp1_0915]) - (([n_avs] - 0.0000008) * [exp2_0915])) / [f_por]) + (([N_RNC0915] *
[q20080915]) / [p_eff0915]) , [p_eff0915] < 0 , ((([n_avs] - 0.0000008) *
[exp1_0915]) - (([n_avs] - 0.0000008) * [exp2_0915])) / [f_por])) * 0.09", c_ron0915,
"D:\nonpointsource_model\data\nutrient\n_avs;D:\nonpointsource_model\data\soil\grid-
soil-
chem\f_por;D:\nonpointsource_model\data\nutrient\N_RNC0915;D:\nonpointsource_model\data
a\nutrient\p_eff0915;D:\nonpointsource_model\data\runoff_sim\cal2\q\q20080915;D:\nonpo
intsource_model\data\nutrient\exp2_0915;D:\nonpointsource_model\data\nutrient\exp1_091
5"

' Process: Flow Accumulation (0915)...
gp.FlowAccumulation_sa flowdirection, ac_ron0915, c_ron0915, "FLOAT"

' Process: N-RNC (0910)...
gp.SingleOutputMapAlgebra_sa "[20080910] * [0.01] * [0.8]", N_RNC0910,
"D:\nonpointsource_model\data\rainfall\idw_r_map\20080910"

' Process: P_EFF (0910)...
gp.SingleOutputMapAlgebra_sa "[20080910] - [total_por]", p_eff0910,
"D:\nonpointsource_model\data\soil\grid-soil-
chem\total_por;D:\nonpointsource_model\data\rainfall\idw_r_map\20080910"

' Process: P_EFF-runoff (0910)...
gp.SingleOutputMapAlgebra_sa "[p_eff0910] - [q20080910]", i_eff0910,
"D:\nonpointsource_model\data\runoff_sim\cal2\q\q20080910;D:\nonpointsource_model\data
\nutrient\p_eff0910"

' Process: Exp_1 (0910)...
gp.toolbox = "C:/Documents and Settings/Administrator/Application
Data/ESRI/ArcToolbox/My Toolboxes/Grid-based Nutrient Yield Model.tbx"
gp.SingleOutputMapAlgebra "EXP (-[n_dmv] * [i_eff0910])", exp1_0910,
"D:\nonpointsource_model\data\nutrient\n_dmv;D:\nonpointsource_model\data\nutrient\i_e
ff0910"

' Process: Exp_2 (0910)...
gp.toolbox = "C:/Documents and Settings/Administrator/Application
Data/ESRI/ArcToolbox/My Toolboxes/Grid-based Nutrient Yield Model.tbx"
gp.SingleOutputMapAlgebra "exp (-[n_dmv] * [i_eff0910] - [n_rmv] * [q20080910])",
exp2_0910,
"D:\nonpointsource_model\data\nutrient\n_dmv;D:\nonpointsource_model\data\nutrient\n_r
mv;D:\nonpointsource_model\data\runoff_sim\cal2\q\q20080910;D:\nonpointsource_model\data
ta\nutrient\i_eff0910"

' Process: C_RON (0910)...
gp.toolbox = "C:/Documents and Settings/Administrator/Application
Data/ESRI/ArcToolbox/My Toolboxes/Grid-based Nutrient Yield Model.tbx"
gp.SingleOutputMapAlgebra "(con ([p_eff0910] > 0 , ((([n_avs] - 0.0000008) *
[exp1_0910]) - (([n_avs] - 0.0000008) * [exp2_0910])) / [f_por]) + (([N_RNC0910] *
[q20080910]) / [p_eff0910]) , [p_eff0910] < 0 , ((([n_avs] - 0.0000008) *
[exp1_0910]) - (([n_avs] - 0.0000008) * [exp2_0910])) / [f_por])) * 0.09", c_ron0910,
"D:\nonpointsource_model\data\nutrient\n_avs;D:\nonpointsource_model\data\soil\grid-
soil-
chem\f_por;D:\nonpointsource_model\data\nutrient\N_RNC0910;D:\nonpointsource_model\data
a\nutrient\p_eff0910;D:\nonpointsource_model\data\runoff_sim\cal2\q\q20080910;D:\nonpo
intsource_model\data\nutrient\exp1_0910;D:\nonpointsource_model\data\nutrient\exp2_091
0"

' Process: Flow Accumulation (0910)...
gp.FlowAccumulation_sa flowdirection, ac_ron0910, c_ron0910, "FLOAT"

' Process: P_EFF (0818)...
gp.SingleOutputMapAlgebra_sa "[20080818] - [total_por]", p_eff0818,
"D:\nonpointsource_model\data\soil\grid-soil-
chem\total_por;D:\nonpointsource_model\data\rainfall\idw_r_map\20080818"

' Process: N-RNC (0818)...
gp.SingleOutputMapAlgebra_sa "[20080818] * [0.01] * [0.8]", N_RNC0818,
"D:\nonpointsource_model\data\rainfall\idw_r_map\20080818"

' Process: P_EFF-runoff (0818)...

```



```

gp.SingleOutputMapAlgebra_sa "[p_eff0818] - [q20080818]", i_eff0818,
"D:\nonpointsource_model\data\nutrient\p_eff0818;D:\nonpointsource_model\data\runoff_sim\cal2\q\q20080818"

' Process: Exp_1 (0818)...
gp.toolbox = "C:/Documents and Settings/Administrator/Application
Data/ESRI/ArcToolbox/My Toolboxes/Grid-based Nutrient Yield Model.tbx"
gp.SingleOutputMapAlgebra "EXP (-[n_dmv] * [i_eff0818])", expl_0818,
"D:\nonpointsource_model\data\nutrient\n_dmv;D:\nonpointsource_model\data\nutrient\i_eff0818"

' Process: Exp_2 (0818)...
gp.toolbox = "C:/Documents and Settings/Administrator/Application
Data/ESRI/ArcToolbox/My Toolboxes/Grid-based Nutrient Yield Model.tbx"
gp.SingleOutputMapAlgebra "exp (-[n_dmv] * [i_eff0818] - [n_rmv] * [q20080818])",
exp2_0818,
"D:\nonpointsource_model\data\nutrient\n_dmv;D:\nonpointsource_model\data\nutrient\n_rmv;D:\nonpointsource_model\data\runoff_sim\cal2\q\q20080818;D:\nonpointsource_model\data\nutrient\i_eff0818"

' Process: C_RON (0818)...
gp.toolbox = "C:/Documents and Settings/Administrator/Application
Data/ESRI/ArcToolbox/My Toolboxes/Grid-based Nutrient Yield Model.tbx"
gp.SingleOutputMapAlgebra "(con ([p_eff0818] > 0 , ((([n_avs] - 0.0000008) *
[expl_0818]) - (([n_avs] - 0.0000008) * [exp2_0818])) / [f_por]) + (([N_RNC0818] *
[q20080818]) / [p_eff0818]) , [p_eff0818] < 0 , ((([n_avs] - 0.0000008) *
[expl_0818]) - (([n_avs] - 0.0000008) * [exp2_0818])) / [f_por])) * 0.09", c_ron0818,
"D:\nonpointsource_model\data\nutrient\n_avs;D:\nonpointsource_model\data\soil\grid-soil-chem\f_por;D:\nonpointsource_model\data\nutrient\p_eff0818;D:\nonpointsource_model\data\nutrient\N_RNC0818;D:\nonpointsource_model\data\runoff_sim\cal2\q\q20080818;D:\nonpointsource_model\data\nutrient\expl_0818;D:\nonpointsource_model\data\nutrient\exp2_0818"

' Process: Flow Accumulation (0818)...
gp.FlowAccumulation_sa flowdirection, ac_ron0818, c_ron0818, "FLOAT"

' Process: Sample...
gp.Sample_sa
"D:\nonpointsource_model\data\nutrient\ac_ron1025;D:\nonpointsource_model\data\nutrient\ac_ron0907;D:\nonpointsource_model\data\nutrient\ac_ron1030;D:\nonpointsource_model\data\nutrient\ac_ron0930;D:\nonpointsource_model\data\nutrient\ac_ron0928;D:\nonpointsource_model\data\nutrient\ac_ron0915;D:\nonpointsource_model\data\nutrient\ac_ron0910;D:\nonpointsource_model\data\nutrient\ac_ron0818", runoff_get_values_shp,
Sample_ac_ron, "NEAREST"

' Process: Table to dBASE (multiple)...
gp.TableToDBASE_conversion "D:\nonpointsource_model\data\nutrient\Sample_ac_ron",
nutrient__2_

' -----
' nutrient_p.vbs
' (generated by ArcGIS/ModelBuilder)
' -----

' Create the Geoprocessor object
set gp = WScript.CreateObject("esriGeoprocessing.GPDispatch.1")

' Check out any necessary licenses
gp.CheckOutExtension "spatial"

' Load required toolboxes...
gp.AddToolbox "C:/Program Files/ArcGIS/ArcToolbox/Toolboxes/Spatial Analyst Tools.tbx"
gp.AddToolbox "C:/Program Files/ArcGIS/ArcToolbox/Toolboxes/Conversion Tools.tbx"
gp.AddToolbox "C:/Documents and Settings/Administrator/Application
Data/ESRI/ArcToolbox/My Toolboxes/Grid-based Nutrient Yield Model.tbx"

' Local variables...
porosity = "D:\nonpointsource_model\data\soil\grid-soil-chem\porosity"
soluble_p = "D:\nonpointsource_model\data\nutrient\soluble_p"
total_por = "D:\nonpointsource_model\data\soil\grid-soil-chem\total_por"
p_fer_pfa = "D:\nonpointsource_model\data\nutrient\p_fer_pfa"

```

```

f_por = "D:\nonpointsource_model\data\soil\grid-soil-chem\f_por"
p_avs = "D:\nonpointsource_model\data\nutrient\p_avs"
p_avr = "D:\nonpointsource_model\data\nutrient\p_avr"
p_dmv = "D:\nonpointsource_model\data\nutrient\p_dmv"
p_rmv = "D:\nonpointsource_model\data\nutrient\p_rmv"
i_eff0818 = "D:\nonpointsource_model\data\nutrient\i_eff0818"
i_eff0907 = "D:\nonpointsource_model\data\nutrient\i_eff0907"
i_eff0910 = "D:\nonpointsource_model\data\nutrient\i_eff0910"
i_eff0915 = "D:\nonpointsource_model\data\nutrient\i_eff0915"
i_eff0928 = "D:\nonpointsource_model\data\nutrient\i_eff0928"
i_eff0930 = "D:\nonpointsource_model\data\nutrient\i_eff0930"
i_eff1025 = "D:\nonpointsource_model\data\nutrient\i_eff1025"
i_eff1030 = "D:\nonpointsource_model\data\nutrient\i_eff1030"
elp_0818 = "D:\nonpointsource_model\data\nutrient\runoff_p_sim\elp_0818"
elp_0907 = "D:\nonpointsource_model\data\nutrient\runoff_p_sim\elp_0907"
elp_1030 = "D:\nonpointsource_model\data\nutrient\runoff_p_sim\elp_1030"
elp_0910 = "D:\nonpointsource_model\data\nutrient\runoff_p_sim\elp_0910"
elp_1025 = "D:\nonpointsource_model\data\nutrient\runoff_p_sim\elp_1025"
elp_0915 = "D:\nonpointsource_model\data\nutrient\runoff_p_sim\elp_0915"
elp_0930 = "D:\nonpointsource_model\data\nutrient\runoff_p_sim\elp_0930"
elp_0928 = "D:\nonpointsource_model\data\nutrient\runoff_p_sim\elp_0928"
e2p_1025 = "D:\nonpointsource_model\data\nutrient\runoff_p_sim\e2p_1025"
q20080818 = "D:\nonpointsource_model\data\runoff_sim\cal2\q\q20080818"
q20080907 = "D:\nonpointsource_model\data\runoff_sim\cal2\q\q20080907"
q20080910 = "D:\nonpointsource_model\data\runoff_sim\cal2\q\q20080910"
q20080915 = "D:\nonpointsource_model\data\runoff_sim\cal2\q\q20080915"
q20080928 = "D:\nonpointsource_model\data\runoff_sim\cal2\q\q20080928"
q20080930 = "D:\nonpointsource_model\data\runoff_sim\cal2\q\q20080930"
q20081025 = "D:\nonpointsource_model\data\runoff_sim\cal2\q\q20081025"
q20081030 = "D:\nonpointsource_model\data\runoff_sim\cal2\q\q20081030"
e2p_1030 = "D:\nonpointsource_model\data\nutrient\runoff_p_sim\e2p_1030"
e2p_0930 = "D:\nonpointsource_model\data\nutrient\runoff_p_sim\e2p_0930"
e2p_0928 = "D:\nonpointsource_model\data\nutrient\runoff_p_sim\e2p_0928"
e2p_0915 = "D:\nonpointsource_model\data\nutrient\runoff_p_sim\e2p_0915"
e2p_0910 = "D:\nonpointsource_model\data\nutrient\runoff_p_sim\e2p_0910"
e2p_0907 = "D:\nonpointsource_model\data\nutrient\runoff_p_sim\e2p_0907"
e2p_0818 = "D:\nonpointsource_model\data\nutrient\runoff_p_sim\e2p_0818"
c_rop0818 = "D:\nonpointsource_model\data\nutrient\runoff_p_sim\c_rop0818"
c_rop1030 = "D:\nonpointsource_model\data\nutrient\runoff_p_sim\c_rop1030"
c_rop0907 = "D:\nonpointsource_model\data\nutrient\runoff_p_sim\c_rop0907"
c_rop1025 = "D:\nonpointsource_model\data\nutrient\runoff_p_sim\c_rop1025"
c_rop0910 = "D:\nonpointsource_model\data\nutrient\runoff_p_sim\c_rop0910"
c_rop0930 = "D:\nonpointsource_model\data\nutrient\runoff_p_sim\c_rop0930"
c_rop0915 = "D:\nonpointsource_model\data\nutrient\runoff_p_sim\c_rop0915"
c_rop0928 = "D:\nonpointsource_model\data\nutrient\runoff_p_sim\c_rop0928"
flowdirection = "D:\nonpointsource_model\data\dem\flowdirection"
ac_rop0818 = "D:\nonpointsource_model\data\nutrient\runoff_p_sim\ac_rop0818"
ac_rop0907 = "D:\nonpointsource_model\data\nutrient\runoff_p_sim\ac_rop0907"
ac_rop1030 = "D:\nonpointsource_model\data\nutrient\runoff_p_sim\ac_rop1030"
ac_rop0910 = "D:\nonpointsource_model\data\nutrient\runoff_p_sim\ac_rop0910"
ac_rop1025 = "D:\nonpointsource_model\data\nutrient\runoff_p_sim\ac_rop1025"
ac_rop0915 = "D:\nonpointsource_model\data\nutrient\runoff_p_sim\ac_rop0915"
ac_rop0930 = "D:\nonpointsource_model\data\nutrient\runoff_p_sim\ac_rop0930"
ac_rop0928 = "D:\nonpointsource_model\data\nutrient\runoff_p_sim\ac_rop0928"
c_rop_table =
"D:\nonpointsource_model\data\nutrient\runoff_p_sim\c_rop_table\c_rop_table"
runoff_get_values_shp =
"D:\nonpointsource_model\data\runoff_measured\runoff_get_values.shp"
c_rop_table__2_ = "D:\nonpointsource_model\data\nutrient\runoff_p_sim\c_rop_table"
c_rop_table__3_ = "D:\nonpointsource_model\data\nutrient\runoff_p_sim\c_rop_table"
soil_chem_shp = "D:\nonpointsource_model\data\soil\soil_chem.shp"
p_cpw = "D:\nonpointsource_model\data\nutrient\p_cpw"
p_fer = "D:\nonpointsource_model\data\nutrient\p_fer"

' Process: P_soil V-to-R...
gp.FeatureToRaster_conversion soil_chem_shp, "P", p_cpw, "30"

' Process: Sol_p...
gp.SingleOutputMapAlgebra_sa "0.1 * [p_cpw] * [porosity]", soluble_p,
"D:\nonpointsource_model\data\soil\grid-soil-
chem\porosity;D:\nonpointsource_model\data\nutrient\p_cpw"

' Process: P_FER * P_fa...

```

```

gp.SingleOutputMapAlgebra_sa "[p_fer] * 0.55", p_fer_pfa,
"D:\nonpointsource_model\data\nutrient\p_fer"

' Process: P_AVS equation...
gp.toolbox = "C:/Documents and Settings/Administrator/Application
Data/ESRI/ArcToolbox/My Toolboxes/Grid-based Nutrient Yield Model.tbx"
gp.SingleOutputMapAlgebra "([soluble_p] + [p_fer_pfa]) * [f_por]", p_avs,
"D:\nonpointsource_model\data\nutrient\soluble_p;D:\nonpointsource_model\data\nutrient
\p_fer_pfa;D:\nonpointsource_model\data\soil\grid-soil-chem\f_por"

' Process: P_AVR equation...
gp.toolbox = "C:/Documents and Settings/Administrator/Application
Data/ESRI/ArcToolbox/My Toolboxes/Grid-based Nutrient Yield Model.tbx"
gp.SingleOutputMapAlgebra "[soluble_p] * [f_por]", p_avr,
"D:\nonpointsource_model\data\nutrient\soluble_p;D:\nonpointsource_model\data\soil\gri
d-soil-chem\f_por"

' Process: total_porosity...
gp.SingleOutputMapAlgebra_sa "[porosity] * 10", total_por,
"D:\nonpointsource_model\data\soil\grid-soil-chem\porosity"

' Process: P_DMV equation...
gp.toolbox = "C:/Documents and Settings/Administrator/Application
Data/ESRI/ArcToolbox/My Toolboxes/Grid-based Nutrient Yield Model.tbx"
gp.SingleOutputMapAlgebra "0.01 / [total_por]", p_dmv,
"D:\nonpointsource_model\data\soil\grid-soil-chem\total_por"

' Process: Exp1phos (0818)...
gp.toolbox = "C:/Documents and Settings/Administrator/Application
Data/ESRI/ArcToolbox/My Toolboxes/Grid-based Nutrient Yield Model.tbx"
gp.SingleOutputMapAlgebra "EXP (-[p_dmv] * [i_eff0818])", elp_0818,
"D:\nonpointsource_model\data\nutrient\i_eff0818;D:\nonpointsource_model\data\nutrient
\p_dmv"

' Process: P_RMV equation...
gp.toolbox = "C:/Documents and Settings/Administrator/Application
Data/ESRI/ArcToolbox/My Toolboxes/Grid-based Nutrient Yield Model.tbx"
gp.SingleOutputMapAlgebra "0.0010 / [total_por]", p_rmv,
"D:\nonpointsource_model\data\soil\grid-soil-chem\total_por"

' Process: Exp2Phos (0818)...
gp.toolbox = "C:/Documents and Settings/Administrator/Application
Data/ESRI/ArcToolbox/My Toolboxes/Grid-based Nutrient Yield Model.tbx"
gp.SingleOutputMapAlgebra "exp (-[p_dmv] * [i_eff0818] - [p_rmv] * [q20080818])",
e2p_0818,
"D:\nonpointsource_model\data\nutrient\p_dmv;D:\nonpointsource_model\data\nutrient\p_r
mv;D:\nonpointsource_model\data\nutrient\i_eff0818;D:\nonpointsource_model\data\runoff
_sim\cal2\q\q20080818"

' Process: C_ROP (0818)...
gp.toolbox = "C:/Documents and Settings/Administrator/Application
Data/ESRI/ArcToolbox/My Toolboxes/Grid-based Nutrient Yield Model.tbx"
gp.SingleOutputMapAlgebra "((((([p_avs] - [p_avr]) * [elp_0818]) - (([p_avs] -
[p_avr]) * [e2p_0818])) / [f_por]) + (([p_avr] * [p_rmv] * [q20080818]) / [f_por])) *
0.09", c_rop0818,
"D:\nonpointsource_model\data\nutrient\p_avs;D:\nonpointsource_model\data\nutrient\p_a
vr;D:\nonpointsource_model\data\nutrient\runoff_p_sim\elp_0818;D:\nonpointsource_model
\data\nutrient\runoff_p_sim\e2p_0818;D:\nonpointsource_model\data\soil\grid-soil-
chem\f_por;D:\nonpointsource_model\data\nutrient\p_rmv;D:\nonpointsource_model\data\ru
noff_sim\cal2\q\q20080818"

' Process: Flow Accumulation (0818)...
gp.FlowAccumulation_sa flowdirection, ac_rop0818, c_rop0818, "FLOAT"

' Process: Exp1phos (0907)...
gp.toolbox = "C:/Documents and Settings/Administrator/Application
Data/ESRI/ArcToolbox/My Toolboxes/Grid-based Nutrient Yield Model.tbx"
gp.SingleOutputMapAlgebra "EXP (-[p_dmv] * [i_eff0907])", elp_0907,
"D:\nonpointsource_model\data\nutrient\p_dmv;D:\nonpointsource_model\data\nutrient\i_e
ff0907"

' Process: Exp2Phos (0907)...

```

```

gp.toolbox = "C:/Documents and Settings/Administrator/Application
Data/ESRI/ArcToolbox/My Toolboxes/Grid-based Nutrient Yield Model.tbx"
gp.SingleOutputMapAlgebra "exp (-[p_dmv] * [i_eff0907] - [p_rmv] * [q20080907])",
e2p_0907,
"D:\nonpointsource_model\data\nutrient\p_dmv;D:\nonpointsource_model\data\nutrient\p_r
mv;D:\nonpointsource_model\data\nutrient\i_eff0907;D:\nonpointsource_model\data\runoff
_sim\cal2\q\q20080907"

' Process: C_ROP (0907)...
gp.toolbox = "C:/Documents and Settings/Administrator/Application
Data/ESRI/ArcToolbox/My Toolboxes/Grid-based Nutrient Yield Model.tbx"
gp.SingleOutputMapAlgebra "((((([p_avs] - [p_avr]) * [elp_0907]) - (([p_avs] -
[p_avr]) * [e2p_0907])) / [f_por]) + (([p_avr] * [p_rmv] * [q20080907]) / [f_por])) *
0.09", c_rop0907,
"D:\nonpointsource_model\data\nutrient\p_avs;D:\nonpointsource_model\data\nutrient\p_a
vr;D:\nonpointsource_model\data\soil\grid-soil-
chem\f_por;D:\nonpointsource_model\data\nutrient\p_rmv;D:\nonpointsource_model\data\nu
trient\runoff_p_sim\elp_0907;D:\nonpointsource_model\data\nutrient\runoff_p_sim\elp_09
07;D:\nonpointsource_model\data\runoff_sim\cal2\q\q20080907"

' Process: Flow Accumulation (0907)...
gp.FlowAccumulation_sa flowdirection, ac_rop0907, c_rop0907, "FLOAT"

' Process: Explphos (0910)...
gp.toolbox = "C:/Documents and Settings/Administrator/Application
Data/ESRI/ArcToolbox/My Toolboxes/Grid-based Nutrient Yield Model.tbx"
gp.SingleOutputMapAlgebra "EXP (-[p_dmv] * [i_eff0910])", elp_0910,
"D:\nonpointsource_model\data\nutrient\p_dmv;D:\nonpointsource_model\data\nutrient\i_e
ff0910"

' Process: Exp2Phos (0910)...
gp.toolbox = "C:/Documents and Settings/Administrator/Application
Data/ESRI/ArcToolbox/My Toolboxes/Grid-based Nutrient Yield Model.tbx"
gp.SingleOutputMapAlgebra "exp (-[p_dmv] * [i_eff0910] - [p_rmv] * [q20080910])",
e2p_0910,
"D:\nonpointsource_model\data\nutrient\p_dmv;D:\nonpointsource_model\data\nutrient\p_r
mv;D:\nonpointsource_model\data\nutrient\i_eff0910;D:\nonpointsource_model\data\runoff
_sim\cal2\q\q20080910"

' Process: C_ROP (0910)...
gp.toolbox = "C:/Documents and Settings/Administrator/Application
Data/ESRI/ArcToolbox/My Toolboxes/Grid-based Nutrient Yield Model.tbx"
gp.SingleOutputMapAlgebra "((((([p_avs] - [p_avr]) * [elp_0910]) - (([p_avs] -
[p_avr]) * [e2p_0910])) / [f_por]) + (([p_avr] * [p_rmv] * [q20080910]) / [f_por])) *
0.09", c_rop0910,
"D:\nonpointsource_model\data\nutrient\p_avs;D:\nonpointsource_model\data\nutrient\p_a
vr;D:\nonpointsource_model\data\soil\grid-soil-
chem\f_por;D:\nonpointsource_model\data\nutrient\p_rmv;D:\nonpointsource_model\data\nu
trient\runoff_p_sim\elp_0910;D:\nonpointsource_model\data\nutrient\runoff_p_sim\elp_09
10;D:\nonpointsource_model\data\runoff_sim\cal2\q\q20080910"

' Process: Flow Accumulation (0910)...
gp.FlowAccumulation_sa flowdirection, ac_rop0910, c_rop0910, "FLOAT"

' Process: Explphos (1030)...
gp.toolbox = "C:/Documents and Settings/Administrator/Application
Data/ESRI/ArcToolbox/My Toolboxes/Grid-based Nutrient Yield Model.tbx"
gp.SingleOutputMapAlgebra "EXP (-[p_dmv] * [i_eff1030])", elp_1030,
"D:\nonpointsource_model\data\nutrient\p_dmv;D:\nonpointsource_model\data\nutrient\i_e
ff1030"

' Process: Exp2Phos (1030)...
gp.toolbox = "C:/Documents and Settings/Administrator/Application
Data/ESRI/ArcToolbox/My Toolboxes/Grid-based Nutrient Yield Model.tbx"
gp.SingleOutputMapAlgebra "exp (-[p_dmv] * [i_eff1030] - [p_rmv] * [q20081030])",
e2p_1030,
"D:\nonpointsource_model\data\nutrient\p_dmv;D:\nonpointsource_model\data\nutrient\p_r
mv;D:\nonpointsource_model\data\nutrient\i_eff1030;D:\nonpointsource_model\data\runoff
_sim\cal2\q\q20081030"

' Process: C_ROP (1030)...
gp.toolbox = "C:/Documents and Settings/Administrator/Application
Data/ESRI/ArcToolbox/My Toolboxes/Grid-based Nutrient Yield Model.tbx"

```

```

gp.SingleOutputMapAlgebra "((((([p_avs] - [p_avr]) * [elp_1030]) - (([p_avs] -
[p_avr]) * [e2p_1030])) / [f_por]) + (([p_avr] * [p_rmv] * [q20081030]) / [f_por])) *
0.09", c_rop1030,
"D:\nonpointsource_model\data\nutrient\p_avs;D:\nonpointsource_model\data\nutrient\p_a
vr;D:\nonpointsource_model\data\soil\grid-soil-
chem\f_por;D:\nonpointsource_model\data\nutrient\p_rmv;D:\nonpointsource_model\data\nu
trient\runoff_p_sim\elp_1030;D:\nonpointsource_model\data\nutrient\runoff_p_sim\e2p_10
30;D:\nonpointsource_model\data\runoff_sim\cal2\q\q20081030"

' Process: Flow Accumulation (1030)...
gp.FlowAccumulation_sa flowdirection, ac_rop1030, c_rop1030, "FLOAT"

' Process: Explphos (0930)...
gp.toolbox = "C:/Documents and Settings/Administrator/Application
Data/ESRI/ArcToolbox/My Toolboxes/Grid-based Nutrient Yield Model.tbx"
gp.SingleOutputMapAlgebra "EXP (-[p_dmv] * [i_eff0930])", elp_0930,
"D:\nonpointsource_model\data\nutrient\p_dmv;D:\nonpointsource_model\data\nutrient\i_e
ff0930"

' Process: Exp2Phos (0930)...
gp.toolbox = "C:/Documents and Settings/Administrator/Application
Data/ESRI/ArcToolbox/My Toolboxes/Grid-based Nutrient Yield Model.tbx"
gp.SingleOutputMapAlgebra "exp (-[p_dmv] * [i_eff0930] - [p_rmv] * [q20080930])",
e2p_0930,
"D:\nonpointsource_model\data\nutrient\p_dmv;D:\nonpointsource_model\data\nutrient\p_r
mv;D:\nonpointsource_model\data\nutrient\i_eff0930;D:\nonpointsource_model\data\runoff
_sim\cal2\q\q20080930"

' Process: C_ROP (0930)...
gp.toolbox = "C:/Documents and Settings/Administrator/Application
Data/ESRI/ArcToolbox/My Toolboxes/Grid-based Nutrient Yield Model.tbx"
gp.SingleOutputMapAlgebra "((((([p_avs] - [p_avr]) * [elp_0930]) - (([p_avs] -
[p_avr]) * [e2p_0930])) / [f_por]) + (([p_avr] * [p_rmv] * [q20080930]) / [f_por])) *
0.09", c_rop0930,
"D:\nonpointsource_model\data\nutrient\p_avs;D:\nonpointsource_model\data\nutrient\p_a
vr;D:\nonpointsource_model\data\soil\grid-soil-
chem\f_por;D:\nonpointsource_model\data\nutrient\p_rmv;D:\nonpointsource_model\data\nu
trient\runoff_p_sim\elp_0930;D:\nonpointsource_model\data\nutrient\runoff_p_sim\e2p_09
30;D:\nonpointsource_model\data\runoff_sim\cal2\q\q20080930"

' Process: Flow Accumulation (0930)...
gp.FlowAccumulation_sa flowdirection, ac_rop0930, c_rop0930, "FLOAT"

' Process: Explphos (0928)...
gp.toolbox = "C:/Documents and Settings/Administrator/Application
Data/ESRI/ArcToolbox/My Toolboxes/Grid-based Nutrient Yield Model.tbx"
gp.SingleOutputMapAlgebra "EXP (-[p_dmv] * [i_eff0928])", elp_0928,
"D:\nonpointsource_model\data\nutrient\p_dmv;D:\nonpointsource_model\data\nutrient\i_e
ff0928"

' Process: Exp2Phos (0928)...
gp.toolbox = "C:/Documents and Settings/Administrator/Application
Data/ESRI/ArcToolbox/My Toolboxes/Grid-based Nutrient Yield Model.tbx"
gp.SingleOutputMapAlgebra "exp (-[p_dmv] * [i_eff0928] - [p_rmv] * [q20080928])",
e2p_0928,
"D:\nonpointsource_model\data\nutrient\p_dmv;D:\nonpointsource_model\data\nutrient\p_r
mv;D:\nonpointsource_model\data\nutrient\i_eff0928;D:\nonpointsource_model\data\runoff
_sim\cal2\q\q20080928"

' Process: C_ROP (0928)...
gp.toolbox = "C:/Documents and Settings/Administrator/Application
Data/ESRI/ArcToolbox/My Toolboxes/Grid-based Nutrient Yield Model.tbx"
gp.SingleOutputMapAlgebra "((((([p_avs] - [p_avr]) * [elp_0928]) - (([p_avs] -
[p_avr]) * [e2p_0928])) / [f_por]) + (([p_avr] * [p_rmv] * [q20080928]) / [f_por])) *
0.09", c_rop0928,
"D:\nonpointsource_model\data\nutrient\p_avs;D:\nonpointsource_model\data\nutrient\p_a
vr;D:\nonpointsource_model\data\soil\grid-soil-
chem\f_por;D:\nonpointsource_model\data\nutrient\p_rmv;D:\nonpointsource_model\data\nu
trient\runoff_p_sim\elp_0928;D:\nonpointsource_model\data\nutrient\runoff_p_sim\e2p_09
28;D:\nonpointsource_model\data\runoff_sim\cal2\q\q20080928"

' Process: Flow Accumulation (0928)...
gp.FlowAccumulation_sa flowdirection, ac_rop0928, c_rop0928, "FLOAT"

```

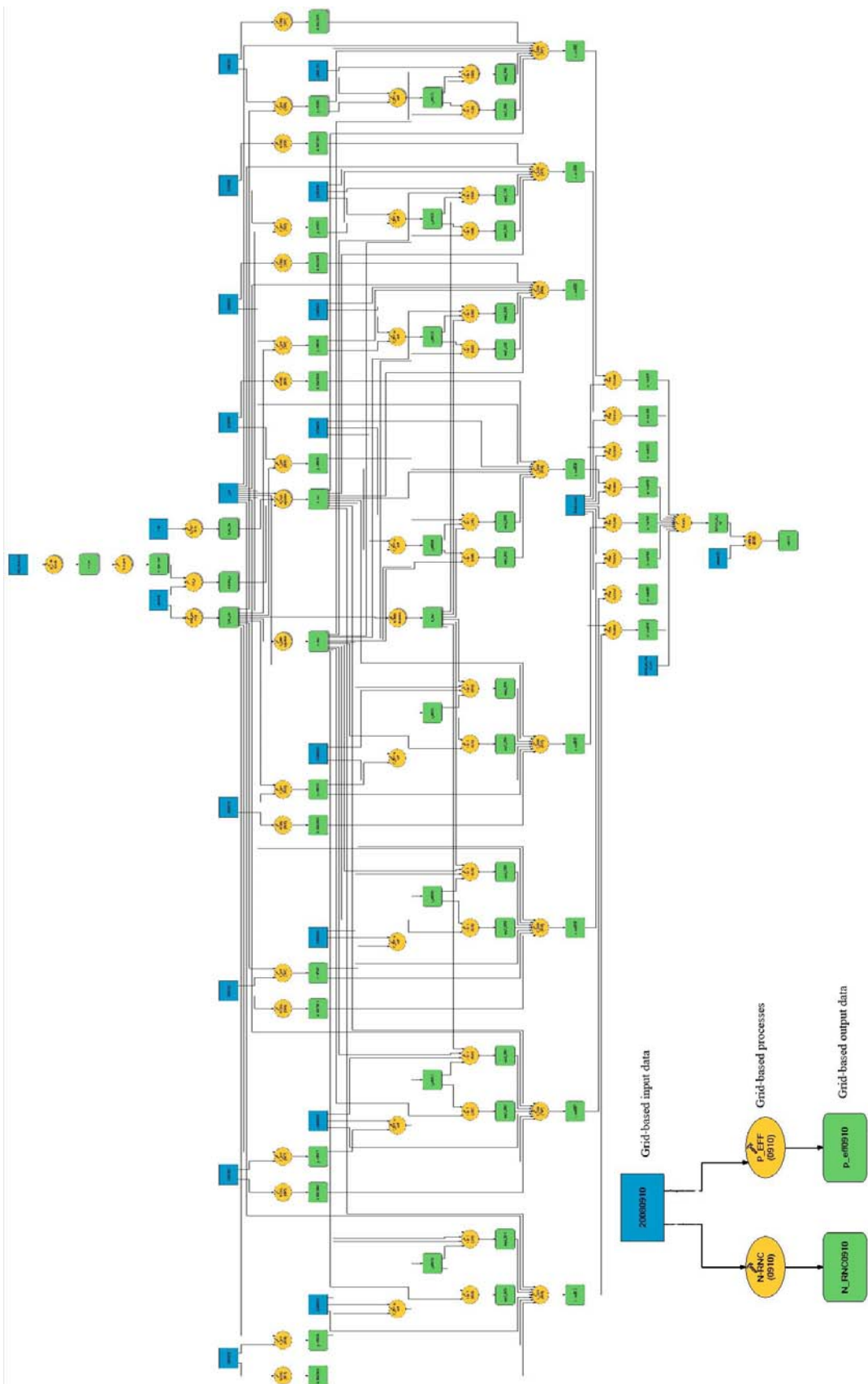
```

' Process: Explphos (1025)...
gp.toolbox = "C:/Documents and Settings/Administrator/Application
Data/ESRI/ArcToolbox/My Toolboxes/Grid-based Nutrient Yield Model.tbx"
gp.SingleOutputMapAlgebra "EXP (-[p_dmv] * [i_eff1025])", elp_1025,
"D:\nonpointsource_model\data\nutrient\p_dmv;D:\nonpointsource_model\data\nutrient\i_e
ff1025"
' Process: Exp2Phos (1025)...
gp.toolbox = "C:/Documents and Settings/Administrator/Application
Data/ESRI/ArcToolbox/My Toolboxes/Grid-based Nutrient Yield Model.tbx"
gp.SingleOutputMapAlgebra "exp (-[p_dmv] * [i_eff1025] - [p_rmv] * [q20081025])",
e2p_1025,
"D:\nonpointsource_model\data\nutrient\p_dmv;D:\nonpointsource_model\data\nutrient\p_r
mv;D:\nonpointsource_model\data\nutrient\i_eff1025;D:\nonpointsource_model\data\runoff
_sim\cal2\q\q20081025"
' Process: C_ROP (1025)...
gp.toolbox = "C:/Documents and Settings/Administrator/Application
Data/ESRI/ArcToolbox/My Toolboxes/Grid-based Nutrient Yield Model.tbx"
gp.SingleOutputMapAlgebra "((((([p_avs] - [p_avr]) * [elp_1025]) - (([p_avs] -
[p_avr]) * [e2p_1025])) / [f_por]) + (([p_avr] * [p_rmv] * [q20081025]) / [f_por])) *
0.09", c_rop1025,
"D:\nonpointsource_model\data\nutrient\p_avs;D:\nonpointsource_model\data\nutrient\p_a
vr;D:\nonpointsource_model\data\soil\grid-soil-
chem\f_por;D:\nonpointsource_model\data\nutrient\p_rmv;D:\nonpointsource_model\data\nu
trient\runoff_p_sim\elp_1025;D:\nonpointsource_model\data\nutrient\runoff_p_sim\elp_10
25;D:\nonpointsource_model\data\runoff_sim\cal2\q\q20081025"
' Process: Flow Accumulation (1025)...
gp.FlowAccumulation_sa flowdirection, ac_rop1025, c_rop1025, "FLOAT"
' Process: Explphos (0915)...
gp.toolbox = "C:/Documents and Settings/Administrator/Application
Data/ESRI/ArcToolbox/My Toolboxes/Grid-based Nutrient Yield Model.tbx"
gp.SingleOutputMapAlgebra "EXP (-[p_dmv] * [i_eff0915])", elp_0915,
"D:\nonpointsource_model\data\nutrient\p_dmv;D:\nonpointsource_model\data\nutrient\i_e
ff0915"
' Process: Exp2Phos (0915)...
gp.toolbox = "C:/Documents and Settings/Administrator/Application
Data/ESRI/ArcToolbox/My Toolboxes/Grid-based Nutrient Yield Model.tbx"
gp.SingleOutputMapAlgebra "exp (-[p_dmv] * [i_eff0915] - [p_rmv] * [q20080915])",
e2p_0915,
"D:\nonpointsource_model\data\nutrient\p_dmv;D:\nonpointsource_model\data\nutrient\p_r
mv;D:\nonpointsource_model\data\nutrient\i_eff0915;D:\nonpointsource_model\data\runoff
_sim\cal2\q\q20080915"
' Process: C_ROP (0915)...
gp.toolbox = "C:/Documents and Settings/Administrator/Application
Data/ESRI/ArcToolbox/My Toolboxes/Grid-based Nutrient Yield Model.tbx"
gp.SingleOutputMapAlgebra "((((([p_avs] - [p_avr]) * [elp_0915]) - (([p_avs] -
[p_avr]) * [e2p_0915])) / [f_por]) + (([p_avr] * [p_rmv] * [q20080915]) / [f_por])) *
0.09", c_rop0915,
"D:\nonpointsource_model\data\nutrient\p_avs;D:\nonpointsource_model\data\nutrient\p_a
vr;D:\nonpointsource_model\data\soil\grid-soil-
chem\f_por;D:\nonpointsource_model\data\nutrient\p_rmv;D:\nonpointsource_model\data\nu
trient\runoff_p_sim\elp_0915;D:\nonpointsource_model\data\nutrient\runoff_p_sim\elp_09
15;D:\nonpointsource_model\data\runoff_sim\cal2\q\q20080915"
' Process: Flow Accumulation (0915)...
gp.FlowAccumulation_sa flowdirection, ac_rop0915, c_rop0915, "FLOAT"
' Process: Sample...
gp.Sample_sa
"D:\nonpointsource_model\data\nutrient\runoff_p_sim\ac_rop0818;D:\nonpointsource_model
\data\nutrient\runoff_p_sim\ac_rop0907;D:\nonpointsource_model\data\nutrient\runoff_p_
sim\ac_rop0910;D:\nonpointsource_model\data\nutrient\runoff_p_sim\ac_rop1030;D:\nonpoi
ntsource_model\data\nutrient\runoff_p_sim\ac_rop0930;D:\nonpointsource_model\data\nutr
ient\runoff_p_sim\ac_rop0928;D:\nonpointsource_model\data\nutrient\runoff_p_sim\ac_rop
1025;D:\nonpointsource_model\data\nutrient\runoff_p_sim\ac_rop0915",
runoff_get_values_shp, c_rop_table, "NEAREST"

' Process: Table to dBASE (multiple)...
gp.TableToDBASE_conversion
"D:\nonpointsource_model\data\nutrient\runoff_p_sim\c_rop_table\c_rop_table",
c_rop_table__3_

```

Model diagram



APPENDIX K

SOME PICTURES OF AREA CHARACTERISTICS



Figure A-1 Direction of tillage for maize often across the contour.



Figure A-2 Maize cropping in undulating-rolling topography.



Figure A-3 Cassava cropping in undulating rolling topography.



Figure A-4 Mungbean cropping.



Figure A-5 Sugarcane cropping.



Figure A-6 Mango orchard.

APPENDIX L

SOME PICTURES OF SAMPLING AND LABORATORY



Figure B-1 M.145 station (Cable way).



Figure B-2 M.171 station (Bridge).



Sounding weight (US.DH 59-40P)



Sample bottle



Different nozzle for suspended sediment
sampling



Winch



Stream velocity instrument



Operated by cable-way

Figure B-3 Sampling instrument.



Figure B-4 Stream flow velocity measurement, suspended sediment sampling, water quality sampling at M.145.



Figure B-5 Stream flow velocity measurement, suspended sediment sampling, water quality sampling at M.171.



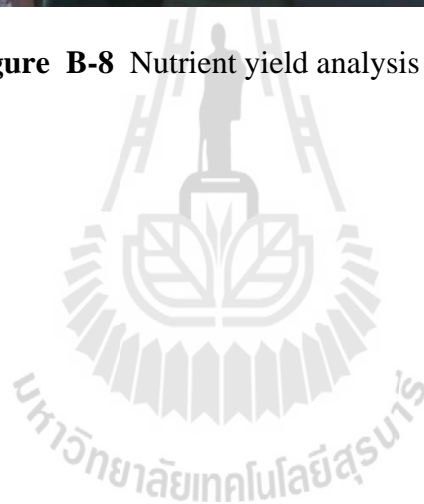
Figure B-6 Sediment yield analysis laboratory.



Figure B-7 Sediment yield analysis by drying at 103°C method.



Figure B-8 Nutrient yield analysis instrument.



CURRICULUM VITAE

Name Mr.Tharapong Phetprayoon

Date of Birth 19 July 1980

Place of Birth Saraburi Province, Thailand

Education

2001 B.Sc. Environmental Science (Resource Management),
Nakhon Ratchasima Rajabhat University.

2004 M.Sc. Geographic Information System,
Nakhon Ratchasima Rajabhat University.

Publications

1) Tharapong Phetprayoon, Sunya Sarapirome, Charlie Navanugraha, and Sodchol Wonprasaid. (2009). **Surface runoff estimation using grid-based curve number method in the Upper Lam Phra Phloeng watershed, Thailand.** In 30th Asian Conference on Remote Sensing, October 18-23, Beijing, China.

2) Tharapong Phetprayoon, Sunya Sarapirome, Charlie Navanugraha, and Sodchol Wonprasaid. (2009). **The revision of spatial MUSLE for event-based sediment yield estimation in Upper Lam Phra Phloeng watershed.** In Geoinfotech2009, December 16-18, Impact Convention Center, Nonthaburi , Thailand.

Position and Place of Work

Lecturer at Program of Geoinformatics, Nakhon Ratchasima Rajabhat University.